

Denman Marine Voyage (NUY2025-V03): Post-survey report



2024/25 Australian Antarctic Program Voyage 3

Of the Research and Supply Vessel *Nuyina*

To the Denman Glacier region in 2025

Contributions by DMV Participants

Edited by James Trihey



AAPP
Australian Antarctic
Program Partnership



© 2025 Author/s retain copyright.

Published by Institute for Marine and Antarctic Studies, College of Sciences and Engineering, University of Tasmania, Hobart, Tasmania, Australia.

This title is published under a Creative Commons Attribution 4.0 International License (CC BY 4.0). The full license terms are available at: <https://creativecommons.org/licenses/by/4.0/>

The views expressed herein are those of the authors and are not necessarily those of the Australian Government or Australian Research Council.

Acknowledgements

We thank the Australian Antarctic Division, the NUY2025-V03 scientific party-led by Science Leads Laura Herraiz-Borreguero, Delphine Lannuzel, Jan Strugnell, and Leonie Suter, Science Coordinator Damien Stringer, AAD support staff and Serco crew members led by Capt. Paul Clarke for their help and support on board the RSV *Nuyina*.

The funding for editing and compiling this report was supported by the Australian Research Council Special Research Initiative, Australian Centre for Excellence in Antarctic Science (ACEAS) (Project Number SR200100008).

Preferred Citation:

Trihey, J., Herraiz-Borreguero, L., Lannuzel, D., Strugnell, J., Suter, L., Stringer, D., and On-board Scientific Party. (2025). *Denman Marine Voyage (NUY2025-V03): Post-survey report*, Institute for Marine and Antarctic Studies, University of Tasmania: Hobart, <https://doi.org/10.25959/247Q-FP34>

Title photo: RSV Nuyina off the Denman Glacier, East Antarctica. Photo: Pete Harmsen, Australian Antarctic Division

2024/25 Australian Antarctic Program Voyage 3

28th February 2025 to 2nd May 2025

Hobart – Hobart

Voyage Title:

Denman Marine Voyage

Science Leads:

Leonie Suter (AAD)

Laura Herraiz Borreguero (AAPP)

Delphine Lannuzel (ACEAS)

Jan Strugnell (SAEF)

Science Coordinator:

Damien Stringer

Voyage Management:

Bruce Payne (Voyage Leader)

Anthony MacFarlane (Deputy Voyage Leader)

Nick Watt (Deputy Voyage Leader)

Contents

1. Summary and Itinerary	10
2. Weather conditions during DMV	15
3. Voyage Participants	17
3.1 Science Team	17
3.2 Scientific support staff	19
3.3 Media	19
3.4 Doctors	20
3.5 Voyage Leadership	20
3.6 RSV <i>Nuyina</i> Crew	20
4. Science overview and objectives.....	22
4.1 Australian Antarctic Division (AAD) – Science Overview and Objectives.....	22
4.2 Australian Antarctic Program Partnership (AAPP) – Science Overview and Objectives	23
4.3 Australian Centre for Excellence in Antarctic Science (ACEAS) – Science Overview and Objectives.....	25
4.4 Securing Antarctica’s Environmental Future (SAEF) – Science Overview and Objectives.	26
5. Physical Oceanography (AAS 4631)	27
5.1 CTD Deployments	27
5.1.1 Overall Aims and Hypotheses.....	27
5.1.2 CTD Deployments and Sample Collection Methods	29
5.1.3 Preliminary results.....	31
5.2 Moorings	38
5.2.1 Overview	38
5.2.2 Deployment	40
5.3 Argo floats	42
5.4 Glider	44
5.5 Data Management	45
5.6 References	45
6. Hydrochemistry (AAS 4630)	46
6.1 Executive Summary	46
6.1.1 Objectives.....	46
6.1.2 General Hydrochemistry Information.....	46
6.1.3 Data Management	46
6.1.4 HydroBox Personnel	46
6.1.5 Summary	47
6.2 Salinity	47

6.3 Dissolved Oxygen.....	48
6.4 Nutrients	49
6.4.1 HyPro Processing Summary for Nutrients	50
6.5 Issues encountered	52
6.6 Recommendations for next voyage	54
6.7 Temperature Plot.....	54
6.8 References	54
7. Trace Metals & Isotopes (AAS 4630).....	56
7.1 General Introduction	56
7.2 Overall Aim and Hypothesis.....	56
7.3 Sample Collection Methods	57
7.4 Station Locations	62
7.5 Deployment details.....	63
7.6 Preliminary results	65
7.6.1 Nutrient results	65
7.6.2 Chlorophyll results	66
7.7 Data Management	68
7.8 Acknowledgments	68
7.9 References	68
8. Atmospheric processes (AAS 4631).....	69
8.1 Background	69
8.2 Methods and Equipment	70
8.3 Challenges	72
8.4 Preliminary Results	73
8.5 Data Management	76
8.6 Acknowledgements	77
8.7 References	77
9. Hydroacoustics	80
9.1 General introduction	80
9.2 Multibeam Echosounders	82
9.2.1 Data acquisition and processing	83
9.2.2 Sound velocity profiles.....	84
9.2.3 Preliminary results.....	85
9.3 Sub-bottom profiling	88
9.3.1 SBP Data acquisition:	88
9.3.2 SBP data processing:	89

9.3.3 Preliminary results.....	89
9.4 Mitigation for cetaceans.....	91
9.5 Acoustics Support for Science Operations.....	94
9.6 Data Management.....	94
9.7 References.....	94
10. Trawling (AAS 4628).....	95
10.1 Introduction.....	95
10.2 Methods and equipment.....	96
10.3 Preliminary results.....	98
10.3.1 Fish.....	104
10.4 Data Management.....	104
10.5 References.....	104
11. Rocks (AAS 4630).....	105
11.1 General Introduction.....	105
11.2 Overall Aims and Hypothesis.....	105
11.3 Methods.....	105
11.3.1 Site Selection.....	105
11.3.2 Equipment.....	106
11.3.3 Dredge deployment workflow.....	106
11.3.4 Rock processing workflow.....	107
11.3.5 Beam (Benthic) Trawls.....	107
11.4 Sample Description and preliminary results.....	108
11.4.1 Rock Dredges.....	108
11.4.2 Beam Trawls.....	111
11.4.3 Sediment coring.....	115
11.5 Data Management.....	116
11.6 Acknowledgements.....	116
11.7 References.....	116
12. Sediment (AAS 4630).....	117
12.1 General Introduction.....	117
12.2 Aims and Hypotheses.....	117
12.3 Diatoms / Underway sampling.....	118
12.3.1 Introduction.....	118
12.3.2 Underway Sampling Protocol.....	119
12.3.3 F. kerguelensis Sampling Protocol.....	121
12.3.4 Underway Nutrient Sampling Protocol.....	121

12.3.5 CTD Sampling Protocol	121
12.3.6 Diatom Assemblage Notes.....	122
12.4 CTD and TMR sampling.....	124
12.4.1 Introduction	124
12.4.2 Sample Collection Methods	125
12.5 Multicores	129
12.5.1 Introduction	129
12.5.2 Site selection & deck operations	129
12.5.3 Sample collection methods	133
12.5.4 Sample description & preliminary results.....	138
12.5.5 Recommendations:	142
12.6 Kasten Cores	143
12.6.1 Introduction	143
12.6.2 Site selection & deck operations	143
12.6.3 Sample Collection Methods	143
12.6.4 Sample description & preliminary results.....	146
12.7 Data Management.....	154
12.8 Acknowledgements.....	154
12.9 References	155
13. Towed camera / Seafloor imagery (AAS 4630).....	156
13.1 Objectives	156
13.2 Methods	156
13.3 Activity on the Voyage.....	160
13.4 Outcomes and data management.....	166
13.5 Acknowledgements.....	166
13.6 References	166
14. Phytoplankton – Biogeochemistry (AAS 4630)	167
14.1 Overview and Acknowledgements	167
14.2 Aim and Hypotheses	167
14.3 Sample Collection Methods	168
14.4 Stations sampled during DMV.....	171
14.5 Preliminary Results	172
14.5.1 Chlorophyll-a concentrations.....	172
14.5.2 Contribution of icebergs to localised ocean fluorescence	173
14.5.3 Iron/manganese additions near the Denman Glacier and within the Shackleton Polynya.....	174

14.5.4 Other secondary metals.....	175
14.5.5 The influence of light and iron-binding ligands on Southern Ocean deep chlorophyll maximas in autumn	176
14.5.6 Iron limitation DFB experiment	177
14.5.7 Krill-Assisted Resuspension of Material to Atmosphere (KARMA) Experiment	177
14.6 Data Management.....	178
14.7 References	178
15. Seal tagging (AAS 4630)	181
15.1 Introduction.....	181
15.2 Methods, equipment and preliminary results	181
15.2.1 Elephant seal tagging at Iles Kerguelen and collection of biological and physical oceanography in the Denman Glacier region.	181
15.2.2 Constructing a new bathymetry for the Denman Glacier Study Area using seal dive data.....	182
15.2.3 Capturing seals on ice floes for the deployment of satellite telemetry tags.....	184
15.2.4 Seal Tag calibrations	186
15.2.5 Seal sightings database.	189
15.3 Potential improvements	190
15.4 Data Management.....	191
16. Environmental DNA (eDNA) and sedimentary ancient DNA sampling (AAS 4556 and AAS 4636) 192	
16.1 General Introduction	192
16.2 Overall Aim and Hypothesis.....	192
16.3 Methods	193
16.3.1 Overview	193
16.3.2 Underway and CTD eDNA sampling.....	193
16.3.3 Autonomous eDNA sampling	196
16.3.4 Sedimentary ancient DNA (<i>seDaDNA</i>) sampling from Kasten cores	196
16.3.5 Sedimentary Ancient DNA (<i>seDaDNA</i>) sampling from Multicores	198
16.4 Issues encountered.....	198
16.5 Recommendations.....	198
16.6 Data Management.....	199
16.7 Acknowledgements.....	199
17. eDNA invasives (AAS 4628)	200
17.1 Introduction.....	200
17.2 Sample Collection Methods	200
17.3 Locations.....	201

17.4 Data Management.....	202
17.5 Acknowledgements.....	202
17.6 References	202
18. Zooplankton / Wet Well (AAS 4631)	203
18.1 General Introduction	203
18.2 Overall Aim and Hypothesis.....	203
18.3 Methods	204
18.3.1 Simulated Plankton tow	204
18.3.2 Zooplankton physiological tolerance experiments.....	205
18.3.3 Pteropod egg development documentation	206
18.4 Recommendations.....	206
18.5 Preliminary Results (Voyage summary)	207
18.5.1 Zooplankton Experiments	210
18.5.2 Continuous Plankton Recorder (CPR) Deployments	211
18.6 Data Management.....	211
18.7 Acknowledgements.....	211
19. Media program	212
20. ACEAS Outreach	214
20.1 Overview	214
21. Appendix.....	219
21.1 Metadata	219
21.2 Station List.....	219
21.3 Fish caught during DMV.....	227
22. Supplementary Material	236

1. Summary and Itinerary

1. Summary and Itinerary

By Damien Stringer

The Denman Marine Voyage brought together researchers from the Australian Antarctic Program Partnership (AAPP – AAS4631, Chief Investigator Dr Laura Herraiz-Borreguero), the Australian Centre for Excellence in Antarctic Science (ACEAS – AAS4630, Chief Investigator Prof. Matthew King), Securing Antarctica’s Environmental Future (SAEF – AAS4628, Chief Investigator Prof. Steven Chown), and the Australian Antarctic Division (AAD – AAS4636 and 4556 Chief Investigators Dr So Kawaguchi and Dr Leonie Suter), on a highly collaborative, multidisciplinary research voyage aboard RSV *Nuyina* to the Denman Glacier region and Shackleton Ice Shelf. The voyage was the first dedicated marine science voyage for RSV *Nuyina* and represented a significant milestone for the Australian Antarctic Program.

The Denman Glacier and related ice shelf system represent a poorly understood region of the East Antarctic Ice Sheet, with potential for significant global impacts. It is presently considered one of the fastest retreating glacier systems in East Antarctica, with the potential to contribute more than 1.5 m rise to global sea-levels. Linking with the Denman Terrestrial Campaign (2022/23 – 2024/25), the voyage sought to address a suite of science objectives, including:

- AAS4630: ACEAS – to understand the risk of ice mass loss from key subglacial basins over the next decades to centuries, and what the consequences are for the local oceans and ecosystems.
- AAS4631: AAPP – to understand the susceptibility of the East Antarctic Ice Sheet to a warming climate, and to contribute to providing decision makers in government, nationally and internationally, with accurate, timely and integrated observations of the earth system to empower assessments of, and responses to, the risks posed by climate variability and change.
- AAS: 4628 SAEF - to improve climate observations and projections and weather forecasts; reduce icesheet uncertainties; provide insight into biodiversity processes and change; assess invasive species pathways and impacts; and develop optimal monitoring methodologies that lead to management decision making.
- AAS:4556/4636 AAD – to inform the sustainable and ecosystem-based management of the East Antarctic krill fishery; and quantify the current and projected impacts of climate change on East Antarctica's krill-based ecosystem.

Each program featured numerous working groups and onboard science leads, with objectives captured in 14 Service Level Agreements:

Table 1: Denman Marine Voyage Service Level Agreements

Project Number	Working Group	Onboard Lead	Research Program	Funding grant number
4628	Biological Invasives	Frances Perry	SAEF	ARC SR200100005
4628	Benthic trawling	Jan Strugnell	SAEF	ARC SR200100005
4630	Sediment coring	Taryn Noble	ACEAS	ARC SR200100008
4630	Rock dredging	Jo Whittaker	ACEAS	ARC SR200100008

1. Summary and Itinerary

4630	Towed camera imaging	Craig Johnson	ACEAS	ARC SR200100008
4630	Trace Metals	Michael Ellwood	ACEAS	ARC SR200100008
4630	Hydroacoustics	Jo Whittaker	ACEAS	ARC SR200100008
4630	Phytoplankton sampling	Pauline Latour	ACEAS	ARC SR200100008
4630	Biogeochemistry	Delphine Lannuzel	ACEAS	ARC SR200100008
4630	Seal Tagging	Mark Hindell	ACEAS	ARC SR200100008
4631	Pelagic Sampling	Haiting Zhang	AAPP	Antarctic Science Collaboration Initiative
4631	Physical Oceanography	Laura Herraiz-Borreguero	AAPP	Antarctic Science Collaboration Initiative
4631	Atmospheric	Jakob Pernov	AAPP	Antarctic Science Collaboration Initiative
4636/4556	eDNA	Leonie Suter	AAD	

To achieve these objectives, a comprehensive suite of deployments and underway activities from a broad range of disciplines were completed across 146 stations, including:

- Underway sampling for eDNA, invasives, phytoplankton
- Continuous Plankton Recorder (CPR) towing during transit
- Multibeam (EM122 & EM712) & TOPAS sub-bottom profiling (59,544 km² mapped)
- Acoustic Doppler Current Profiling (ADCP)
- Expendable bathythermographs (XBTs – 57 deployments)
- Underway air-chemistry sampling
- Wet-well sampling – 47 sessions
- Conductivity, Temperature and Depth (CTD) rosette – 102 deployments
- Trace metal free CTD rosette (TMR) – 28 deployments
- Trace metal free in situ pump (ISP) – 3 deployments
- Rock dredging – 7 deployments
- Multicoring – 14 deployments of the 6-core multi-corer
- Kasten coring – 6 deployments
- Towed camera seafloor imaging – 23 deployments (approx. 1 km each tow)
- Benthic beam trawling – 16 deployments
- Moorings – 3 long string mooring deployments
- Argo floats – 13 float deployments
- Moving Vessel Profiler (MVP) – approx. 90 hours during transit
- Radiosonde deployments – 150 launches
- Process stations – 2 stations
- Phytoplankton and zooplankton incubation experiments
- Seal tagging – 2 attempts

The voyage departed Hobart on 1st March 2025 with a team of 60 scientists, 25 AAD support and management staff, and 45 crew. The science team brought together researchers from 14 institutions, with two-thirds being early career scientists. Of the 60 scientists, 40 identified as female and 20 as male, and three-quarters were based at Australian universities.

1. Summary and Itinerary

A range of underway science activities were performed throughout the south-bound transit including the deployment of three large biogeochemistry floats, underway sampling for air-chemistry, eDNA, invasives and phytoplankton, wet-well sampling, CPR tows, radiosonde releases, hydroacoustics and ADCP operations. Aft deck operations in the target region commenced with a rock dredge on the Bruce Rise on the 9th March 2025.

Operations then continued in the Bruce Rise and Central Denman region through until 2nd April, and included:

- Argo Floats – 8 deployments
- Multicoring - 7 deployments
- Kasten coring – 3 deployments
- Benthic beam trawling – 7 deployments
- CTD - 60 deployments
- TMR - 15 deployments
- Towed Camera – 10 deployments
- Moorings – 2 deployments
- Smith McIntyre grab – 1 deployment
- 1 Process Station
- ISP – 1 deployment
- 68 Radiosonde balloons

Low sea-ice conditions allowed unprecedented access to the Denman Glacier, with CTD transects performed within a nautical mile of the glacier's edge. In one area close proximity to the glacial tongue enabled bathymetric data to be obtained from beneath the floating ice shelf. General operations cycled through hydroacoustics, CTD transects and aft-deck operations as the voyage worked through the region. The central region was the priority area for the physical oceanography team, and CTDs and float deployments were prioritised more heavily in this period. Four days of operational time in this region were impacted by adverse weather, however hydroacoustic activities continued throughout.

On the 2nd April the voyage then transited to the West Shackleton operational area and completed a further:

- Argo Floats – 3 deployments
- Multicoring - 7 deployments
- 3 Kasten coring – 3 deployments
- Benthic beam trawling – 9 deployments
- CTD - 42 deployments
- TMR - 13 deployments
- Towed Camera - 13 deployments
- 1 Mooring – 1 deployment
- 1 Process Station
- ISP – 2 deployments
- 54 Radiosonde balloons
- 24 hours of ship time dedicated to seal tagging

A similar operational cycle was employed in the West Shackleton region, with a greater focus on biological projects including benthic trawling, towed camera and seal-tagging. A further six days were impacted by adverse weather, however CTD operations using the vessel's moonpool were able to continue – in conditions impacted by sea-ice and with winds gusting above 50 knots.

1. Summary and Itinerary

Upon completion of activities in the West Shackleton on the 21st April, the voyage then returned via the East Bruce Rise and seamounts to the North, completing a further four rock dredges. Final underway activities including sampling for air-chemistry, eDNA, invasives and phytoplankton, wet-well sampling, CPR tows, radiosonde releases, hydroacoustics, ADCP operations and MVP tows were completed during the return transit, with RSV *Nuyina* returning to port in Hobart on the 2nd May 2025.

Throughout the voyage, weather and ice conditions significantly influenced planning decisions – notably how, where and when operations could be performed - however a high operational tempo was maintained throughout, with minimal time lost. Conditions at night adjacent to the Denman Glacier proved particularly challenging, where strong local currents and numerous icebergs, combined with adverse winds, generated conditions not conducive to operations. Notwithstanding the above, steady progress in this region was made and two CTD transects across the Northern and Eastern flanks of the glacier were successfully completed.

Similarly, the ship's systems performed well throughout the voyage, with minimal lost time due to mechanical or other failure. For a ~14 hr period on the 1st April the A-frame was not operational, however the ship transitioned into an 8-CTD transect during this time, and minimal operational time was lost whilst the A-frame was rectified.

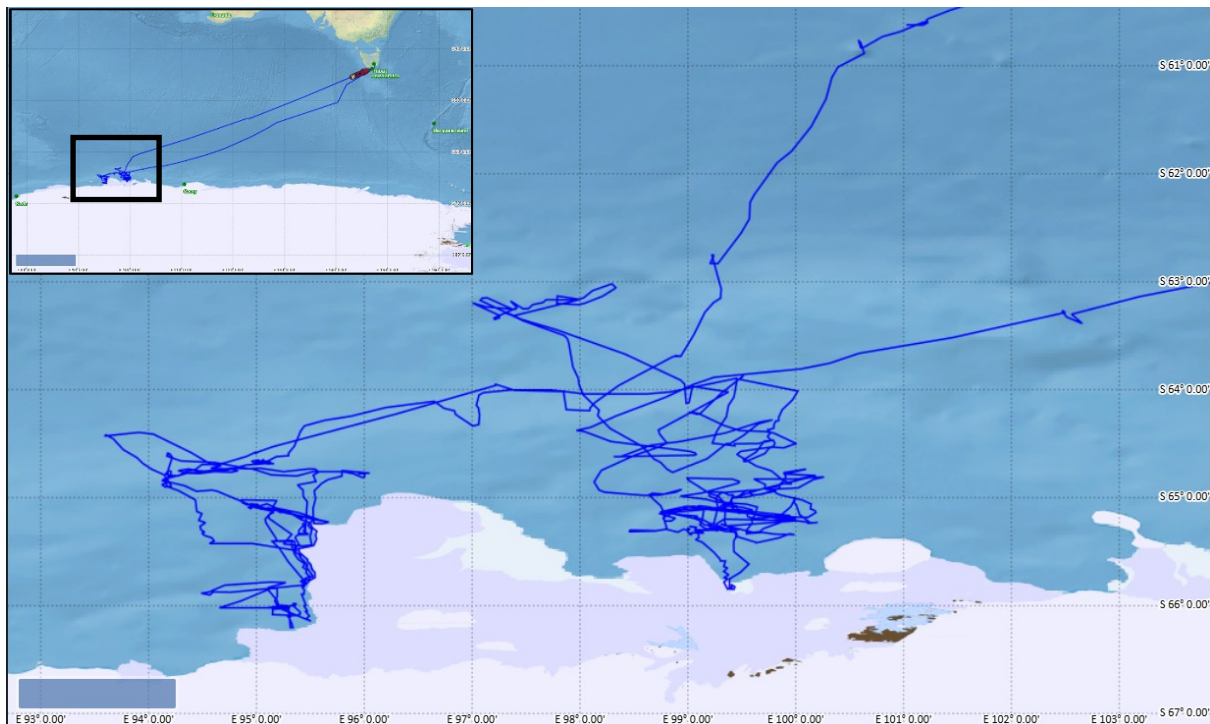


Figure 1: Voyage track

1. Summary and Itinerary

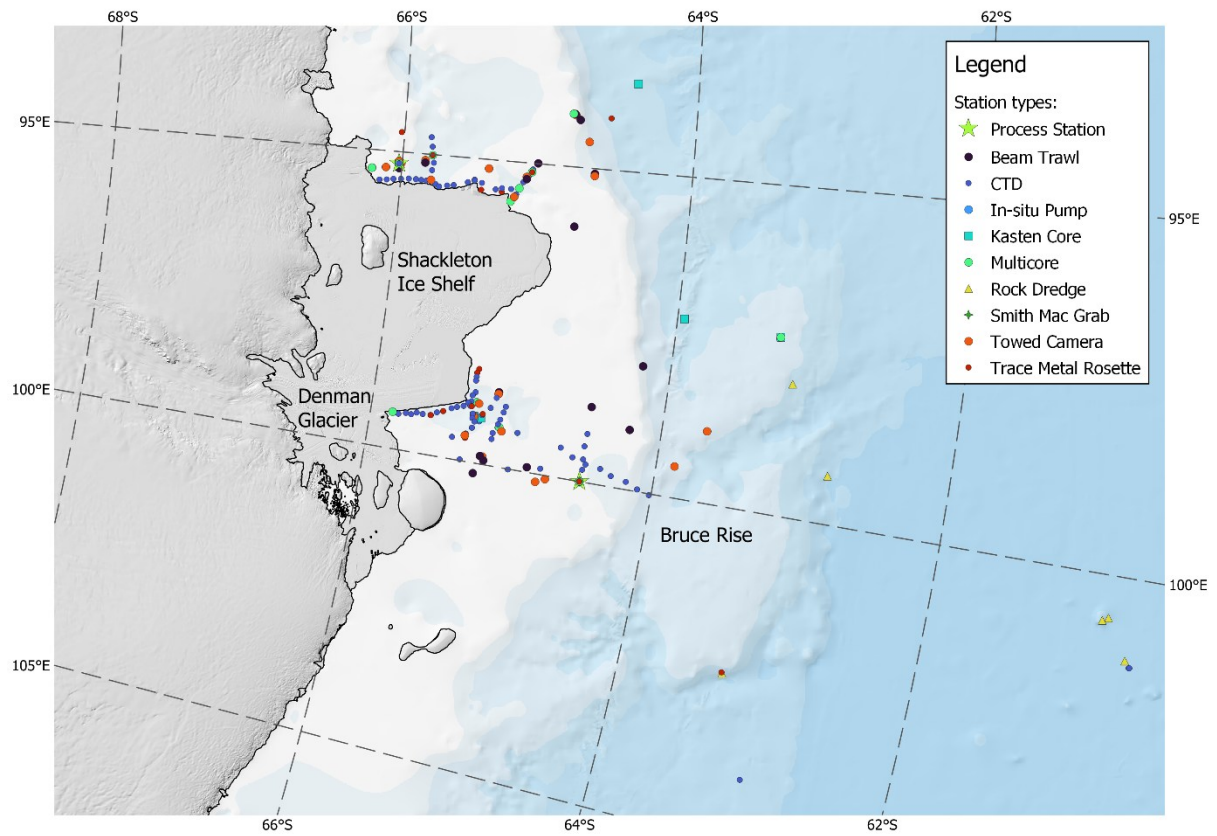


Figure 2: All stations from the Denman / Shackleton region. Basemap from Quantarctica (Matsuoka et al., 2021).

2. Weather conditions during DMV

2. Weather conditions during DMV

By Bruce Payne

Departed Hobart in the AM of Saturday 01 March 2025. Weather conditions early in the transit from Hobart to the Denman Glacier region were reasonable before deteriorating on Tuesday the 4th of March. A cold front generated showers and large swell with wave heights up to 6.5 m and winds up to 45 knots continuing through to Thursday, which prevented the deployment of equipment over the side of the vessel.

Conditions improved on 6 March as a weak ridge of high pressure moved through before deteriorating again on the evening of 7 March as a low-pressure system approached. This saw wave heights up to 6 m and snow showers through 8 March before improving again on the evening of 8 March 2025. The *Nuyina* crossed 60 °S at approximately 1000 hrs entering Antarctic waters.

A large deep low approached on Sunday evening, 9 March, bringing winds up to 45 knots and wave heights of up to 6.5 m. Conditions improved on Tuesday with wind speed falling to 20-30 knots and waves reducing to 4-5 m. A second large low-pressure system was approaching at this point.

The large low brought heavy sea conditions, snow showers and strong winds on Monday 10 March with winds over 50 knots and waves over 10 m and isolated snow showers. Conditions prevented operational activities apart from Hydroacoustics.

This weather system cleared quickly allowing activities to resume on 11 March and continue relatively trouble free until 19 March.

From 19 March we were operating in areas with icebergs that affected operations due to their movement. This was especially an issue at night when there was limited visibility. A frontal band attached to a low came through on 20 March with high winds affecting operations. Winds of 40 knots and 4 m swells on the 21st continued through the 22nd before clearing on the 23rd. Good weather continued through to the 29th when a series of lows came through and the weather started deteriorating again with high winds and swell but activities were still able to be conducted.

On the 3rd of April weather in the morning prevented a beam trawl being conducted before improving in the afternoon. The 4th and 5th of April saw a deep low come in from the west bringing wind gusts over 45 knots and 40 knots respectively with temperatures falling to below -15 °C by the 6th of April. Temperatures of -15 °C or below continued with wind chill factor of -30 °C at night. On the 9th of April we were unable to do a rock dredge due to high winds from the wrong direction.

Low temperatures continued with below -25 °C being recorded on 11 and 12 April with sea ice forming. On the 13th we had winds gusting up to 60 knots at times which made deployment of equipment difficult. This continued into the 14th where we had -20 °C overnight and winds of 40-50 knots before the winds dropped and the sun came out briefly on the 15th.

Weather again worsened with a deep low from the West approaching on the 17th with winds averaging around 40 knots and gusting up to 60 knots on the 17th and 80 knots on the 18th along

2. Weather conditions during DMV

with snow limiting visibility and hampering operations. Wind speeds started falling on the 19th though still over 50 knots overnight,

From early April until mid-April we were operating in conditions with large amounts of ice, and icebergs around, which, combined with reduced visibility at night severely hampered nighttime operations.

The weather then remained reasonable until the 25th when we started our transit back to Hobart. The trip home passed without incident apart from some large swell (6-7 m) on the 28th of April.

3. Voyage Participants

3. Voyage Participants

3.1 Science Team

Name	Funding body	Institute*	Profession	Discipline
Matthis Auger	ACEAS	UTAS	Scientist	Physical Oceanography
Kelsey Barber	AAPP	U of U	Scientist	Atmospherics
Chelsea Bekemeier	AAPP	CSU	Masters student	Atmospherics
Luke Brokensha	AAPP	UTAS	Scientist	Plankton
Jesselyn Brown	SAEF	JCU	Research assistant	Beam Trawl
Neve Clippingdale	ACEAS	UTAS	Honours student	Sediments & Rock Dredging
Matthew Corkill	ACEAS	UTAS	Scientist	Phytoplankton Biogeochemistry
Inessa Corney	AAPP	UTAS	PhD student	Plankton
Yuhao Dai	ACEAS	ANU	Scientist	Trace Metals & Isotopes & Sediments
Michael Ellwood	ACEAS	ANU	Scientist	Trace Metals & Isotopes
Annie Foppert	AAPP	UTAS	Scientist	Physical Oceanography
Noémie Friscourt	ACEAS	UTAS	Scientist	Deep Sea Camera
Dave Green	ACEAS	UTAS	Scientist	Seal Tagging
Laura Herraiz Borreguero	AAPP	CSIRO	Scientist	Physical Oceanography
Mark Hindell	ACEAS	UTAS	Scientist	Seal Tagging
Katharina Hochmuth	ACEAS	UTAS	Scientist	Hydroacoustics, Rock Dredging & Sediments
Molly Husdell	ACEAS	UQ	PhD student	Sediments & Rock Dredging
Julie Janssens	AAPP	CSIRO	Scientist	Hydrochemistry
Craig Johnson	ACEAS	UTAS	Scientist	Deep Sea Camera
Rosie Kidman	SAEF	JCU	Research assistant	Beam Trawl
Delphine Lannuzel	ACEAS	UTAS	Scientist	Trace Metals & Isotopes

3. Voyage Participants

Pauline Latour	ACEAS	UTAS	Scientist	Phytoplankton Biogeochemistry
Sally Lau	SAEF	JCU	Scientist	Beam Trawl
Rose Leeger	SAEF	CU-Boulder	PhD student	Beam Trawl
Benoit Legresy	AAPP	CSIRO	Scientist	Physical Oceanography
Joshua Lesicar	SAEF	JCU	Honours student	Beam Trawl
Yuhang Liu	AAPP	UTAS	PhD student	Physical Oceanography
Merinda McMahon	AAPP	CSIRO	Scientist	Hydrochemistry
Noah Menner	ACEAS	UTAS	Honours student	Sediments & Rock Dredging
Rachel Meyne	ACEAS	Mines	PhD student	Sediments & Rock Dredging
Katie Nawrath	ACEAS	UTAS	Honours student	Trace Metals & Isotopes
Talitha Nelson	ACEAS	UTAS	PhD student	Trace Metals & Isotopes
Taryn Noble	ACEAS	UTAS	Scientist	Sediments & Rock Dredging
Karin Orth	ACEAS	UTAS	Scientist	Rock Dredging & Sediments
Christian Pagel	SAEF	JCU	Research assistant	Beam Trawl
Tom Paynter	AAPP	AAD	Scientist	Atmospherics
Jakob Pernov	AAPP	QUT	Scientist	Atmospherics
Frances Perry	SAEF	UoA	PhD student	eDNA invasives & Beam Trawl
Ole Rieke	AAPP	UTAS	PhD student	Physical Oceanography
Pimnara Riengchan	AAPP	UTAS	PhD student	Plankton
Nicola Rodewald	SAEF	JCU	PhD student	Beam Trawl
Vishwadeep Rout	ACEAS	UTAS	PhD student	eDNA
Christina Schmidt	ACEAS	UNSW	PhD student	Hydrochemistry
Abbie Smith	AAPP	AAD	Scientist	Trace Metals & Isotopes
Salvatore Sodano	AAPP	UTAS	PhD student	Atmospherics
Ilaria Stollberg	ACEAS	UTAS	PhD student	Deep Sea Camera
Jan Strugnell	SAEF	JCU	Scientist	Beam Trawl
Leonie Suter	AAD	AAD	Scientist	eDNA

3. Voyage Participants

Esther Tarszisz	ACEAS	UTAS	Scientist	Seal Tagging
Jim Trihey	ACEAS	UTAS	PhD student	Sediments & Rock Dredging
Robin Van Dijk	ACEAS	UTAS	PhD student	Trace Metals & Isotopes
Jakob Weis	ACEAS	UTAS	Scientist	Seal Tagging
Amy Wells	ACEAS	UTAS	PhD student	Sediments & Rock Dredging
Jasmin Wells	SAEF	GA	Scientist	Acoustics & Beam Trawl
Joanne Whittaker	ACEAS	UTAS	Scientist	Rock Dredging & Sediments
Nerida Wilson	SAEF	CSIRO	Scientist	Beam Trawl
Kaihe Yamazaki	ACEAS	UTAS	Scientist	Physical Oceanography
Claire Yung	ACEAS	ANU	PhD student	Hydrochemistry
Haiting Zhang	AAPP	UTAS	Scientist	Plankton

*Refer to Table 2 for institute abbreviations

3.2 Scientific support staff

Name	Institution	Role
Alison Herbert	AAD	Acoustician
Floyd Howard	AAD	Acoustician
Anton Rocconi	AAD	Aquaria Technician
Tess Chapman	AAD	Data Officer
Lewis Rockliffe	AAD	Data Officer
Mick Stapleton	AAD	Field Training Officer (Seal Tagging team)
Trent Wickham	AAD	Gear Officer
Adam Duraj	AAD	Gear Officer
Jamie Derrick	CSIRO	Gear Officer
Michael Santarossa	AAD	Science Systems Engineer
Anthony Hay	AAD	Science Systems Engineer
Roland Painter	AAD	Science Systems Engineer
Dominic Weller	AAD	Science Systems Engineer
William Rigby	AAD	Science Systems Engineer
Nick Burleigh	AAD	Science Systems Engineer
Hugh Matthys	AAD	Science Systems Engineer
Liam Byrne	AAD	Science Systems Engineer
Jacob Yates	AAD	Science Systems Engineer

3.3 Media

Name	Company	Role
Pete Harmsen	AAD	Camera Operator
Lily West	AAD	Media Representative

3. Voyage Participants

3.4 Doctors

Name	Company	Role
Cath Deacon	AAD	Antarctic Medical Practitioner
Jess Johnson Ling	AAD	Antarctic Medical Practitioner

3.5 Voyage Leadership

Name	Company	Role
Bruce Payne	AAD	Voyage Leader
Anthony Macfarlane	AAD	Deputy Voyage Leader
Nick Watt	AAD	Deputy Voyage Leader
Damien Stringer	AAD	Science Coordinator

3.6 RSV *Nuyina* Crew

Name	Company	Role
Paul Clarke	Serco	Master
Tim Sharpe	Serco	Chief Officer
Katrina Beams	Serco	2 nd Officer
Henry Goodfellow	Serco	2 nd Officer
Brett Cross	Serco	3 rd Officer
Tom Leaversuch	Serco	3 rd Officer
Pete Flynn	Serco	3 rd Officer
Danielle McCarthy	Serco	3 rd Officer
Ayla Rance	Serco	Deck Cadet
Gerrit Oplaat	Serco	Chief Engineer
Tom O'Neil	Serco	1 st Engineer
Damien Betts	Serco	2 nd Engineer
Steve Ayers	Serco	3 rd Engineer
Francesco Polez	Serco	3 rd Engineer
John Murphy	Serco	4 th Engineer
John Clauss	Serco	4 th Engineer
Kian Dalton	Serco	Engineering Cadet
Levi Dubbelman	Serco	ETO
Mykyta Yarzhemski	Serco	ETO
Ilya Dryakhlov	Serco	ETO
Joe McMenemy	Serco	Bosun
Phil Brouillette	Serco	Integrated Rating
Amy Norman	Serco	Integrated Rating
Nathan Cox	Serco	Integrated Rating
Grant Smith	Serco	Integrated Rating
Darren McDougall	Serco	Integrated Rating
Alex Burenkov	Serco	Integrated Rating
Finn Zanoni	Serco	Integrated Rating
Trent Stephens	Serco	Integrated Rating
Damian Adkins	Serco	Integrated Rating
Darrel Barker	Serco	Integrated Rating

3. Voyage Participants

Shane Eccarius	Serco	Integrated Rating
David Ibbs	Serco	Integrated Rating
Stephen Boddy	Serco	Integrated Rating
Lincoln Hillier	Serco	Trainee Integrated Rating
Jordan Rogers	Serco	Trainee Integrated Rating
Darcy Chalker	Serco	Chief Steward
Amanda Allwood	Serco	Steward
Trudi Gallagher	Serco	Steward
Maja Veit	Serco	Steward
Tracey Lunson	Serco	Steward
Tim Scott	Serco	Chief Cook
Anne-Marie Bensley	Serco	Cook
Bret Brooker	Serco	Cook
Reece Wheldale	Serco	Cook

Table 2: Abbreviations of participating institutes

Abbreviation	Institute
AAD	Australian Antarctic Division
AAPP	Australian Antarctic Partnership Program
ACEAS	Australian Centre for Excellence in Antarctic Science
ANU	Australian National University
CSIRO	Commonwealth Scientific and Industrial Research Organisation
CSU	Colorado State University
CU-Boulder	University of Colorado, Boulder
GA	Geoscience Australia
JCU	James Cook University
Mines	Colorado School of Mines
QUT	Queensland University of Technology
SAEF	Securing Antarctica's Environmental Future
U of U	University of Utah
UNSW	University of New South Wales
UoA	University of Adelaide
UQ	University of Queensland
UTAS	University of Tasmania

4. Science overview and objectives

4.1 Australian Antarctic Division (AAD) – Science Overview and Objectives

The main aim of AAD Science on the DMV was to describe the metazoan biodiversity between Hobart to Antarctica and in the Denman region, both in surface waters as well as throughout the water column, by collecting and filtering small volumes of seawater (5 L) either from the uncontaminated seawater line (surface) or from CTD casts (multiple depths) and analysing the environmental DNA (eDNA) contained in these samples. Comparing the eDNA biodiversity data to physical and chemical ocean variables will allow us to identify drivers of regional biodiversity. To assess whether autonomous eDNA sampling could provide comparable data to manual filtration, we tested two state-of-the-art autonomous eDNA samplers loaned to us by the Monterey Bay Aquarium Research Institute (MBARI) throughout the voyage. Through collaboration with IMAS scientist Dr Linda Armbricht, we also investigated the biodiversity of the past by collecting sedimentary ancient DNA (sedaDNA) samples from kasten cores and multicores, to understand how the local ecosystem has responded to changing climates in the past. Combining past (sedaDNA) and present (eDNA) biodiversity data will allow us to understand how the current ecosystem may respond to future climate change.

Specifically, we investigate the following questions:

- i) What is the animal biodiversity of the Denman Glacier region in surface waters and throughout the water column, and what physical and chemical ocean variables are shaping the observed diversity?
- ii) What is the animal biodiversity between Hobart and the survey area, how does it compare to eDNA data collected on past voyages, what are the drivers of biodiversity and can autonomous eDNA sampling provide comparable data to manual filtration?
- iii) How did the biodiversity change over the past glacial and interglacial periods, and how does it compare to current biodiversity?

4. Science overview and objectives

4.2 Australian Antarctic Program Partnership (AAPP) – Science Overview and Objectives

The Australian Antarctic Territory has contributed as much as one quarter of the total recent Antarctic ice-mass loss. Here, the Denman Glacier, which holds a potential sea level rise of 1.5 m, is one of the fastest retreating glaciers. However, the causes behind these changes remain a mystery. This project will carry out a systematic hydrographic and atmospheric survey to determine: 1) the ocean's role behind the current retreat, 2) feedbacks from environmental change to ocean circulation, 3) its ability to exchange CO₂ with the atmosphere and the marine biota, and 4) role of biological emissions on cloud and aerosol formation. The project will inform the susceptibility of the East Antarctic Ice Sheet to a warming climate, and contributes to providing decision makers in government, nationally and internationally, with accurate, timely and integrated observations of the earth system to empower assessments of, and responses to, the risks posed by climate variability and change.

The main AAPP objectives of the project are:

1. To quantify the ocean heat flux towards the Denman Glacier grounding line.

Ocean temperature, salinity, volume, and current velocity measurements will be used to quantify the transport of ocean heat flux into the Denman ice tongue cavity, and towards the deep grounding line. New bathymetry measurements from the continental slope and towards the glacier tongue will inform us of Circumpolar Deep Water (CDW) pathways from the continental slope to the Denman cavity. Together these measurements will inform us of the susceptibility of the glacier to rapid melting. Moorings within the deep trough adjacent to the Denman ice tongue will provide the first information to understand the processes and temporal variability in ocean heat transport towards the glacier for, at least, a full seasonal cycle. Ice-capable Argo floats will inform us about the spatial variability of water masses and of ocean heat content within the continental shelf.

2. To map the distribution of inorganic carbon and nutrients and the physical and chemical processes driving them.

The distribution of inorganic carbon and nutrients will be combined with information on water mass properties and circulation to infer sinks and sources of trace elements and assess the impact on local and remote marine environments, including Vulnerable Marine Ecosystems. A combination of underway seawater, CTD (Conductivity, Temperature, Depth), and net sampling will be used to quantify zooplankton composition, and ship-based environmental manipulation experiments will be used to investigate the sensitivity of the zooplankton to changes in environmental conditions.

3. Identify the source water masses driving basal melt under the Denman Glacier tongue, and assess the glacier's vulnerability to climate change forcing.

Trace metals (e.g., Al, Mn) and their isotopes (with ACEAS) and oxygen isotopes will be used to (i) determine the water mass driving basal melt, (ii) distinguish sources of glacier freshwater (i.e. discharged glacial freshwater and basal glacial meltwater), (iii) give accurate estimates of basal melt rates, and (iv) track glacial meltwater distribution within the continental shelf. The meltwater spatial distribution will inform us about its role in the transport of biologically important limiting elements, such as Fe, towards the surface layers, and will provide a

4. Science overview and objectives

benchmark to assess the impacts of increasing glacial freshwater discharge on the primary productivity of the Antarctic shelf.

4. Identify Cross-slope exchange processes.

Temperature, salinity profiles from repeat glider sections across the continental slope will be used to characterise the Antarctic Slope Front, a key player in the cross-slope upwelling of CDW. The glider profiles will also be used to provide geostrophic velocities and calculate heat fluxes across the slope towards the Denman Glacier. The continental slope forms a transition zone that has largely been neglected in biogeochemical studies. Conventional ship-based measurements of water column hydrochemistry across the slope will be compared to the glider's and used to characterise nutrients and carbon in the water masses that are transported between the shelf and the open ocean via the slope.

5. Characterize the cloud, aerosol and precipitation properties of the atmosphere over the Southern Ocean and assess how these properties are influenced by compounds released by marine biota.

We will characterise the complete pathway from biological emissions through aerosols to cloud formation inside the Polar Front during high summer peak biological activity. The pathways and characteristics of aerosols, clouds and precipitation differ substantially from those present further north in the warm Southern Ocean, modulating the surface radiation bias observed over the Southern Ocean at different latitudes. The Denman voyage will sample air directly coming from the continent, allowing closure on the circulation component of these processes, and determining whether biogenic gases and aerosols are still prevalent. We will use the observational insights obtained at these high latitudes to test our understanding of model representations of these processes and develop new ones specifically tailored for the region south of the Polar Front. These observations will also contribute to the ground validation program of the European Space Agency EarthCARE cloud radar / lidar satellite. We will also sample aerosol particles for trace metals such as Fe that may be delivered from the atmosphere and may be a source of this micronutrient for coastal ecosystems.

These objectives will be addressed with an innovative multi-disciplinary approach that combines full-depth oceanographic transects, deep sea gliders transects, tall moorings, novel profiling floats, and modelling efforts; and that integrates ocean physics, biogeochemistry, biology and atmospheric physics and chemistry.

4. Science overview and objectives

4.3 Australian Centre for Excellence in Antarctic Science (ACEAS) – Science Overview and Objectives

ACEAS key objectives for DMV are to answer what is the risk of ice mass loss from key subglacial basins over the next decades to centuries, and what the consequences are for the local oceans and ecosystems. ACEAS through the DMV will:

1. Quantify mass outputs from the Denman Glacier through basal melt (with Denman terrestrial) coupled with measurements and modelling of ocean circulation pathways and variability within the cavity and upstream on the continental shelf;
2. Examine retreat processes and feedbacks: bedrock uplift rates, glacier sliding and linkages with subglacial hydrology, geothermal heat flow and sedimentation for grounding line wedge stabilization, local atmospheric and oceanic forcing;
3. Obtain high-resolution geometry of continental shelf, subglacial basins, sub ice shelf ocean cavities and grounding zone conditions to constrain the models (with Denman terrestrial) including geological mapping, and airborne and ship-based geophysics;
4. Use marine sediment cores recovered from the slope to reconstruct ice sheet state for past climates warmer than present;
5. Determine historical ice sheet volumes and retreat rates through bathymetric mapping, offshore geophysical data and land-based approaches (with Denman terrestrial);
6. Collect remote and in-situ observations (moorings) to evaluate the influence of interannual variability in ice shelf melting and subglacial discharge events on primary productivity and seafloor biodiversity; and
7. Use biogeochemical and seafloor ecosystem mapping as well ship-board bioassays to evaluate the drivers of marine productivity (including nutrient sources, pathway and sinks) in the Denman and Shackleton regions.

4. Science overview and objectives

4.4 Securing Antarctica's Environmental Future (SAEF) – Science Overview and Objectives

Securing Antarctica's Environmental Future (SAEF) aims to forecast environmental change and to deploy effective environmental stewardship in the face of this change. The program draws on the integration of multiple fields, and a combination of quantitative and qualitative approaches, to address these aims, founded on the social-ecological systems approach.

SAEF research during the DMV provides an integrated view of the interactions between the living and non-living environments, delivering fresh insights into cryosphere dynamics, biodiversity processes and change, and the future contributions of the Denman Glacier region to Earth System change and Southern Ocean conservation. The research completed during this expedition will lead to an increased understanding of diversity, connectivity and biogeographic history, and the results will provide important data for conservation, elucidating ice sheet history, and understanding of the forces that have shaped evolution of life in the Southern Ocean.

SAEF key objectives from DMV (approved AASP project #4628) are to improve climate observations and projections and weather forecasts; reduce icesheet uncertainties; provide insight into biodiversity processes and change; assess invasive species pathways and impacts; and develop optimal monitoring methodologies that lead to management decision making. In seeking to achieve these objectives, DMV component of SAEF will [seek] to:

1. Use recent field observations and satellite observations to better understand the dynamical and microphysical processes that deliver precipitation to the Denman Glacier, the adjacent ice shelf and the coastal Southern.
2. Based on targeted modelling experiments and synthesis of observations and paleoclimate records, produce constrained decadal-centennial CMIP6 projections of Antarctic and Southern Ocean climate.
3. Use a combination of offshore bathymetric mapping, imagery, onshore geomorphology, high-precision geochronology and ecological genomics approaches, (in close conjunction with the Denman terrestrial campaign), to reconstruct Antarctic ice sheet history during periods of past rapid environmental changes.
4. Characterise and understand the biogeographic history and current spatio-temporal dynamics of species populations in the Antarctic, their spatial scales of connectivity and pathways of movement, including populations of introduced species, by combining surveys (e.g. benthic trawls, eDNA surveys, imagery), ecological genomics, biodiversity informatics and dispersal modelling approaches, to (i) understand biodiversity trends, (ii) build new ecoregional classifications, and (iii) develop a risk assessment framework for biological invasion.
5. Develop new data science methods to quantify and integrate uncertainty in model inputs (e.g. observational error, differences in resolution), structure (e.g. lack of scientific understanding of the process), and parameters (e.g. measurements of water ocean properties and bathymetry) within and across model outputs, to improve the analysis and interpretation of Antarctic data. The model outputs produced by these methods will facilitate visualisation and improve evidence-based policy made in the presence of uncertainty.

5. Physical Oceanography (AAS 4631)

Team: Laura Herraiz Borreguero, Annie Foppert, Benoit Legresy, Kaihe Yamazaki, Matthis Auger, Ole Rieke, Yuhang Liu

Note: CTD log sheets are published separately on the IMAS database as a part of the 'Supplementary Material'. There will also be a separate data processing report for the work completed by the Physical Oceanography team. This report will contain information on the CTD sensors (calibrations, serial numbers, etc.) and the post-voyage data processing methods employed.

5.1 CTD Deployments

5.1.1 Overall Aims and Hypotheses

During the Denman Marine Voyage, we conducted an extensive series of CTD (Conductivity–Temperature–Depth) deployments to investigate the physical and biogeochemical properties of the ocean in front of Denman Glacier and along the Shackleton Ice Shelf (Figure 3). A total of 105 CTD casts were completed (Table 3), including 69 side-door and 26 moon pool deployments, aimed at characterising the water masses entering and exiting the cavity, which had never been visited before. CTD stations were arranged in tightly spaced lines (~5 km apart) to resolve fine-scale features, guided by the local Rossby radius of deformation. This spatial resolution ensured that hydrographic continuity was captured between stations, allowing us to observe coherent structures such as currents and eddies, which can influence ice shelf melt rates.

Based on the bathymetry in front of Denman Glacier, we completed three east-west transects across the trough in front of the Denman Glacier, one saddle section near the continental shelf break, and two additional transects extending toward the glacier front. To examine the evolution of water masses along the trough, we also conducted a north-south section extending toward open water. West of the Shackleton Ice Shelf, we conducted a long transect along the ice shelf front as well as two west-east cross-sections to investigate ice-ocean interactions and the influence of ice shelf water. Collectively, these observations enabled us to characterise water mass distribution, current pathways and variability in mixing and stratification. In addition to our planned CTD sections, we supported other research groups on board by providing targeted water samples when needed.

5. Physical Oceanography (AAS 4631)

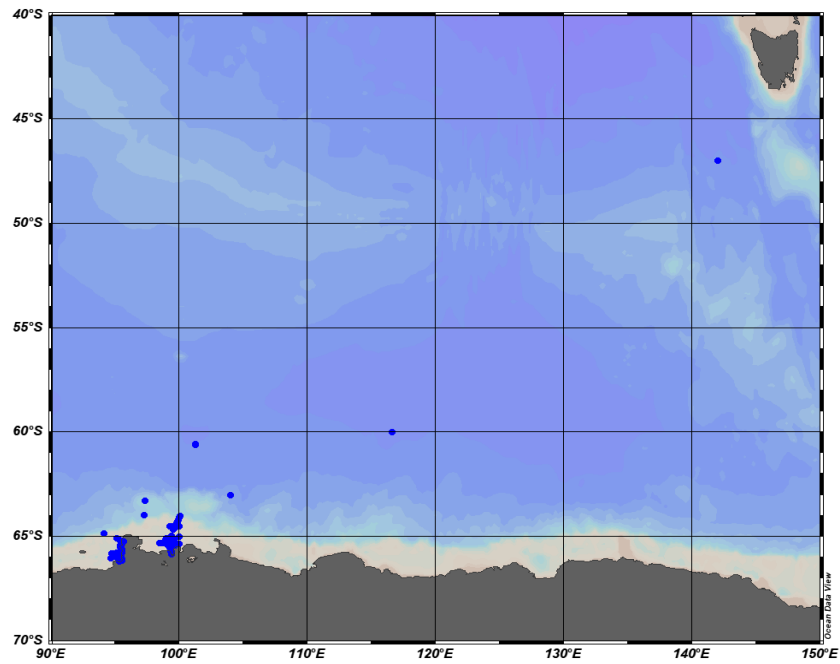


Figure 3. Overview map of the study area during Denman Marine Voyage 2025. The blue dots indicate the locations of the CTD.

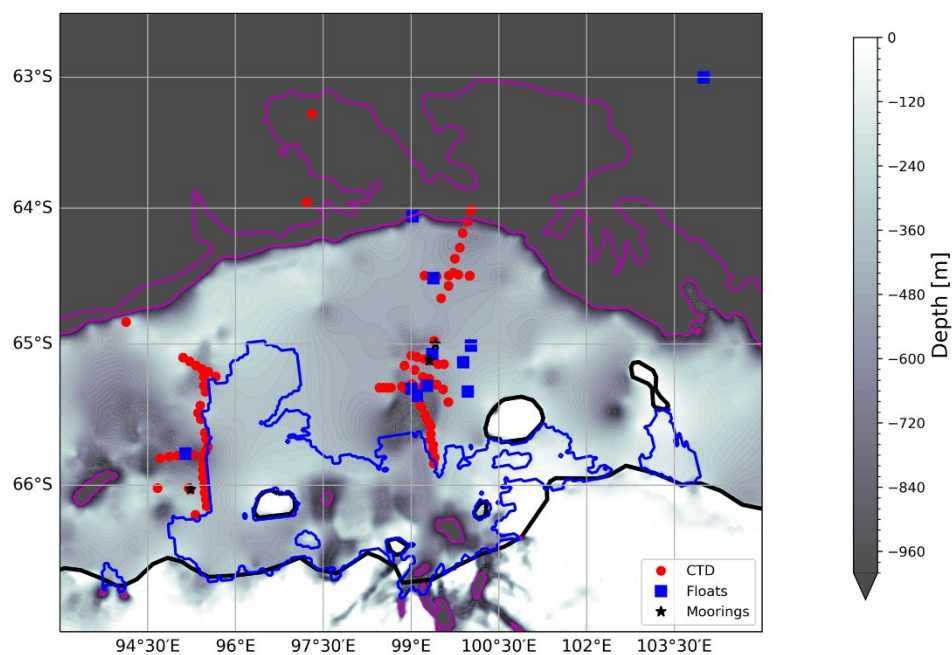


Figure 4. Enlarged map focussing on the continental shelf, showing the locations of Argo floats, CTD stations, and moorings. The Antarctic coastline is represented by a dark black line, the ice sheet extent by blue lines, and the 1000 m and 2000 m isobaths by purple lines.

5.1.2 CTD Deployments and Sample Collection Methods

The CTD system is mounted on a circular metal rosette frame equipped with up to 36 Niskin bottles, each with a 12 L capacity for water sampling. In addition to water collection, the rosette is equipped with multiple sensors (sensor details to be published separately in the data processing report), such as Acoustic Doppler Current Profilers (ADCPs) to measure current velocity, an oxygen sensor for dissolved oxygen, and fluorescence sensors to detect chlorophyll-a fluorescence. These instruments provide real-time insights into water column structure and biogeochemistry.

While deployments were traditionally conducted from the side door of the vessel (Figure 5), we also had a backup plan: the moon pool (Figure 6). This alternative was used in bad weather and heavy sea ice conditions. The moon pool is a 4 m x 4 m opening through the hull, featuring two hydraulic upward-opening doors at the bottom to prevent ice ingestion and two downward-opening doors at Deck 4 level. This setup allows the CTD to be lowered through the moon pool using the CTD winch, even in challenging environments. There were two CTD rosettes on board: “BOB” and “PAT”. “BOB” was our primary CTD rosette. Each rosette had its own set of Niskin bottles and sensors. At the beginning of the voyage, CTD deployments were primarily conducted using “BOB” via side deployment, while moonpool deployments used “PAT”. However, due to heavy sea ice later in the voyage, we increasingly relied on moonpool deployments for efficiency. As a result, we swapped the rosettes at CTD cast 72, and from that point onward, all moonpool deployments were conducted using “BOB”.

The CTD rosette was initially lowered to 20 m to start pump systems, then brought back to the surface to begin the downcast. The top 15 m were lost during moon pool deployments. The lowering speed was reduced when approaching the seafloor, with the CTD typically stopped 5-10 m above the bottom, depending on weather conditions, sea ice, ship movement, and bottom topography. Individual Niskin bottles were fired during the upcast and the water sampling was conducted. Clean glass bottles with screw lids were flushed three times with sea water from the Niskin bottles, before fully filling the bottles bubble-free in overflow without air reservoir. The water sampling started with the deepest and proceeded to the shallowest depth. During water sampling, we filled out the log sheets to verify that the correct depths were sampled and properly labelled. We also measured the temperature of the dissolved oxygen (DO) and recorded it in the log sheets, which is used by the Hydrochemistry team for DO calibration.

5. Physical Oceanography (AAS 4631)



Figure 5. The CTD rosette is deployed from an extendable arm through the side of the ship.

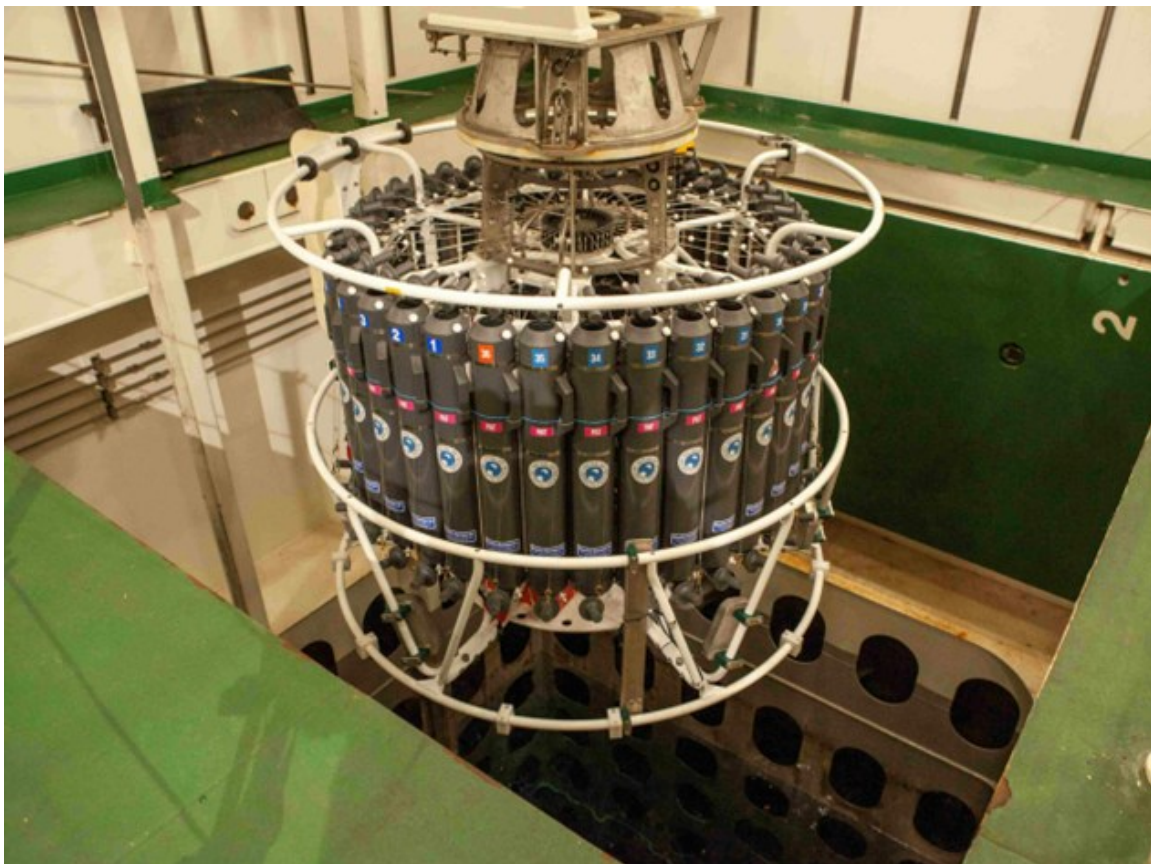


Figure 6. The CTD rosette is lowered through the moon pool inside the ship when sea ice or weather conditions do not allow deployment over the side.

5. Physical Oceanography (AAS 4631)

Nuyina DMV - CTD-36 sampling sheet				Voyage : <i>NUYINA-05-V3</i> 2025 V3		Station no.: <i>015</i>																			
				Cruise : <i>Denman Marine</i>		Section/region: <i>Denman Front</i>																			
				Date (UTC) : <i>17/03/2025</i>		Sta <i>17. (w.TMR)</i>																			
				Date (dd/m/yy - hh:mm)																					
approx. volume (ml) (including rinse)				750	200	750	750	750	100	40	500	250	10500	10500	100	1500	1500	10000	1500	2500	2500	700	1000	700	
N.E. Start at bottom (i.e. at no. 1, the deepest)	Row No.	Stk No.	Nominal Pressure	D.O.	chl a	D.L.C	ALK	Salinity	chl a	chl b	chl c	chl d	chl e	chl f	chl g	chl h	chl i	chl j	chl k	chl l	chl m	chl n	chl o	chl p	chl q
Shallowest	36		<i>10</i>																						
	35		<i>10</i>																						
	34		<i>10</i>	✓				✓	✓		✓								✓	✓					✓
	33		<i>30</i>																						
	32		<i>30</i>																						
	31		<i>30</i>	✓				✓	✓		✓								✓	✓					✓
	30		<i>50</i>																						
	29		<i>50</i>																						
	28		<i>50</i>	✓				✓	✓		✓								✓	✓					✓
	27		<i>85</i>																						
	26		<i>85</i>																						
	25		<i>85</i>	✓				✓	✓		✓								✓	✓					✓
	24	<i>MID</i>	<i>190</i>																						
	23	<i>TOP</i>	<i>190</i>																						
	22	<i>TOP</i>	<i>190</i>	✓				✓	✓		✓								✓	✓					✓
	21		<i>230</i>																						
	20		<i>230</i>																						
	19		<i>230</i>	✓				✓	✓		✓								✓	✓					✓
	18		<i>330</i>																						
	17		<i>330</i>																						
	16		<i>330</i>	✓				✓	✓		✓								✓	✓					✓
	15		<i>440</i>																						
	14		<i>440</i>																						
	13		<i>440</i>	✓				✓	✓		✓								✓	✓					✓
	12		<i>550</i>																						
	11		<i>550</i>																						
	10		<i>550</i>	✓				✓	✓		✓														
	9		<i>700</i>																						
	8		<i>700</i>																						
	7		<i>700</i>	✓				✓	✓		✓								✓	✓					✓
	6		<i>800</i>																						
	5		<i>800</i>																						
	4		<i>800</i>	✓				✓	✓		✓														
	3		<i>850</i>																						
	2		<i>850</i>																						
Deepest	1		<i>850</i>	✓				✓	✓		✓								✓	✓					✓

Comments :

Figure 7: Example of a CTD sampling sheet (CTD36) with various parameters collected. Approximate volumes (mL) collected for each sample type is shown as one of the top rows.

5.1.3 Preliminary results

Most stations were located on the continental shelf, with typical cast depths shallower than 1000 m. Preliminary results reveal several notable features:

- Modified Circumpolar Deep Water (mCDW) was observed in the deepest parts of the Denman trough (Figure 8).

5. Physical Oceanography (AAS 4631)

- In front of Denman Glacier, remnants of summer surface water led to a warm subsurface layer (Figure 8).
- A deep fluorescence maximum was observed around 300 m, indicating biological activity at depth in the front of the Denman Glacier (Figure 8).
- We observed the influence of icebergs on the surrounding water masses, and the influence of ice shelf water was observed along the Denman side of the shelf (Figure 9).

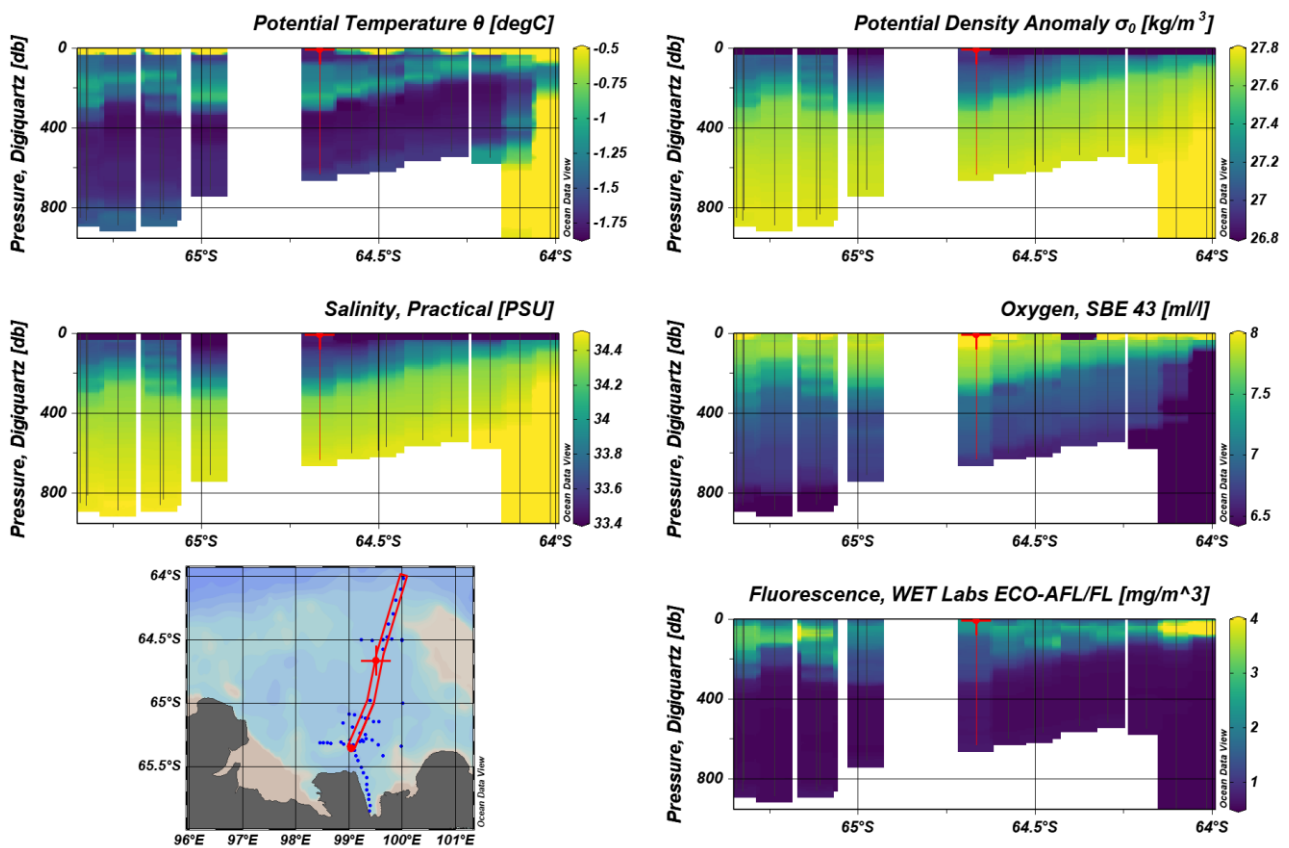


Figure 8. Potential temperature, potential density anomaly, salinity, oxygen and fluorescence along the north-south section of the Denman trough.

5. Physical Oceanography (AAS 4631)

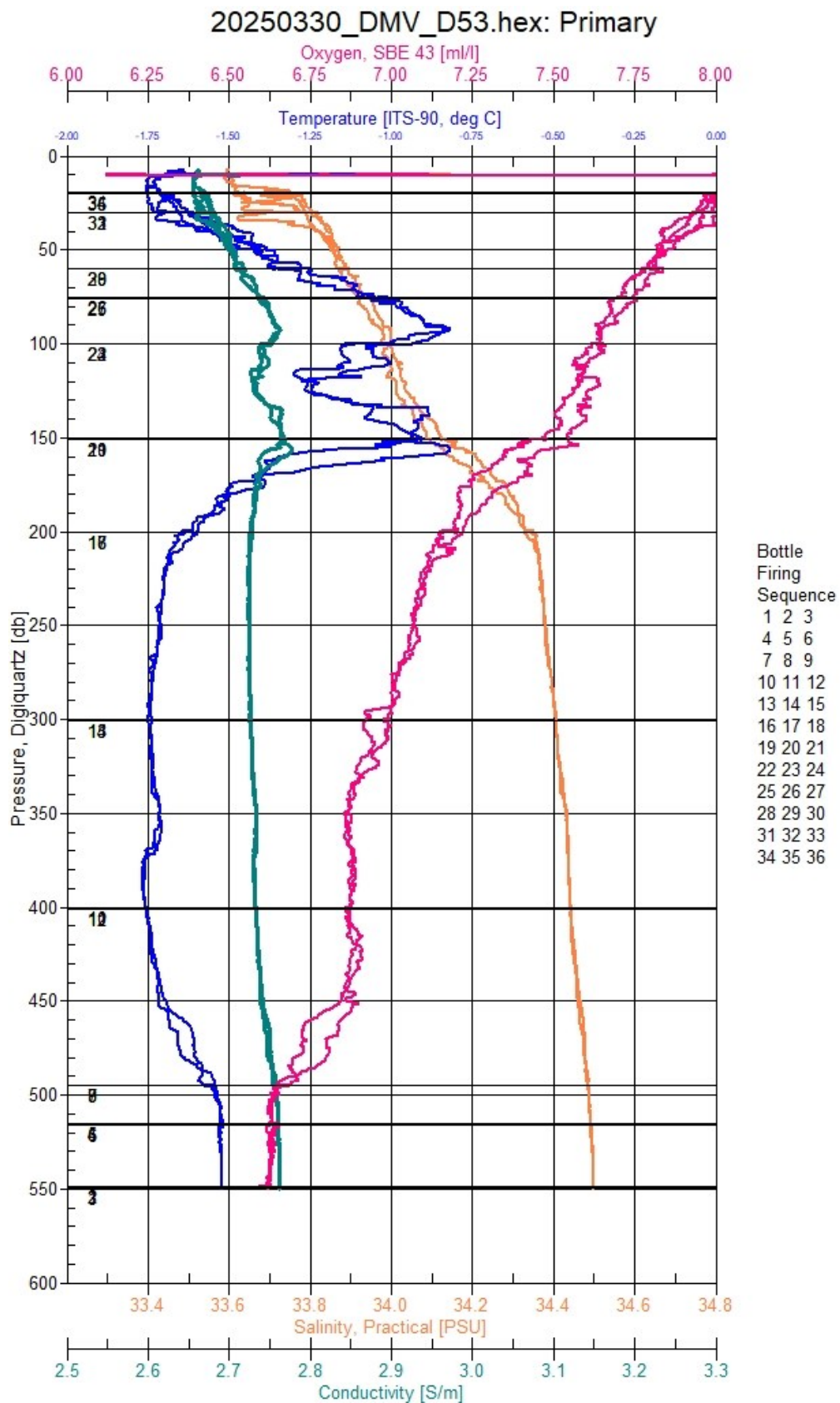


Figure 9. Depth profile from CTD cast 53 (Process station), illustrating the influence of the iceberg on the local water column (100 m - 150 m).

5. Physical Oceanography (AAS 4631)

Table 3. Meta-data of all CTD casts from Denman Marine Voyage.

Cast	Latitude (DD)	Longitude (DD)	Date & Time [UTC]	Deployment Method	CTD Rosette	Depth [m]	Note
1	-46.9992	142.0034	2025-03-02T09:47:26+00:00	Side Deployment	BOB	3503.64	
2	-59.993	116.5736	2025-03-06T23:20:13+00:00	Side Deployment	BOB	4525.97	
3	-63	104.0012	2025-03-08T13:00:00+00:00	Side Deployment	BOB	3610.48	
4	-63.2831	97.3054	2025-03-12T16:15:52+00:00	Side Deployment	BOB	1648.81	
5	-65.3036	98.4583	2025-03-15T04:16:44+00:00	Side Deployment	BOB	587.09	
6	-65.3136	98.5232	2025-03-15T07:37:22+00:00	Side Deployment	BOB	621.6	
7	-65.3134	98.5899	2025-03-15T11:10:04+00:00	Side Deployment	BOB	636.57	
8	-65.3139	98.6539	2025-03-15T13:50:55+00:00	Side Deployment	BOB	651.97	pumps frozen
9	-65.3139	98.6539	2025-03-15T17:26:52+00:00	Side Deployment	BOB	652.25	
10	-65.3041	98.8436	2025-03-15T20:59:59+00:00	Side Deployment	BOB	755.45	
11	-65.3211	98.9014	2025-03-16T00:56:06+00:00	Side Deployment	BOB	778.4	
12	-65.2871	99.0096	2025-03-16T06:14:01+00:00	Side Deployment	BOB	801.54	
13	-65.3231	99.0038	2025-03-16T12:02:17+00:00	Side Deployment	BOB	804.84	
14	-65.3434	99.0328	2025-03-16T15:30:42+00:00	Side Deployment	BOB	837.84	
15	-65.3254	99.0804	2025-03-16T23:48:06+00:00	Side Deployment	BOB	849.19	
16	-65.3713	99.0989	2025-03-17T03:54:30+00:00	Side Deployment	BOB	771.28	
17	-65.4152	99.1336	2025-03-17T06:13:56+00:00	Side Deployment	BOB	723.1	
18	-65.4511	99.1696	2025-03-17T08:16:12+00:00	Side Deployment	BOB	716.03	
19	-65.505	99.2378	2025-03-17T10:46:44+00:00	Side Deployment	BOB	676.95	
20	-65.5462	99.2754	2025-03-17T14:14:49+00:00	Side Deployment	BOB	594.05	
21	-65.5867	99.3362	2025-03-17T22:18:11+00:00	Side Deployment	BOB	562.19	
22	-65.6409	99.3404	2025-03-18T01:41:58+00:00	Side Deployment	BOB	558.36	
23	-65.6835	99.3329	2025-03-18T03:50:27+00:00	Side Deployment	BOB	617.6	
24	-65.72	99.3751	2025-03-18T05:57:31+00:00	Side Deployment	BOB	695.18	
25	-65.7566	99.3698	2025-03-18T07:51:31+00:00	Side Deployment	BOB	735.81	
26	-65.8065	99.4030	2025-03-18T11:17:16+00:00	Side Deployment	BOB	638.43	
27	-65.8483	99.3858	2025-03-18T13:43:32+00:00	Side Deployment	BOB	833.69	
28	-64.7803	99.9043	2025-03-20T09:26:55+00:00	Moon pool	PAT	556.01	No data, unsuccessful test

5. Physical Oceanography (AAS 4631)

							deployment to 11 m.
29	-65.3264	99.5439	2025-03-22T13:18:34+00:00	Side Deployment	BOB	620.9	
30	-65.2486	99.3112	2025-03-22T19:08:10+00:00	Side Deployment	BOB	901.79	
31	-65.291	99.4325	2025-03-22T22:52:04+00:00	Side Deployment	BOB	793.35	No bottle, misfire
32	-65.291	99.4325	2025-03-23T00:06:13+00:00	Side Deployment	BOB	793.15	
33	-65.2355	99.1999	2025-03-23T06:37:53+00:00	Side Deployment	BOB	876.93	
34	-65.1852	99.0618	2025-03-23T10:44:20+00:00	Side Deployment	BOB	754.65	
35	-65.1551	98.8839	2025-03-23T14:03:47+00:00	Side Deployment	BOB	679.13	
36	-65.0831	99.0035	2025-03-23T16:32:21+00:00	Side Deployment	BOB	-999	
37	-65.092	99.1012	2025-03-23T19:01:09+00:00	Side Deployment	BOB	685	
38	-65.1071	99.2269	2025-03-24T06:20:10+00:00	Side Deployment	BOB	823.21	
39	-65.1168	99.3618	2025-03-24T09:00:00+00:00	Side Deployment	BOB	850.44	
40	-65.144	99.4629	2025-03-24T19:52:52+00:00	Side Deployment	BOB	761.17	
41	-65.1451	99.5634	2025-03-24T22:16:28+00:00	Side Deployment	BOB	681.13	
42	-64.9988	100.0073	2025-03-25T07:51:45+00:00	Side Deployment	BOB	505.73	
43	-65.3375	99.9811	2025-03-25T20:30:18+00:00	Side Deployment	BOB	436.13	
44	-65.4158	99.6358	2025-03-26T00:02:52+00:00	Side Deployment	BOB	463.6	
45	-65.289	99.2407	2025-03-26T06:41:48+00:00	Side Deployment	BOB	999	
46	-65.3002	99.2018	2025-03-26T16:34:39+00:00	Side Deployment	BOB	856.3	
47	-65.2986	99.2732	2025-03-26T19:15:17+00:00	Side Deployment	BOB	876.19	
48	-65.281	99.3255	2025-03-26T21:32:19+00:00	Side Deployment	BOB	885.43	
49	-64.9761	99.3953	2025-03-27T18:45:49+00:00	Side Deployment	BOB	698.41	
50	-65.1179	99.3084	2025-03-27T23:42:44+00:00	Side Deployment	BOB	858.84	
51	-64.5001	99.9997	2025-03-29T19:11:35+00:00	Side Deployment	BOB	546.2	
52	-64.502	99.9987	2025-03-30T14:39:13+00:00	Side Deployment	BOB	544.43	
53	-64.5021	99.9983	2025-03-30T15:00:09+00:00	Moon pool	PAT	544.15	
54	-64.0146	100.0204	2025-03-31T14:57:00+00:00	Side Deployment	BOB	1462.43	
55	-64.1009	99.9641	2025-03-31T18:17:05+00:00	Side Deployment	BOB	1083.37	
56	-64.1859	99.8776	2025-03-31T21:16:22+00:00	Side Deployment	BOB	595.04	
57	-64.2943	99.8283	2025-03-31T23:49:34+00:00	Side Deployment	BOB	514.71	
58	-64.3744	99.7449	2025-04-01T02:59:58+00:00	Side Deployment	BOB	524.11	

5. Physical Oceanography (AAS 4631)

59	-64.4787	99.7154	2025-04-01T06:22:43+00:00	Side Deployment	BOB	559.97	
60	-64.5755	99.6369	2025-04-01T09:00:22+00:00	Side Deployment	BOB	598.15	
61	-64.6653	99.5142	2025-04-01T12:13:34+00:00	Side Deployment	BOB	629.1	
62	-64.4947	99.8066	2025-04-01T16:31:32+00:00	Moon pool	PAT	563.86	
63	-64.5006	99.6418	2025-04-01T19:06:18+00:00	Side Deployment	BOB	580.89	
64	-64.5063	99.4320	2025-04-01T21:51:52+00:00	Moon pool	PAT	598.8	
65	-64.5	99.2294	2025-04-02T00:49:05+00:00	Side Deployment	BOB	571.52	
66	-64.8396	94.1286	2025-04-04T19:28:39+00:00	Side Deployment	BOB	290.2	
67	-65.2325	95.6596	2025-04-05T07:15:05+00:00	Side Deployment	BOB	507.23	
68	-65.1979	95.5323	2025-04-05T11:46:08+00:00	Side Deployment	BOB	550.71	
69	-65.1797	95.4251	2025-04-05T13:27:36+00:00	Side Deployment	BOB	556.17	
70	-65.156	95.3211	2025-04-05T16:15:40+00:00	Side Deployment	BOB	614.99	
71	-65.1236	95.2167	2025-04-05T19:13:18+00:00	Moon pool	PAT	581.35	
72	-65.0976	95.1007	2025-04-05T22:01:50+00:00	Moon pool	PAT	566.92	
73	-65.8129	94.7108	2025-04-07T21:20:04+00:00	Moon pool	BOB	748.5	Bob Moonpool
74	-65.801	94.8687	2025-04-07T23:54:37+00:00	Moon pool	BOB	748.62	
75	-65.795	95.0116	2025-04-08T04:21:03+00:00	Moon pool	BOB	724.55	
76	-65.783	95.1358	2025-04-08T09:15:17+00:00	Moon pool		862.19	Backfilled entry after it happened again on April 13th. Lost comms with fish for several minutes. Resolved with deckbox and SeaSave restart.
77	-65.7908	95.2628	2025-04-08T12:18:43+00:00	Moon pool	BOB	936.39	
78	-66.021	94.6659	2025-04-08T19:19:20+00:00	Moon pool	BOB	495.95	
79	-66.0281	95.2196	2025-04-09T21:15:03+00:00	Moon pool	BOB	691.92	
80	-66.205	95.3135	2025-04-10T13:26:19+00:00	Moon pool	BOB	395.66	
81	-66.0217	95.1995	2025-04-11T19:49:31+00:00	Moon pool	BOB	755.54	
82	-66.0218	95.1997	2025-04-12T05:35:09+00:00	Moon pool	BOB	754.97	

5. Physical Oceanography (AAS 4631)

83	-66.1465	95.5043	2025-04-12T09:37:32+00:00	Moon pool	BOB	286	
84	-66.0969	95.4907	2025-04-12T11:39:00+00:00	Moon pool	BOB	248.13	
85	-66.0511	95.4695	2025-04-12T13:27:09+00:00	Moon pool	BOB	696.4	
86	-65.9989	95.4579	2025-04-12T15:21:02+00:00	Moon pool	BOB	644.74	
87	-65.9454	95.4415	2025-04-12T17:30:41+00:00	Moon pool	BOB	428.09	
88	-65.8957	95.4389	2025-04-12T19:55:54+00:00	Moon pool	BOB	711.09	
89	-65.8592	95.4438	2025-04-12T21:57:14+00:00	Moon pool	BOB	533.03	
90	-65.8235	95.4481	2025-04-13T01:45:39+00:00	Moon pool	BOB	1051.57	
91	-65.7911	95.4462	2025-04-13T04:47:19+00:00	Moon pool	BOB	1289.64	
92	-65.7602	95.4877	2025-04-13T08:50:37+00:00	Moon pool	BOB	813.91	
93	-65.733	95.5251	2025-04-13T11:42:48+00:00	Moon pool	BOB	839.27	
94	-65.6774	95.4967	2025-04-13T13:59:53+00:00	Moon pool	BOB	426.81	
95	-65.6327	95.4767	2025-04-13T16:08:23+00:00	Moon pool	BOB	585.08	
96	-65.5381	95.4077	2025-04-13T19:00:01+00:00	Moon pool	BOB	488.34	
97	-65.4923	95.3555	2025-04-13T21:12:19+00:00	Moon pool	BOB	223.55	
98	-65.4917	95.3702	2025-04-17T07:00:30+00:00	Moon pool	BOB	186.12	
99	-65.4404	95.3974	2025-04-17T09:17:00+00:00	Moon pool	BOB	270.23	
100	-65.3421	95.4825	2025-04-17T12:47:15+00:00	Moon pool	BOB	999	
101	-65.2998	95.4542	2025-04-17T14:59:53+00:00	Moon pool	BOB	488.17	
102	-65.2363	95.4531	2025-04-17T17:58:53+00:00	Moon pool	BOB	536.09	
103	-63.9542	97.2165	2025-04-20T19:11:24+00:00	Side Deployment	PAT	2165.26	
104	-60.5869	101.2188	2025-04-24T03:51:27+00:00	Side Deployment	PAT	4477.59	
105	-60.5829	101.2168	2025-04-24T10:03:24+00:00	Side Deployment	PAT	4476.02	

5.2 Moorings

5.2.1 Overview

On the Denman Marine Voyage three moorings were deployed, two on the eastern side of the Denman Glacier in the deep canyon (M2, M3) and one on the western side of the Shackleton Ice Shelf in the Shackleton Polynya (M1; Table 4, Figure 10).

Table 4. Moorings position, depth and release codes summary.

M1: BGC in Shackleton Polynya

	Activation 1	Activation 2	Disable	Release
1 st release	670030	670055	670076	645377
2 nd release	667632	667657	667674	645331
Latitude	-66° 01.77' S		Longitude	95° 13.66' E
Deployment Date (UTC)	10/04/2025		Time (UTC)	5:20
Deployment depth (m)	647			

M2: Denman trough

	Activation 1	Activation 2	Disable	Release
1 st release	660175	660217	660234	635270
2 nd release	622201	622222	622247	632344
Latitude	-65° 00.00' S		Longitude	99° 24.82' E
Deployment Date (UTC)	29/03/2025		Time (UTC)	1:35
Deployment depth (m)	729			

M3: Denman trough

	Activation 1	Activation 2	Disable	Release
1 st release	670124	670141	670162	645456
2 nd release	622106	622125	622140	632321
Latitude	-65° 07.05' S		Longitude	99° 18.91' E
Deployment Date (UTC)	28/03/2025		Time (UTC)	10:06
Deployment depth (m)	860			

5. Physical Oceanography (AAS 4631)

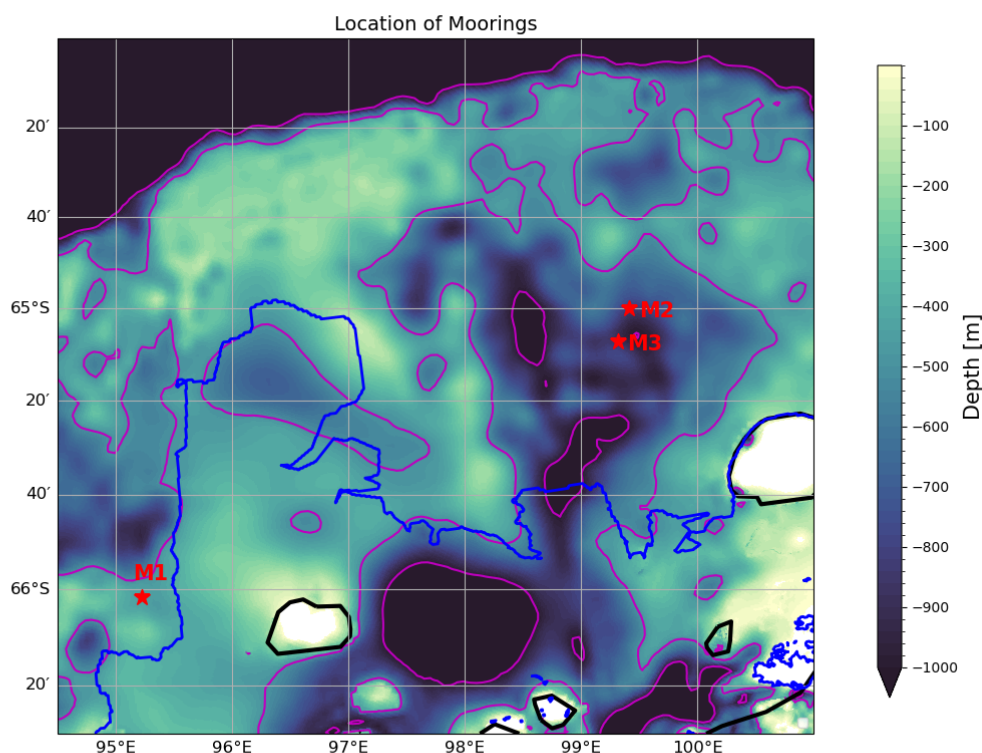


Figure 10: Location of moorings M1, M2, and M3. The colourmap shows the bathymetry of the region, from Charrassin et al. (2025).

The Denman canyon provides a deep connection between the continental shelf break and the Denman Glacier and has previously been found to occupy warm modified circumpolar deep water (mCDW) (van Wijk et al., 2022) in a relatively thin bottom layer, providing a potential inflow pathway for warm water to the ice shelf front. A main target of the moorings is to investigate the temporal variability of this warm water layer. The moorings M2 and M3 are placed in the centre of the trough within 8 nm from each other and have the same suite of instruments attached (Table 5, Table 6, Table 7). Several CTDs and current meters are installed throughout the length of the mooring to capture the variability of the circulation and water properties in the water column. A CTD attached to the acoustic releases right above the anchor at 20 m depth, and a current meter right above ensure a good coverage of the mCDW-layer that covers the bottom of the water column. The height of the mooring (300 m) is a compromise between getting a good coverage of the water column and the threat of getting hit by icebergs that can reach drafts of up to 300 m.

The Shackleton Polynya has previously been found to be an area of strong sea ice formation, dense water production and high bioproductivity. The aim of mooring M1 in this area is to monitor all these parameters, and how they are interconnected. CTD and current metres are placed throughout the water column to capture the variability of the water properties and currents. A trace metal sampler is installed at the top of the mooring, and a sediment trap at mid-depth.

5. Physical Oceanography (AAS 4631)

5.2.2 Deployment

All instruments were calibrated, tested and turned on before the voyage. The acoustic releases were tested onboard the ship before deployment.

Due to heavy sea ice conditions, a stream-out (headfirst) of the first mooring (M3) was aborted. Instead, all moorings were deployed anchor first. The acoustic releases were tested after deployment and connection was established successfully.

All moorings are scheduled to be picked up by the RSV *Nuyina* during resupply voyages during the next summer season 2025/2026. However, should this not be possible due to sea ice conditions or other circumstances, a later pickup is possible. The batteries of the acoustic releases will last for five years.

Table 5. Instrument configuration for mooring M1, deployed in 629 m depth.

Depth above sea floor (m)	Instrument Type	Serial Number
580	SBE37SMP CTD	9176
570	Trace metal sampler	
495	Aquadopp Current meter	9890
495	SBE37SMP-ODO CTD	26388
430	SBE37SMP CTD	9179
365	SBE37SMP CTD	9882
300	SBE37SMP CTD	9889
235	SBE37SMP CTD	9909
170	McLane Sediment Trap 13 cups	9911
170	SBE37SMP CTD	22652
100	LR75 ADCP	14397
30	Aquadopp Current meter	9841
25	SBE37SMP-ODO CTD	26407
20	SBE39 TP	8664
20	ACR Releases	25692 & 25690

Table 6. Instrument configuration for mooring M2, deployed in 856 m depth.

Depth above sea floor (m)	Instrument Type	Serial Number
300	SBE37SMP CTD	9908
225	SBE37SMP CTD	9911
160	SBE37SMP CTD	15021
100	LR75 ADCP	16375
40	Aquadopp Current meter	9496
35	SBE37SMP CTD	15131
20	SBE39 TP	4891
20	ACR Releases	22172 & 25599

5. Physical Oceanography (AAS 4631)

Table 7. Instrument configuration for mooring M3, deployed in 733 m depth.

Depth above sea floor (m)	Instrument Type	Serial Number
300	SBE37SMP CTD	15134
225	SBE37SMP CTD	15884
160	SBE37SMP CTD	20272
100	LR75 ADCP	16374
40	Aquadopp Current meter	9894
35	SBE37SMP CTD	22595
20	SBE39 TP	6272
20	ACR Releases	29298 & 29301

5. Physical Oceanography (AAS 4631)

5.3 Argo floats

A total of 13 Argo floats were deployed during the voyage (Table 8): three BGC-Argo floats in the open Southern Ocean, two EM-Apex floats in the Antarctic Slope Current (including one equipped with a microstructure sensor), and eight Ice-Argo floats on the continental shelf (seven near the Denman Glacier and one in the Shackleton Polynya that was equipped with a dissolved oxygen sensor). The floats will provide invaluable information about ocean variability and circulation by regularly measuring ocean properties throughout the water column for several years. Data is transmitted ashore via satellite communications. The Argo program on board the Denman Marine Voyage represents an international collaboration and Australian support to the international Argo program.

Table 8. Argo deployments

Float Type	Float ID#	CTD on deploy. (CTD#)	Deployment time (UTC)	Deployment latitude (DD)	Deployment longitude (DD)	Seafloor depth (m)	Comments
BGC Argo	P53865 - 24AU001	no	05/03/2025 00:34	-54.31	128.49	4321.7	
BGC Argo	P53865 - 24AU002	yes, #002	07/03/2025 02:30	-59.99	116.57	4525.7	BGC sampling on CTD
BGC Argo	P53879 - 24AU001	yes, #003	08/03/2025 15:52	-63.00	104.00	3607.1	BGC JUMBO; bio sampling on CTD
EM-APEX	10834	no	13/03/2025 20:54	-64.0593	99.0168	1095	Equipped with microstructure
ALAMO	9450	yes, #013	16/03/2025 11:59	-65.3231	99.0038	814	Lowered by hand over side
ARVOR	24DE022	yes, #016	17/03/2025 05:05	-65.3713	99.099	773	
ARVOR	Al2600 - 24IT001	no	25/03/2025 10:41	-65.1417	99.8922	504	Deployed not far from cast #042
APEX	10398	yes, #043	25/03/2025 21:36	-65.3445	99.9667	474	Float remained horizontal after deployment; snow was heavy so float shortly disappeared
APEX	10754	no	26/03/2025 10:14	-65.304	99.2665	867	Deployed not far from cast #045; float remained horizontal at surface post-deployment and slushy ice surrounded float until out of sight
ALAMO	9451	no	28/03/2025 11:29	-65.0667	99.3573	809	Lowered by hand over side

5. Physical Oceanography (AAS 4631)

EM-APEX	10833	yes, #054	31/03/2025 16:49	-64.0145	100.0205	1471	Deployed with crane from starboard side
ARVOR	AI2600 - 24DE023	no	01/04/2025 23:24	-64.5143	99.377	602	Deployed with A-frame into puddle surrounded by young ice, ~26 mins after removing magnet (between CTDs #064-065)
APEX	10342	yes, #076	08/04/2025 10:40	-65.783	95.1358	871	Deployed with A-frame

EM-Apex float #10833 was faulty and it was immediately recognised by partners on shore that it was not relaying any oceanographic data. The float was put into recovery mode and its location was tracked with regularly updated GPS locations (that were integrated into DiRT). Fortuitously, the float's location aligned with the ship's track and the crew were able to recover the float via fast rescue boat. The float has been returned to Hobart for a diagnostic assessment and potential future deployment.

5.4 Glider

The primary question addressed by the Seaglider is how cross-slope exchange processes allow warm Circumpolar Deep Water inflows in the Denman region. Temperature and salinity profiles from repeat glider sections across the continental slope were intended to characterise the Antarctic Slope Front, a key player in the cross-slope upwelling of CDW. The glider profiles were also intended to be used to provide geostrophic velocities and calculate heat fluxes across the slope towards the Denman Glacier. The continental slope forms a transition zone that has largely been neglected in biogeochemical studies. Conventional ship-based measurements of water column hydrochemistry across the slope can be compared to the glider's and used to characterise nutrients (including Fe) and carbon in the water masses that are transported between the shelf and the open ocean via the slope to constrain the sources and transport mode of Fe from productive to barren waters.

Unfortunately, we encountered a series of issues with the glider that prevented the early deployment of the instrument. Early checks suggested that the below freezing conditions impacted the performance of the cable used to communicate the glider with the computer during sea launch procedure. Self-tests and pre-sea launch tests had to be carried out in the open during the days prior to deployment and the cable may have been affected during these tests. While comms were interrupted at times, the final test was when we were ready to launch the Seaglider and the final command was not read by the glider. Under these conditions, the glider could not be deployed.



Figure 11. Glider on the RSV Nuyina's helideck

5.5 Data Management

All preliminary data will be published through the Australian Antarctic Data Centre (AADC) (<https://data.aad.gov.au/>) following standard AADC procedures, and subject to the moratorium of 2 years.

5.6 References

Charrassin, R., Millan, R., Rignot, E., & Scheinert, M. (2025). Bathymetry of the Antarctic continental shelf and ice shelf cavities from circumpolar gravity anomalies and other data. *Scientific Reports*, 15(1), 1214. <https://doi.org/10.1038/s41598-024-81599-1>

Van Wijk, E. M., Rintoul, S. R., Wallace, L. O., Ribeiro, N., & Herraiz-Borreguero, L. (2022). Vulnerability of Denman Glacier to Ocean Heat Flux Revealed by Profiling Float Observations. *Geophysical Research Letters*, 49(18). <https://doi.org/10.1029/2022GL100460>

6. Hydrochemistry (AAS 4630)

Team: Merinda McMahon, Julie Janssens, Claire Yung, Christina Schmidt

6.1 Executive Summary

6.1.1 Objectives

The Hydrochemistry team, referred to as the HydroBox team on the Denman Marine Voyage (DMV), analysed dissolved oxygen (DO), salinity and macro-nutrients. Macro-nutrients analysed were Silicate (SiO_4^{4-} as Si), Phosphate (PO_4^{3-} as P), Nitrate (NO_3^- as N) plus Nitrite (NO_2^- as N) referred to as NO_x , Nitrite (NO_2^- as N) and Ammonium (NH_4^+ as N).

The HydroBox team provided macro-nutrient measurements in support of 4 of the 8 science packages delivered on the DMV: Physical oceanography, Pelagic sampling, Trace metals and isotopes, and Sediments. Macro-nutrients, DO and salinity samples were collected and measured from each CTD cast deployment where samples were taken. The team also analysed macro-nutrient samples from underway samples (UWY), trace metal rosette (TMR) casts, pore water from kasten, multi-core sediments and Smith-McIntyre grab (CORE), and phytoplankton incubation (INC) experiments. In addition to that, the HydroBox team collected and measured salinity samples (TSG) from the underway system.

6.1.2 General Hydrochemistry Information

Macro-nutrients, dissolved oxygen, and PortaSal salinity measurements were performed in the HydroBox, the CSIRO's containerised hydrochemistry lab. Salinity measurement on the AutoSal were performed in Dry Lab 1. The HydroBox was set up on Deck 5 aft.

6.1.3 Data Management

Final hydrology data, analytical methods, related log sheets and processing notes can be obtained from the Australian Antarctic Data Centre (AADC) <https://data.aad.gov.au>.

6.1.4 HydroBox Personnel

Table 9: Key personnel list

Name	Analysis	Organisation
Julie Janssens	Nutrients	CSIRO
Merinda McMahon	Nutrients	CSIRO
Claire Yung	Salinity	ANU
Christina Schmidt	Dissolved Oxygen	UNSW

6. Hydrochemistry (AAS 4630)

6.1.5 Summary

Table 10: Sample type and number of samples assayed

Analysis	Samples Assayed	Type
Salinity	1140	CTD
	41	TSG
Dissolved Oxygen	1129	CTD
Nutrients	1141*	CTD
	68	Underway
	547	Pore water
	231	Trace metal
	194	Incubations

* This number does not include the duplicate sample taken from the first Niskin of each cast. Sample 2 in the results file is the duplicate sample, please use an average of the two results.

6.2 Salinity

Table 11: Salinity Measurement Parameters

Details	
HyPro Version	5.9
Instruments	Guildline Autosal Laboratory Salinometer 8400B – SN 71-611. Bath temperature 24.0 °C Guildline Portasal Salinometer 8410A – SN 74995. Bath temperature 24.0°C
Software	Ocean Scientific International Ltd (OSIL) Data Logger version 1.2
Hydrochemistry Methods	Sampling: WI_Sal_002 Analysis: SOP 006 (Autosal) SOP 008 (Portasal)
Accuracy	± 0.001 practical salinity units
Reference Material	OSIL IAPSO – Batch P167, use by 21/02/2026, $K_{15} = 0.99988$
Sample Container	200 mL volume OSIL bottles made of type II glass (clear) with disposable plastic insert and plastic screw cap.
Sample Storage	Stored in Dry Lab 1 lab for minimum of 8 hrs before the measurement.
Lab Temperature	Ambient lab temperature
Analysts	Claire Yung
Comments	CTD 3, 12 – 104, TSG 1, 2, 3, 7 – 45 and INC 1 – 2 analysed on Autosal 71-611. CTD 1, 2, 4 – 9 and TSG 4 – 6 analysed on Portasal 74995.

Salinity samples were measured on both a Guildline Autosal 8400B salinometer and Guildline Portasal 8410A Salinometer. Both instruments were operated in accordance with their relevant SOP and technical manual. The measured value on both instruments was recorded with an OSIL data logger.

Practical salinity unit (PSU) is defined in terms of the ratio (K_{15}) of the electrical conductivity measured at 15 °C 1 atm of seawater to that of a potassium chloride (KCl) solution of mass fraction 32.4356×10^{-3} .

6. Hydrochemistry (AAS 4630)

Before each lot of sample measurements, the Salinometer is calibrated with standard seawater (OSIL, IAPSO) of known K_{15} ratio. A new bottle of OSIL standard is used for each calibration. The frequency of calibration is at least one per run.

Method: The salinity sample is collected in a 200 mL OSIL bottle. The bottle is rinsed then filled from the bottom, via a polytetrafluoroethylene (PTFE) straw, till overflowing. The bottle is removed from the straw and the sample is decanted to allow a headspace of approximately 25 cm³. A dry plastic insert is fitted, the bottle inverted and rinsed with water then capped and stored cap-down until measured. To measure, the Autosal cell is flushed three times with the sample and then measured after the fourth and fifth flush. The OSIL data logger software captures the conductivity ratio and calculates the practical salinity. The output from the data logger is imported into HyPro.

The instrument was calibrated with OSIL standard seawater lot P167.

Table 12: OSIL standard seawater lot P167 details.

OSIL IAPSO Standard Seawater	
Batch	P167
Use by date	21/02/2026
K_{15}	0.99988
PSU	34.995

6.3 Dissolved Oxygen

Table 13: Dissolved oxygen measurement parameters.

Details	
HyPro Version	5.9
Instrument	Automated Photometric Oxygen System
Software	Scripps Institution of Oceanography (SIO)
Hydrochemistry Methods	Sampling: WI_DO_001 Analysis: SOP 005
Accuracy	$\pm 0.5 \mu\text{mol L}^{-1}$
Lab Temperature	Mean 21.1 °C SD 1.4 °C
Sample Container type	140 mL glass iodine determination flasks with glass stopper.
Sample Storage	Samples stored in the HydroBox until analysis.
Analysts	Christina Schmidt
Comments	N/A

Scripps Institution of Oceanography method used. The method is based on the whole bottle modified Winkler titration of Carpenter (1965) plus modifications by Culberson *et al* (1991).

Method: The sample is collected in an iodine determination flask of known volume. 1 mL of manganese (II) chloride solution followed by 1 mL of alkaline iodide solution is added to the sample, the flask stoppered and inverted a minimum of 30 times. The dissolved oxygen oxidizes an equivalent amount of Mn (II) to Mn (IV) which precipitates. Just before titration, the sample is acidified, Mn (IV) is reduced to the divalent state liberating iodine. The iodine is titrated with a standardised thiosulphate solution using a Metrohm 876 Dosimat fitted with a 1 mL burette. The endpoint is determined by measuring the decrease in the UV absorption 365 nm.

6. Hydrochemistry (AAS 4630)

The thiosulphate solution is standardised by titrating it against a 10 mL aliquot of potassium iodate primary standard. A blank correction is also determined from the difference between two titres of consecutive additions of 1 mL aliquots of potassium iodate to the same blank sample. The standardisation is done at least once per 12-hour shift, when samples are being assayed.

The output from the SIO instrument software is imported into HyPro.

6.4 Nutrients

Table 14: Nutrient measurement parameters analysed with Seal AA500 segmented flow analyser. All instrument parameters, reagent batches and instrument events are logged for each analysis run. This information is available on request.

Details					
Instrument	Seal AA500 segmented flow analyser				
HyPro version	5.9				
Operating Software	AACE 8.03 SP1				
Hydrochemistry Sampling Method	WI_Nut_001				
Hydrochemistry analysis method	SOP001	SOP002	SOP003	SOP003	SOP004
Nutrients Analysed	Silicate SiO_4^{4-} as Si	Phosphate PO_4^{3-} as P	Nitrate + Nitrite $\text{NO}_3^- + \text{NO}_2^-$ as N	Nitrite NO_2^- as N	Ammonium NH_4^+ as N
Top concentration ($\mu\text{mol L}^{-1}$)	140.0	3.0	42.0	1.4	2.0
Method detection limit ($\mu\text{mol L}^{-1}$)	0.2	0.02	0.02	0.02	0.02
Reference Material	KANSO RMNS lot CP				
Sample Container	CTD/TMR: 50 mL High-Density Polyethylene (HDPE) with screw cap lids. Reused after acid wash with 10 % HCl solution. CORE/UWY: 10 mL polypropylene (PP) with screw cap lids. Reused after acid wash with 10 % HCl solution. INC: 10 mL PP with crew cap lids, new for each sample.				
Sample Storage	< 4 hours at room temperature after collection or < 12 hours at 4 °C after collection				
Sample preparation	Assayed as neat. No filtration for CTD, TMR, UWY and INC samples. For Core sampling procedure please refer to the voyage report, Sediment and Solid Earth section. Please refer to Core log sheet for sample dilution factors.				
Lab Temperature (°C)	Mean 21.1 °C SD 1.4 °C. Temperature probe was located above the AA500 autosampler, as close to the samples as possible.				
Analysts	Merinda McMahon and Julie Janssens				
Comments	Refer to metadata for sample log sheets. Log sheet for TMR 001 and 002 not available.				

Nutrient samples are assayed on a Seal AA500 segmented flow auto-analyser fitted with 1 cm flow-cells for colorimetric measurements and a JASCO FP2020 fluorescence instrument as the ammonium detector.

6. Hydrochemistry (AAS 4630)

Silicate (SOP001): colourimetric, molybdenum blue method. Based on Armstrong et al. (1967). Silicate in seawater is reacted with acidified ammonium molybdate to produce silicomolybdic acid. Tartaric acid is added to remove the phosphate molybdic acid interference. Tin (II) chloride is then added to reduce the silicomolybdic acid to silicomolybdous acid and its absorbance is measured at 660 nm.

Phosphate (SOP002): colourimetric, molybdenum blue method. Based on Murphy and Riley (1962) with modifications from the NIOZ-SGNOS¹ Practical Workshop 2012 optimizing the antimony catalyst/phosphate ratio and the reduction of silicate interferences by pH. Phosphate in seawater forms a phosphomolybdenum complex with acidified ammonium molybdate. It is then reduced by ascorbic acid and its absorbance is measured at 880 nm.

Nitrate (SOP003): colourimetric, Cu-Cd reduction – naphthylenediamine method. Based on Wood et al. (1967). Nitrate is reduced to nitrite by first adding an ammonium chloride buffer then sending it through a copper – cadmium column. Sulphanilamide is added under acidic conditions to form a diazo compound. This compound is coupled with 1-N-naphthyl-ethylenediamine dihydrochloride to produce a reddish purple azo complex and its absorbance is measured at 540 nm.

Nitrite (SOP003): colourimetric, naphthylenediamine method. As per nitrate method without the copper cadmium reduction column and buffer. Absorbance measured at 540 nm.

Ammonium (SOP004): fluorescence, ortho-phthalaldehyde method. Based on K rouel and Aminot (1997). Ammonium reacted with ortho-phthalaldehyde and sulphite at a pH of 9.0-9.5 to produce an intensely fluorescent product. Its emission is measured at 460 nm after excitation at 370 nm.

SOP methods can be obtained from the CSIRO Hydrochemistry Group.

Sediment core pore water samples were analysed for nutrients as per nutrient methods above. Due to the concentration range of these methods the core samples were required to be diluted. All sample ID's and dilution factors are recorded in NUY2025_V3_Core logheets file. Samples were prepared for analysis by the Sediment team, please refer to 'Nutrients, Ferrozine and Sulphide methods' of the Sediment section of the voyage report for more information. The final reported results are corrected for refractive index effect and have had the dilution factor calculation applied. Any sample where the instrument measurement, prior to applying corrections and dilution factor calculation falls below the method detection limit has been flagged.

¹ Royal Netherlands Institute for Sea Research – Study Group on Nutrient Standards.

6.4.1 HyPro Processing Summary for Nutrients

After a run, the raw absorbance/ fluorescence data is exported from the instrument and processed by HyPro. For each analyte, HyPro re-creates the peak traces, defines the region on the peak's plateau (peak window) used to determine the peak heights, constructs the calibration curve, applies corrections for carry-over, baseline and sensitive drifts then, derives the nutrient concentrations for each sample. The corrections are quantified using dedicated solutions included in every run.

6. Hydrochemistry (AAS 4630)

HyPro uses criteria to identify suspect calibration points, noisy peaks, method detection limits that are above the nominal limit and duplicate sample results that do not match.

Suspect calibration points are weighted less when fitting the calibration curve. The cut-off limits for good calibration data are:

- $\pm 0.5\%$ of the concentration of the top standard for silicate and nitrate+nitrite (as per WOCE¹).
- $0.02 \mu\text{mol L}^{-1}$ for phosphate, nitrite and ammonium.

¹ World Ocean Circulation Experiment

Table 15: HyPro 5.9 Processing Parameters. All instrument parameters, reagent batches, and operation events are logged for each analysis run. This information is available on request.

Result Details	Silicate	Phosphate	Nitrate + Nitrite (NOx)	Nitrite	Ammonium
Data Reported as	$\mu\text{mol L}^{-1}$	$\mu\text{mol L}^{-1}$	$\mu\text{mol L}^{-1}$	$\mu\text{mol L}^{-1}$	$\mu\text{mol L}^{-1}$
Calibration Curve degree	Linear	Linear	Quadratic	Quadratic	Quadratic
# of points in Calibration	7	6	7	6	6
Forced through zero	N	N	N	N	N
Matrix correction	N	N	N	N	N
Blank correction	N	N	N	N	N
Refractive Index Correction (HyPro)	Y	Y	Y	Y	N/A
Peak window defined by	HyPro	HyPro	HyPro	HyPro	HyPro
Carryover correction (HyPro)	Y	Y	Y	Y	Y
Baseline drift correction (HyPro)	Y	Y	Y	Y	Y
Sensitivity drift correction (HyPro)	Y	Y	Y	Y	Y
Data Adj for RMNS variance.	N	N	N	N	N
Medium of Standards	Low nutrient seawater (LNSW, bulk on PW1 wharf, CSIRO Hobart) collected in June 2021 and October 2022. Sub-lot passed through a 5-micron filter (October 2024) and stored in 20 L carboys in the Heli-hanger.				
Medium of Baseline	18.2 Ω water. Dispensed from the Milli-Q IQ 7010 system.				
Duplicate samples.	CTD: Niskins fired at the greatest depth were analysed in duplicate. Single samples were analysed for remaining depths.				
Comments					

6.5 Issues encountered

HydroBox:

- Temperature control in the HydroBox was at times challenging. Large influxes of cold air into the HydroBox occurred when the door was open, resulting in frozen plumbing.
- The HydroBox is equipped with two panel heaters near floor level and a reverse cycle unit near the roof. However, due to the natural rise of heat and poor floor insulation, a sharp air temperature gradient developed inside the unit. The inadequate insulation allowed extreme Antarctic conditions to affect the floor, which at times became frozen when temperatures dropped below -20°C . This caused small amounts of spilled water to freeze, occasionally affixing boxes to the floor
- The cold-water inflow from the ship froze on 28/03/2025, 07/04/2025 and 14/04/25 date, causing the Milli-Q system to also run out of water. Rectified by use of a heat gun and mitigated by regularly running water.
- The wastewater drain froze on evening of 07/04/25 when temperatures dropped to -21°C with wind chills of -35°C . The issue was resolved after 24 hours through a heat gun and installing heat trace on the outer piping and valve connecting the HydroBox waste to the ship's holding tank and mitigated by half-hourly (and at times continuous) water flow in the sink.

CTD Sampling:

- Dissolved Oxygen sampling temperature probe was slow to reach temperature reading on the first sample. On casts 041, 042 and 044 duplicate samples were taken one using the primary thermometer and the duplicates using the spare thermometer. This experiment showed that the two thermometers were reading the temperature differently. An experiment was conducted in an ice bath with the two sampling probes, along with the AutoSal calibrated thermometer. Both sampling probes read the same temperature as the Autosal thermometer, however it took a bit of time for them to reach this reading. It is possible the positioning of the thermometer tip in the sampling tube was the cause as during the experiments the thermometers were removed from the sample tubing. It is recommended to work with the CSIRO Calibration Facility to design and built a more robust, purpose fit sampling thermometer that is able to be calibrated.
- There were no samples from CTD008 (sensors froze), CTD028 (failed moonpool deployment) and CTD031 (all bottles closed together).

Salts:

- PortaSal 74945 OSIL standardisation requires a large volume of water. Therefore, often the first readings of the OSIL did not match the standardised conductivity and salinity (off by 0.001). Often two OSILs were required for PortaSal standardisation.
- The OSIL pump flush speed was slower than recommended in the salinometer SOP, reducing the efficiency of salinity analysis. Measurements using a measuring cylinder showed a read speed of 10 mL/min (mode 1) and a flush speed of 16 mL/min (mode 3). The flush speed was below the SOP speed of 25 mL/min. To address this, from CTD029 (24/3/25), a variable-speed peristaltic pump (Masterflex EasyLoad II model 77200-60), borrowed from Leonie Suter (AAD), was installed alongside the AutoSal, along with a 3D-printed sample holder provided by Liam from the AAD Science Systems team. The AutoSal 71-611 was used from CTD012 (18/3/25) onward. Duplicate samples were collected on casts 003, 067, 079, 081, and 103 and run on the PortaSal 74945 to allow instrument comparison. Subsequent AutoSal analyses used the new pump setup, while

6. Hydrochemistry (AAS 4630)

duplicate PortaSal measurements continued with the original OSIL pump due to space constraints in the HydroBox.

- The AutoSal 71-611 had a large bubble at the inlet tube of the glass cell, first observed during CTD003 (first time used). Cleaning with bleach, triton-x and ethanol/deacon solution did not remove the bubble. Upon consultation with the Guildline calibration and maintenance team at CSIRO, it was confirmed that this bubble would not affect the readings as it was not interfering with the conductivity coils. To remove the bubble the instrument would need to be opened up and the cell removed, it was determined that the risk to the instrument's performance was too high to do this. As the bubble was not affecting the results it was determined to continue operating with the bubble in place. Occasional cleaning was required when the bubble became difficult to pop during flushing.
- Both the HydroBox and Dry Lab 1 did not have a constant air temperature, with HydroBox temperatures recorded during salinity analysis varying between 18.6 and 22.7 °C and Dry Lab 1 between 19.3 to 25 °C (with most temperatures between 20.3 and 21.1 °C).
- During CTD015 analysis (sal010 run), the waste carboy filled up so that the salinometer cell drainpipe could not access the ambient air, and back pressure resulted in formation of bubbles. Sample TSG007 was therefore not analysed. After cleaning with bleach and triton-x the salinometer was standardised and the run was resumed in sal011.
- During CTD07411 sample analysis (sal040 run), salinometer gave highly variable readings (large drift up and down). After flushing with saltwater, readings were stable and run was continued.
- During CTD101 analysis (sal055 run), salinometer gave highly variable readings. Salinometer was cleaned with bleach and triton-x. Sample CTD10121 was not analysed.

Dissolved oxygen:

- On 12/4/2025, a leak occurred on the thiosulphate dosimat. The 3-way connector was removed, pulled apart and cleaned. Upon re-installing the leak still occurred, after further investigation the leak was observed to be due to a damaged flange on the end of the tubing. The tubing was replaced with the equivalent tube from the spare dosimat and the leak was resolved. It is recommended to re-flange the tubes once home and purchase a spare set for the HydroBox.
- While resolving the dosimat leak, a communications error between the dosimat and the computer occurred. This was a result of a broken usb-RS232 adapter and was resolved with help from the AAD Support team.

Nutrients:

- The signal on the silicate channel would flatline due to small bubbles entering the system through the tartaric line. During a run this was managed by pinching the waste line, building enough pressure to dislodge the bubble. The cause of the issue was determined to be the vertical 10 turn reagent inlet coil. This was replaced with a horizontal 10 turn coil and separate reagent inlet part which resolved the issue.
- The automatic Cd-column valve was removed and replaced with a manual 4-way valve.
- The door to the HydroBox was open for an extended period of time while issues with the frozen plumbing were being resolved. At this time a nutrient analysis run was occurring. The influx of cold air into the lab over that period of time caused a large amount of drift in the ammonia channel. These samples were repeated, once the lab returned to ambient temperature.

6. Hydrochemistry (AAS 4630)

6.6 Recommendations for next voyage

- Improve heat insulation of HydroBox floor and pipes for Antarctic conditions
- Get a purpose fit DO sampling temperature probe made
- Buy heat gun, ethernet to usb dongle, network box
- Better cable management in the Box

6.7 Temperature Plot

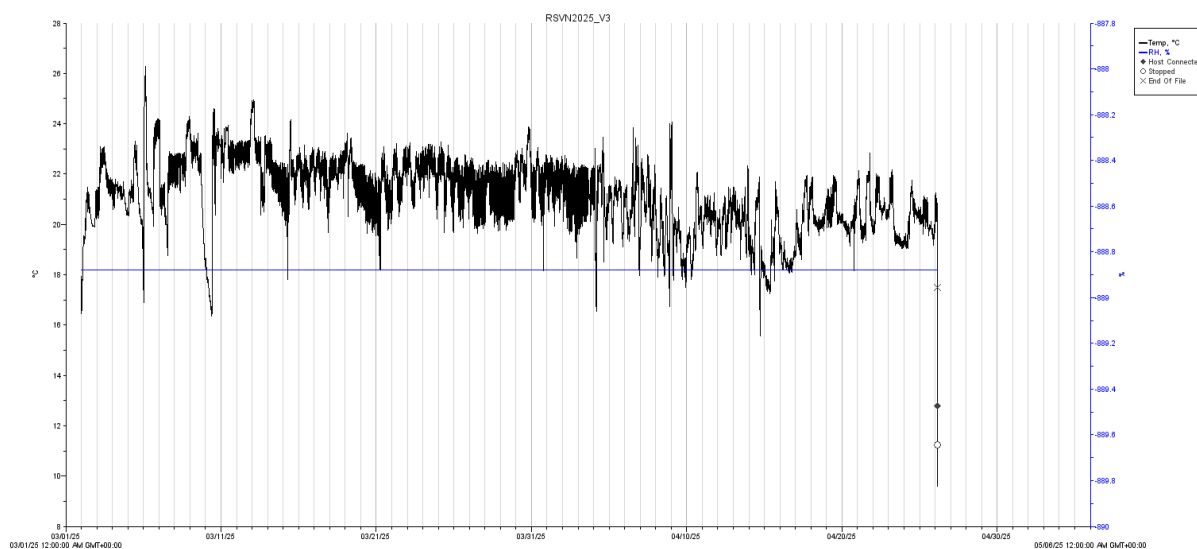


Figure 12: Plot of the temperature in the HydroBox for the duration of the voyage. The temperature probe was mounted on the wall near the nutrient analyser sampler. Note: there was a temperature gradient in the HydroBox, temperatures were colder closer to the floor.

6.8 References

Armishaw, P. (2003) “*Estimating measurement uncertainty in an afternoon. A case study in the practical application of measurement uncertainty.*” *Accred Qual Assur*, 8: pp. 218-224

Armstrong, F.A.J., Stearns, C.A., and Strickland, J.D.H. (1967) “*The measurement of upwelling and subsequent biological processes by means of the Technicon Autoanalyzer and associated equipment,*” *Deep-Sea Res.*, 14: pp.381-389. [doi: 10.1016/0011-7471\(67\)90082-4](https://doi.org/10.1016/0011-7471(67)90082-4)

Becker, S., Aoyama, M., Woodward, E. M.S., Bakker, K., Coverly, S., Mahaffey, C., and Tanhua, T. (2020). “GO-SHIP Repeat Hydrography Nutrient Manual: The precise and accurate determination of dissolved inorganic nutrients in seawater, using continuous flow analysis methods.” *Front. Mar. Sci.*, Sec. Ocean observation volume 7. <https://doi.org/10.3389/fmars.2020.581790>

6. Hydrochemistry (AAS 4630)

- Hood, E.M. (2010). *“Introduction to the collection of expert reports and guidelines.”* The GO-SHIP Repeat Hydrography Manual: A Collection of Expert Reports and Guidelines. IOCCP Report No 14, ICPO Publication Series No. 134, Version 1, 2010.
- Hydes, D., Aoyama, M., Aminot, A., Bakker, K., Becker, S., Coverly, S., Daniel, A.G., Dickson, O., Grosso, R., Kerouel, R., van Ooijen, J., Sato, K., Tanhua, T., Woodward, E.M.S., and Zhang, J.Z. (2010). *“Determination of dissolved nutrients (N, P, Si) in seawater with high precision and inter-comparability using gas-segmented continuous flow analysers.”* The GO-SHIP Repeat Hydrography Manual: A Collection of Expert Reports and Guidelines. IOCCP Report No 14, ICPO Publication Series No. 134, Version 1, 2010. (UNESCO/IOC)
- K erouel, R., and Aminot, A. (1997) *“Fluorometric determination of ammonia in sea and estuarine waters by direct segmented flow analysis”*. Mar. Chem., 57: pp. 265-275. [doi:10.1016/S0304-4203\(97\)00040-6](https://doi.org/10.1016/S0304-4203(97)00040-6)
- Murphy, J. And Riley, J.P. (1962) *“A Modified Single Solution Method for the Determination of Phosphate in Natural Waters”*, Anal. Chim. Acta, 27: p.30. [doi:10.1016/S0003-2670\(00\)88444-5](https://doi.org/10.1016/S0003-2670(00)88444-5)
- Rees, C., Janssens, J., Sherrin, K., Hughes, P., Tibben, S., McMahon, M., McDonald, J., Camac, A., Schwanger, C. and Marouchos, A., (2021) *“Method for Reproducible Shipboard Segmented Flow Analysis Ammonium Measurement Using an In-House Reference Material for Quality Control.”*Frontiers in Marine Science, 8. [doi:10.3389/fmars.2021.581901](https://doi.org/10.3389/fmars.2021.581901)
- Rees, C., L. Pender, K. Sherrin, C. Schwanger, P. Hughes, S. Tibben, A. Marouchos, and M. Rayner. (2018) *“Methods for reproducible shipboard SFA nutrient measurement using RMNS and automated data processing.”* Limnol. Oceanogr: Methods, 17(1): pp. 25-41. [doi:10.1002/lom3.10294](https://doi.org/10.1002/lom3.10294)
- Wood, E.D., Armstrong, F.A.J., and Richards, F.A. (1967) *“Determination of nitrate in seawater by cadmium-copper reduction to nitrite.”* Journal of the Marine Biological Association of U.K. 47: pp. 23-31.

7. Trace Metals & Isotopes (AAS 4630)

Team: Robin Van Dijk, Katie Nawrath, Talitha Nelson, Yuhao Dai, Abbie Smith, Delphine Lannuzel and Michael Ellwood

Note: TMR log sheets are published separately on the IMAS database as a part of the 'Supplementary Material'.

7.1 General Introduction

The Denman Glacier is one of the largest and fastest-melting glaciers in East Antarctica. It holds the potential to contribute up to 1.5 m of global sea level rise. Recent research indicates that the glacier has retreated approximately five kilometres over the past two decades (1996 to 2017/18), highlighting its vulnerability to climate-driven change. This accelerated melting not only impacts global sea levels but also plays a crucial role in the supply of trace elements to surrounding marine ecosystems. The coastal environment shaped by ice-ocean interactions regulates biogeochemical cycles, including the cycling of trace metals such as iron (Fe) in the water column. Iron in polar waters is essential for sustaining marine productivity, serving as a vital micronutrient that regulates phytoplankton growth and ecosystem dynamics. However, current ocean biogeochemical models often struggle to capture the complexity of trace metal biogeochemistry in these regions, leading to uncertainties in climate change projections and ocean productivity forecasts.

Iron and light are key drivers of primary productivity in the Antarctic coastal environment. Macronutrients are abundant in Antarctic coastal waters, but biological growth remains limited by micronutrient availability. Iron enters the Antarctic marine system through ice melt, sediment resuspension, and benthic fluxes. As climate change accelerates ice melt and alters ocean circulation patterns, Fe availability is expected to shift, influencing biological and chemical dynamics in the Southern Ocean. The interplay between trace metal supply and seasonal variations in light exposure plays a crucial role in stimulating phytoplankton blooms, which drive carbon cycling and export, sustain pelagic and benthic marine food webs, and contribute to deep-sea carbon sequestration.

7.2 Overall Aim and Hypothesis

The Denman Marine Voyage (DMV) aims to improve our understanding of the Denman Glacier region's role in shaping ocean biogeochemistry. A key aspect of this research is characterising dissolved and particulate trace metal distributions, metal speciation (e.g. Fe and copper), and other trace elements and isotopes throughout the water column. Denman Marine Voyage has been approved by the international program GEOTRACES.

High-resolution sampling at selected stations along the eastern and western edges of the Denman and Shackleton ice fronts, as well as at two process stations, will allow us to monitor fluxes of particulate and dissolved trace metals, providing insights into key processes such as

7. Trace Metals & Isotopes (AAS 4630)

metal scavenging, organic ligand interactions, and biological uptake across euphotic zone and their regeneration at depth in the mesopelagic and on the seafloor.

Given the significance of iron and other trace metals in stimulating productivity, dissolved and particulate samples and water column sensor data collected on the DMV will be used to explore links between trace metal availability and phytoplankton productivity. Additionally, this work will be integrated with analyses of Kasten sediment cores and shorter multicores collected by the sediments team. These cores will provide insights into the contribution of sediment-derived trace metals, including Fe, via pore water fluxes into the overlying water column. By examining these sediments, we aim to quantify sources of benthic iron release, evaluate the role of sediment resuspension in metal transport to the overlying water column, and assess how glacial meltwater influences trace element availability.

We also collaborated with the biological team to conduct phytoplankton incubations with amendments of Fe, copper, cobalt, zinc and various Fe-binding ligands to assess their influence on biological productivity. These experiments will help us determine how varying trace metal concentrations impact phytoplankton growth, bacterial production, and community composition, thereby offering a better understanding of the biogeochemical connections within the water column for the Denman/Shackleton glacier region.

7.3 Sample Collection Methods

The Trace Metal Rosette (TMR) is a custom-built, fit for purpose instrument used for the non-contaminating collection of seawater suitable for trace metal oceanography. The TMR can sample seawater throughout the water column to a maximum of 6000 m depth. The TMR was deployed from the ship with a Dyneema™ line. The TMR consists of a Sea-Bird Electronics (SBE) 12-position, multi-bottle sampler. It is compatible with integrated CTD and auxiliary equipment, including the SBE 17plus Searam, SBE32 Carousel and the SBE 9plus CTD underwater unit with auto fire module, with modular temperature and conductivity sensors as standard. The Rosette was equipped with an USBL transponder to be able to track the current depth of the TMR during deployments.

The TMR uses externally closing 12 Niskin 12-litre bottles (Ocean Test Equipment) with SeaBird titanium carousel mount brackets. Niskin bottles have been modified for trace metal sampling; this includes replacement of o-rings, drain taps, clips, crimps, and pins with materials suitable for trace metal sampling. The inside of the X-Niskins is Teflon-lined, and the external springs are Teflon-coated. The TMR guard frame is made from all-welded aluminium with a polyurethane electrostatic powder coat finish. Only high-quality stainless and titanium metal parts are used where non-metallic components are not possible. Once retrieved, the Niskin bottles were transported to a trace metal-clean containerised laboratory equipped with an ISO 5 HEPA filtered air system.

The TMR was deployed 30 times, of which 4 deployments failed, and two shallow test deployments were performed.

A general challenge throughout the voyage was the cold temperatures, causing the lanyards on the Niskin bottles to contract. This occasionally led to improper sealing of the bottles and therefore leaking, or lower bottle caps closing at deployment when the rosette touched the

7. Trace Metals & Isotopes (AAS 4630)

surface of the water. We would recommend replacing all lanyards before the next voyage as lengths were inconsistent between Niskins.

The SBE 9plus CTD unit's battery required replacement on multiple occasions. The frequency of replacements suggested higher-than-expected power consumption, possibly exacerbated by cold conditions.

Another general challenge that was encountered during the voyage is Niskin freezing when the air temperature dropped below $-5\text{ }^{\circ}\text{C}$. At the start of the voyage, the TMR was placed in front of the storage container, from where the Niskins were transferred to the sampling container. After this, the TMR rosette was placed back in the container. The significant time that the rosette was on deck resulted in freezing of both the seawater in the Niskins, as well as the tubing that leads to the sensors on the rosette/CTD package. Particularly, the freezing of the pressure sensor led to draining oil out and, ultimately, caused a malfunction resulting in incorrect pressure readings and a failed bottle firing sequence. We adjusted our methods by placing the TMR inside the storage container immediately upon retrieval, but despite the heaters placed inside the storage container, freezing would still occur. As a final solution, the TMR was stored in Hold 2 deck 4 after the Niskins were transferred to the sampling container. Storing the TMR in this location resulted in fast thawing of the sensors on the rosette, but risks of contamination by surrounding metals were higher.

The freezing of the seawater inside the Niskin bottles resulted in delays as the bottles needed to be left for approximately an hour to thaw before sampling. The freezing process may have altered some trace metal properties in the collected seawater, potentially impacting the quality of the samples. Strategies to mitigate the freezing of the sensors in future deployments could include enhanced thermal insulation for the storage container and/or cover, in addition to thawing of the tubing after each deployment and checking oil levels. We would also recommend placing the TMR storage container and sampling container closer together on the deck, which decreases time spend on deck and therefore chances of freezing of both the rosette and the seawater inside the Niskins.

Unfiltered samples for macro nutrients (ammonia (NH_4^+), nitrate + nitrite (NO_x), nitrite (NO_2^-), phosphate (PO_4^{3-}) and silicate ($\text{Si}(\text{OH})_4^-$)) were taken at every depth using three times sample-rinsed 50 mL HDP tubes. Samples were analysed on board by the hydrochemistry team and preliminary results can be found in Figure 15. The results were used to compare with the CTD and check if the bottles closed at the pre-programmed depths. No major issues were identified during the voyage. Samples for $\delta^{18}\text{O}$ and biological parameters were taken from the TMR at stations with no complimentary CTD deployment.

All trace metal sampling and analysis techniques followed the GEOTRACES cookbook (Cutter et al., 2017). Briefly, new 60 mL, 125 mL, 250 mL and 1 L Low Density Polyethylene (LDPE) sample bottles were cleaned pre-voyage in 2 % v:v Decon-90 for one week to remove any residue from manufacturing. At ANU, the 250 mL and 1 L bottles were then rinsed four times with deionized water and thrice in ultra-high purity (UHP) water. The bottles were filled with 6 M hydrochloric acid (HCl) and placed in a 1.2 M HCl bath for one month. At UTAS, the 60 mL and 125 mL bottles were rinsed five times with deionised water, filled with 6M HCl and placed in 1.2M HCl bath on a hotplate at $80\text{ }^{\circ}\text{C}$ for one week. Bottles were rinsed again seven times with UHP water, filled with trace metal grade UHP pH = 1.8 and triple-bagged for transportation. Bottles were rinsed thrice with freshly collected seawater prior to sampling. For incubation experiments (see biology voyage report), 125 mL LDPEs were used for initial and final trace metal sampling. New bottles were

7. Trace Metals & Isotopes (AAS 4630)

cleaned in 2 % v/v Decon-90 for one week at room temperature, then rinsed four times with deionised water and thrice in ultra-high purity water under a ducted laminar flow hood. The bottles were then filled with 6M HCl and placed in a 1.2M HCl bath at 80 °C for one week. Bottles were rinsed four times with ultra-high purity water under a ducted laminar flow hood before being filled with 1 % distilled HCl. Bottles were double-bagged for transport. Fluorinated high-density polyethylene (FLPE) bottles were used for ligand samples. Briefly, new 500 mL FLPE were soaked in a 2 % v:v Decon-90 for one week at room temperature. Bottles were then rinsed four times with deionized water and three times in ultra-high purity water under a ducted laminar flow hood. The bottles were then filled with 6 M HCl and placed in a 1.2 M HCl bath for one week at 80 °C. Each bottle was then rinsed seven times with Milli-Q, filled with Milli-Q to remove any remaining acid, and then stored at room temperature and double bagged for transportation.

Unfiltered seawater samples were taken from each depth for total dissolvable metals, in 60 mL acid cleaned LDPE bottles. 125 mL, 250 mL, and 1 L samples collected for dissolved metal analysis were collected from each depth using acid-washed AcroPak 0.2 µm filter membranes. All bottles were sample rinsed three times. Both unfiltered and filtered metal samples were acidified with double distilled HCl to ~1.8 pH in a clean laminar flow bubble and double bagged in LDPE resealable bags for trace element analysis at IMAS and ANU. At two stations, 125 mL environmental blanks for dissolved metals were taken to check for any background contamination. 3-5 bottles were left open in different locations inside the sampling container for 3 hours during sampling. These bottles were treated similar as seawater samples and acidified. Samples ranging from 1-5 L filtered seawater were collected for Pb isotopes and acidified to pH = 1.8-2.0 using double distilled HCl. Up until TMR9, acidification level of the Pb isotope samples was checked using a pH meter (LAQUATwin, Horiba). Due to a malfunction of the pH meter, the pH was not checked after TMR9. All acidified samples were stored at ambient temperature. The filter membranes were discarded after each section of the voyage, roughly every 5-7 stations. We would recommend for future voyages to keep track more accurately of filter membranes by numbering them, separating shallow and deep Niskin bottle sampling, and tracking for how many stations they have been used.

Filtered seawater was collected in 500 mL FLPE bottles for Fe-binding ligands. These bottles were filled to 80 % and frozen at -20 °C without acidification. At two deployments, duplicates were taken in LDPE bottles for comparison. At the process stations, 2 L of filtered seawater was collected in polycarbonate bottles for siderophores analysis. These polycarbonate bottles were cleaned with a minimum 48 hour 2 % neutracon soak, followed by a thorough RO rinse and then one week in 10 % HCl at room temperature. Bottles are then rinsed > 4 times with Milli-Q water and left to dry in a ducted laminar flow hood before being double-bagged for transport.

At the final two deployments, filtered seawater was collected in carboys for in-house trace metal and for phytoplankton culturing media at IMAS. Two 20 L carboys were filled completely and stored at +4 °C in the dark. A 20 L carboy was filled and acidified with 21.5 mL HCl, and ~10 L of leftover filtered seawater was collected in a 50 L and acidified with 9.8 mL HCl. Their pH will be checked upon return at IMAS.

At two stations, the CTD was sampled for trace metals for a contamination comparison (CTD78 and CTD87). At process station 2, both the CTD and TMR were sampled for cross calibration. From the CTD, 500 mL unfiltered seawater was taken from the sampled depths and frozen at -20 °C without acidification. At IMAS, these samples will be filtered and acidified prior to analysis. Additionally, 60 mL unfiltered seawater was taken and acidified to a pH ~1.8 and stored at ambient temperature for total dissolvable metals. These results can be used to measure

7. Trace Metals & Isotopes (AAS 4630)

contamination levels for different metals from the CTD. We expect certain metals to have higher contamination than others. Be aware that the CTD casts that were samples for trace metals were deployed through the moonpool. Deployments using the outside winch might have different contamination levels.

A transect starting at process station 2 towards the southeast was chosen to test the underway uncontaminated system for trace metals. The first sample was taken at the process station, and every 1.5 nm (~20 minutes). The sampling followed the same method as the CTD sampling, where a 500 mL and 60 mL bottle were filled. Information can be found in Table 17.

To meet the GEOTRACES program, one station (TMR23) was added to the voyage program that was visited in early 2024 by RV *Polarstern* on the EASI-2 campaign.

In-situ pumps were deployed with the aim of quantifying particulate trace metals (pTMs), particulate organic carbon (POC) and environmental DNA (eDNA) from different depths across the water column. These data may be used to infer the composition and attenuation of sinking particles to carbon fluxes and identify sources of trace elements to surface waters (such as sediment resuspension). Particles were sampled from the water column using McLane WTS-LV, Challenger Stand Alone Pumps. The ISP's allow for the collection of particles from large volumes (up to 10,000 L) of seawater simultaneously at a range of depths (pumps are rated to 5000 m). The pumps were battery operated, requiring custom-made batteries to provide 36 V per unit. Each unit held two baffled 142 mm filter heads (Multiple Unit Large Volume in-situ Filtration System, MULVFS) comprising a QMA filter for eDNA and POC analyses and an acid-cleaned 0.2 μm Supor filter for particulate trace elements.

Six pump units were deployed at three sites. ISP01 and ISP03 corresponded with Process Station 1 and 2 respectively (Figure 13). No water was pumped across ISP02 filters (due to technical difficulties with bubblers) and as a result these filters may be considered blank measurements. Pump units were deployed evenly between the surface 30 m and 500 m. Pumps were programmed with a minimum flow rate of 4000 ml min⁻¹ for 120 min or a maximum sampling volume of 2000 L (whichever occurred first). Flow meter readings were recorded prior to and following each deployment, and each unit filtered between 579 – 772 L of seawater. Pump units were clamped in series onto a Dyneema line during deployment. ISP01 was deployed from the starboard aft of the trawl deck, whereas ISP02 and ISP03 were deployed from the A-Frame which resulted in a smoother deployment and retrieval process.

The extremely cold temperatures on-deck during retrieval resulted in seawater rapidly freezing inside the pumps, therefore all pumps were swiftly returned to the heated containerised lab before disassembly. Once retrieved, pumps heads were removed and any overlying water removed by sucking through the remaining water using a vacuum system. All filter heads were transferred in ziploc bags to the trace metal sampling van, and QMA filters were subsampled for eDNA and POC ahead of Supor filters to prevent rapid degradation of eDNA. QMA filters were sub-sampled for eDNA in triplicates with a 25 mm stainless steel punch and stored in polycarbonate vials at -80 °C. POC was sub-sampled using a 10 mm stainless steel punch, stored in well-plates and dried at 60 °C for several days before being stored in activated silica beads for analysis onshore. The remaining punched QMA filter was also preserved in polycarbonate at -20 °C. Supor filters were left intact and stored in acid-cleaned 50 mL polyethylene tubes at -20 °C until analysis at Central Science Laboratories, University of Tasmania.

7. Trace Metals & Isotopes (AAS 4630)

Table 16: List of key variables for DMV parameters collected.

Key Variable	Reason for interest	Collected from:
<i>Trace elements</i>		
Fe	Essential micronutrient	TMR
Al	Terrestrial input tracer	TMR
Zn	Micronutrient	TMR
Mn	Micronutrient	TMR
Cd	Micronutrient when Zn is limiting	TMR
Ni	Micronutrient	TMR
Co	Micronutrient	TMR
Cu	Micronutrient	TMR
<i>Isotopes</i>		
$\delta^{18}\text{O}$	Tracer of glacial meltwater	CTD
^{14}C	Aging of water masses and dissolved organic material	TMR
<i>Radiogenic isotopes</i>		
Pb isotopes	Tracer of natural and contaminant sources to the ocean	TMR
<i>Biological tracers</i>		
DOC/DON	Recycled from POC/PON	CTD
Fe-binding ligands	Marker of iron bio-availability	TMR
Siderophores	Marker of iron bio-availability	TMR
<i>Nutrients and C cycling</i>		
Alkalinity	Ocean's buffering capacity against acidity	CTD
DIC	Non-biological carbon in seawater	CTD
NO_x	Macronutrient for phytoplankton	CTD/TMR
PO_4^{3-}	Macronutrient for phytoplankton	CTD/TMR
$\text{Si}(\text{OH})_4^-$	Macronutrient for diatoms	CTD/TMR
NH_4^+	Macronutrient recycled from phytoplankton	CTD/TMR
NO_2^-	Macronutrient recycled from phytoplankton	CTD/TMR

7. Trace Metals & Isotopes (AAS 4630)

7.4 Station Locations

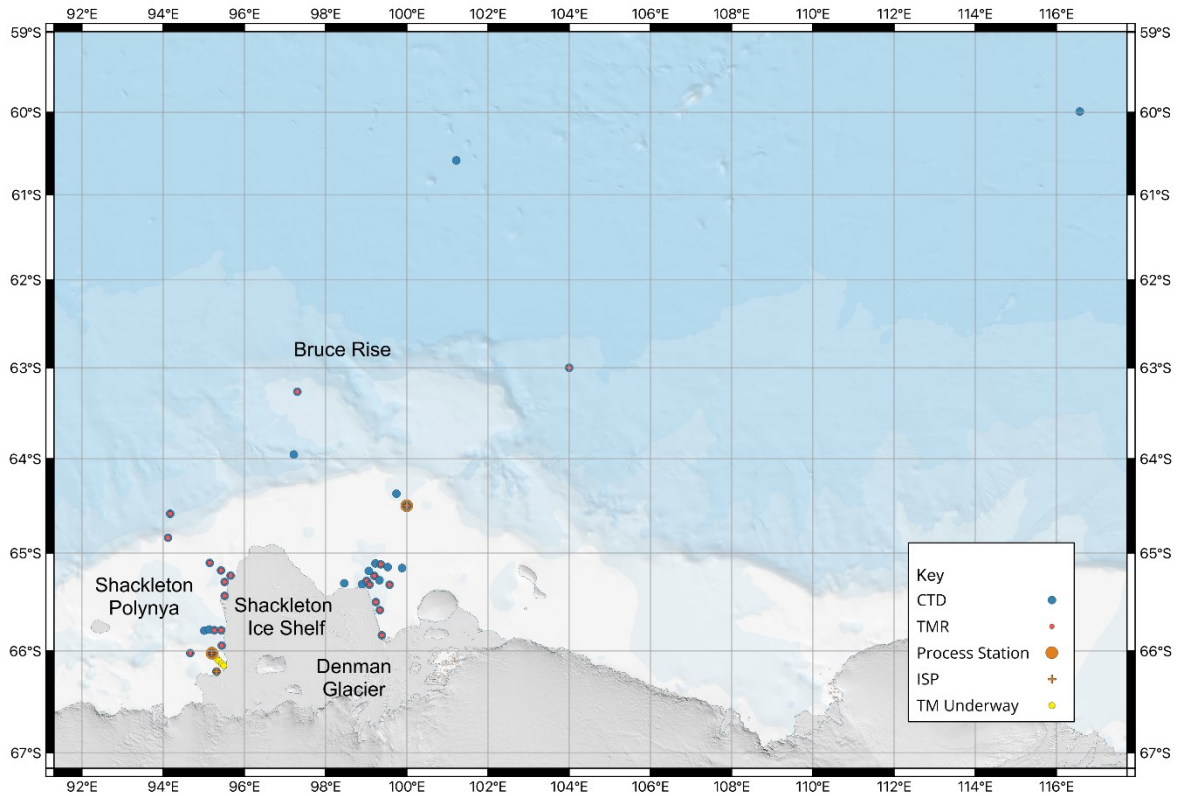


Figure 13: Map of trace metal rosette (TMR), combined CTD and TMR, process station, and trace metal underway sampling stations. Antarctica and the Southern Ocean basemap, British Antarctic Survey, <https://arcg.is/1S1jmi>.

7. Trace Metals & Isotopes (AAS 4630)

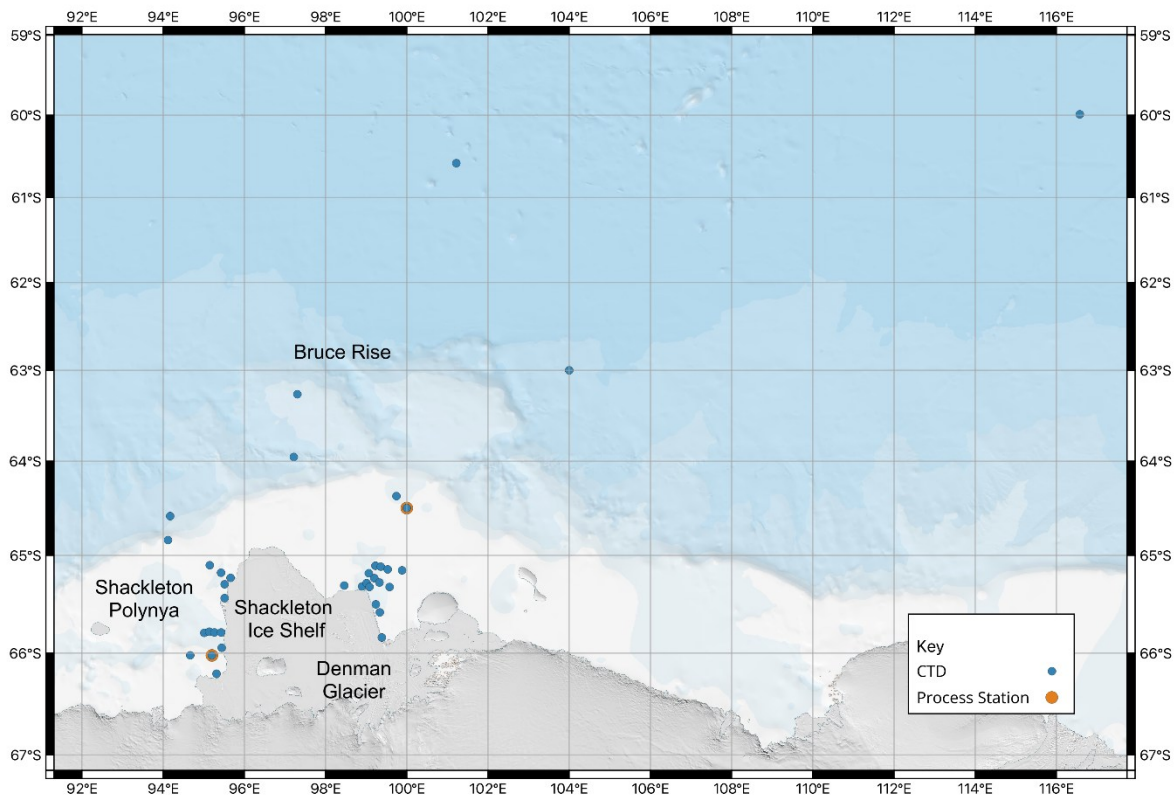


Figure 14: Map of stations sampled for CTD's, TMR casts and process stations. Antarctica and the Southern Ocean basemap, British Antarctic Survey, <https://arog.is/1S1jmi>

7.5 Deployment details

Table 17: Deployment details for TMR and ISP casts

Station	Cast	Location name	Date (UTC)	Time (UTC)	Latitude (DD)	Longitude (DD)	Depth (m)
4	TMR1	Bruise Rise E	9/03/2025	08:07:00 AM	-63.2897	102.4821	2111.89
6	TMR2	Bruise Rise W1	12/03/2025	07:27:00 PM	-63.2930	97.3320	1651.81
8	Failed TMR		15/03/2025		-65.3036	98.4583	587.09
9	Failed TMR		15/03/2025		-65.3136	98.5232	621.6
14	TMR3	Denman Transect 1	16/03/2025	07:57:21 AM	-65.2869	99.0085	800.02
17	TMR4	Denman Transect 2	17/03/2025	02:19:22 AM	-65.3153	99.0828	849.32
21	TMR5	Denman Transect 3	17/03/2025	12:14:32 PM	-65.5047	99.2385	674.5
23	TMR6	Denman Transect 4	17/03/2025	11:55:42 PM	-65.5841	99.3382	570
29	TMR7	Denman Transect 5	18/03/2025	03:10:00 PM	-65.8487	99.3858	833.38

7. Trace Metals & Isotopes (AAS 4630)

34	TMR8		22/03/2025	03:26:24 PM	-65.3262	99.6169	563.83
38	TMR9		23/03/2025	08:04:11 AM	-65.2324	99.1814	872.43
44	TMR10		24/03/2025	11:56:45 AM	-65.1114	99.3508	855.48
64	TMR11	Process station 1	29/03/2025	08:38:36 PM	-64.5000	99.9990	546.51
64	TMR12	Process station 1	30/03/2025	06:05:00 PM	-64.5020	99.9980	545.86
64	TMR13	Process station 1	30/03/2025	9:15:07 PM	-64.5004	100.0001	547.13
83	TMR14	Shackleton Ice Shelf transect EW1	4/04/2025	09:06:00 PM	-64.8393	94.1283	290.05
84	TMR15	Shackleton Ice Shelf transect EW4	5/04/2025	08:06:00 AM	-65.2325	95.6597	507.56
86	TMR16	Shackleton Ice Shelf transect EW3	5/04/2025	03:03:00 PM	-65.1798	95.4255	556
92	TMR17	Shackleton Ice Shelf transect EW2	6/04/2025	10:06:00 PM	-65.1022	95.1472	546.03
96	Failed TMR18		8/04/2025	6:24:00 AM	-65.795	95.0116	724.55
100	Failed TMR19		8/04/2025	8:43:15 PM	-66.021	94.6659	495.95
106	TMR20	Shackleton Ice Shelf transect NS4	10/04/2025	02:29:56 PM	-66.2050	95.3135	395.82
109	TMR21	Process station 2	11/04/2025	09:47:24 PM	-66.0217	95.1995	755.5
109	TMR22	Process station 2	12/04/2025	04:21:00 AM	-66.0218	95.1997	753.14
125	TMR23	Shackleton Ice Shelf transect NS3, Polarstern repeat	14/04/2025	08:30:53 AM	-65.7915	95.4274	1264.64
129	TMR24	Shackleton Ice Shelf transect NS2	15/04/2025	11:27:25 AM	-65.4408	95.5126	272.27
130	TMR25	Shackleton Ice Shelf transect NS1	15/04/2025	03:05:00 PM	-65.2991	95.5134	487.07
138	TMR26	Bruce Rise W2	19/04/2025	12:20:18 PM	-64.5883	94.1748	2404.43
64	ISP 1	Process station 1	30/03/2025	08:00:00 AM	-64.5000	100.0000	556

7. Trace Metals & Isotopes (AAS 4630)

106	ISP 2	Shackleton Ice Shelf transect NS4	10/04/2025	05:48:00 PM	-66.2050	95.3133	395.82
109	ISP 3	Process station 2	11/04/2025	12:15:00 PM	-66.0220	95.1995	760
100	CTD78	Shackleton Ice Shelf transect EW1	08/04/2025	07:19:20 PM	-66.021	94.6659	495.95
109	CTD82	Shackleton Ice Shelf transect EW2 (PS2)	12/04/2025?	05:35:09 AM	-66.0218	95.1997	754.97
114	CTD87	Shackleton Ice Shelf transect EW3	12/04/2025	05:30:41 PM	-65.9454	95.4415	428.09
109	UWYR1	Underway transect 1	13/04/2025	06:23:00 AM	-66.0218	95.19967	NA
NA	UWYR2	Underway transect 2	13/04/2025	07:26:00 AM	-66.0482	95.25867	NA
NA	UWYR3	Underway transect 3	13/04/2025	07:43:00 AM	-66.0718	95.3105	NA
NA	UWYR4	Underway transect 4	13/04/2025	08:03:00 AM	-66.098	95.36917	NA
NA	UWYR5	Underway transect 5	13/04/2025	08:23:00 AM	-66.1262	95.439	NA
NA	UWYR6	Underway transect 6	13/04/2025	08:39:00 AM	-66.1453	95.491	NA

7.6 Preliminary results

7.6.1 Nutrient results

Preliminary nutrient results for each trace metal rosette cast are presented in Figure 15. Most casts show a slight depletion of NO_x, phosphate, and silicate in surface waters. In contrast, ammonia and nitrite concentrations are elevated at the surface and decline with depth between approximately 100 and 150 m. However, some stations exhibit elevated concentrations below 200 m.

7. Trace Metals & Isotopes (AAS 4630)

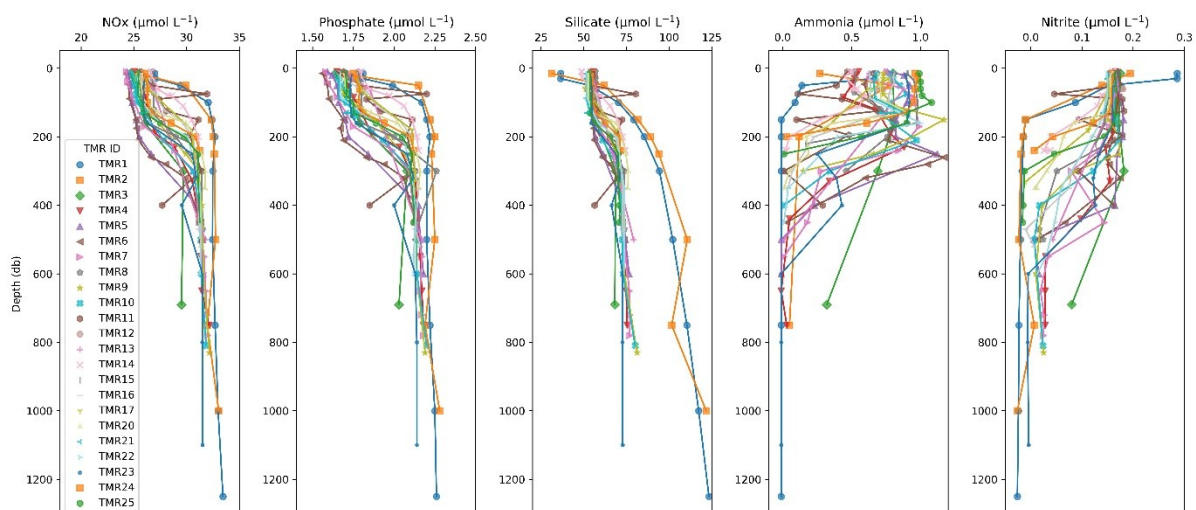


Figure 15: Nutrient concentrations plotted versus pressure for all TMR casts.

7.6.2 Chlorophyll results

Table 18: Deployment details for CTD and TMR casts sampled for biology.

Station	Cast	Location Description	Date (UTC)	Time Start (UTC)	Latitude (DD)	Longitude (DD)
2	CTD002	BGC Float 2	6/03/2025	23:12	-59.990	116.574
3	CTD003	BGC Float 3	8/03/2025	12:52	-63.000	104.000
6	CTD004	Bruce Rise W	12/03/2025	16:12	-63.2831	97.305
8	CTD005	Denman Front W	15/03/2025	03:53	-65.3036	98.4583
13	CTD011	Denman Glacier Front	16/03/2025	00:49	-65.321	98.901
14	CTD012	Denman Glacier Front	16/03/2025	06:09	-65.287	99.010
17	CTD015	Denman Glacier Front	16/03/2025	23:46	-65.326	99.081
21	CTD019	Denman Glacier Front	17/03/2025	10:36	-65.505	99.238
23	CTD021	Denman Glacier Front	17/03/2025	22:09	-65.587	99.336
29	CTD027	Denman Glacier Front	18/03/2025	13:35	-65.842	99.386
34	CTD029	Denman Transect 3	22/03/2025	13:15	-65.327	99.544
38	CTD033	Denman Transect 3	23/03/2025	06:34	-65.236	99.200
39	CTD034	Denman Transect 3	23/03/2025	10:40	-65.185	99.064
40	CTD035	Denman Transect 3	23/03/2025	14:00	-65.155	99.884

7. Trace Metals & Isotopes (AAS 4630)

43	CTD038	Denman Transect 4	24/03/2025	06:10	-65.107	99.227
44	CTD039	Denman Transect 4	24/03/2025	08:57	-65.117	99.361
46	CTD041	Denman Transect 4	24/03/2025	22:15	-65.145	99.563
57	CTD048	Denman	26/03/2025	21:31	-65.281	99.326
64	CTD052	Process Station #1	30/03/2025	14:39	-64.502	99.999
71	CTD058	Denman	1/04/2025	02:59	-64.375	99.745
83	CTD066	NE Shackleton #1	4/04/2025	19:25	-64.840	94.129
84	CTD067	Shackleton Iceshelf Front	5/04/2025	7:13	-65.233	95.660
86	CTD069	Shackleton Iceshelf Front	5/04/2025	13:27	-65.180	95.425
91	TMR17	Shackleton Iceshelf Front	6/04/2025	22:06	-65.102	95.147
92	CTD075	Shackleton EW 2	8/04/2025	04:12	-65.795	95.012
97	CTD076	Shackleton EW 2	8/04/2025	09:14	-65.783	95.136
98	CTD077	Shackleton EW 2	8/04/2025	12:17	-65.791	95.263
100	CTD078	Shackleton	8/04/2025	19:13	-66.021	94.666
106	TMR20	Shackleton NS	10/04/2025	14:29	-66.205	95.314
109	CTD082	Process Station 2	12/04/2025	05:50	-66.022	95.200
114	CTD087	Shackleton NS	12/04/2025	17:22	-65.945	95.442
125	TMR23	Shackleton NS	14/04/2025	08:30	-65.791	95.427
129	TMR24	Shackleton NS	15/4/2025	11:27	-65.441	95.513
130	TMR25	Shackleton NS	15/4/2025	15:05	-65.299	95.513
145	CTD103	Continental slope	20/4/2025	19:04	-63.954	97.216
146	CTD104	Seamount	24/4/2025	3:48	-60.587	101.219

7. Trace Metals & Isotopes (AAS 4630)

7.7 Data Management

All preliminary data will be published through the Australian Antarctic Data Centre (AADC) (<https://data.aad.gov.au/>) following standard AADC procedures, and subject to the moratorium of 2 years. All trace metal data will also be published in the GEOTRACES Process Study 'GPpr17'.

7.8 Acknowledgments

We would like to express our gratitude towards the organisational body that realised this voyage, both the Voyage Management Team on board and the team at the AAD in Kingston, Tasmania. The TMR team would like to thank the Serco crew, DVLs, Sci ops, door holders (Noah, Claire, Jo, Taryn, Dave, Ilaria, etc) for all their help during the voyage. A special thanks to those who helped when there were technical problems with the TMR.

7.9 References

- Cutter, Gregory, Casciotti, Karen, Croot, Peter, Geibert, Walter, Heimbürger, Lars-Eric, Lohan, Maeve, Planquette, Hélène, van de Flierdt, Tina (2017) Sampling and Sample-handling Protocols for GEOTRACES Cruises. Version 3, August 2017. Toulouse, France, GEOTRACES International Project Office, 139pp. & Appendices. DOI: <http://dx.doi.org/10.25607/OBP-2>
- Rees, C., L. Pender, K. Sherrin, C. Schwanger, P. Hughes, S. Tibben, A. Marouchos, and M. Rayner. 2018. Methods for reproducible shipboard SFA nutrient measurement using RMNS and automated data processing. *Limnol. Oceanogr: Methods* [doi:10.1002/lom3.10294](https://doi.org/10.1002/lom3.10294)
- Rees, C., Janssens, J., Sherrin, K., Hughes, P., Tibben, S., McMahon, M., McDonald, J., Camac, A., Schwanger, C. and Marouchos, A., (2021) "Method for Reproducible Shipboard Segmented Flow Analysis Ammonium Measurement Using an In-House Reference Material for Quality Control." *Frontiers in Marine Science*, 8. [doi:10.3389/fmars.2021.581901](https://doi.org/10.3389/fmars.2021.581901)

8. Atmospheric processes (AAS 4631)

Ship-based team: Jakob Pernov (Lead), Kelsey Barber, Chelsea Bekemeier, Tom Paynter, Salvatore Sodano

Onshore team: Marc Mallet, Ruhi Humphries, Simon Alexander, Alain Protat, Joel Alroe, Jay Mace, Branka Miljevic, Jessie Creamean

8.1 Background

The Southern Ocean (SO) is one of the most remote and cloud-covered regions on Earth (McCoy et al., 2015; McFarquhar et al., 2021) and is considered one of the few remaining pristine environments left on Earth (Hamilton et al. 2014). In this region, the aerosol–cloud interactions are primarily driven by natural processes (Mallet et al., 2023). Natural, marine gaseous emissions (e.g., dimethyl sulfide) are emitted into the atmosphere where they undergo a series of physical and chemical transformations to form aerosol particles, which occurs especially during spring and summer (Kang et al., 2025; Mallet et al., 2025), when favorable conditions (such as increased light availability, warmer temperatures, and reduced sea ice formation), lead to enhanced biological emissions (Joge et al., 2024). Depending on their size and chemical composition, aerosol particles can become activated as cloud condensation nuclei (CCN), thus forming the initial seeds for liquid clouds. Other particles which are emitted directly from the oceanic or ice-free terrestrial environments, can act as ice nucleating particles (INPs), depending on their morphology and composition, thus initiating the formation of ice crystals and thus mixed-phase clouds or MPCs (Kanji et al., 2017). In the Southern Ocean, these mixed-phase clouds are common and consist of both liquid droplets and ice particles (Xi et al., 2022). Aerosols can directly affect the climate by scattering and absorbing solar radiation. Aerosols also indirectly interact with clouds by modifying key cloud microphysical properties, such as the droplet radius, number concentration, and cloud phase (i.e., liquid or ice containing or mixed phase clouds) (Bellouin et al., 2020). These indirect interactions can suppress or alter precipitation patterns (Ackerman et al., 2000) and influence cloud albedo (the fraction of solar radiation that is reflected back into space) (Bellouin et al., 2020; Christensen et al., 2024), resulting in a cooling effect on the climate (Boucher, 2015; Intergovernmental Panel on Climate Change (IPCC), 2023).

Earth system models face significant challenges in accurately representing clouds over the SO, which is largely due to misrepresentation of aerosol sources and processes leading to cloud formation and phase. Satellite observations and cloud-resolving models remain limited due to sparse validation data, primarily from ship and aircraft campaigns (Reddington et al., 2017; Stier, 2016). Increased measurements of aerosol processes spatially and seasonally are crucial for reducing uncertainties in estimating aerosol forcing in climate models (Fiddes et al., 2024; Reddington et al., 2017; Virtanen et al., 2025). However, due to its remoteness and extreme weather conditions, there remains a significant lack of observations of aerosols, clouds and precipitation over the SO (Humphries et al., 2023; Mallet et al., 2023). For these reasons, ship-based observations over the SO during all seasons are particularly valuable, providing a unique opportunity to study the interaction between aerosols and cloud (Hamilton et al., 2014; Humphries et al., 2021). While most voyages occur during the summer, there are limited observations during austral autumn. The Denman Marine Voyage is uniquely situated to add to

8. Atmospheric processes (AAS 4631)

the dearth of aerosol, cloud, and precipitation measurements in the SO and Antarctic coast during this understudied time of year.

The purpose of the atmospheric measurements is to increase the spatial and temporal coverage in the Southern Ocean/Antarctic region and investigate the sources, processes, and fate of cloud forming particles and to provide detailed information about low level clouds and katabatic winds as well as relating cloud and precipitation properties. Together this provides information about the sources of cloud forming aerosol particles, the meteorological conditions conducive for cloud formation, and how these effects precipitation patterns in a data sparse region and time of year.

8.2 Methods and Equipment

In the Air Chemistry Laboratory (Figure 16), in the bow of RSV *Nuyina*, detailed measurements of aerosol particle microphysical properties including particle number size distribution (PNSD) using a Scanning Mobility Particle Sizer (SMPS; TSI Shoreview, MN, USA), total particle number concentration using a Condensation Particle Counter (CPC, TSI Shoreview, MN, USA) model number 3776 and 3772 for diameters greater than 3 and 10 nm, respectively, and Cloud Condensation Nuclei (CCN) number concentration using a CCN counter (CCNc; Droplet Measurement Technologies Longmont, CO, USA) were undertaken continuously since leaving Hobart.

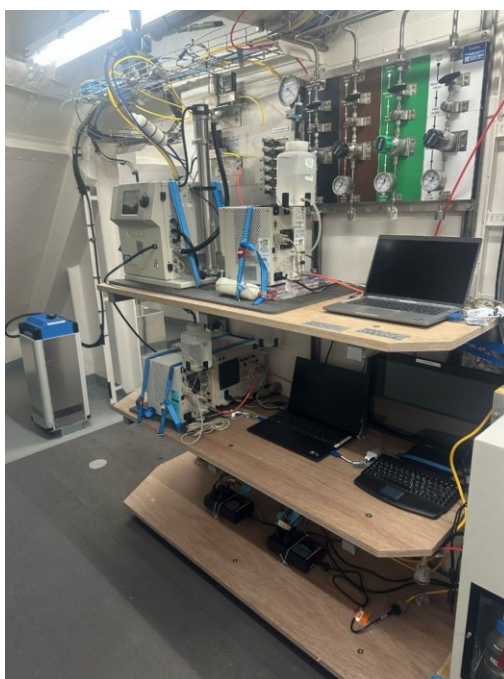


Figure 16: Aerosol instrumentation installed inside the Air Chemistry Laboratory at the bow of the ship.

On Deck 9 behind the Observation lounge (Figure 17), 0.2 μm (INP) and 0.4 μm (DNA) filters were collected which will be analysed for INP concentrations and aero-DNA content, respectively. These filters sampled air continuously for 24 hours, with flow maintained by pumps and flow meters at around 15-20 litres per minute. Blank filters (both INP and DNA) were sampled once a week and will be used for blank correction. Post-sampling, these filters were carefully extracted

8. Atmospheric processes (AAS 4631)

into petri dishes in Dry Lab 1 and stored at $-80\text{ }^{\circ}\text{C}$. In addition to the filters, INP team also collected CTD and wet well water and Sterivex samples to be analysed for Chlorophyll-a and DNA, respectively. Samples were shipped frozen and will be analysed back at Colorado State University. Insights will help elucidate INP sources across the Southern Ocean and their impact on ice fraction in MPCs.



Figure 17: Sampling apparatus for INP and aero-DNA filter collection. Pictured is Chelsea Bekemeier (right) and Jakob Boyd Pernov (left) during a filter exchange.

Profiles of the vertical thermodynamic structure (temperature, pressure, relative humidity, wind direction/speed) were measured using radiosondes attached to weather balloons (Figure 18), which were launched from the helideck every at 00 and 12 UTC, weathering permitting (wind less than 40 knots).

8. Atmospheric processes (AAS 4631)



Figure 18: Launch of a radiosonde attached to a weather balloon. Pictured is Kelsey Barber.

Remote sensing instrumentation located on Deck 8 and 11 measured microphysical cloud/precipitation properties including brightness temperatures across 35 channels, precipitable water, and liquid water path using the microwave radiometer (MWR). The MWR also provides retrieved atmospheric profiles of temperature, relative humidity, and precipitable water. Precipitation properties were measured with a microrain radar (MRR) which measures reflectivity, vertical velocity, and doppler spectra properties. Cloud properties were detected with the Micropulse lidar (MPL) which measures co-polarization power and cross-polarization power.

8.3 Challenges

The Deman Marine Voyage represents the first scientific mission of RSV *Nuyina* and the first use of the Air Chemistry Laboratory and the Meteorological Laboratory so it is expected that hurdles and challenges would have to be overcome in the beginning.

In the Air Chem Lab, we began the voyage by troubleshooting flowrate issues for several instruments. For instance, we suspect the SMPS experienced flowrate variation due to the inherent movement and vibrations of the ship in the rough sea state. The data are still valid and useable although with a little added uncertainty. The CPC3776 malfunctioned and therefore had unstable flowrates, after reconfiguring the internal tubing we were able to remedy the issues.

The MRR, located originally on Deck 11 portside, was detecting interference from one of the ship's radars. This was easily diagnosed with help from the crew and the instrument was relocated to one of the radars blind spots at the rear of the ship.

The Atmospheric Team experienced their fair share of struggles due to the harsh conditions of the Southern Ocean. Throughout the voyage, and especially during the transit south, there were

8. Atmospheric processes (AAS 4631)

periods where the weather conditions caused the radiosonde launches to be cancelled due to the strong winds (> 40 kts).

During certain periods, the INP filters were saturated with water and snow, which is less than optimal although we are hopeful the filters can still be successfully analysed.

During certain operations, the ship was required to be facing certain directions regardless of the wind direction. When the wind was coming from the stern, the Air Chemistry Laboratory sampled pollution from the ship's exhaust. This is an unfortunate and sometimes unavoidable aspect of shipborne atmospheric science.

After several weeks at sea, the main air blower in the Air Chemistry Laboratory, which brings ambient air into the main sampling line at high flowrates, experienced an unexplained drop in the flowrate. After completing a thorough diagnostic inspection, we discovered a filter was clogged with sea salt. After cleaning, the main blower was operational again.

8.4 Preliminary Results

During the voyage, a preliminary amount of data processing and investigation was undertaken. Interesting conditions in terms of the cloud and precipitation data were observed from March 17th to 19th. The conditions on the 17th started with low-level, likely mixed phase, cumulus clouds. We decided to launch radiosondes every 3 hours based on those conditions and observed a layer of katabatic, dry air move over the ship. The katabatic layer is essentially free tropospheric air and was directly above the cloud layer inviting interesting questions about how this layer and the cloud interact (i.e. are the cloud forming aerosols coming from the free tropospheric air?) The katabatic layer persisted into the night, and technician Tom Paynter continued radiosonde launches through the night. By the 18th, the katabatic layer was no longer present, and we continued routine launches at 0 UTC and 12 UTC. The morning was free of low-level clouds, but we were in offshore flow meaning that the air masses were coming from the continent. On the 19th, there were multiple cloud decks, the bottom of which was a low-level cumulus cloud layer. On this day we continued 3 hourly launches from 0 UTC to 12 UTC when the conditions shifted to more frontal conditions. Via remote sensing data, we observed precipitation events from the low-level clouds and potential seeder-feeder events, where precipitation is initiated in higher-altitude clouds which then feed into the lower-level mixed phase clouds.

We recently observed an interesting nanoparticle event with our aerosol instrumentation. On the 10th April, we observed the largest concentration of nanoparticles (< 30 nm) so far on the voyage (Figure 19). The entire team jumped into action; we launched weather balloons every three hours, capturing the beginning and end of the event. We collaborated with the biology team to collect samples of seawater for chlorophyll analysis every hour. We successfully measured the whole event without pollution from the ship's exhaust thanks to the help of voyage management. We have observed similar events but not of this magnitude. Our early interpretation is that air masses spent time near the coast several days prior which picked up gaseous marine emissions, were lifted to high altitudes where the lower temperatures and high sunlight allowed gases to be photochemically oxidized and form particles, then the air masses descended to surface where they were measured (Figure 20). This event even influenced the number of cloud-forming particles despite their small size.

8. Atmospheric processes (AAS 4631)

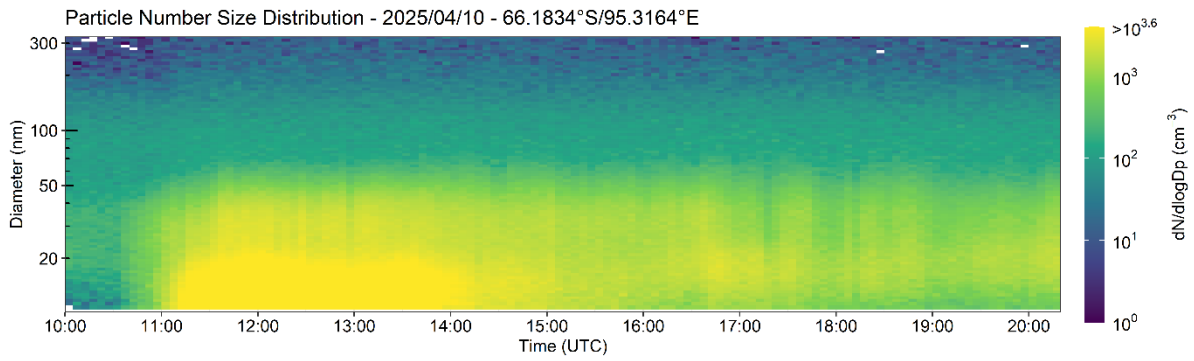


Figure 19: Time series of the particle number size distribution with time on the x axis, particle diameter in nanometres on the y axis, and concentration depicted in the colour bar.

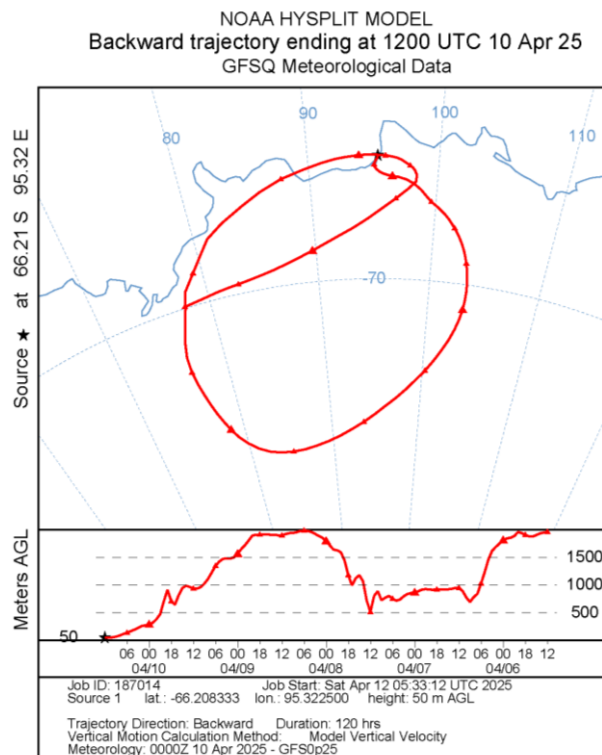


Figure 20: Air mass back trajectories with the geographic location in the top panel and the vertical location on the bottom panel.

8. Atmospheric processes (AAS 4631)

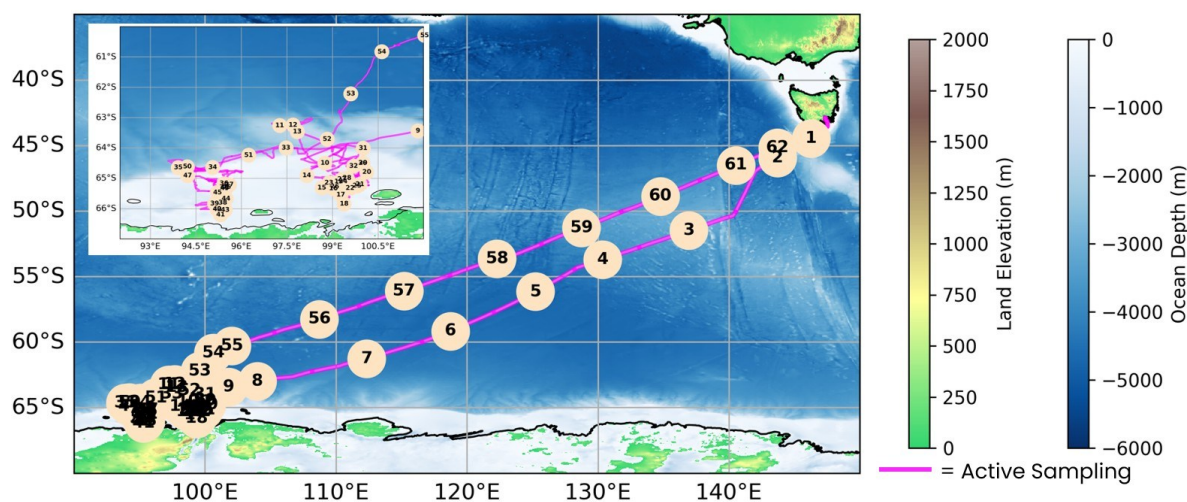


Figure 21: Location of INP and DNA sample collection (beige circles, sample number within the circle) periods (active sampling indicated by pink along the ship track) with an inlay (top left) of samples between 60 °S to 67 °S and 91 °E to 102 °E, for clarity. Bathymetry and topography imagery are reproduced using the General Bathymetric Chart of the Oceans 2024 data. Land elevation and ocean depth data are from 2024 (last accessed June 2025). Land elevation is coloured from 0 to 2000 m (Land Elevation colour bar, m) and ocean depth is coloured from 0 m to -6000 m depth (Ocean Depth colour bar, m).

The Atmospheric Team had a successful voyage, although not without our own trials and tribulations that accompany practicing polar science. Throughout the voyage, the Atmospheric Team successfully:

- Collected 62 filters for ice nucleating particles and 62 filters for aero-DNA filters (Figure 21)
- Launched 155 weather balloons (Figure 22)
- Collected 78 water and 75 Sterviex DNA samples
- Collected 62 continuous days of precipitation and cloud based remote sensing and aerosol microphysical data.

8. Atmospheric processes (AAS 4631)

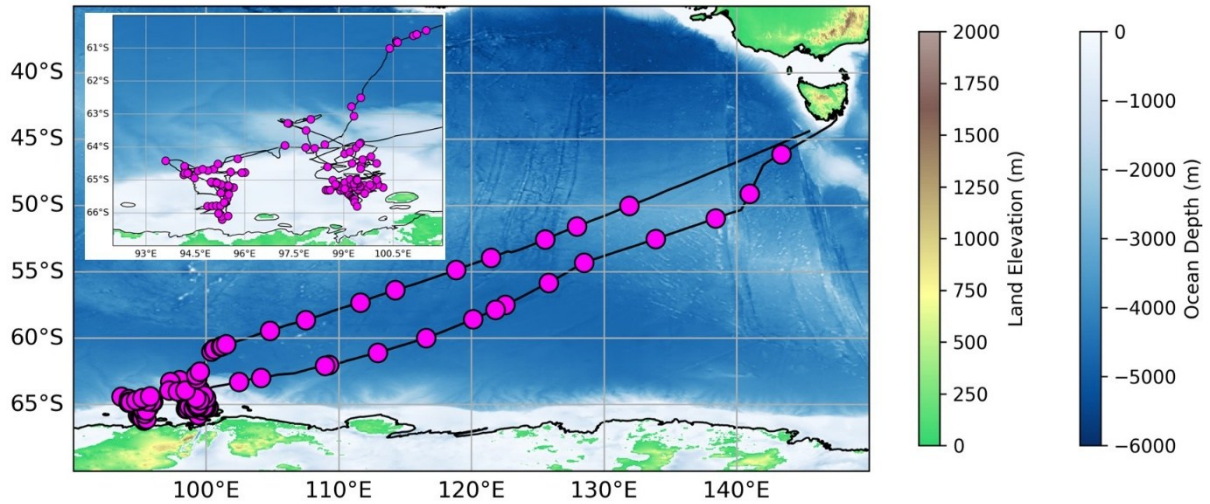


Figure 22: Radiosonde launch locations (pink circles) along the ship track (black line) with an inlay (top left) of radiosonde launches between 60°S to 67°S and 91°E to 102°E, for clarity. Refer to Figure 21 for bathymetry and topography data.

8.5 Data Management

All preliminary data will be published through the Australian Antarctic Data Centre (AADC) (<https://data.aad.gov.au/>) following standard AADC procedures, and subject to the moratorium of 2 years.

8. Atmospheric processes (AAS 4631)

8.6 Acknowledgements

The atmospheric science team would like to extend our gratitude to all of the SERCO crew members for an efficient and safe voyage. Special thanks to the bridge for clearance in radiosonde launches/filter changes. Thanks to IRs Stephen Boddy, Trent Stephens, and Daza (Darrel Barker) for assisting in radiosonde launches.

Michael Santarossa, Nick Burleigh, and Ant (Anthony Hay) are acknowledged for their excellent technical and IT support throughout the voyage.

Ruhi Humphries, Marc Mallet, Branka Miljevic, and Joel Alroe are acknowledged for their excellent onshore support for the aerosol instrumentation. Ruhi Humphries is also acknowledged for excellent support and guidance in installing the aerosol instrumentation.

Jay Mace, Luis Ackerman, Simon Alexander are acknowledged for their support with installing and maintaining the remote sensing equipment.

We would also like to thank to Dr. Annie Foppert, Dr. Laura Herraiz-Borreguero, and the other oceanographers for helping to organize the CTD collections. Another special thanks to Anton Rocconi and the zooplankton team for allowing us to use their facilities to take surface (4 m) and 9 m water samples. Thank you to Dr. Delphine Lannuzel and the biology team for assistance in chlorophyll-a samples.

Much gratitude to all of the Science Leads, the Deputy Voyage Leaders, and the Australian Antarctic Division for a well-executed voyage. A special thank you to Dr. Simon Alexander at AAD for and Dr Marc Mallet (UTAS) for coordinating the Atmosphere deployment of DMV.

This project received grant funding from the Australian Government as part of the Antarctic Science Collaboration Initiative program, under the Australian Antarctic Program Partnership, ASCI000002. This project received grant funding from the Australian Research Council Discovery Project scheme (DP240100389).

8.7 References

- Ackerman, A. S., Toon, O. B., Taylor, J. P., Johnson, D. W., Hobbs, P. V., & Ferek, R. J. (2000). Effects of Aerosols on Cloud Albedo: Evaluation of Twomey's Parameterization of Cloud Susceptibility Using Measurements of Ship Tracks. *Journal of the Atmospheric Sciences*, 57(16), 2684–2695. [https://doi.org/10.1175/1520-0469\(2000\)057<2684:EOAOCA>2.0.CO;2](https://doi.org/10.1175/1520-0469(2000)057<2684:EOAOCA>2.0.CO;2)
- Bellouin, N., Quaas, J., Gryspeerdt, E., Kinne, S., Stier, P., Watson-Parris, D., Boucher, O., Carslaw, K. S., Christensen, M., Daniau, A.-L., Dufresne, J.-L., Feingold, G., Fiedler, S., Forster, P., Gettelman, A., Haywood, J. M., Lohmann, U., Malavelle, F., Mauritsen, T., ... Stevens, B. (2020). Bounding Global Aerosol Radiative Forcing of Climate Change. *Reviews of Geophysics*, 58(1), e2019RG000660. <https://doi.org/10.1029/2019RG000660>
- Boucher, O. (2015). Atmospheric Aerosols. In *Atmospheric Aerosols: Properties and Climate Impacts* (pp. 9–24). Springer Netherlands. https://doi.org/10.1007/978-94-017-9649-1_2

8. Atmospheric processes (AAS 4631)

- Christensen, M. W., Wu, P., Varble, A. C., Xiao, H., & Fast, J. D. (2024). Aerosol-induced closure of marine cloud cells: Enhanced effects in the presence of precipitation. *Atmospheric Chemistry and Physics*, 24(11), 6455–6476. <https://doi.org/10.5194/acp-24-6455-2024>
- Fiddes, S. L., Woodhouse, M. T., Mallet, M. D., Lamprey, L., Humphries, R. S., Protat, A., Alexander, S. P., Hayashida, H., Putland, S. G., Miljevic, B., & Schofield, R. (2024). The ACCESS-AM2 climate model strongly underestimates aerosol concentration in the Southern Ocean, but improving it could be problematic for the modelled climate system. *EGUsphere*, 2024, 1–38. <https://doi.org/10.5194/egusphere-2024-3125>
- Hamilton, D. S., Lee, L. A., Pringle, K. J., Reddington, C. L., Spracklen, D. V., & Carslaw, K. S. (2014). Occurrence of pristine aerosol environments on a polluted planet. *Proceedings of the National Academy of Sciences*, 111(52), 18466–18471. <https://doi.org/10.1073/pnas.1415440111>
- Humphries, R. S., Keywood, M. D., Gribben, S., McRobert, I. M., Ward, J. P., Selleck, P., Taylor, S., Harnwell, J., Flynn, C., Kulkarni, G. R., Mace, G. G., Protat, A., Alexander, S. P., & McFarquhar, G. (2021). Southern Ocean latitudinal gradients of cloud condensation nuclei. *Atmospheric Chemistry and Physics*, 21(16), 12757–12782. <https://doi.org/10.5194/acp-21-12757-2021>
- Humphries, R. S., Keywood, M. D., Ward, J. P., Harnwell, J., Alexander, S. P., Klekociuk, A. R., Hara, K., McRobert, I. M., Protat, A., Alroe, J., Cravigan, L. T., Miljevic, B., Ristovski, Z. D., Schofield, R., Wilson, S. R., Flynn, C. J., Kulkarni, G. R., Mace, G. G., McFarquhar, G. M., ... Griffiths, A. D. (2023). Measurement report: Understanding the seasonal cycle of Southern Ocean aerosols. *Atmospheric Chemistry and Physics*, 23(6), 3749–3777. <https://doi.org/10.5194/acp-23-3749-2023>
- Intergovernmental Panel on Climate Change (IPCC) (Ed.). (2023). The Earth's Energy Budget, Climate Feedbacks and Climate Sensitivity. In *Climate Change 2021 – The Physical Science Basis: Working Group I Contribution to the Sixth Assessment Report of the Intergovernmental Panel on Climate Change* (pp. 923–1054). Cambridge University Press; Cambridge Core. <https://doi.org/10.1017/9781009157896.009>
- Joge, S. D., Mahajan, A. S., Hulswar, S., Marandino, C. A., Galí, M., Bell, T. G., & Simó, R. (2024). Dimethyl sulfide (DMS) climatologies, fluxes, and trends – Part 1: Differences between seawater DMS estimations. *Biogeosciences*, 21(19), 4439–4452. <https://doi.org/10.5194/bg-21-4439-2024>
- Kang, L., Marchand, R., Ma, P.-L., Huang, M., Wood, R., Jongebloed, U., & Alexander, B. (2025). Impacts of DMS Emissions and Chemistry on E3SMv2 Simulated Cloud Droplet Numbers and Aerosol Concentrations Over the Southern Ocean. *Journal of Advances in Modeling Earth Systems*, 17(5), e2024MS004683. <https://doi.org/10.1029/2024MS004683>
- Kanji, Z. A., Ladino, L. A., Wex, H., Boose, Y., Burkert-Kohn, M., Cziczo, D. J., and Krämer, M. (2017). Overview of Ice Nucleating Particles. *Meteorological Monographs* (58), 1.1-1.33. <https://doi.org/10.1175/AMSMONOGRAPHS-D-16-0006.1>

8. Atmospheric processes (AAS 4631)

- Mallet, M. D., Humphries, R. S., Fiddes, S. L., Alexander, S. P., Altieri, K., Angot, H., Anilkumar, N., Bartels-Rausch, T., Creamean, J., Dall'Osto, M., Dommergue, A., Frey, M., Henning, S., Lannuzel, D., Lapere, R., Mace, G. G., Mahajan, A. S., McFarquhar, G. M., Meiners, K. M., ... Woodhouse, M. T. (2023). Untangling the influence of Antarctic and Southern Ocean life on clouds. *Elementa: Science of the Anthropocene*, 11(1), 00130. <https://doi.org/10.1525/elementa.2022.00130>
- Mallet, M. D., Miljevic, B., Humphries, R. S., Mace, G. G., Alexander, S. P., Protat, A., Chambers, S., Cravigan, L., DeMott, P. J., Fiddes, S., Harnwell, J., Keywood, M. D., McFarquhar, G. M., McRobert, I., Moore, K. A., Mynard, C., Osuagwu, C. G., Ristovski, Z., Selleck, P., ... Williams, A. (2025). Biological enhancement of cloud droplet concentrations observed off East Antarctica. *Npj Climate and Atmospheric Science*, 8(1), 113. <https://doi.org/10.1038/s41612-025-00990-5>
- McCoy, D. T., Burrows, S. M., Wood, R., Grosvenor, D. P., Elliott, S. M., Ma, P. L., Rasch, P. J., & Hartmann, D. L. (2015). Natural aerosols explain seasonal and spatial patterns of Southern Ocean cloud albedo. *Sci. Adv.*, 1.
- McFarquhar, G. M., Bretherton, C. S., Marchand, R., Protat, A., DeMott, P. J., Alexander, S. P., Roberts, G. C., Twohy, C. H., Toohey, D., Siems, S., Huang, Y., Wood, R., Rauber, R. M., Lasher-Trapp, S., Jensen, J., Stith, J. L., Mace, J., Um, J., Järvinen, E., ... McDonald, A. (2021). Observations of Clouds, Aerosols, Precipitation, and Surface Radiation over the Southern Ocean: An Overview of CAPRICORN, MARCUS, MICRE, and SOCRATES. *Bulletin of the American Meteorological Society*, 102(4), E894–E928. <https://doi.org/10.1175/BAMS-D-20-0132.1>
- Reddington, C. L., Carslaw, K. S., Stier, P., Schutgens, N., Coe, H., Liu, D., Allan, J., Browse, J., Pringle, K. J., Lee, L. A., Yoshioka, M., Johnson, J. S., Regayre, L. A., Spracklen, D. V., Mann, G. W., Clarke, A., Hermann, M., Henning, S., Wex, H., ... Zhang, Q. (2017). The Global Aerosol Synthesis and Science Project (GASSP): Measurements and Modeling to Reduce Uncertainty. *Bulletin of the American Meteorological Society*, 98(9), 1857–1877. <https://doi.org/10.1175/BAMS-D-15-00317.1>
- Stier, P. (2016). Limitations of passive remote sensing to constrain global cloud condensation nuclei. *Atmospheric Chemistry and Physics*, 16(10), 6595–6607. <https://doi.org/10.5194/acp-16-6595-2016>
- Virtanen, A., Joutsensaari, J., Kokkola, H., Partridge, D. G., Blichner, S., Seland, Ø., Holopainen, E., Tovazzi, E., Lipponen, A., Mikkonen, S., Leskinen, A., Hyvärinen, A.-P., Zieger, P., Krejci, R., Ekman, A. M. L., Riipinen, I., Quaas, J., & Romakkaniemi, S. (2025). High sensitivity of cloud formation to aerosol changes. *Nature Geoscience*, 18(4), 289–295. <https://doi.org/10.1038/s41561-025-01662-y>
- Xi, B., Dong, X., Zheng, X., & Wu, P. (2022). Cloud phase and macrophysical properties over the Southern Ocean during the MARCUS field campaign. *Atmospheric Measurement Techniques*, 15(12), 3761–3777. <https://doi.org/10.5194/amt-15-3761-2022>

9. Hydroacoustics

Science Acoustic Officers: Jasmin Wells (Geoscience Australia), Katharina Hochmuth (University of Tasmania) and Jo Whittaker (University of Tasmania)

Acoustic Officers: Alison Herbert (AAD) and Floyd Howard (AAD)

9.1 General introduction

Hydroacoustic measurements allow the mapping of the seafloor as well as the subseafloor. The continental shelf of Antarctica remains poorly mapped (Dorschel et al. 2022), however high-resolution information of the seafloor morphology is required for navigational as well as scientific purposes. The seafloor geomorphology and subseafloor geometry of the Denman/Shackleton continental shelf has been formed by the advancing and retreating icesheet over multiple geological periods. The detailed maps of the geomorphology report on paleo ice extent (e.g. Consortium et al. 2014), flow style and direction (e.g. Carson et al. 2017; Smith et al. 2019) as well as subglacial meltwater pathways (Fernandez et al. 2018). Large scale structures such as cross-shelf glacial troughs serve as potential pathways for warmer modified circumpolar deep water to reach the grounded ice sheet (e.g. Nitsche et al. 2017). However, the resolution of the currently available bathymetric data can only rudimentarily display the complexity of the (sub)seafloor environment introducing large uncertainties to modern ocean and ice sheet modelling studies and limit our understanding of previous retreat scenarios (e.g. Consortium et al. 2014).

Prior to this expedition only very limited data from the Denman/Shackleton continental shelf has been available. The available data has been collected by Japanese, US, French and German vessels, whereas only the data collected on PS-140/141 (2023-24 season) covers sections of the continental shelf and included sub-bottom profiling data. During planning, these datasets have been collated and assessed for their quality. Whereas older data has been freely available, the German PS-140/141 dataset has been obtained from the Alfred Wegener Institute through a data sharing agreement and will only be used for operational support given the ongoing moratorium on this dataset.

Three scientists from the science party were assigned to assist the AAD Acoustic Officers with watch keeping, data cleaning, site selections and providing advice and support for science operations. The Science Acoustic Officers held the responsibility for the sub-bottom profiling, including marine mammal mitigation.

Hydroacoustic data were acquired throughout the entire voyage in accordance with the Environmental Authorisation to operate multibeam echosounder and sub-bottom profiling instruments throughout the Denman Marine Voyage.

Our main objective was to acquire multibeam bathymetry and sub-bottom profiler data in the Denman Marine area for scientific, navigational and operational purposes. Particularly to:

1. Characterise and understand seabed and subseafloor features that record past ice sheet behaviour, provide pathways for warm ocean water to flow up onto the continental shelf and undermine ice shelves, and provide habitats for benthic marine invertebrates.

9. Hydroacoustics

The dataset was additionally used to:

2. Inform sediment coring, rock dredge, towed camera and benthic trawl site selections. Commonly, this equipment cannot be deployed until the seabed is well characterised.

Hydroacoustic instruments were activated on 2 March 2025 when out of the Australian Exclusive Economic Zone (EEZ) and all Biologically Important Areas (BIAs). The hydroacoustic instruments were deactivated on 30 April 2025, prior to entering the Southern right whale migration BIA.

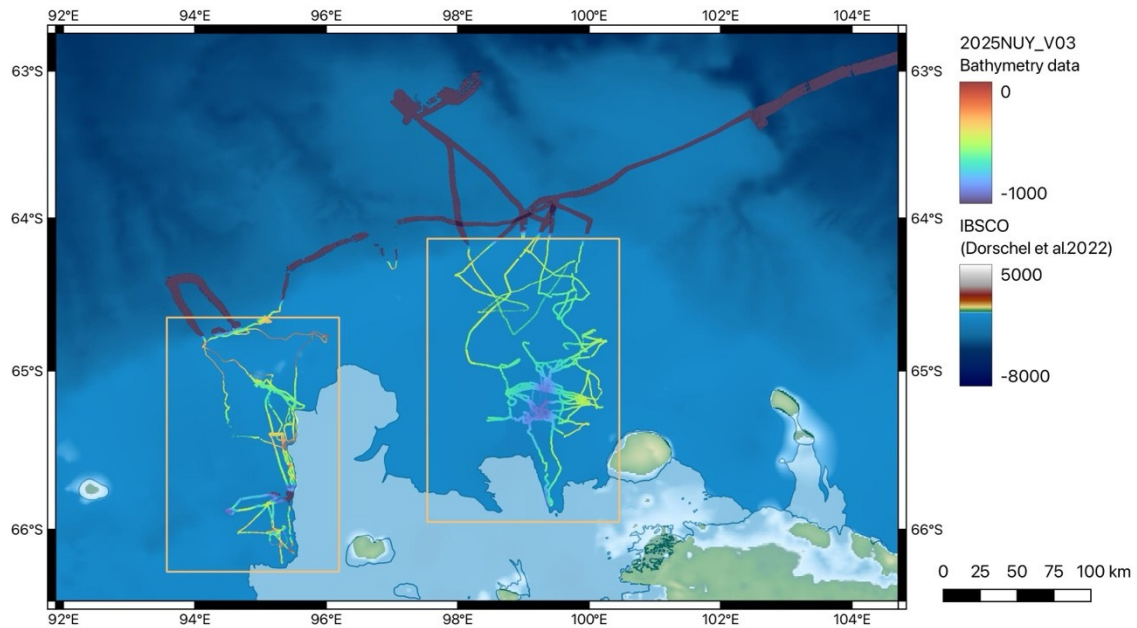


Figure 23: Overview of the data acquired during 202425030 in the main research area.

9.2 Multibeam Echosounders

During DMV bathymetric data were acquired using two multibeam echosounders to map the seafloor geometry. The hull mounted EM122 deep water multibeam echosounder which operates at 10.5 to 13.5 kHz and the drop-keel EM712 shallow water multibeam echosounder which operates at 40 to 100 kHz.

The Kongsberg Deepwater EM122 Multibeam Echosounder and the Kongsberg Shallow water EM712 Multibeam Echosounder are both 1° x 1° vessel-mounted multibeam sonar that transmits narrow beams of sound in a wide swath across the ship to produce detailed 3D maps of the seabed. The multibeam echosounders receive array measures two-way travel time and elevation angle of many reflected echo returns across the transmitted signal to make up to 2 x 432 for the EM122 and 2 x 400 for the EM712 simultaneous depth measurements per transmit (ping) cycle. The receiver array simultaneously measures the intensity of the reflected echo returns, which is referred to as backscatter or the seabed image. This backscatter provides an indication of the relative hardness and composition of the seabed. For further information refer to the *RSV Nuyina - Kongsberg Deep Water EM122 Multibeam Echosounder overview* (Content Manager Reference: D21/136879) and the *RSV Nuyina – Kongsberg Shallow Water EM712 Multibeam Echosounder overview* (Content Manager Reference: D21/136880), both available on request.

The EM712 is the preferred multibeam echosounder to use in the shallower areas of the continental shelf. During this voyage, the EM712 was used only while the drop keel was in working position (i.e. fully deployed), in water depths <1000 m and in appropriate ice conditions as determined by the Master. As a result, the drop-keel could not always be in operational position (Figure 24).

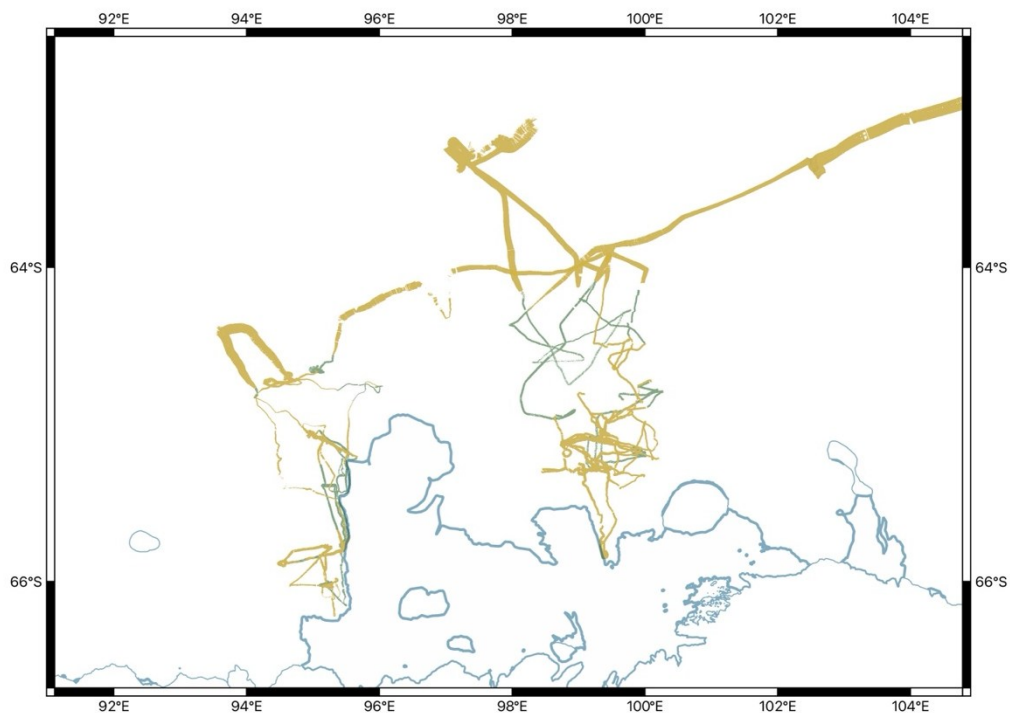


Figure 24: Overview on the collected hydroacoustic data with the data collected by the EM122 in yellow and the data collected on the EM712 in green

9. Hydroacoustics

9.2.1 Data acquisition and processing

Bathymetric data were acquired throughout the entire voyage in Seafloor Information System (SIS) software version 4.3.3 for EM712 and version 4.3.2 for EM122. For immediate use of the data for operational purposes, the hydroacoustics team as well as volunteers cleaned the data throughout their shifts. This included assessing the individual swaths for erroneous readings and signal introduced by other hydroacoustic instruments. Data acquisition during the night in the research area was particularly difficult and often had to be restricted to small areas due to prevailing sea-ice conditions and other operational constraints.

During the voyage EM122 and EM712 data were processed using QPS Qimera v2.5.3 following the procedure in *Acoustic Support – Qimera for Bathymetry Data Processing* (Content Manager Reference: D25/5851[v1]). As the multibeam data was collected across multiple UTM zones the Qimera project coordinate system for both was WGS84/World Mercator + EGM2008 height (EPSG6893). A total of 2,009 files of multibeam were acquired and processed during the voyage. For further information on multibeam data acquisition and processing please refer to *202425030 DMV Acoustics Voyage Report*, available on request.

Mapping occurred in the research areas, the central Denman region (Figure 25) and the western region off the Shackleton Ice Shelf (Figure 26).

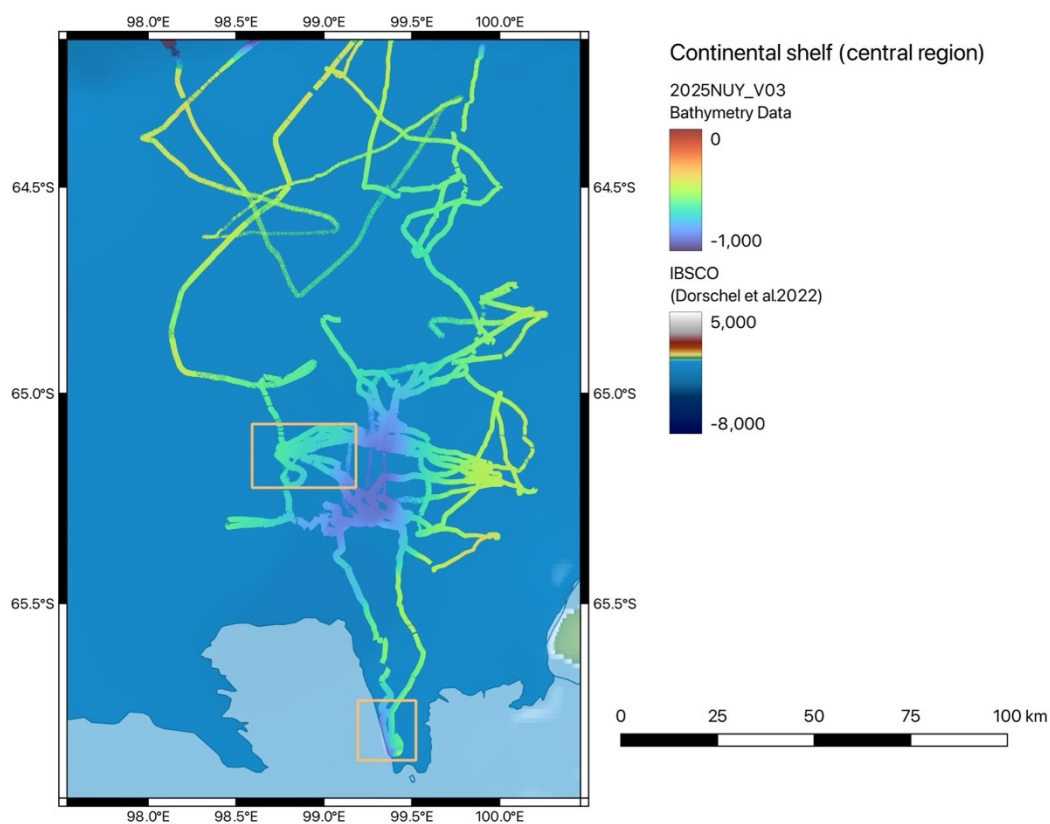


Figure 25: Bathymetric data collected in the central Denman Area; orange boxes refer to close-up images highlighted further in the report (Figure 28, Figure 29).

9. Hydroacoustics

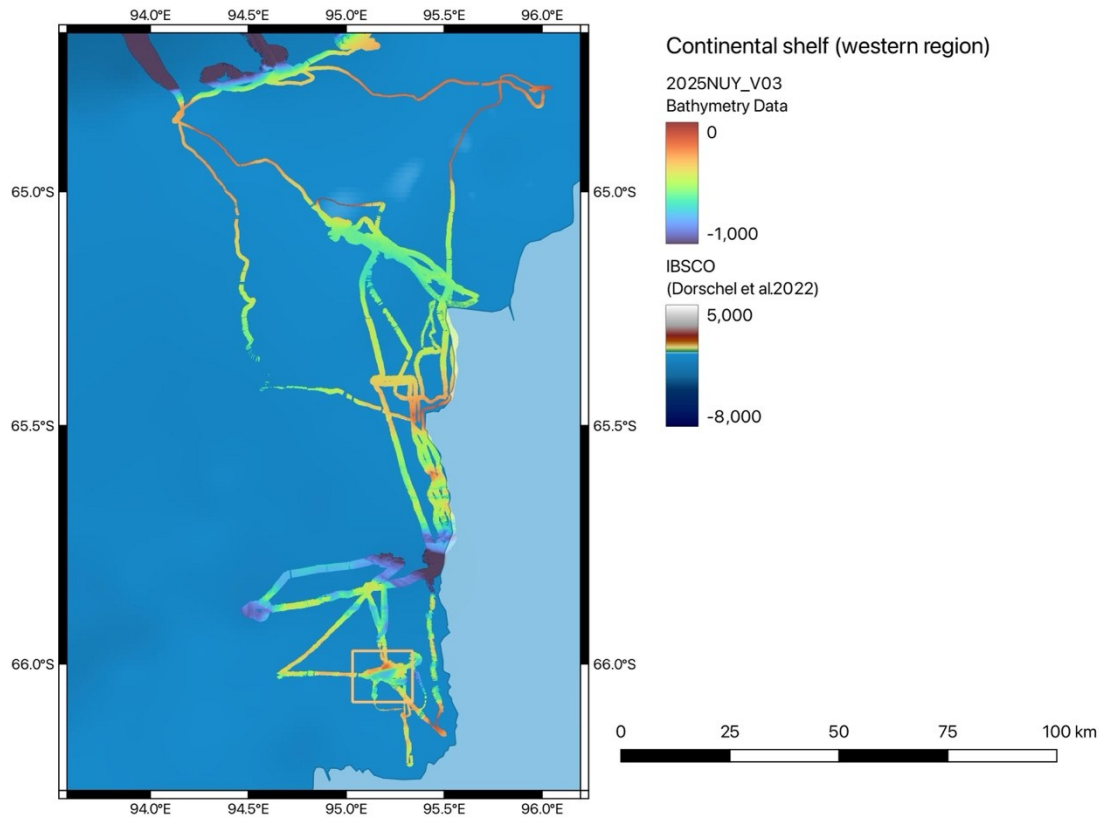


Figure 26: Bathymetric data collected in the western area off the Shackleton Ice Shelf, orange box indicates close-up images highlighted further in the report (Figure 30).

9.2.2 Sound velocity profiles

During the voyage expendable bathythermograph (XBT), moving vessel profiler (MVP), and CTD data were processed into sound speed profiles using HydrOffice Sound Speed Manager Software following the procedure in *SOP – RSV Nuyina - Sound Speed Manager* (Content Manager Reference: D22/22389[v1]). Sound speed profiles were used for ray tracing by EM122 and EM712. We launched 57 XBTs, deployed 105 CTDs (see CTD Deployments section), and obtained 733 MVP profiles (Figure 27).

9. Hydroacoustics

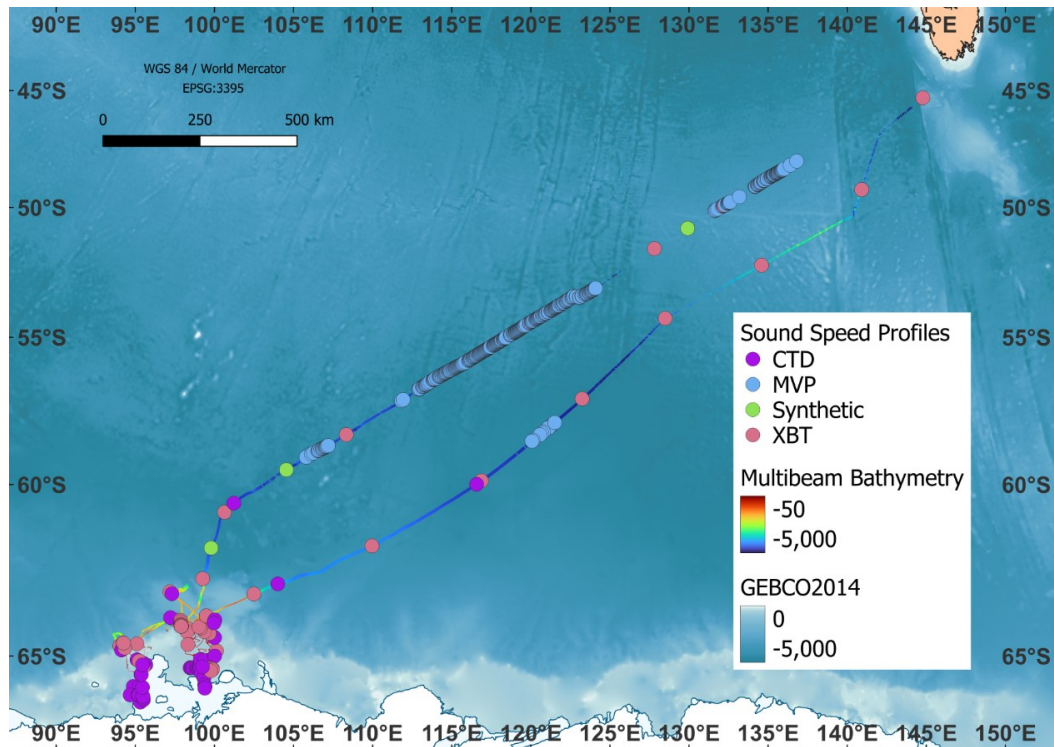


Figure 27: Overview of the location and sources for sound speed profiles.

9.2.3 Preliminary results

During the entire voyage we collected 59,544 km² of multibeam data. Geomorphologically, we mapped glacial and ocean current related features in the deep sea, the continental rise and slope as well as on the continental shelf. Due to the exceptional sea ice conditions during the early part of the voyage, we were able to map large areas of previously completely unmapped seafloor in the central Denman region. The outer and middle shelf in this area was dominated by iceberg scours as well as underlying megascale glacial lineations, which can be used to reconstruct paleo-ice drainage in this rapidly changing region (Figure 28).

9. Hydroacoustics

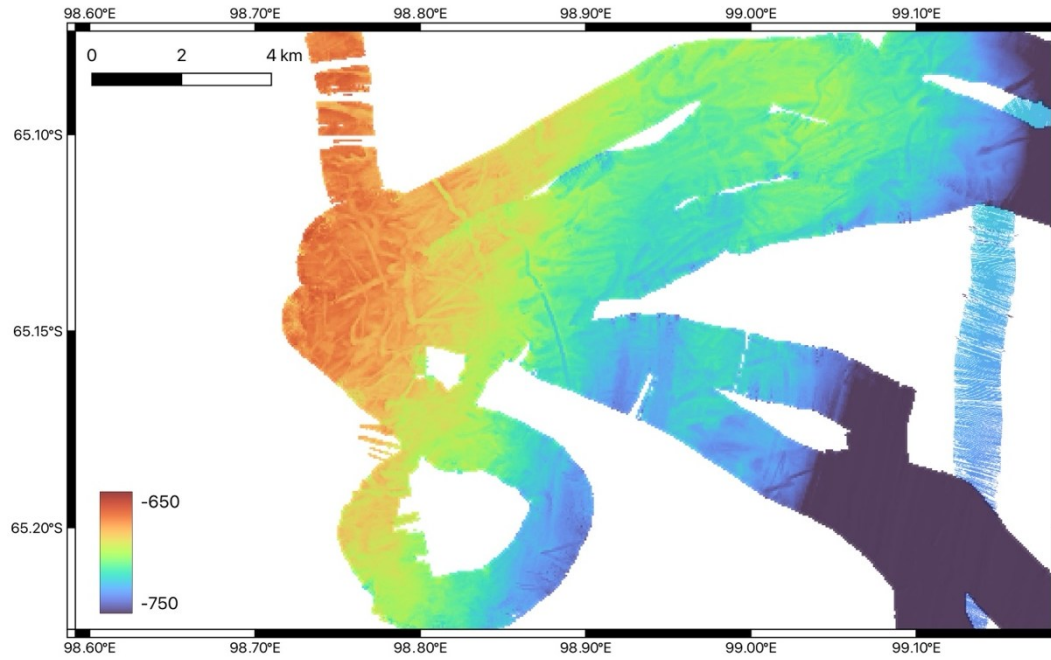


Figure 28: Example bathymetric dataset from the middle shelf of the central Denman region. This data has been collected with the EM712 and has been cleaned on board. The depth between 650 m and 700 m is dominated by iceberg scours, whereas the deeper areas display megascale lineations

The optimal sea-ice conditions during the voyage allowed passes close to the current iceshelf edge to map below the currently floating ice (Figure 29). We mapped for approximately 90 km along the edge of the Denman Glacier and approximately 110 km along the edge of the Shackleton Ice Shelf. Our beams reached 850 m underneath the Denman Glacier and 300 m underneath the Shackleton Ice Shelf.

9. Hydroacoustics

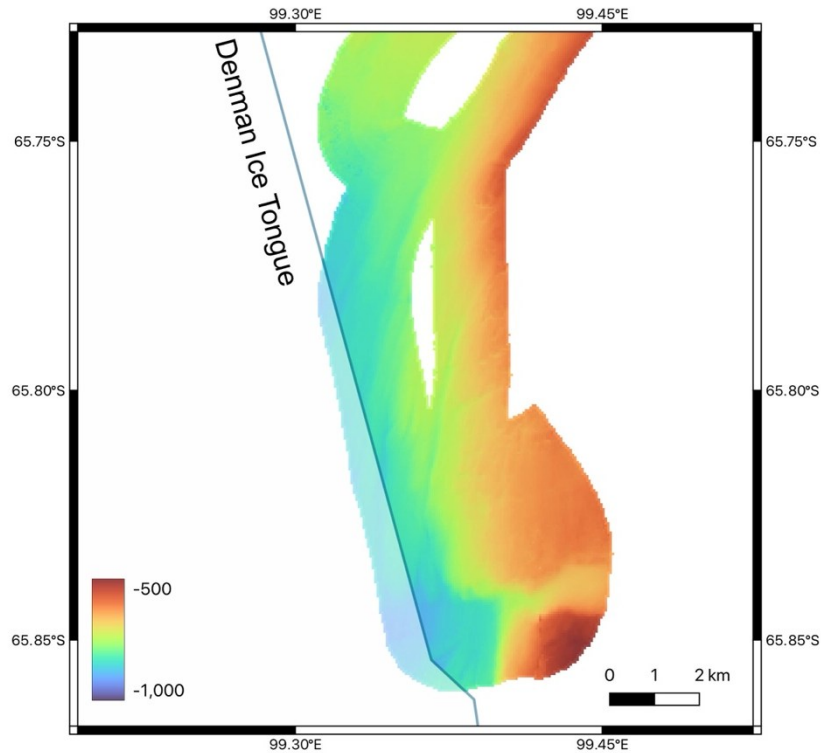


Figure 29: Bathymetric data collected below the Denman Ice Tongue.

The western research area off the Shackleton Ice Shelf presents as highly structured with multiple deep channels of up to 1200 m and shallow areas of up to 85 m. Multiple small basins were identified in the inner and middle continental shelf. Some of these basins displayed especially varied morphology (Figure 30) and allowed the deployment of various scientific equipment in close vicinity, which normally required larger transits. The steep northern edge of the basin was chosen for a rock dredging attempt, whereas the flatter area around 600 m depth was photographed with the towed camera and sampled by the beam trawl. The deepest part of the basin was cored with the Kasten corer and serves as a deployment site for the oceanic mooring, which will be recovered on return to this area.

9. Hydroacoustics

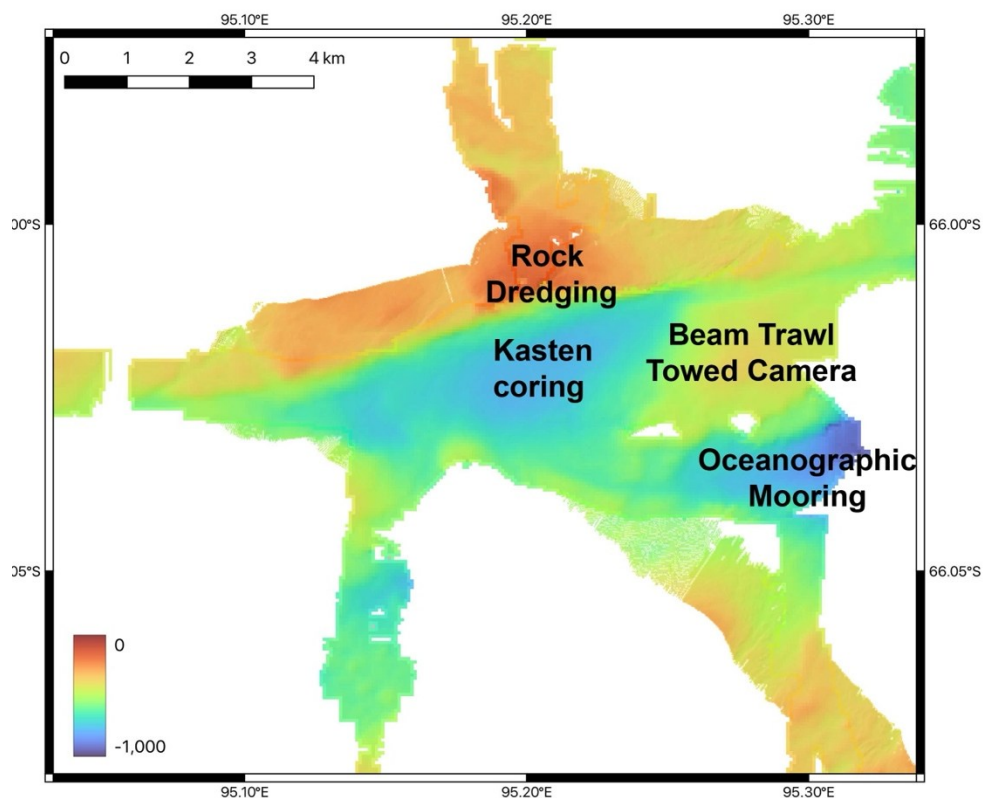


Figure 30: Small inner shelf basin the science operations in this area included the deployment of an oceanographic mooring, rock dredging, towed camera, beam trawling and sediment coring.

9.3 Sub-bottom profiling

Sub-bottom profiling data were fundamental in informing site selection for the Kasten core and multicore science operations. The sub-bottom profiler is used to image geological layering in the shallow seabed (tens of metres). Due to the over compaction by the ice load of the sediments deposited on the continental shelf the penetration of the sub bottom profiler signal is often limited.

9.3.1 SBP Data acquisition:

Data were acquired through the Kongsberg TOPAS PS18 Sub Bottom Profiler version 3.2. software. The system operates at frequencies of 3.5 kHz and is mounted on the hull of RSV *Nuyina*. The position of the sensor is factored into the navigational position displayed.

Two file types, .raw and .seg were acquired in the Kongsbeg TOPAS PS18 Sub Bottom Profiler software. The raw files contained the raw SBP data while the seg files contained the processed data which were obtained by using real-time processing for optimal data display for example, Time Variable Gain (TVG), pulse type and other filter settings. Overall, we collected 470 sub bottom profile lines during the whole voyage.

9. Hydroacoustics

After testing some settings during transit, we decided on the below settings for the rest of the voyage. These settings changed occasionally depending on the weather and depth of the seafloor:

- Pulse Form: LFM
- Auto gain unchecked, value updated as required. The gain was usually set to low values while in the Denman region and increased while transiting to, between and from the Denman region. In poor weather conditions, the gain was increased to improve the signal to noise ratio.
- Data collection was difficult under certain weather conditions. The ship's heading, prevailing wave and wind directions, aeration/bubbles in the water column and occasional interference with other acoustic systems on board limited the resolution of the SBP. This made watchkeeping and bottom-tracking challenging.

While stationary for science operations we would reduce the ping rate of the SBP to allow other acoustic instruments to ping freely and stopped logging data. For further information on the Topas acquisition settings used during 202425030 refer to the *202425030 DMV Acoustics Voyage Report*.

For ad-hoc site selection and visualisation, we used Kingdom Seismic Suite (IHS). We imported the rudimentary processed datasets from the Kongsberg system (see Kasten Cores section).

9.3.2 SBP data processing:

Preliminary processing of SBP data was conducted in SonarWiz version 8.2.3 by Chesapeake Technology. Data were split into three projects while onboard containing data from the Denman research area and transit. Metadata and comments on how the data were processed were recorded. Due to time constraints not all SBP data could be processed while onboard. Processing will continue back onshore and provided to the AADC when finished for archiving. Some files were not processed because of stationary data or where the seabed was lost.

Settings to process the files included bottom tracking, adjusting duration and threshold as needed and manual picking where required, applying Auto TVG and adjusting the scalar as necessary, blanking the water column and applying settings from the detected sea floor. The figures below (Figure 31 to Figure 34) are examples of some of the data we have processed through SonarWiz.

9.3.3 Preliminary results

The sub-bottom profiler data collected during the Denman Marine Voyage depicts various geomorphological features. Data collected on the slope and on the Bruce Rise shows exceptional penetration to up to 200 m into the subsurface. Along the slope various channel levee deposits were imaged (Figure 31) preserving the shelf to slope transport from the Denman Glacier and Shackleton Ice Shelf. As expected, the data acquisition on the continental shelf itself proved challenging. The outer and middle shelf consist of older seaward dipping sediment packages, which have been heavily compacted by previously extended ice sheets (Figure 34). The inner shelf showed a variable structure with exposed basement at the seafloor (e.g. Figure

9. Hydroacoustics

34) as well as smaller and larger basins, which are around 900 m deep and show a sedimentary package of up to 40 m (Figure 31 and Figure 32). The horizontal layering of the sediment suggests a sedimentation environment, which is undisturbed by ocean currents and mass wasting events potentially in a previous sub-ice setting.

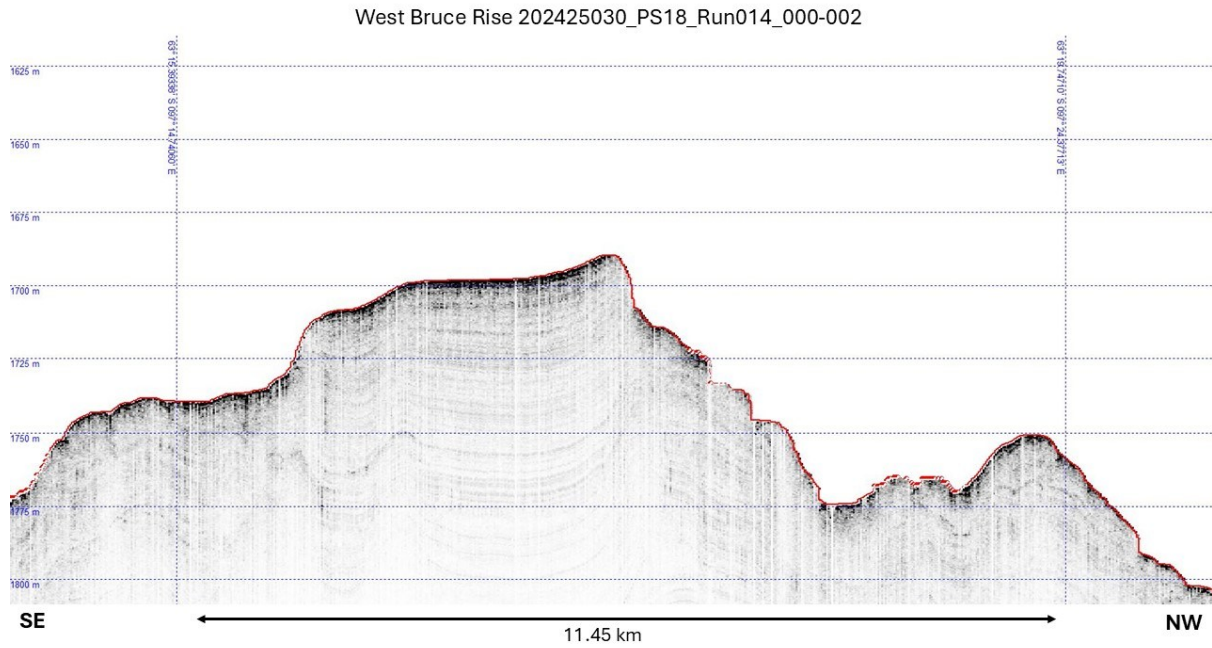


Figure 31: KC01 site. Example of channel levee.

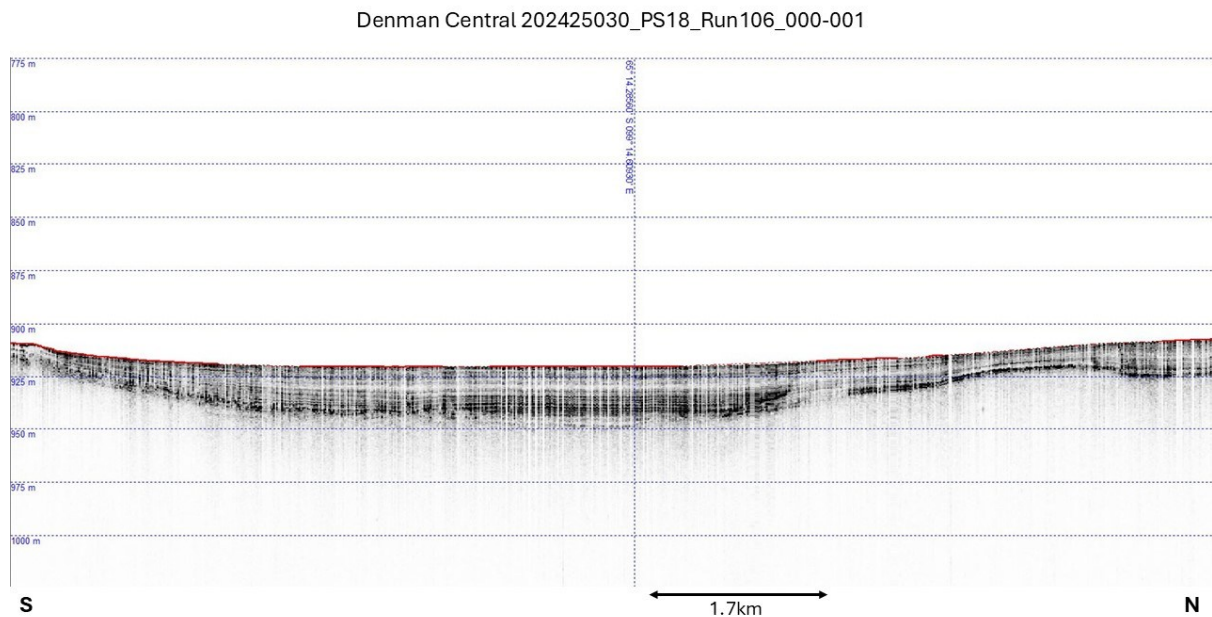


Figure 32: KC02 & KC03 sites. Example of inner shelf sedimentary basin.

9. Hydroacoustics

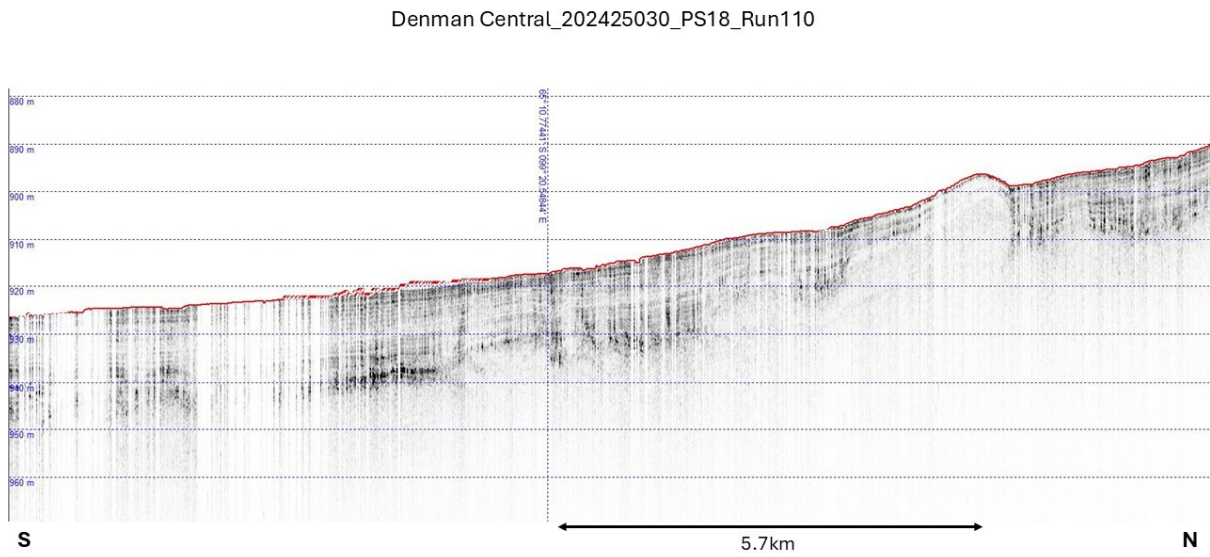


Figure 33: MC04 site. Example of inner shelf sedimentary basin.

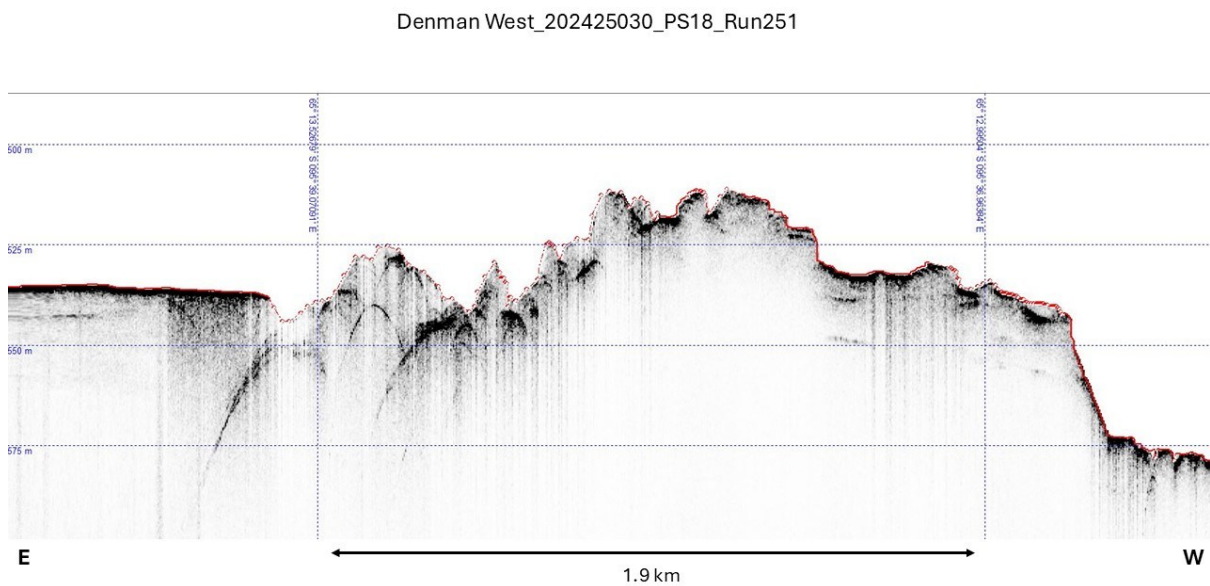


Figure 34: MC08 site. Heavily consolidated sediment towards the east followed by outcropping basement.

9.4 Mitigation for cetaceans

Within the self-assessment and for the purpose of the voyage, cetacean is defined as including all whales and dolphins. Marine mammal observations were coordinated by the Science Acoustic Officers. A total of 27 expeditioners from the science party volunteered to be cetacean

9. Hydroacoustics

observers during the voyage and were trained by a qualified MMO on board (Jasmin Wells). Training included a presentation and a practical session on how to use reticule binoculars to measure distance, bearing of the cetacean and location of the bridge wings. The ‘SOP for Cetacean Monitoring for TOPAS18 survey during DMV on RSV Nuyina’ was made available to all volunteers via DiRT along with the presentation and additional reference sheets.

In accordance with the self-assessment, bridge officers kept a look out for cetaceans as part of their ongoing watch duties. Every 30 minutes the Science Acoustics Officer would eLog no whales were observed by the bridge if the bridge had not raised an alarm. When either a whale or dolphin were spotted by the bridge, the officer on duty called Science Operations and the on-duty Science Acoustics Officer coordinated two trained observers to take over observations on the bridge. Overall, the communication between bridge and acousticians worked well and the mitigation process was initiated swiftly with immediate shut-down of the instrument and dedicated observers on the bridge within minutes. In case that there were no science party members available for marine mammal observations, the hydroacoustic team undertook their own observations.

Opportunistic cetacean sightings from expeditioners were also reported via the voyage WhatsApp group. These sightings were recorded and the same mitigation measures outlined in the self-assessment were implemented.

Each trained observer had a radio, reticule binoculars and a reference sheet for observations. From Science Operations, the Science Acoustics Officer checked in with the observers every 15 minutes and recorded in eLog. The role of the observers was to constantly scan the ocean around the vessel and look for visual cues either with the naked eye and then confirm with the binoculars. If a cetacean was sighted, the observers would radio the Science Acoustics Officer and provide relevant information for the Science Acoustics Officer to record in the Whale Sightings eLog. The information is also provided to the Acoustics Officer to determine if and what mitigation was required.

A total of 53 cetacean sightings were reported during the voyage and at least 100 cetaceans observed, the majority being whales. Species able to be identified were Minke, Humpback, Orca and Pilot. A total of 11 shutdowns were required due to cetaceans being within 500 m of the vessel i.e. the shut-down zone (Table 19).

Table 19: Summary of SBP shutdowns as a result of cetaceans sighted within 500 m of the vessel.

Date	Time (UTC)	Latitude (DD)	Longitude (DD)	Sighting number	Species	Mitigation
08/03/2025	17:55:32	-63.101	103.394	1	Whale no ID	Shut-down
14/03/2025	03:30:08	-64.223	99.019	2	Whale no ID	Shut-down
05/04/2025	00:12:38	-64.840	94.139	2	Humpback	Shut-down
05/04/2025	01:21:37	-64.843	94.129	1	Humpback	Shut-down
05/04/2025	04:14:25	-65.029	94.826	1	Minke	Shut-down

9. Hydroacoustics

06/04/2025	00:31:09	-65.087	94.967	2	Orca	Shut-down
15/04/2025	02:12:14	-65.068	95.019	2	Minke	Shut-down
15/04/2025	08:40:31	-65.361	95.313	2	Whale no ID	Shut-down
16/04/2025	09:34:56	-64.821	94.168	1	Minke	Shut-down
26/04/2025	02:53:48	-56.991	112.481	5	Pilot whale	Shut-down
28/04/2025	02:04:59	-52.343	126.129	4	Pilot whale	Shut-down

Cetaceans were mostly sighted in the Denman region near the ice shelf, with a few observed transiting in and out of the region (Figure 35).

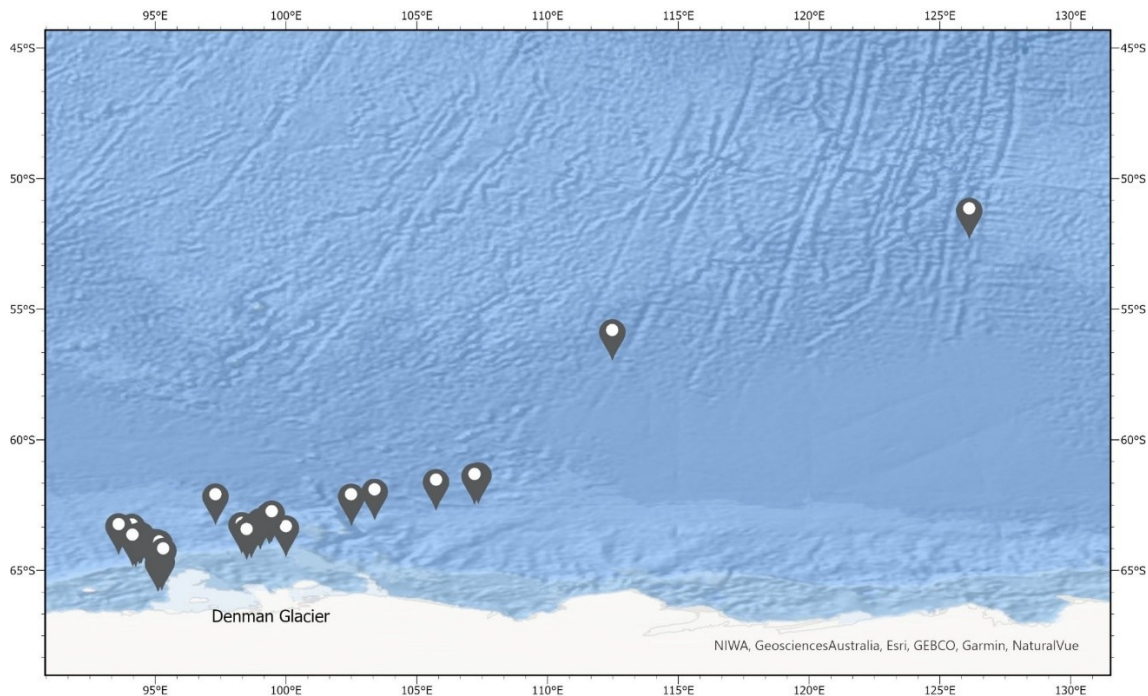


Figure 35: Locations of cetacean sightings and voyage track.

Determining the total number of cetaceans sighted was difficult at times, due to sea state/weather or inconsistencies between surfacing behaviour and blows. The total numbers of cetaceans are indicative and there were most likely more cetaceans present within the same observations.

All SBP protocols were followed in line with the self-assessment produced by Geoscience Australia and University of Tasmania in consultation with the AAD and MNF. The hydroacoustic team are happy to share the self-assessment for the purpose of future research voyages.

9.5 Acoustics Support for Science Operations

For information on how acoustic support was provided for various science operations please refer to 202425030 DMV Acoustics Voyage Report (available on request).

9.6 Data Management

All preliminary data will be published through the Australian Antarctic Data Centre (AADC) (<https://data.aad.gov.au/>) following standard AADC procedures, and subject to the moratorium of 2 years.

9.7 References

- Carson, C. J., Post, A. L., Smith, J., Walker, G., Waring, P., Bartley, R., & Raymond, B. (2017). The seafloor geomorphology of the Windmill Islands, Wilkes Land, East Antarctica: Evidence of Law Dome ice margin dynamics. *Geomorphology*, 292, 1–15. <https://doi.org/10.1016/j.geomorph.2017.04.031>
- Consortium, T. R., Bentley, M. J., Cofaigh, C. Ó., Anderson, J. B., Conway, H., Davies, B., et al. (2014). A community-based geological reconstruction of Antarctic Ice Sheet deglaciation since the Last Glacial Maximum. *Quaternary Science Reviews*, 100, 1–9. <https://doi.org/10.1016/j.quascirev.2014.06.025>
- Dorschel, B., Hehemann, L., Viquerat, S., Warnke, F., Dreutter, S., Tenberge, Y. S., et al. (2022). The International Bathymetric Chart of the Southern Ocean Version 2. *Scientific Data*, 9(1), 275. <https://doi.org/10.1038/s41597-022-01366-7>
- Fernandez, R., Gulick, S., Domack, E., Montelli, A., Leventer, A., Shevenell, A., et al. (2018). Past ice stream and ice sheet changes on the continental shelf off the Sabrina Coast, East Antarctica. *Geomorphology*, 317, 10–22. <https://doi.org/10.1016/j.geomorph.2018.05.020>
- Nitsche, F. O., Porter, D., Williams, G., Cougnon, E. A., Fraser, A. D., Correia, R., & Guerrero, R. (2017). Bathymetric control of warm ocean water access along the East Antarctic Margin. *Geophysical Research Letters*, 44(17), 8936–8944. <https://doi.org/10.1002/2017gl074433>
- Smith, J. A., Graham, A. G. C., Post, A. L., Hillenbrand, C.-D., Bart, P. J., & Powell, R. D. (2019). The marine geological imprint of Antarctic ice shelves. *Nature Communications*, 10(1), 5635. <https://doi.org/10.1038/s41467-019-13496-5>

10. Trawling (AAS 4628)

Team: Jan Strugnell, Nerida Wilson, Sally Lau, Nicola Rodewald, Jesselyn Brown, Christian Pagel, Joshua Lesicar, Rosie Kidman, Frances Perry, Jasmin Wells, Rose Leeger

10.1 Introduction

Marine East Antarctica is the largest under-sampled region of continental shelf around Antarctica. A lack of sampling of benthic life has prevented progress in understanding connectivity and diversity across space and time, not only in the ocean off East Antarctica, but also the Southern Ocean as a whole. Obtaining whole benthic marine invertebrate specimens and their genomic samples from the Denman Glacier region will provide crucial knowledge for understanding diversity, connectivity, and environmental drivers on spatial and temporal scales.

Genomic data contains information about historical connectivity between populations, and past changes in population size. Genomic signatures of benthic marine species living in Antarctica now can, therefore, be used to investigate the past stability and configuration of the Antarctic ice sheet. For example, by testing alternative scenarios of connectivity or significant bottlenecks and expansion in population size, marked changes in available shelf habitat due to ice expansion/contraction could be inferred (e.g. Lau et al. 2023). Investigation of historical signatures of connectivity and population changes will provide insight into the history of the Antarctic Ice Sheet and help in improving projections of the Antarctic contribution to sea level rise. The whole benthic marine invertebrate specimens act as voucher specimens to enable us to match their genetic data to their specific taxonomic and morphological characteristics. Voucher specimens permanently preserve the characteristics by which species and biodiversity patterns can be distinguished and serve as a basis of future studies. The Denman Glacier region is very data poor in terms of fish sampling. Occasional bycatch fish caught in the beam trawl will provide a unique opportunity to identify and sample fish. This will increase our knowledge of Antarctic fish distribution, genetics, age and growth, and ecology. Significant amounts (thousands) of rocks (mostly ice rafted debris) were also caught as bycatch and opportunistically sampled by the geology team on DMV (Rocks (AAS 4630)).

This research will lead to an increased understanding of diversity, connectivity and biogeographic history, and the results will provide important data for conservation, elucidating ice sheet history, and understanding of the forces that have shaped evolution of life in the Southern Ocean.

Our objective was to collect marine benthic invertebrate specimens from the Denman Marine area. We will use these marine benthic invertebrates to:

- Characterise and understand the biogeographic history and current spatio-temporal dynamics of species populations in the Southern Ocean to understand biodiversity trends and build new ecoregional classifications.
- Reconstruct ice sheet history during periods of past rapid environmental changes.
- Provide reference material to support eDNA monitoring activities.
- Fish opportunistically caught as bycatch will enable us to expand knowledge of Antarctic fish distribution, life history, and ecology.

10.2 Methods and equipment

The equipment used was an AAD benthic trawl (research beam trawl) (Figure 36). The research beam trawl is a heavy-duty net attached to a beam that holds the net open next to the seafloor. The main body of the net was a 15 mm mesh, and the cod-end was a 10 mm mesh. Attached to the research beam trawl was a forward and backwards facing camera to visualise the *in-situ* trawl operation. The research beam trawl was deployed from the stern of the ship using a deep towed winch or the trawl winch. Camera operations were only possible when using the deep towed winch.



Figure 36: Beam trawl and winch used for all trawls except trawl D, E, F and G, in which the trawl winch was utilised.

Benthic invertebrates and fish were collected through trawl surveys. Several factors were considered for site selection including depth (target depth ~400-600 m), slope (ideally less than 15 %) and substrate type (minimising rocks and mud). For sites in the Western region, we were guided by previous informative imagery of the benthos from the Shackleton Ice Shelf (project led by Andrew Constable in December-January 2009/10 on RV *Aurora Australis*). Hydroacoustic data was used to inform site selection for all beam trawls. A total of 16 trawls (trawls A to P) were deployed (Figure 37).

10. Trawling (AAS 4628)

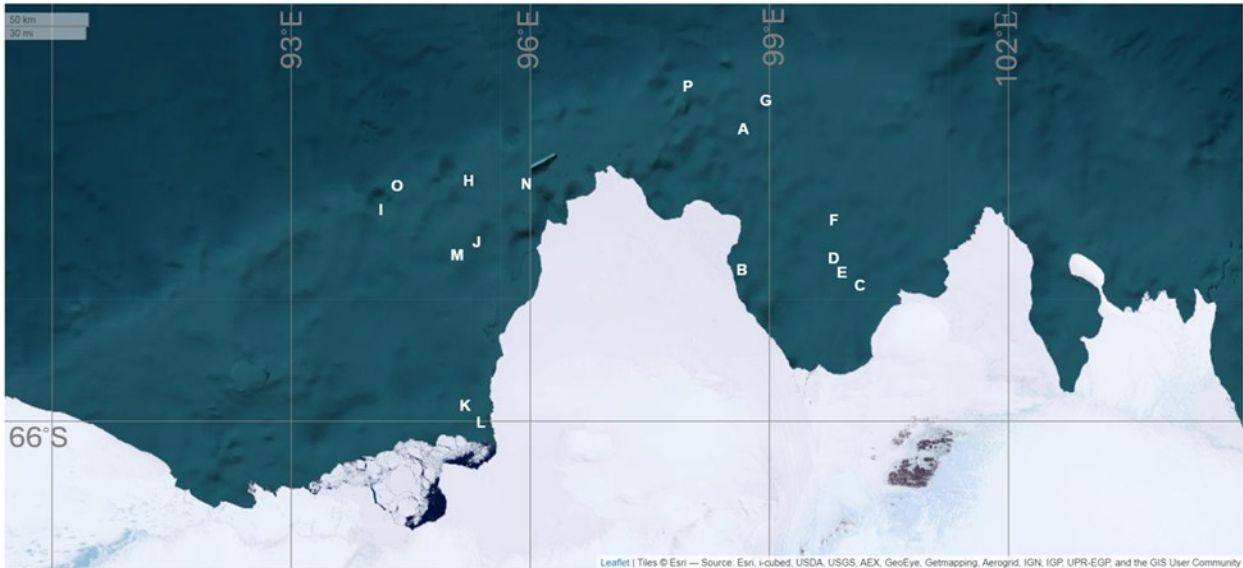


Figure 37: Map indicating benthic trawl sites in the Shackleton Ice Shelf and Denman Glacier region, East Antarctica.

The speed at which the trawl was operated ranged between 1.5 to 1.8 knots. When deployed using the ‘deep towed’ winch the trawl could be ‘porpoised’ to some degree to avoid non target areas and large rocks which were identified using the research beam trawl camera.

After retrieval of the catch on the back deck animals were collected into buckets of seawater and taken to the laboratory for processing. In the laboratory buckets were sieved and initially sorted into higher taxonomic groups (e.g. phyla), before being sorted to lower taxonomic levels, including to species where possible.

Specimens were cleaned with paint brushes and photographed with a unique identification number. Tissue samples from many specimens were collected and stored in either 100 % ethanol, RNAlater or snap frozen in liquid nitrogen for subsequent genetic research. Whole animals were either preserved in 70 % ethanol, 10 % formalin or frozen, enabling their use in future studies. Some dead corals were also retained, in which case they were soaked in freshwater, dried and frozen for transport. Many specimens were preserved individually. After at least three individuals of a species were preserved individually, in many cases several individuals were preserved together in a group and therefore assigned a specimen number to the group. Not all individuals that were collected were kept. In these cases, live animals were returned to the sea as quickly as possible. All squid were returned in this way. It is important to note that the data collected and provided does not represent abundances from each trawl.

Bycatch from trawling included marine fishes which were photographed and opportunistically sampled. Bycatch not sampled, including all skates, rock cod and live fishes not euthanized were returned to the ocean as quickly as possible. Total length, standard length, and stomach content analysis was recorded for dead and euthanized fishes following the CCAMLR bycatch fishing guidelines from fisheries observers. Each of these fishes were photographed individually.

10. Trawling (AAS 4628)

Otoliths from sampled fishes were extracted and dried and will be brought back to Colorado University (CU) Boulder for age and growth analysis. The second otolith will be subsampled and analysed for both trace metal microchemistry analysis and stable isotope analysis at CU Boulder to complete life history characteristics. Lastly, a small subsample of understudied Antarctic fish tissue was collected in 2 mL vials of ethanol and will be sent to Dr. Christopher Jones at NOAA's Antarctic Ecosystem Research Division to add to their fisheries database.

10.3 Preliminary results

Animals were successfully collected in 15 of the 16 trawls which were deployed between 14 March to 21 April 2025 (Table 21). The net tore on trawls C and K during retrieval and some animals were lost from these catches as a result. Trawl P yielded no specimens due to a loose cod end. Winch repairs necessitated that the trawl winch was used from trawls C to E (not the deep tow winch) and no camera footage was available for these trawls. Trawl duration ranged from 2 minutes, 29 seconds (trawl M) to 18 minutes, 7 seconds (trawl A) (Table 21). Trawl depths ranged from 192 m (trawl N) to 770 m (trawl P) (Table 21).

A total of 4,641 individual benthic invertebrates were processed and retained across all trawls (Table 20). After trawl P (which yielded no specimens), the smallest number of specimens were processed from trawl D (n = 84). The largest number of specimens were processed from trawl I (n = 796).

Table 20: Total numbers of benthic invertebrates processed from each trawl.

Trawl ID	Number of animals processed
A	94
B	193
C	95
D	84
E	225
F	172
G	233
H	571
I	796
J	440
K	554
L	384
M	323
N	241
O	236
P	0
Total	4641

10. Trawling (AAS 4628)

Table 21: Benthic trawls deployed during the Denman Marine Voyage

Trawl	Winch (deep tow or trawl)	Camera present	Date (UTC)	On bottom latitude (DD)	On bottom longitude (DD)	On bottom depth (m)	Off bottom latitude (DD)	Off bottom longitude (DD)	Off bottom depth (m)	On bottom time (UTC)	Off bottom time (UTC)	Time on bottom (hr:min: sec)	Comment
A	deep	yes	14/03/25	-64.500	98.795	478	-64.506	98.782	477	08:28:05	08:46:12	0:18:07	
B	deep	yes	19/03/25	-65.145	98.787	639	-65.146	98.801	635	04:35:40	04:46:04	0:10:24	
C	trawl	yes	25/03/25	-65.232	100.167	511	-65.232	100.153	514	03:51:54	04:02:49	0:10:55	net broke
D	trawl	no	27/03/25	-65.204	99.869	484	-65.203	99.873	484	02:58:35	03:03:20	0:04:45	
E	trawl	no	27/03/25	-65.176	99.933	474	-65.174	99.937	473	04:55:03	05:01:58	0:06:55	
F	deep	no	29/03/25	-64.873	99.918	545	-64.874	99.922	543	06:05:32	06:11:19	0:05:47	
G	deep	no	31/03/25	-64.218	99.060	424	-64.223	99.067	426	04:18:21	04:29:37	0:11:16	
H	deep	yes	3/04/25	-64.672	95.083	367	-64.672	95.072	376	09:04:21	09:14:21	0:10:00	
I	deep	yes	5/04/25	-64.837	94.147	280	-64.839	94.138	284	00:02:23	00:13:06	0:10:43	
J	deep	yes	7/4/2025	-65.135	95.267	584	-65.135	95.274	583	06:42:56	06:49:40	0:06:44	
K	deep	yes	9/4/2025	-65.842	95.147	433	-65.842	95.154	444	02:28:14	02:34:42	0:06:28	net broke- large rock
L	deep	yes	11/4/202 5	-66.019	95.280	367	-66.018	95.283	393	07:22:28	07:25:26	0:02:58	towed camera first
M	deep	yes	15/04/25	-65.066	94.994	412	-65.066	94.992	411	02:29:00	02:31:29	0:02:29	
Na	deep	yes	16/04/25	-64.778	95.960	199	-64.778	95.960	199	01:42:55	01:43:14	0:00:19	2 touch down points
Nb	deep	yes	16/04/25	-64.777	95.970	196	-64.777	95.973	192	01:51:07	01:53:59	0:02:52	
Oa	deep	yes	20/04/25	-64.799	94.236	383	-64.800	94.240	375	02:10:10	02:13:48	0:03:38	2 touch down points
Ob	deep	yes	20/04/25	-64.801	94.242	373	-64.801	94.247	372	02:16:54	02:22:25	0:05:31	
P	deep	yes	21/04/25	-64.192	98.037	764	-64.192	98.042	771	08:09:07	08:15:03	0:05:56	cod end broke

10. Trawling (AAS 4628)

Benthic invertebrates were collected from 14 phyla (Figure 38). The largest number of lots were processed from the phyla Echinodermata (n = 928), followed by Arthropoda (n = 441), Annelida (n = 237), and Mollusca (n = 192).

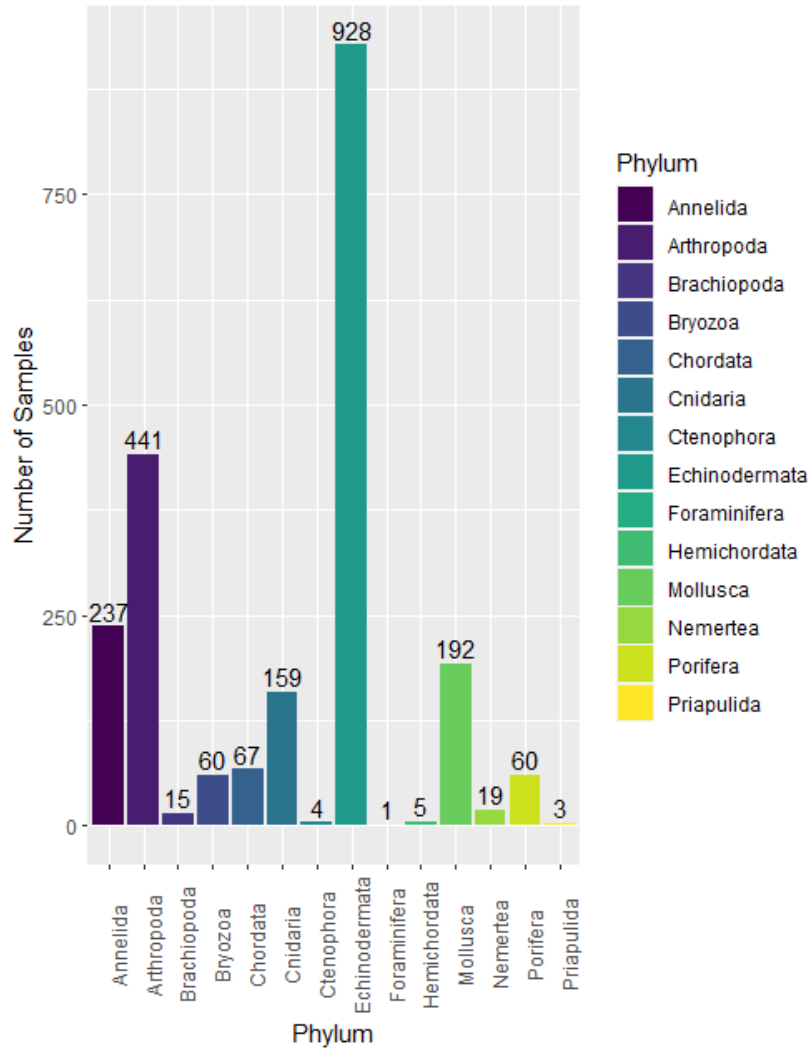


Figure 38: Bar plot indicating the number of lots (that include individual or multiple samples) that were processed from each phylum during the voyage.

10. Trawling (AAS 4628)

The class Polychaeta (n = 218) dominated the numbers of lots processed within Annelida (Figure 39), followed by Sipuncula (n = 15) and Clitellata (n = 4).

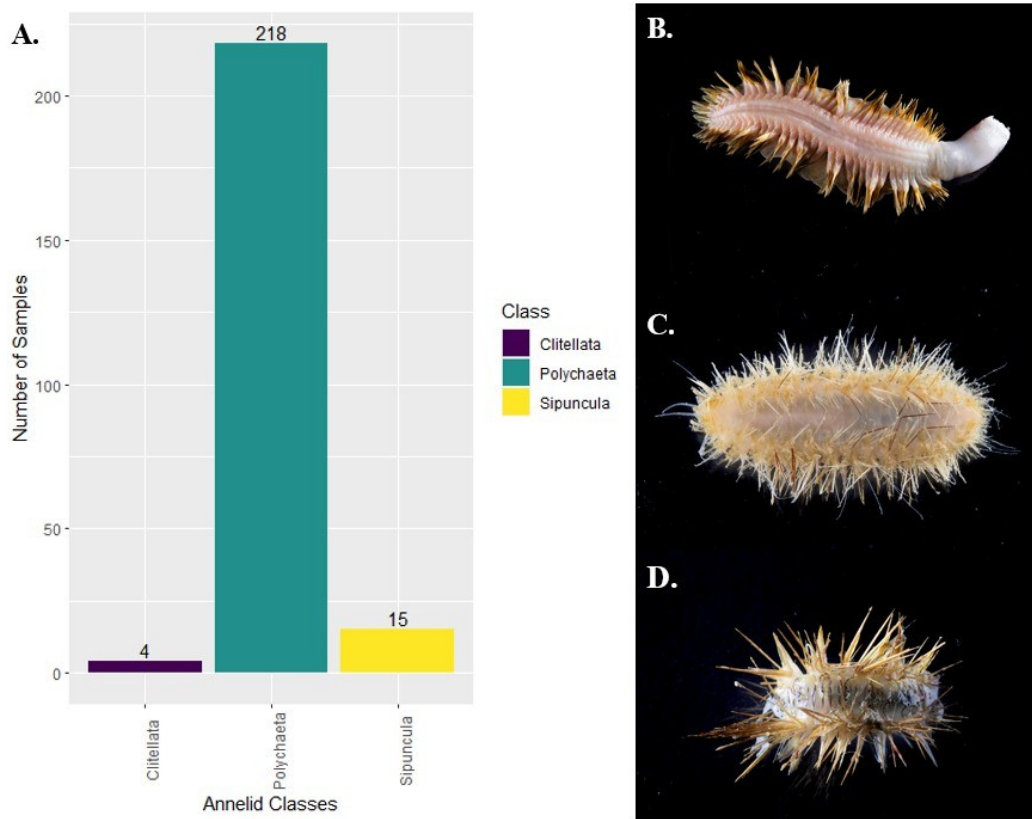


Figure 39: A) Bar plot indicating the number of lots (that include individual or multiple samples) in each class of the phylum Annelida that were processed. Classes included Clitellata, Polychaeta, Sipuncula. Examples of the specimens collected included scales worms, e.g. B) *Eulagisca gigantea*, C) *Laetmonice producta*, D) *Antarctinoe ferox*. Photo credit: Pete Harmsen, AAD.

10. Trawling (AAS 4628)

Malacostracans (n = 290) comprised the majority of the arthropod lots processed, followed by Pycnogonida (n = 132), Thecostraca (n = 6), and Copepoda (n = 5). There were a small number of unidentified crustaceans (n = 8) (Figure 40).

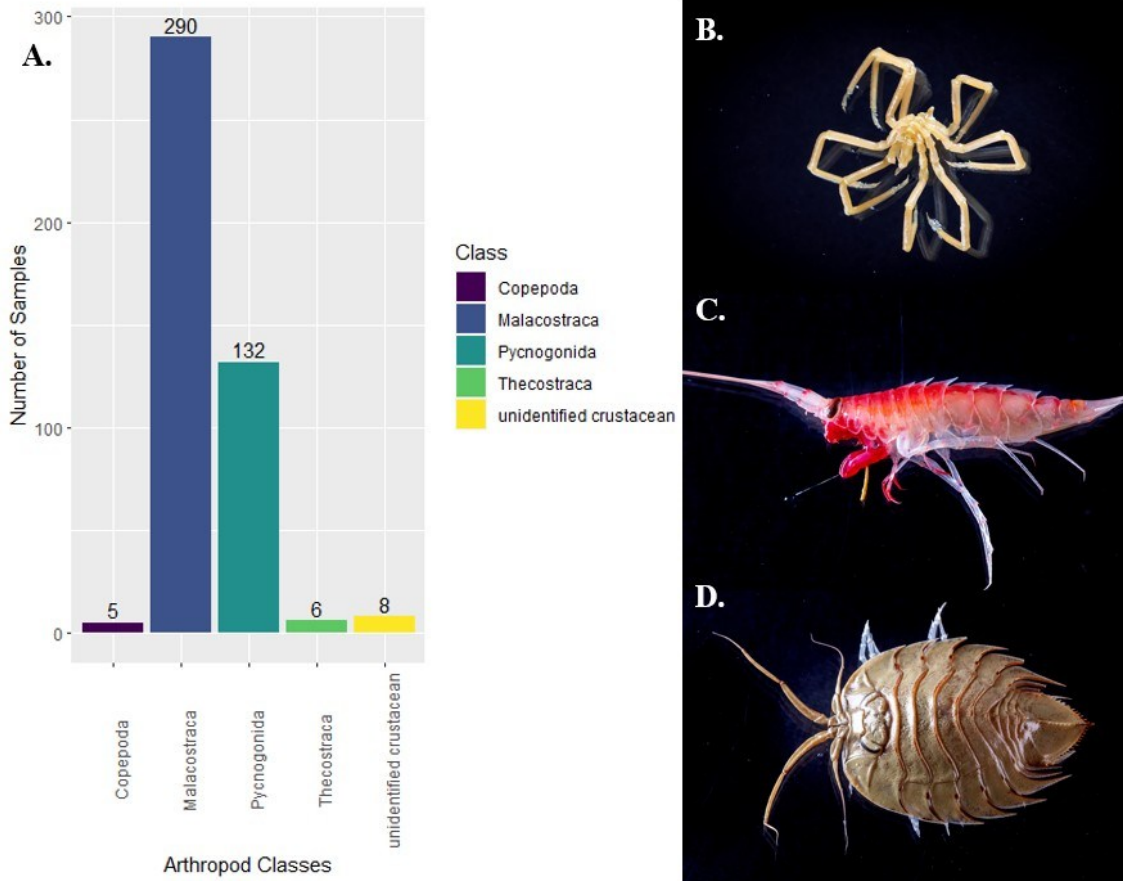


Figure 40: Bar plot indicating the number of lots (that include individual or multiple samples) in each class of the phylum Arthropoda that were processed. Classes included Copepoda, Malacostraca, Pycnogonida, Thecostraca, unidentified crustaceans. Examples of the specimens collected included B) pycnogonids, e.g. *Nymphon* sp., C) amphipods, e.g. *Eusirus perdentatus*, D) isopods, e.g. *Ceratoserolis trilobitoides*. Photo credit: Pete Harmsen, AAD.

10. Trawling (AAS 4628)

All echinoderm classes were represented in the samples processed (Figure 41). The class Ophiuroidea comprised the largest number of lots processed ($n = 310$), followed by Holothuroidea ($n = 194$), Asteroidea ($n = 185$), Crinoidea ($n = 127$) and Echinoidea ($n = 111$).

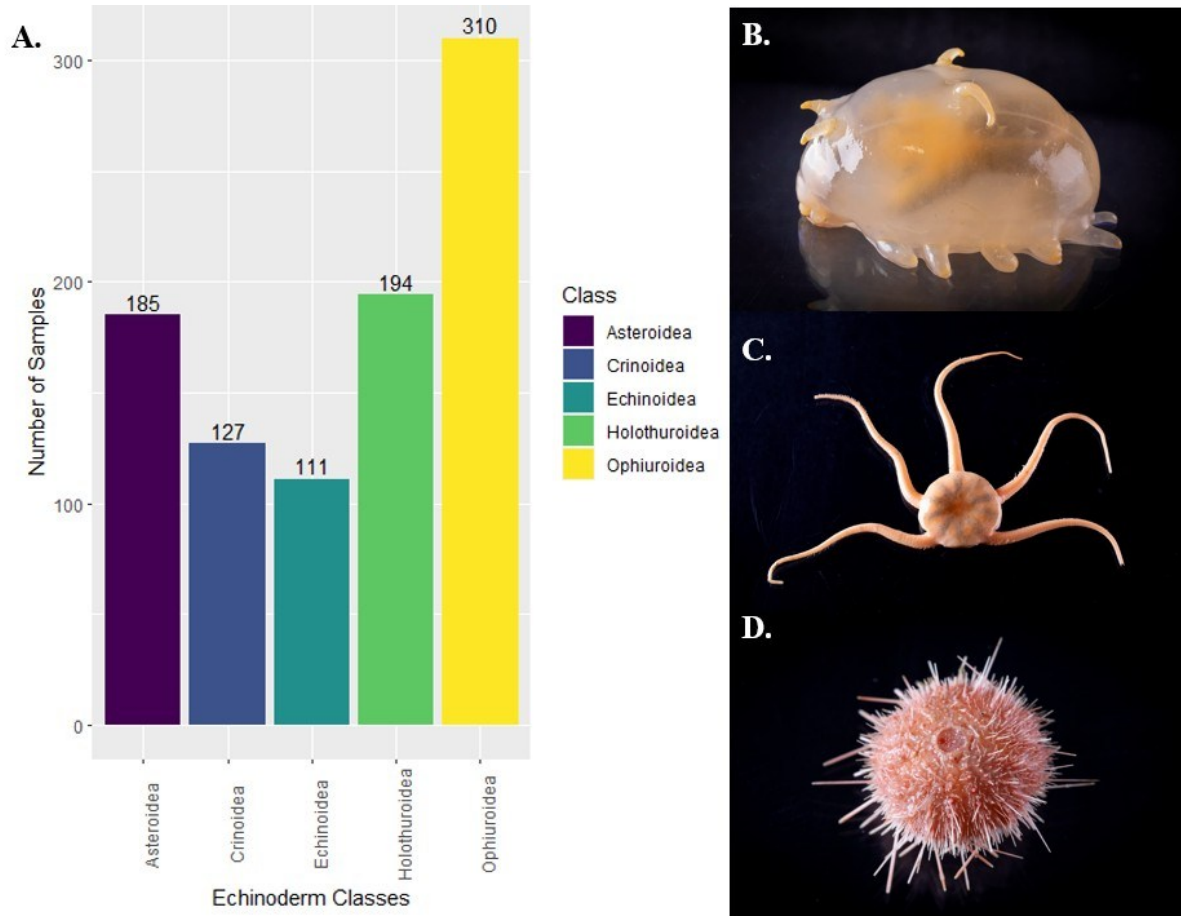


Figure 41: A) Bar plot indicating the number of lots (that include individual or multiple samples) in each class of the phylum Echinodermata that were processed. Classes included Asteroidea, Crinoidea, Echinoidea, Holothuroidea and Ophiuroidea. Examples of the specimens collected included B) holothurians, e.g. sea pigs *Protelpidia murrayi*, C) brittle stars, e.g. *Ophionotus victoriae*, D) sea urchins, e.g. *Sterechinus* sp. Photo credit: Pete Harmsen, AAD.

10. Trawling (AAS 4628)

10.3.1 Fish

A total of 540 fish were caught as bycatch in the beam trawls (Table 22). Of these 32 were euthanized and 146 were returned live to the sea. Fish species caught include *Bathyraco antarcticus*, *Bathyraco marri*, *Chaenodraco wilsoni*, *Channichthys rhinoceros*, *Harpagifer antarcticus*, *Lindbergichthys mizops*, *Macrourus carinatus*, *Macrourus carinatus*, *Macrourus whitsoni*, *Neopagetopsis ionah*, *Notolepis coatsi*, *Nototheniops larseni*, *Pachycara brachycephalum*, *Pleuragramma antarctica*, *Racovitzia glacialis*, *Trematomus hansonii* and an unidentified skate species (see 'Fish caught during DMV' in the Appendix).

Table 22: Total numbers of fish processed from each trawl.

Trawl ID	Date (UTC)	Fish total	Fish euthanized	Live fish returned
A	14/3/2025	30	1	0
B	19/3/2025	17	9	0
C	25/3/2025	2	0	0
D	27/3/2025	9	3	0
E	27/3/2025	28	15	8
F	29/3/2025	24	0	12
G	31/3/2025	14	0	2
H	3/4/2025	37	0	21
I	5/4/2025	134	0	64
J	7/4/2025	138	0	2
K	9/4/2025	19	0	4
L	11/4/2025	27	0	9
M	15/4/2025	11	2	2
N	16/4/2025	22	1	4
O	20/4/2025	28	0	18
P	21/4/2025	0	0	0

10.4 Data Management

All preliminary data will be published through the Australian Antarctic Data Centre (AADC) (<https://data.aad.gov.au/>) following standard AADC procedures, and subject to the moratorium of 2 years.

10.5 References

Lau, S.C.Y., Wilson, N.G., Golledge, N.R., Naish, T.R., Watts, P.C., Silva, C.N., Cooke, I.R., Allcock, A.L., Mark, F.C., Linse, K., Strugnell, J.M. (2023). Genomic evidence for West Antarctic Ice Sheet collapse during the Last Interglacial Period. *Science*. 382:1384-1389

11. Rocks (AAS 4630)

Team: Joanne Whittaker, Karin Orth, Taryn Noble, Katharina Hochmuth, Jim Trihey, Neve Clippingdale, Rachel Meyne, Amy Wells, Noah Menner, Molly Husdell

Note: There was significant overlap between the Sediment and Rock teams on the Denman Marine Voyage. Detailed Rock Dredge reports are published separately on the IMAS database as a part of the 'Supplementary Material'.

11.1 General Introduction

Rock dredges were deployed to collect physical rock samples from the seafloor to understand the geology of the seafloor in, and near, the Denman region. Rock samples were additionally opportunistically recovered from beam trawls on the shelf and slope.

11.2 Overall Aims and Hypothesis

Seamounts (extinct volcanoes) located offshore the Denman region rise ~2000 m from the abyssal seafloor (~5000 m). Some of these seamounts have previously been geophysically imaged (bathymetry and seismic reflection data), which reveals steep, likely rocky slopes, and patterns of interaction with the surrounding sediments that suggest these seamounts have penetrated through existing sediment layers, suggesting geologically recent eruption. A key goal is to recover rock samples from the seamounts to constrain (1) when they formed, (2) and the driving mechanism. We want to understand if these features reveal a more regional raised heat flow, with potential impacts on the Denman region, including basal heating (and melting) of glaciers. We plan to sample rocks from the seamounts and the adjacent Bruce Rise to understand when and how they formed, and prevalence and timing of volcanism, which will inform inferences regarding regional heat flow.

There were three main goals of this voyage:

1. To map and sample volcanic rocks from the Bruce Rise and offshore seamounts to understand the history of volcanism in the region and the linked regional mantle temperature.
2. To sample in situ continental samples from the Bruce Rise to understand the basement geology.
3. To recover ice-rafted debris which are directly linked to the onshore sample collection during last season's Denman Terrestrial Campaign, to understand the geometry of onshore drainage basins at the Denman and Shackleton.

11.3 Methods

11.3.1 Site Selection

The general area of dredge sites was mapped out prior to the voyage based on available geophysical data, principally bathymetry maps that combine low resolution data from satellite

11. Rocks (AAS 4630)

altimetry with shiptrack single beam and multibeam profiles where available. In a few cases existing seismic profiles were available to guide the choice of general dredge areas. However, in all cases the dredge areas were mapped using the RSV *Nuyina* multibeam system and specific sites chosen based on the maps generated from these new data. The steeper slopes with bright backscatter were the most preferred dredge targets due to a combination of inferred rocky slopes and low ooze accumulation.

Along with geological considerations, site selection was also heavily influenced by wind direction and sea ice conditions.

11.3.2 Equipment

Three CSIRO rock dredges were on board at the beginning of the cruise. One dredge was lost during a difficult deployment in heavy sea-ice (Dredge 3).

11.3.3 Dredge deployment workflow

Dredging was undertaken using either the 'fly-in' or 'stop and drop' techniques. For a 'fly in' dredge the ship slowly moves towards the dredge site while the dredge is being deployed. For the 'stop-and-drop' technique, the ship positions directly over the start of the chosen transect and the dredge deployed to the seafloor. The ship then moves slowly to the final position whilst laying out additional wire. There are pros and cons to each approach, with the 'stop-and-drop' ultimately preferred by the bridge crew as being easier to compensate for weather conditions.

Refer to Figure 42 for the fly-in technique procedures.

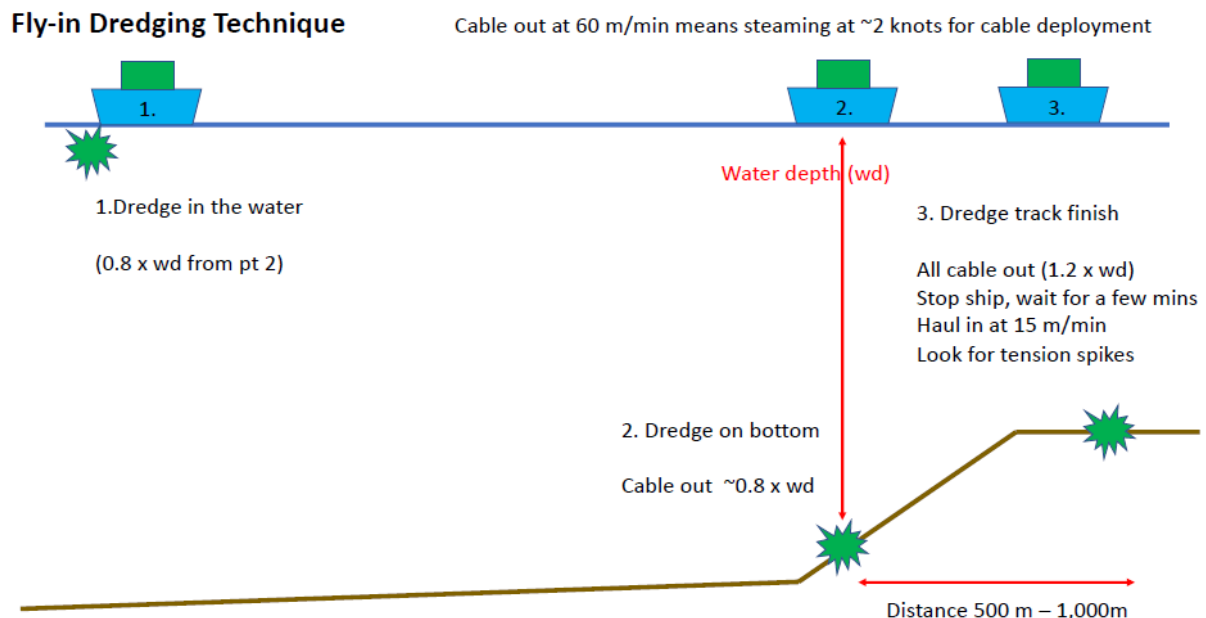


Figure 42: Procedural schematic for the 'Fly-in' dredging technique.

11. Rocks (AAS 4630)

The amount of cable deployed relative to the water depth of the target was the subject of some experimentation between different dredges. Past experience has shown that values between 110 % and 150 % of water depth have been successful. On this voyage, the value chosen varied between 110 % and 130 %. A smaller value allows for more precise targeting of specific parts of a slope and may reduce the degree to which cable is dragged across (and thus potentially damaged by) rough seafloor. On the other hand, smaller values increase the likelihood of missing the seafloor entirely. At least one geoscientist remained with the winch operator during dredging, working closely to determine the stages of dredge deployment and recovery.

11.3.4 Rock processing workflow

The *Nuyina*'s Integrated Ratings (IRs) emptied the contents of the dredge bag and pipe dredges on the back deck and secured the dredge. Then the geology team was allowed to approach, examine and sample the material. Photos were taken of the entire rock haul lying on the deck. The pile of rocks was thoroughly examined, using hammers to reduce sample size where appropriate. The rocks were transported to the cutting container in buckets or (especially for large hauls) using a large fish bin. The IRs then hosed the deck and dredge ready for the next deployment.

In the cutting container the rocks were sawn in half. Rock samples were given sequential identifiers of the form NUY2025_V03-DR01_1, DR01_2, DR01_3, etc. Samples from the two sediment traps on the rock dredge were always assigned sample numbers 1 & 2 for each dredge (where recovered). Where recovered, a modern seabed ooze sample was also retained. Samples were stored in ziplocked or stapled plastic bags with sample number written on a waterproof plastic label.

After being assigned sample numbers, rocks were visually described, photographed (wet and dry), and weighed. They are all stored at the University of Tasmania.

11.3.5 Beam (Benthic) Trawls

Beam trawls were opportunistically sampled due to the large number of rocks brought up by each trawl. For Beam Trawl deployment methods, please refer to Voyage Report section 'Methods and equipment'. Any rocks found during Beam Trawls were set aside in fish bins or buckets by the beam trawl team. These rocks were then washed (most in 1M HCl, the rest in fresh water), grouped (Figure 43), and then visually described and named. Beam trawl rocks were then photographed, counted, and weighed. For some trawls where > 1000 rocks were brought up, some rock groups were winnowed onboard at the end of this process.

11. Rocks (AAS 4630)



Figure 43: Geology team beginning to sort Beam Trawl G in the cutting container

11.4 Sample Description and preliminary results

11.4.1 Rock Dredges

The collection of rock and sediment samples with the dredge was highly successful. We undertook dredging at 7 sites, with successful sample recovery at 6 locations. A key aim is to date when these underwater features erupted and we obtained suitable, datable samples from the seamounts and Bruce Rise. We also recovered a suite of continental, ice-rafted samples that can be used in conjunction with the Beam Trawl samples to understand the under-ice geology of the adjacent onshore Denman region.

Detailed dredge reports are published separately and can be found in the Supplementary Material on the IMAS database.

11. Rocks (AAS 4630)

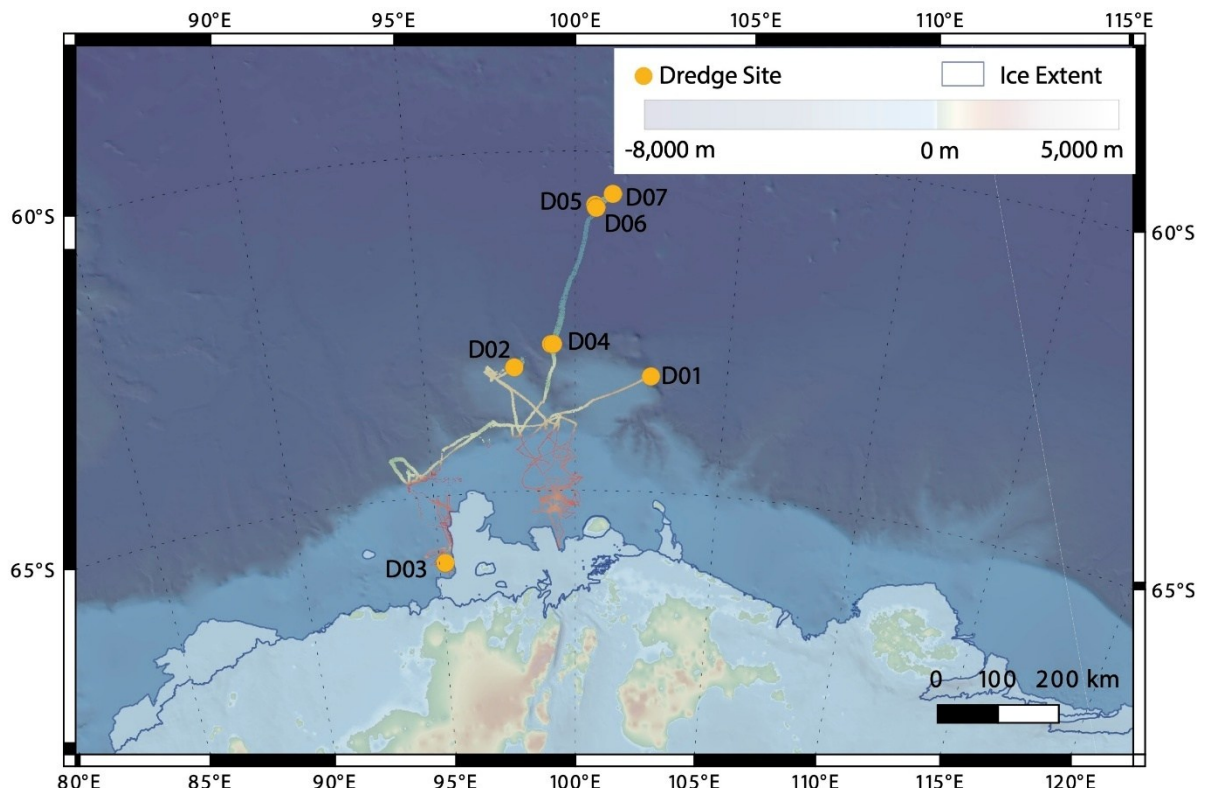


Figure 44: Map with Rock Dredge locations.

11. Rocks (AAS 4630)

Table 23: Rock dredge details

Station	Date (UTC)	ID	Start Latitude (DD)	Start Longitude (DD)	Start water depth (m)	End Latitude (DD)	End Longitude (DD)	End water depth (m)	Number of samples	Length of dredge (m)	Comments
4	9/03/2025	D01	-63.286	102.4949	2625	-63.289	102.487	2170	53	521	
5	12/03/2025	D02	-63.161	97.989	2405	-63.163	97.999	2254	13	549	
105	10/04/2025	D03	-66.011	95.2062	425	-66.0055	95.20948	179	0	632	Failed deployment - no samples
143	22/04/2025	D04	-62.8316	99.2773	3698	-62.8316	99.27734	3609.1	4		Fly-in - ~500 m.
144	23/04/2025	D05	-60.7854	100.5907	4480	-60.8218	100.6053	3520	29		Fly-in - ~500 m.
145	23/04/2025	D06	-60.824	100.6379	3281.21	-60.8303	100.6281	3264.3	15	885	
146	24/04/2025	D07	-60.6226	101.1314	2810.57	-60.6236	101.1161	2358.09	17	839	

11.4.2 Beam Trawls

Opportunistic collection of rock samples from biological beam trawl operations was undertaken on the continental shelf in both the eastern Denman Glacier and the western Shackleton Ice Shelf areas (Figure 45). The majority of these rocks are ice rafted debris (IRD) although the finer fraction may be windblown with current reworking in the marine environment possible for some smaller clasts.

The trawls varied in length from around 1 km (BT B and BT K) to ~150-200 m (BT M and N). Most trawls drag along the seafloor, but in some areas it may have dug down into the substrate to a depth less than 0.5 m.

Rock abundances varied between trawls with some collecting no (BT D) or very few (BT M and N) rocks and others many (hundreds) rocks. The most rocks, 1700, were collected in BT G. Rocks ranged in size from very large metre-sized blocks to small gravel. All the rocks collected were washed and many were treated in 1M HCl to remove biota. Some of the larger samples were cut onboard. Rocks were then grouped and assigned names. The named groups of samples were counted, weighed and, in some cases, the longest dimensions of the largest clasts were recorded. All samples were photographed in their groups. Some samples of particular interest underwent preliminary geochemistry onboard using the pXRF (a Delta handheld, set to 'Geochem' mode, with a powdered vial of 'Tas Bas' used as the standard).

Numerous rocks from some trawls made keeping all samples impractical and so for these groups only representative samples were retained.

11. Rocks (AAS 4630)

Table 24: Beam trawls where rocks were collected. No rocks collected from BT D or BT P due to mechanical failures with the trawl.

Station	Date	ID	Start Latitude (DD)	Start Longitude (DD)	Start water depth (m)	End Latitude (DD)	End Longitude (DD)	End water depth (m)	Number of samples	Length of trawl (m)	Comments
7	14/03/2025	BT A	-64.500	98.795	478	-64.506	98.782	477	162	797	Samples winnowed
30	19/03/2025	BT B	-65.145	98.787	639	-65.146	98.801	635	355	1061	Samples winnowed
47	25/03/2025	BT C	-65.232	100.167	511	-65.232	100.153	514	46	276	
59	27/03/2025	BT E	-65.176	99.933	474	-65.174	99.937	473	59	361	
63	29/03/2025	BT F	-64.873	99.918	545	-64.874	99.922	543	178	264	
65	31/03/2025	BT G	-64.218	99.060	424	-64.223	99.067	426	1485	478	Samples winnowed
79	3/04/2025	BT H	-64.672	95.083	367	-64.672	95.072	376	19	627	
83	5/04/2025	BT I	-64.837	94.147	280	-64.839	94.138	284	69	511	Samples winnowed
93	7/04/2025	BT J	-65.135	95.267	584	-65.135	95.274	583	4	404	
101	9/04/2025	BT K	-65.842	95.147	433	-65.842	95.154	444	1028	1002	Samples originally filled a 'fish bin' on the back deck. Were winnowed at random from this to meet the total of 1028 which was then described, counted and weighed. Further winnowing then followed after this step.
108	11/04/2025	BT L	-66.019	95.280	367	-66.018	95.283	393	103	299	Samples winnowed.
128	15/04/2025	BT M	-65.066	94.994	412	-65.066	94.992	411	2	149	
131	16/04/2025	BT N	-64.7778	95.96465	199	-64.7774	95.9686	199	1	193	
132	20/04/2025	BT O	-64.799	94.236	383	-64.800	94.240	375	399	586	

11. Rocks (AAS 4630)

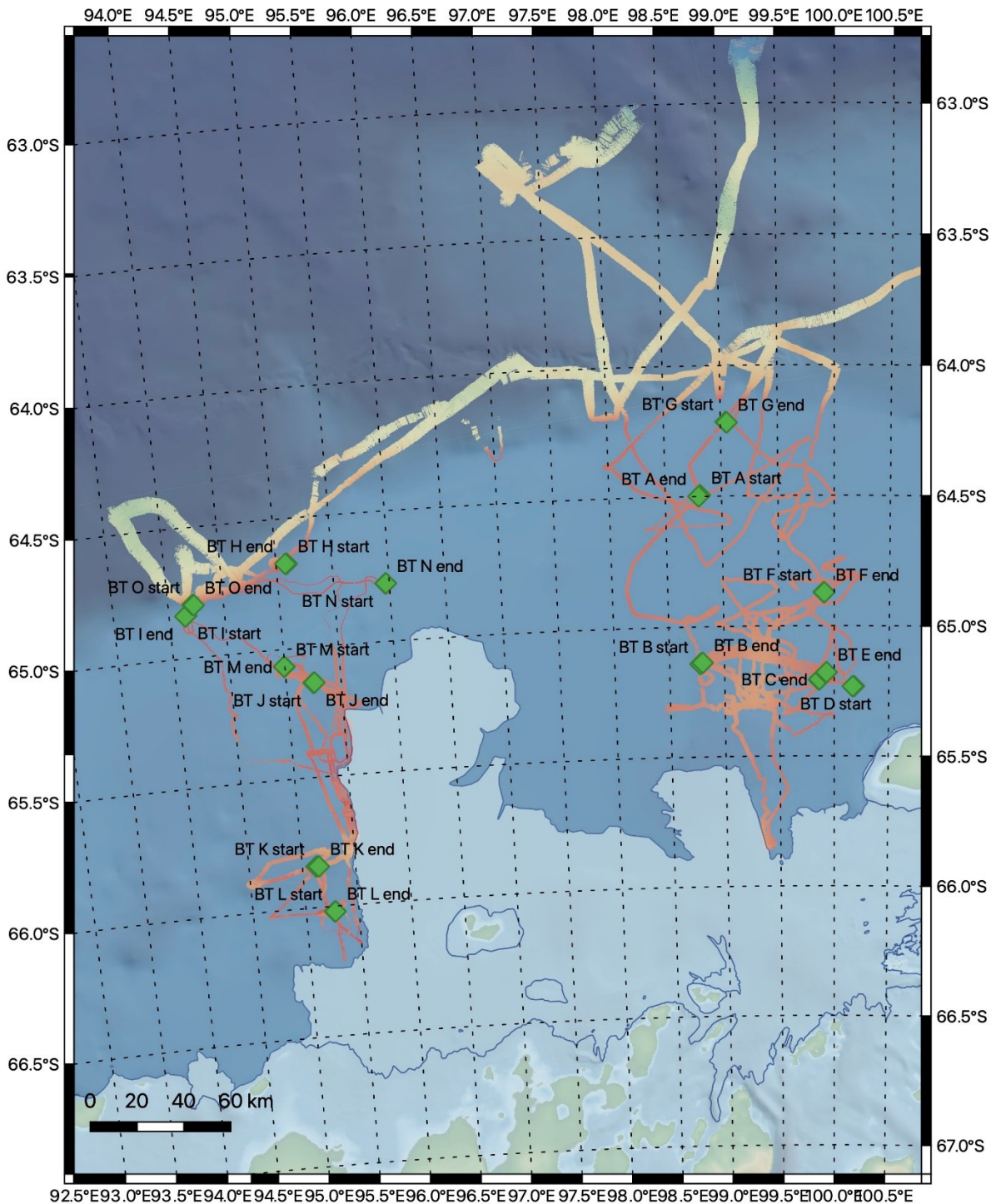


Figure 45: Map with locations of Beam Trawls undertaken during DMV.

11.4.2.1 Overview results

Denman Glacier Area

In the eastern Denman Glacier area, some soft sedimentary clasts were present. These included sandstone, siltstone and possible glauconite rocks as well as diamictite and a

11. Rocks (AAS 4630)

phosphatic elongate rock that may be a fossil. These rocks appear to belong to basinal successions which currently have no known outcrop. Harder sedimentary rocks include abundant red sandstone and siltstone that are probably from the Neoproterozoic Sandow Group (Sheraton and Tingey; 1994).

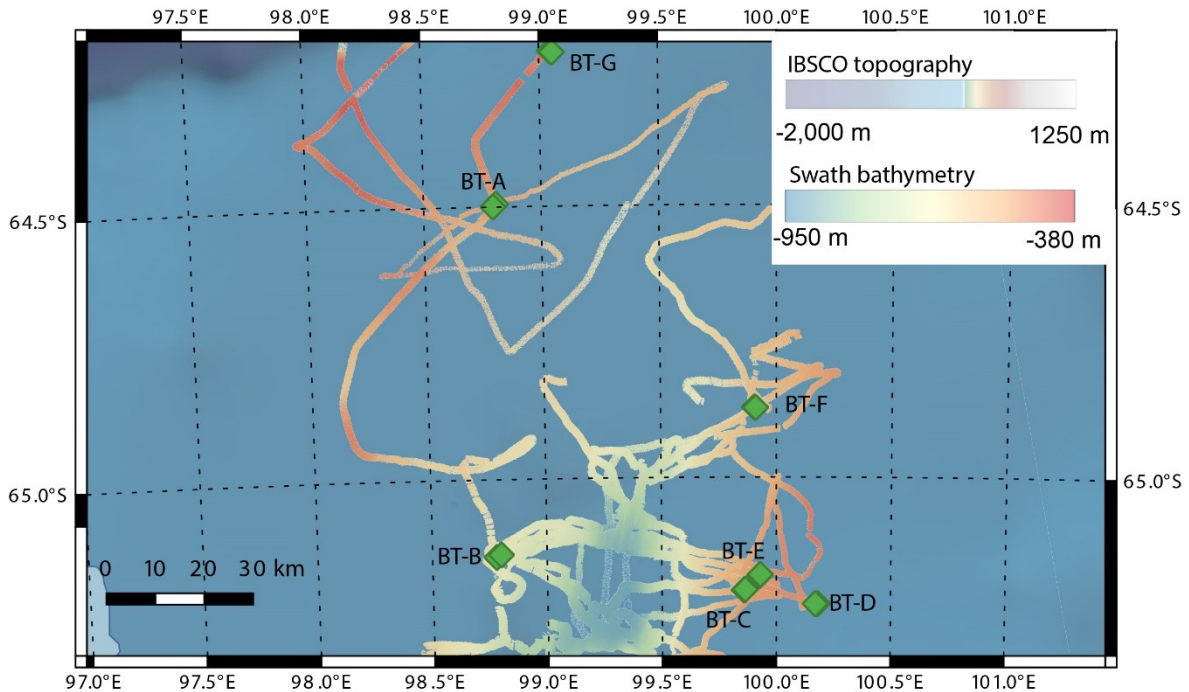


Figure 46: Eastern section of survey area, with beam trawl locations and multibeam bathymetry shown.

There are also a wide variety of metamorphosed mafic and sedimentary rocks which are up to amphibolite grade. Feldspar+quartz+biotite gneisses are abundant. Grey and pink granite are common in some trawls. Mafic rocks are metamorphosed to greenschist or amphibolite grade. Most basalt clasts are further from the glacier in BT G which was a rock-rich trawl which sampled the grounding wedge of the Denman Glacier.

Shackleton Polynya

Fewer soft sedimentary rocks were trawled in the western Shackleton Ice Shelf area than in the Denman area but there are some small clasts of friable diamictite. A few clasts of solid red diamictite is present in BT K. Red sandstone and siltstone of the Sandow Group are in most trawls but the abundance and size of these clasts is notably reduced from the east Denman Glacier area. Prominent are clasts of reddish to pink K-feldspar rich syenogranites and monzogranites of various grain size. The largest and often most abundant IRDs are feldspar+biotite+ quartz gneiss with pink, K-feldspar dominated planar and irregular leucosomes and porphyroblastic domains. Metamorphosed mafic rocks are less abundant in this area and basalts are not common. The multibeam and sub bottom profile data suggests that BT K may have collected some of the in-situ bedrock. While not confirmed, this theory is backed up by an extremely large boulder collected (approx. 1 m³) (K-feldspar-biotite-quartz gneiss), along with hundreds of smaller fragments of rocks of similar lithology.

11. Rocks (AAS 4630)

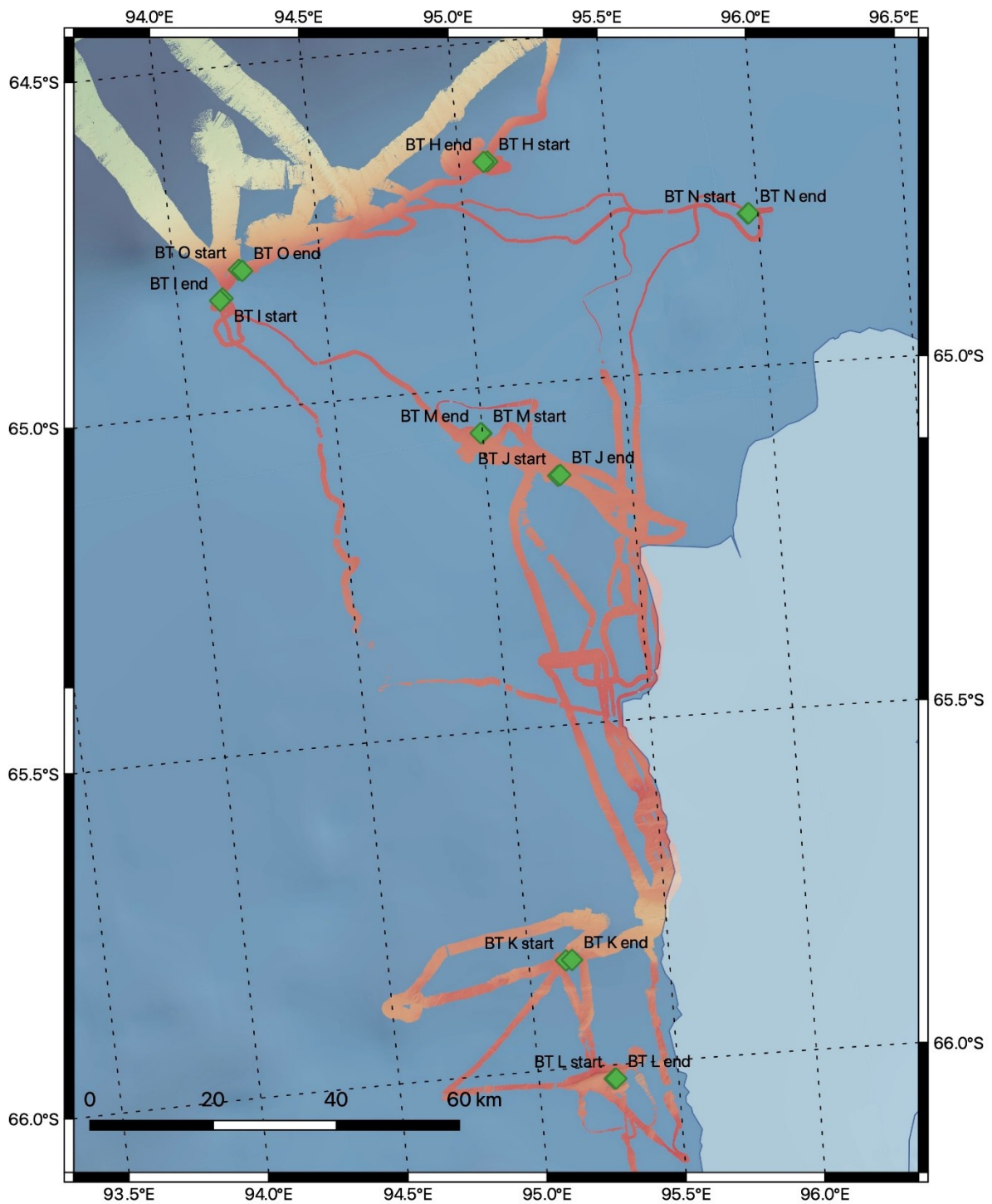


Figure 47: Western section of survey area, with beam trawl locations and multibeam bathymetry shown.

11.4.3 Sediment coring

Where present, dropstones were collected and recorded from kasten and multi cores (Table 25). These have all been visually described and are stored at IMAS.

11. Rocks (AAS 4630)

Table 25: Locations of rocks collected from sediment coring operations

Station	Date (UTC)	Operation	ID	Latitude (DD)	Longitude (DD)	Ocean Depth (m)	Number of samples
6	13/03/2025	Kasten core	KC01	-63.283	97.307	1647	15
53	26/03/2025	Kasten core	KC03	-65.289	99.24	868	1
82	4/04/2025	Kasten core	KC04	-64.421	93.599	2677	31
103	9/04/2025	Kasten core	KC05	-66.022	95.199	749	17
140	20/04/2025	Kasten core	KC06	-63.9536	97.2159	2164	40
14	16/03/2025	Multicore	MC02	-65.286	99.004	793	1
29	18/03/2025	Multicore	MC03	-65.848	99.386	834	8
84	5/04/2025	Multicore	MC08	-65.233	95.66	507	3
96	8/04/2025	Multicore	MC11	-65.795	95.012	725	3
132	16/04/2025	Multicore	MC14	-64.8485	94.1449	289	37
64	30/03/2025	Smith McIntyre Grab	SMG	-64.5001	99.9998	544.63	6

11.5 Data Management

All preliminary data will be published through the Australian Antarctic Data Centre (AADC) (<https://data.aad.gov.au/>) following standard AADC procedures, and subject to the moratorium of 2 years.

11.6 Acknowledgements

The Rocks team would like to thank all AAD and SERCO technicians and crew for their help throughout the voyage. A big thank you to the SAEF (Beam Trawl) team for always setting aside any rocks collected during trawls.

11.7 References

SHERATON, J.W AND TINGEY, R. J., (1994). Bedrock geology of the Bunger Hills-Denman Glacier area, 1:250 000 map, AGS

12. Sediment (AAS 4630)

Team: Taryn Noble, Karin Orth, Katharina Hochmuth, Joanne Whittaker, Yuhao Dai, Molly Husdell, Rachel Meyne, Jim Trihey, Amy Wells, Neve Clippingdale, Noah Menner

Note: The Sediment and Rock teams worked as one for the duration of the voyage. Visual core logs and more expansive core reports (for kasten and multi cores) are published separately on the IMAS database as a part of the ‘Supplementary Material’.

12.1 General Introduction

The Australian Antarctic Territory has contributed as much as one quarter of the total recent Antarctic ice-mass loss. The Denman Glacier, which holds a potential sea level rise of 1.5 m, is one of the fastest retreating glaciers. However, the causes behind these changes remain a mystery. Similarly, the potential impacts of this melt on the surrounding ocean biogeochemistry are unclear- including the impact on trace metal supply from the sediment, and the impact on carbon burial.

Seamounts located offshore the Denman region rise from the abyssal seafloor (~5000 m) to ~3000 mbsl. Some of these seamounts have previously been mapped using multibeam and seismic reflection data, which reveal steep sided slopes (likely rock) and patterns of sediment interaction that suggest these seamounts have penetrated through existing sediment layers after they were deposited. This information suggests that these seamounts may be relatively young and formed via volcanism driven by a hot thermal anomaly in the underlying mantle. Hot mantle anomalies with associated volcanism can raise regional heat flow, with potential impacts on the Denman region, including basal heating of glaciers.

The sediments team sampled more than just sediments. The team conducted sampling and analysis of the water column, marine sediments and rocks to understand the susceptibility of the Denman Glacier to a warming climate, and the risks posed by climate variability and change.

12.2 Aims and Hypotheses

Determine biogeochemical budgets Sediment and sediment porewater samples were collected to close the biogeochemical budgets for this region. We aim to determine the rate at which carbon, silica and trace metals accumulate on the seafloor and, using porewater samples, determine whether the sediments are a source of essential (or toxic) metals to the water column. This work will inform whether the Antarctic margin becomes a stronger or weaker sink for carbon and silica in a warming world, with implications for the global cycles of these important elements.

Validate paleo-proxies: Sampling of the water column and surficial sediments was conducted in order to validate and refine paleo-proxies. This includes diatom shape as a surface temperature proxy, Nd isotopes to trace water-masses, N isotopes to trace nitrate utilisation, Th-230 to trace particle accumulation and ice rafted debris samples to trace ice sheet erosion.

12. Sediment (AAS 4630)

Reconstruct paleo-environments: Longer sediment cores were collected in order to understand how the Denman Glacier and surrounding ocean responded to past climate change. These cores will allow us to a) understand past ice sheet behaviour under different climate conditions and b) reconstruct how the ecosystem and carbon cycle responded to past climate change, including warmer-than-present conditions that serve as analogues to human-driven climate change.

Assess regional volcanism and heat flow: We sampled rocks from seamounts to understand when and how they formed, which will inform inferences regarding regional volcanism and heat flow. We also measured heat flow directly during coring, to inform modelling of heat flow and improve estimates of basal melting.

12.3 Diatoms / Underway sampling

12.3.1 Introduction

Underway sampling was undertaken every six hours along the transect to and from Antarctica in addition to more occasional samples taken south of 60 °S. Three main sample types were taken from the ship's underway system, and these included those for a diatom community analysis study (Figure 48), *Fragilariopsis kerguelensis* samples for an Honours project (Figure 49), and nutrient samples which were analysed by the on-board CSIRO hydrochemistry team (Figure 50). The samples were collected over a variety of latitudes and oceanic conditions to determine the impact of these conditions and areas on the observed diatom assemblages.

Additional samples were opportunistically taken from the CTD instead of the underway to enable comparison of surface communities, phytoplankton communities at depth, and sinking assemblages through the water column.

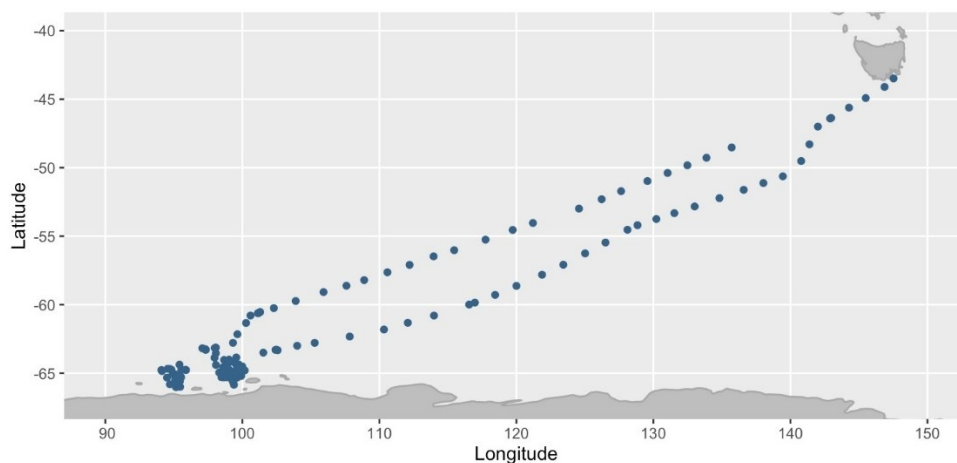


Figure 48: Plot of the underway sampling locations on NUY2025_V03 from UTC 01/03/2025 – 19/04/2025 in relation to Tasmania and Antarctica.

12. Sediment (AAS 4630)

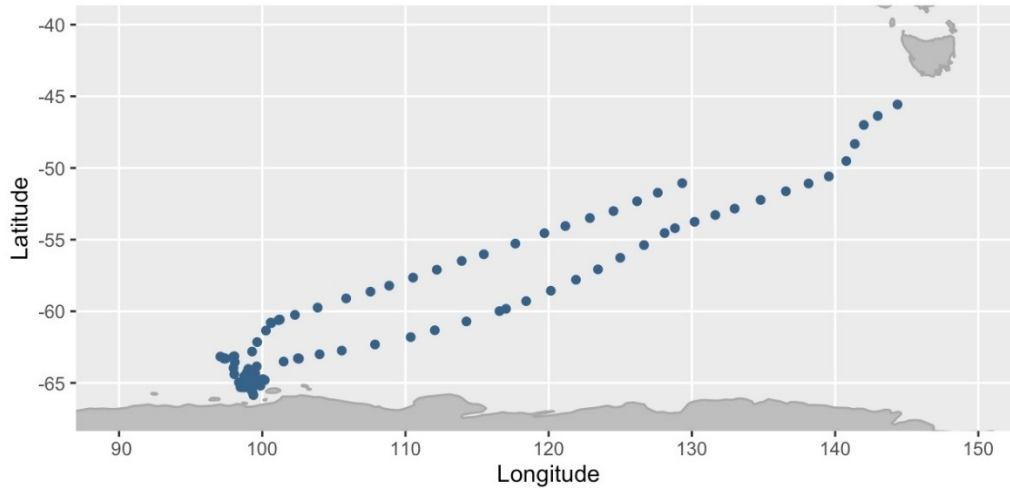


Figure 49: Plot of the underway sampling locations for *F. kerguelensis* on NUY2025_V03 from UTC 01/03/2025 – 22/03/2025 and 22/04/2025 – 28/04/2025 in relation to Tasmania and Antarctica.

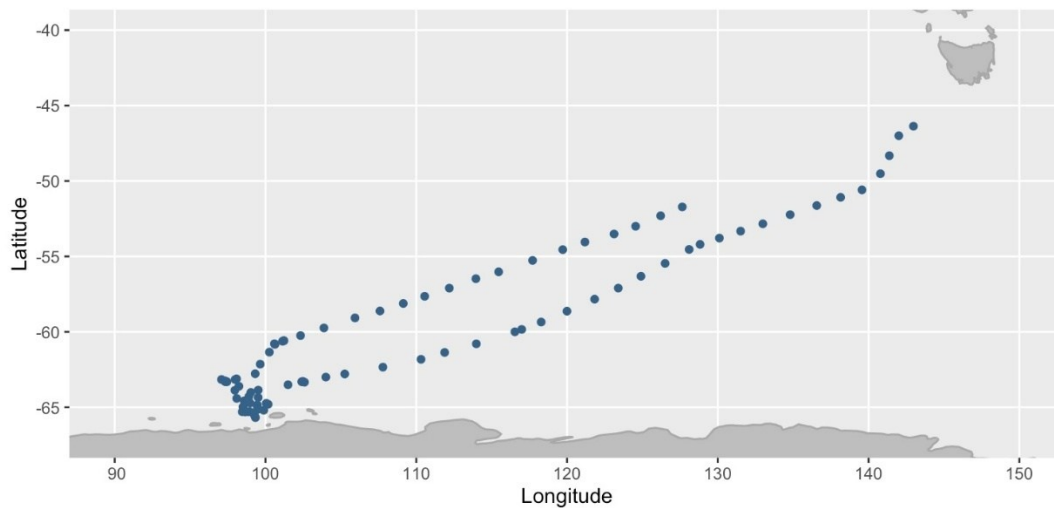


Figure 50: Plot of the underway sampling locations for nutrients on NUY2025_V03 from UTC 02/03/2025 – 22/03/2025 and 22/04/2025 – 28/04/2025 in relation to Tasmania and Antarctica.

12.3.2 Underway Sampling Protocol

Poly-bottles (1000 mL) were filled with sample seawater from the uncontaminated seawater line every six hours, when crossing an oceanographic front, and/or when in areas of interesting sea ice/chlorophyll conditions. When water was collected from the uncontaminated seawater line they were assigned a station number and labelled in ascending order starting with UWY001. Samples were also taken from the CTD at a variety of depths. Before samples were taken the 1000 mL poly-bottles were rinsed three times with the seawater being collected.

12. Sediment (AAS 4630)



Figure 51: Neve, Rachel and Molly taking the first underway sample of the DMV.

Samples were refrigerated (4 °C) and in the dark for a short time (<1 day), until they could be filtered. This allowed for multiple samples to be taken per day while only filtering once a day. Samples were filtered using the 0.45 μm pore size 25 mm diameter HAWG gridded filters, placed on a polysulfone funnel base, wetted slightly with Milli-Q water, and then screwed to the funnel on top. The samples were shaken to re-suspend the diatoms and then added to the filter funnel.



Figure 52: The filtering set up used during the DMV for underway samples.

12. Sediment (AAS 4630)

The volume of seawater filtered ranged from 100 mL in high chlorophyll areas and 1000 mL in low chlorophyll areas. The amount filtered was determined by considering the value on the fluorometer at the time of sampling and observing the pigmentation of the filter. After filtering was completed, the filters were left to dry in a petri dish for approximately 24 hours before they were cut in half – one being used for future SEM and the other being used for light microscopy. The light microscopy slides were prepared by placing a few drops of immersion oil on a slide and then placing the dry filter on top. The oil was then left to completely penetrate the filter for 24 hours, before another few drops of oil were added and a 25 mm square coverslip. It was important to ensure the filter was completely dry before adding the immersion oil to prevent the slides from being “milky”. Slides were then observed at sea and stored upright in a slide case to prevent the oil from sticking to the other slides.

12.3.3 *F. kerguelensis* Sampling Protocol

F. kerguelensis was sampled for using the underway system during the transect to and from Antarctica. Some sampling was also conducted along the glacier to collect samples from a wide range of temperatures with a station and label being assigned to each sample in ascending order beginning with Fk001. The underway system was run for 5-10 minutes to flush out old water before a 10 µm filter was attached to collect diatoms. Water was then run through the filter for approximately 30 - 60 minutes to collect as many diatoms as possible, while being careful to not allow it to overflow and lose any sample. This sample filter was then left to dry before being removed and stored in a tube with a lid in the 4 °C fridge aboard the RSV *Nuyina*. Because this sampling protocol commenced after the Underway sampling it was given a new station number and labelled in ascending order starting with FK001.

12.3.4 Underway Nutrient Sampling Protocol

After the *F. kerguelensis* and underway samples were taken a 10 mL water sample was collected for nutrients from the underway system. These samples were associated with the *F. kerguelensis* sampling stations – with the first nutrient sample being collected with Fk002 and were labelled in ascending order from UWY002. The tube was rinsed thrice before the sample was collected, and after collection was taken to the on-board CSIRO hydrochemistry team for analysis. On the return transect to Hobart underway nutrient samples were collected in 30 mL tubes and frozen in a -20 °C freezer on the *Nuyina* for later analysis back in Hobart. Where possible duplicate samples were taken. Samples were given labels corresponding to the *F. kerguelensis* sample taken at the same location.

12.3.5 CTD Sampling Protocol

CTDs were sampled opportunistically instead of taking an underway sample whenever our team sampled for Th/Nd starting at CTD 29. Nalgene bottles (1 L) were DI rinsed before collection and when possible replicate bottles were filled from the shallowest Niskin triggered and the Niskin

12. Sediment (AAS 4630)

bottle triggered at the deep chlorophyll maximum (DCM). Starting at CTD 39, samples were from Niskin bottles triggered at the surface, DCM, the deep temperature maximum, the pycnocline, the bottom and somewhere in between the pycnocline and the bottom of the CTD. Slides were prepared using the same methods as the underway phytoplankton samples.

12.3.6 Diatom Assemblage Notes

CTD sampling initially aimed to qualitatively compare the phytoplankton community population of the surface and DCM. Samples from CTD 12, 29, 33, and 35 sampled only these two depths and showed similar diatom assemblages to each other as well as to the underway samples, with the DCM having a notably higher concentration of phytoplankton. The most common genera observed were *Probocia*, *Corethron*, *Chaetoceros*, and *Fragillariopsis*. The rest of the CTD casts (39, 51, 66, 67, 78, 81, and 103) sampled multiple depths targeting the different water masses and interesting physical oceanography profiles. For example, CTD 39 (Figure 53) showed two sub surface thermal maxima and samples from each depth show similar phytoplankton community structure. The basal relatively warm, salty, and anoxic water mass has physical oceanographic signatures of modified circumpolar deep water (mCDW). The phytoplankton community within this water mass was sampled at 820 m and 850 m and both depths have a distinct diatom assemblage from the rest of the CTD. They are enriched in *F. kerguelensis*, a species that is prolific in the permanently open ocean zone and has been used as an indicator of CDW in palaeoceanographic studies. CTD 51 also showed the presence of mCDW and was enriched in *F. kerguelensis* in its deepest sample.

12. Sediment (AAS 4630)

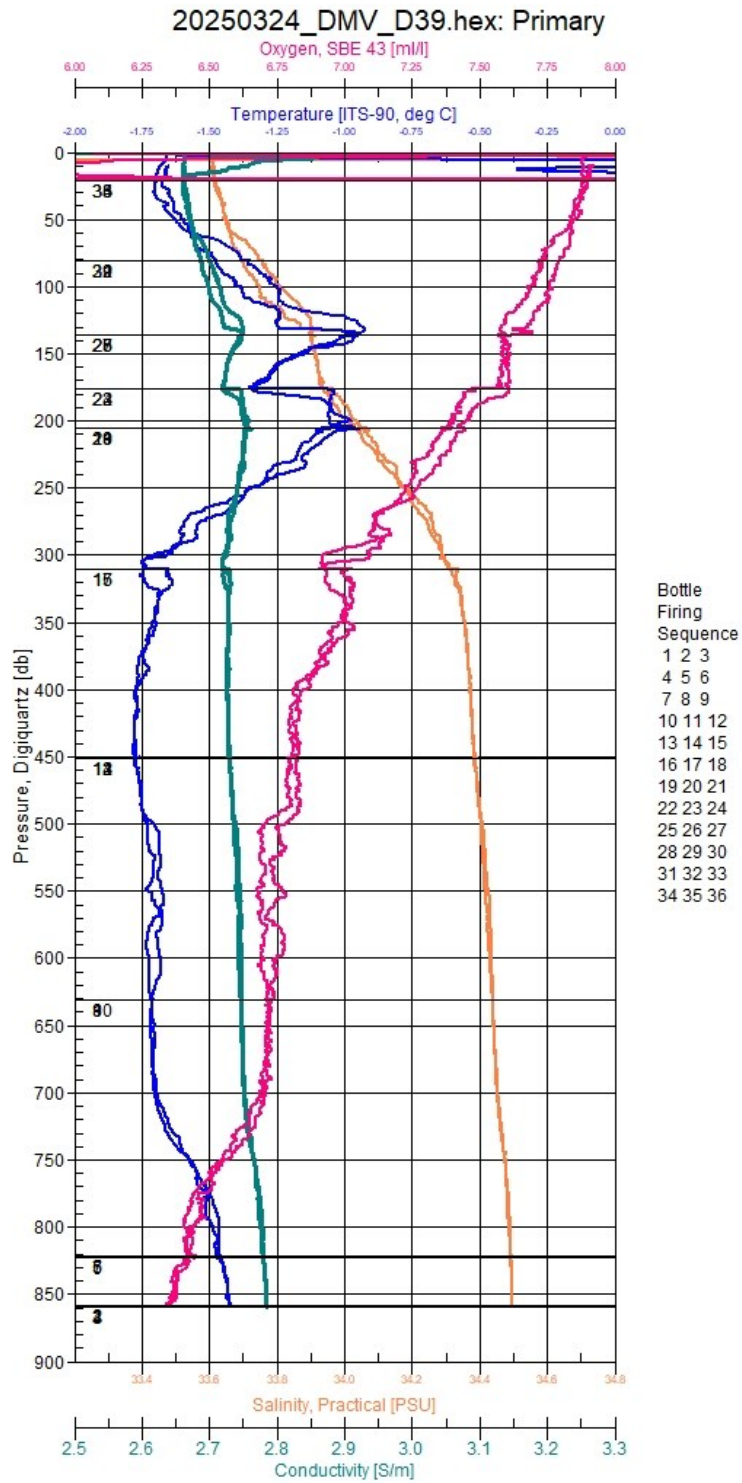


Figure 53: CTD profile from cast 39 showing interesting bifurcated deep thermal maxima and modified circumpolar deep water.

12.4 CTD and TMR sampling

12.4.1 Introduction

The sediments team sampled from the CTD and TMR to obtain a variety of samples. The CTD was sampled to collect samples for nitrogen and oxygen isotopes of nitrate (collaboration with Abby Ren, National Taiwan University), rare earth elements (REE), thorium (Th), neodymium (Nd) and beryllium (Be) isotope analysis. This sampling was completed in a relatively clean manner to reduce contamination, using a clean hands/dirty hands system. Nitrogen isotopes, REE and Th/Nd samples were taken from 25 CTD deployments. Beryllium samples were taken from 2 CTD deployments. The TMR was sampled to collect samples for lead (Pb) isotope analysis. This sampling was conducted in the trace metal container, with trace metal clean protocols employed to ensure that contamination was minimised. Pb samples were collected from 19 TMR deployments.



Figure 54: CTDs sampled by the Sediment team (blue dots). Basemap from *Quantarctica* (Matsuoka et al., 2021).

12. Sediment (AAS 4630)

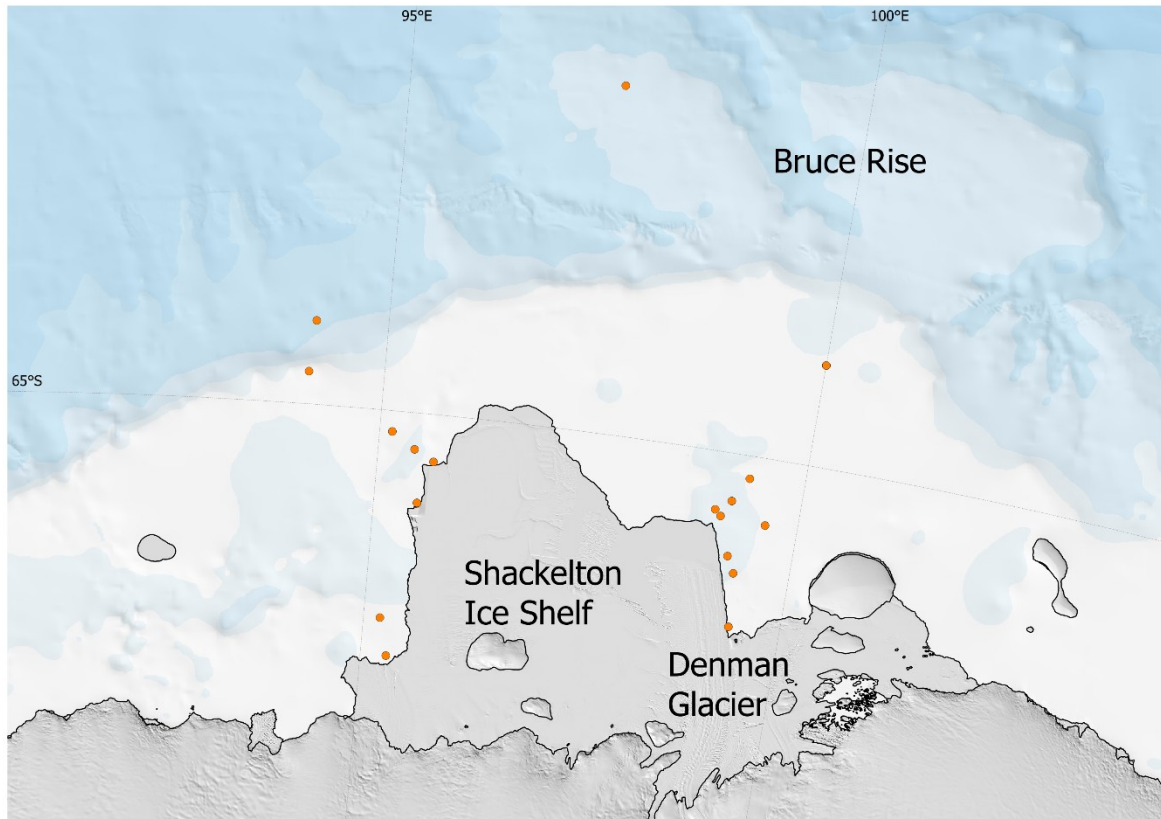


Figure 55: TMRs sampled by the Sediment team (orange dots). Basemap from *Quantarctica* (Matsuoka et al., 2021).

12.4.2 Sample Collection Methods

Cleaning: Jerry cans (10 L) for Th/Nd and beryllium isotopes, 5 L jerry cans and 1 L PPE bottles for Pb isotopes, and 250 mL bottles for REE were cleaned according to the GEOTRACES cookbook, with minor adjustments (Cutter et al., 2017). Bottles were cleaned in the IMAS acid lab in 2 % v:v Decon-90 for one week to remove any residue from manufacturing. The bottles were rinsed with deionised water four times and filled with 6 M hydrochloric acid (HCl). The 1 L bottles were placed in a 1.2 M HCl bath on a hotplate at 80 °C for one week. The 250 mL bottles were placed on a hotplate at 80 °C for one week. The 10 L and 5 L jerry cans were stored, filled with 6 M HCl, for four weeks. All bottles were rinsed four times with ultra-high purity (UHP) water. Bottles were filled with UHP water and 0.2 mL of distilled HCl was added per litre of UHP water. After at least two weeks, bottles were rinsed three times with UHP water and double bagged for transportation. Filters used to connect the Niskin bottles and the sample bottles were 0.45 µm AcroPak capsule filters. Capsule filters were acid cleaned at IMAS using a peristaltic pump. A chain of five filters was created using tubing, and ultrapure (UHP) water was pumped through for 15 minutes, followed by 0.1 M hydrochloric acid (HCl) for 10 minutes. The chain was sealed by connecting the end tubing with the first filter, and the acid was stored for two weeks. Afterward, UHP water was pumped through the chain for 20 minutes, and each filter was stored with UHP water inside by linking one length of tubing to both ends of the filter. All bottles and filters were double bagged and stored away for use on the voyage.

12. Sediment (AAS 4630)

Labelling: Filter cartridges and sample bottles were labelled with the following convention: “NUY2025_V03_v_CTDw_x_y_z” where v = station number, w = CTD number, x = rosette position, y = sample depth, and z = parameter sampled. The labelling procedure for Nitrogen isotopes was different, and each sample bottle had its own ID (e.g. bottle #84) that was recorded in the CTD sampling sheet. TMR sample bottles were labelled with the following convention: “NUY2025_V03_w_TMRx_y_z” where w = station number, x = TMR number, y = rosette position, and z = sample depth.

Samples collected and volume of each sample is shown in Table 26 and Table 27.

Table 26: CTD sample parameters collected

Parameter	Volume collected (L)
Nitrogen isotopes	0.06
REE	0.125
Th/Nd	10
Beryllium isotopes	10

Table 27: TMR sample parameters collected

Parameter	Volume collected (L)
Pb isotopes	2-5

CTDs were sampled by the Sediments team in teams of four. Two people were “clean hands” and wore clean blue nitrile gloves and only handled the Niskin bottle spigot, capsule filters, and opened the clean sampling bottle. One person was “dirty hands” (who also wore blue nitrile gloves) and handled everything else. The remaining person was the “cop” and kept track of writing everything down on the CTD log sheets, directing which Niskin bottles to sample from, etc. The “dirty hands” and “cop” roles were completed by one person when only two people were available.

12.4.2.1 Sample collection in CTD hangar

Samples were collected using the following procedure:

1. Tubing attached from Niskin bottle outflow to filter cartridge* inflow. Tubing + filter rinsed with Niskin bottle seawater.
2. 125 mL nitrogen sample bottle rinsed thrice with ~ 40 mL of filtered seawater. Collected a 125 mL sample for nitrogen isotope analysis (< 5 min).
3. 250 mL bottle rinsed thrice with ~80 mL of filtered seawater. Collected a 250 mL sample for REE analysis (< 5 min).
4. Fitted dummy lids with holes onto sample bottle. Bagged original lids into a clean Ziploc lab. Fitted the filter cartridge outflow into the hole of the dummy lid. 10 L jerry cans rinsed thrice with ~ 0.5 L of filtered seawater. Bungy-strapped sample bottles to the CTD frame. Collected 10 L of filtered seawater into jerry can for Th/Nd analysis (~ 1 hr).
5. Took a Milli-Q blank in the CTD room, opened it and placed a capsule filter above it just like samples to have ship blank as realistic as possible.

12. Sediment (AAS 4630)

*Filters had capacity to filter ~ 100 L, which varied slightly according to how much biota was in the samples. After this volume, filters were replaced.

12.4.2.2 Post CTD hangar processing

Nitrogen isotopes were immediately stored in the -20 °C freezer.

Other samples (Th/Nd, REE, Be) were processed using the following procedure:

1. Removed the (dirty) outside bag before putting sample under the hood.
2. Acidified REE samples with 500 µL 6M HCl, using a 1 mL pipette.
3. Estimated the Th/Nd sample volume using the jerry can pre-marked with 1 L increments. Recorded volume in log-sheet.
4. Acidified Th/Nd samples with 2 mL/L of 6M HCl using the adjustable volume dispenser squeeze bottle. Acidified blanks using the same amount as for a seawater sample. Samples were acidified as soon as possible after filtration.
5. Shook samples, poured a small volume into a small container and checked that the pH is < 2 using pH-meter or pH paper. Adjusted pH using more acid where necessary.
6. Recorded the amount of acid used, time of acidification and final pH in the log-sheet. Put sample back in original outside bag.
7. Rinsed filters and tubing with Milli-Q, bagged and stored these in the fridge. Rinsed the dummy lids with Milli-Q and stored in Ziploc bag or put in acid bath if dirty.
8. Re-checked the pH the following day (> 12 h later), added more acid if necessary.
9. Wrapped parafilm around the lid of the bottles, double bagged samples, put a quarantine tape on if required and stored in grey box.

TMRs were sampled by the trace metal team as described in depth in section 'Sample Collection Methods'. Pb isotope samples were collected in 1 L and 5 L acid cleaned LDPE bottles. Duplicate or triplicate samples were taken when 1 L bottles were used.

Table 28: CTD casts sampled by the Sediments team

Station number	CTD cast	Latitude (DD)	Longitude (DD)	Ocean depth (m)	Parameters collected
2	2	-59.993	116.5736	4525.97	Th/Nd
3	3	-63	104.0012	3610.48	Nitrogen isotopes, REE, Th/Nd
6	4	-63.2831	97.3054	1648.81	Nitrogen isotopes, REE, Th/Nd
8	5	-65.3036	98.4583	587.09	Nitrogen isotopes, REE, Th/Nd
11	9	-65.3139	98.6539	652.25	Nitrogen isotopes, REE, Th/Nd
14	12	-65.2871	99.0096	801.54	Nitrogen isotopes, REE, Th/Nd, Diatoms
27	25	-65.7566	99.3698	735.81	Nitrogen isotopes, REE, Th/Nd
29	27	-65.8483	99.3858	833.69	Nitrogen isotopes, REE, Th/Nd
34	29	-65.3264	99.5439	620.9	Nitrogen isotopes, REE, Th/Nd, Diatoms
38	33	-65.2355	99.1999	876.93	Nitrogen isotopes, REE, Th/Nd, Diatoms
44	39	-65.1168	99.3618	850.44	Nitrogen isotopes, REE, Th/Nd, Diatoms

12. Sediment (AAS 4630)

48	42	-64.9988	100.0073	505.73	Be
64	51	-64.5001	99.9997	546.2	Nitrogen isotopes, REE, Th/Nd, Diatoms
83	66	-64.8396	94.1286	290.2	Nitrogen isotopes, REE, Th/Nd, Diatoms
84	67	-65.2325	95.6596	507.23	Nitrogen isotopes, REE, Th/Nd, Diatoms
86	69	-65.1797	95.4251	556.17	Nitrogen isotopes, REE, Th/Nd
96	75	-65.795	95.0116	724.55	Nitrogen isotopes, REE, Th/Nd
100	78	-66.021	94.6659	495.95	Nitrogen isotopes, REE, Th/Nd, Diatoms
106	80	-66.205	95.3135	395.66	Nitrogen isotopes, REE, Th/Nd
109	81	-66.0217	95.1995	755.54	Nitrogen isotopes, REE, Th/Nd, Diatoms
118	91	-65.7911	95.4462	1289.64	Nitrogen isotopes, REE, Th/Nd
134	99	-65.4404	95.3974	270.23	Nitrogen isotopes, REE, Th/Nd
136	101	-65.2998	95.4542	488.17	Nitrogen isotopes, REE, Th/Nd
140	103	-63.9542	97.2165	2165.26	Nitrogen isotopes, REE, Th/Nd, Be, Diatoms
146	104	-60.5869	101.2188	4477.59	Nitrogen isotopes, REE, Th/Nd

Table 29: TMR casts sampled for Pb Isotopes

Station number	Cast	Date (UTC)	Depth (m)	Latitude (DD)	Longitude (DD)
6	TMR2	12/03/2025	1651.81	-63.2930	97.3320
14	TMR3	16/03/2025	800.02	-65.2869	99.0085
17	TMR4	17/03/2025	849.32	-65.3153	99.0828
21	TMR5	17/03/2025	674.5	-65.5047	99.2385
23	TMR6	17/03/2025	570	-65.5841	99.3382
29	TMR7	18/03/2025	833.38	-65.8487	99.3858
34	TMR8	22/03/2025	563.83	-65.3262	99.6169
38	TMR9	23/03/2025	872.43	-65.2324	99.1814
44	TMR10	24/03/2025	855.48	-65.1114	99.3508
64	TMR11	29/03/2025	546.51	-64.5000	99.9990
64	TMR13	30/03/2025	547.13	-64.5004	100.0001
83	TMR14	4/04/2025	290.05	-64.8393	94.1283
84	TMR15	5/04/2025	507.56	-65.2325	95.6597
86	TMR16	5/04/2025	556	-65.1798	95.4255
92	TMR17	6/04/2025	546.03	-65.1022	95.1472
106	TMR20	10/04/2025	395.82	-66.2050	95.3135

12. Sediment (AAS 4630)

109	TMR22	12/04/2025	753.14	-66.0218	95.1997
129	TMR24	15/04/2025	272.27	-65.4408	95.5126
138	TMR26	19/04/2025	2404.43	-64.5883	94.1748

12.5 Multicores

12.5.1 Introduction

Multicores were taken on the DMV for a variety of analyses. Solid sediment was sampled for bulk geochemical, porosity and dry bulk density, microfossil, eDNA, grain size, silica, biomarkers, and ice rafted debris analysis. Porewaters were sampled for macronutrient, trace metal, rare earth element, dissolved oxygen, sulphide and iron, silica, lead and uranium isotope analysis.

12.5.2 Site selection & deck operations

Multicore sites were selected to coincide with TMR stations, enabling comparison between the water column and surface sediments. Sites for multicoring were selected using bathymetry and sub-bottom profiling data collected by the hydroacoustics teams on board the RSV *Nuyina*. The analysis of these data provided potential target sites for longer kasten coring. The sites were selected to create both latitudinal and longitudinal multicore transects in the Denman and the Shackelton regions.

12. Sediment (AAS 4630)

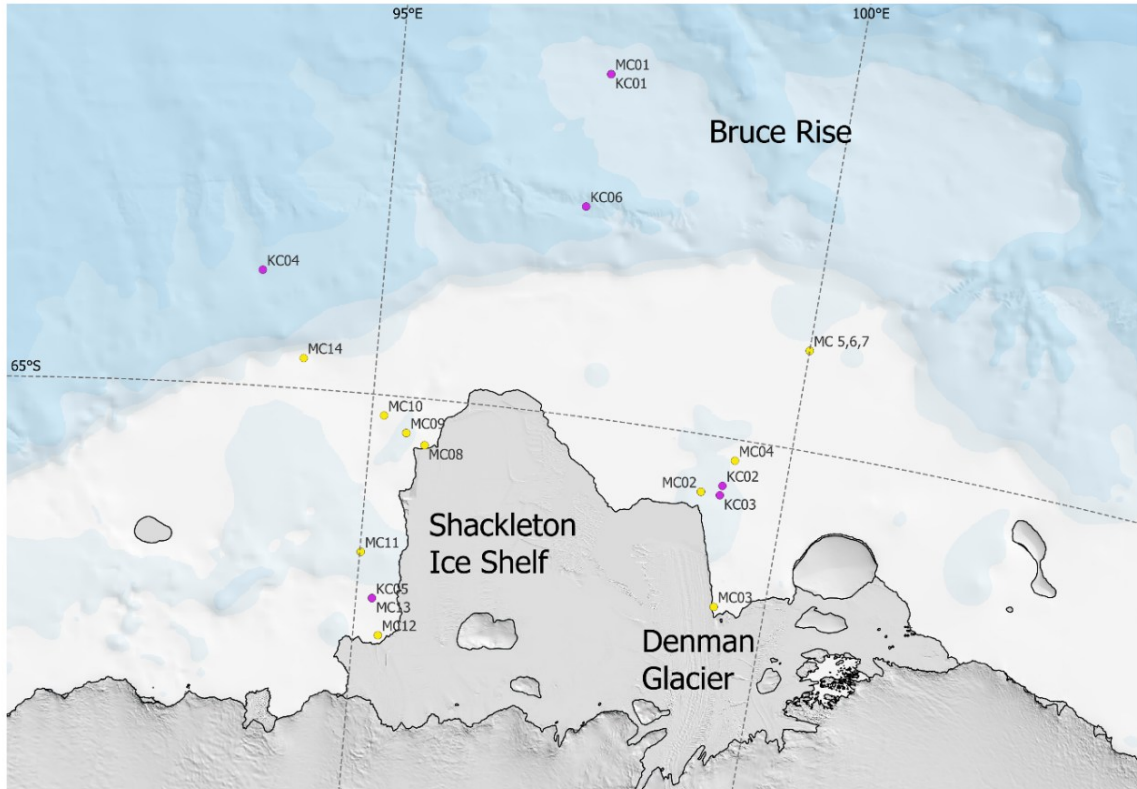


Figure 56: Coring locations during DMV. Kasten cores (purple dots) and multicores (yellow dots) are both shown. Basemap from Quantarctica (Matsuoka et al., 2021).

The multicorer sampler contained six cores each with an 800 mm long barrel, and an internal diameter of 105 mm, with the technical capability to capture a maximum of 30 cm of surface seafloor sediment (KC Denmark, 2025). The first deployment over the western Bruce Rise failed due to rough sea state but the deployment went ahead as a training operation for the crew. The multicore system initially had issues related to early firing of the shutter gates likely due to shrinking of the firing cords in the cold water, and slightly different cord lengths. After three failed deployments at the Denman region process station (5, 6, 7) the multicore system was modified by the MNF gear officer (Jamie Derrick) which allowed successful subsequent deployments (except at MC12 where the location was not optimised for sediment collection).

12. Sediment (AAS 4630)



Figure 57: Multicorer being deployed using the RSV Nuyina's aft deck A-frame

The multicorer was deployed via the A-frame on the aft deck using the trawl winch. It was lowered at 60 m/min to the seafloor. The corer remained on the seafloor for five minutes to allow the cores to settle into the seafloor, and was then recovered at 60 m/min. The descent of the corer through the water column was tracked using the USBL run by part of the Sci-Ops team. When the core was on deck, the multicorer was secured, and the protective net was removed. Two people were required to remove the cores from the multicorer, while one transported the cores to the lab. One person slid a puck into the core while another person opened the gate. The seal on the top of the core tube was removed and the tube was capped on the top and bottom. The core was transported into the lab, dried with paper towel, labelled, and the caps were sealed with electrical tape. The cores were stored upright in the walk-in fridge at 3 °C, in the dark.

12. Sediment (AAS 4630)



Figure 58: Multicorer back on deck after a successful deployment (MC11)

Table 30: DMV multi core locations and core recoveries. Smith-McIntyre grab taken at Station 64 after failed multicore deployments.

Station	Multicore	Latitude (DD)	Longitude (DD)	Ocean Depth (m)	Cores recovered	Average recovered depth (cm)	Deployment date (UTC)
6	1	-63.2829	97.3068	1647.43	0	0	13/03/2025
14	2	-65.2858	99.0044	792.76	6	38	16/03/2025
29	3	-65.8483	99.3858	833.66	6	31	18/03/2025
44	4	-65.1064	99.3507	855.04	6	42	24/03/2025
64	5	-64.5001	99.9998	544.63	0	0	29/03/2025
	6	-64.5001	99.9998	544.63	0	0	29/03/2025
	7	-64.5012	99.99931	544.63	0	0	30/03/2025
84	8	-65.2325	95.6597	503.99	6	21	5/04/2025
91	9	-65.1802	95.4287	559.94	6	32	6/04/2025
92	10	-65.1024	95.1461	546.21	6	34	6/04/2025
96	11	-65.7950	95.0116	724.12	6	17	8/04/2025
106	12	-66.2058	95.3148	425.57	0	0	10/04/2025
109	13	-66.0218	95.1995	754.24	6	32	12/04/2025
132	14	-64.8485	94.1449	289	6	10	16/04/2025

12.5.3 Sample collection methods

Each core was taken out of the fridge to be photographed, measured and described. Descriptions of core depth, quality of overlying water, bioturbation, sediment types and colours, and the boundaries of different layers in the core were made and the layers of the core were sketched.

Oxygen profiles were taken immediately on one replicate core (Core a). Four cores (Cores b, c, d, e) were allocated for collection of porewater. The longest core which was representative of the general layering of the remaining multicores was used for onboard analysis of the porewaters (Core b). The final core (Core f) was sampled for sedimentary ancient DNA, and geotechnical analyses.

Table 31: Multicore sampling order

Core of each multicore	Sampling order from MC02-MC08	Sampling order from MC09-MC14	Samples taken
Core a	1 st	5 th	Overlying water, oxygen profile, microfossils, bulk geochemistry.
Core b	2 nd	1 st	Overlying water, DBD, porewaters, dissolved nutrients, dissolved iron, dissolved hydrogen sulphide, centrifuged sediment.
Core c	3 rd	2 nd	Overlying water, porewaters, centrifuged sediment.
Core d	4 th	3 rd	Overlying water, porewaters, centrifuged sediment.
Core e	5 th	4 th	Overlying water, porewaters, centrifuged sediment.
Core f	6 th	6 th	Ancient DNA, geotechnical analysis.

Before processing each core, the overlying seawater was removed in a temperature-controlled container at 4 °C. The seawater was syphoned through a 0.45 µm AcroPak filter into an acid washed 10 L jerrycan using a peristaltic pump (Cytiva, 2025). 10 cm of water was left over the top of the sediment, to allow for transport to the lab without disrupting the upper layers of the sediment. The overlying seawater for each of the six multicores was collected in one 10 L jerry

12. Sediment (AAS 4630)

can. Once the core was transported to the lab, the lower cap was removed, and the core was fastened to the extruder.

Samples were labelled using the following naming convention: Voyage ID (NUY2025_V03), station number, multicore number, core number, parameter sampled for (e.g. 'F' for Ferrozine). E.g. "NUY2025_V03_14_MC02_C3_F".

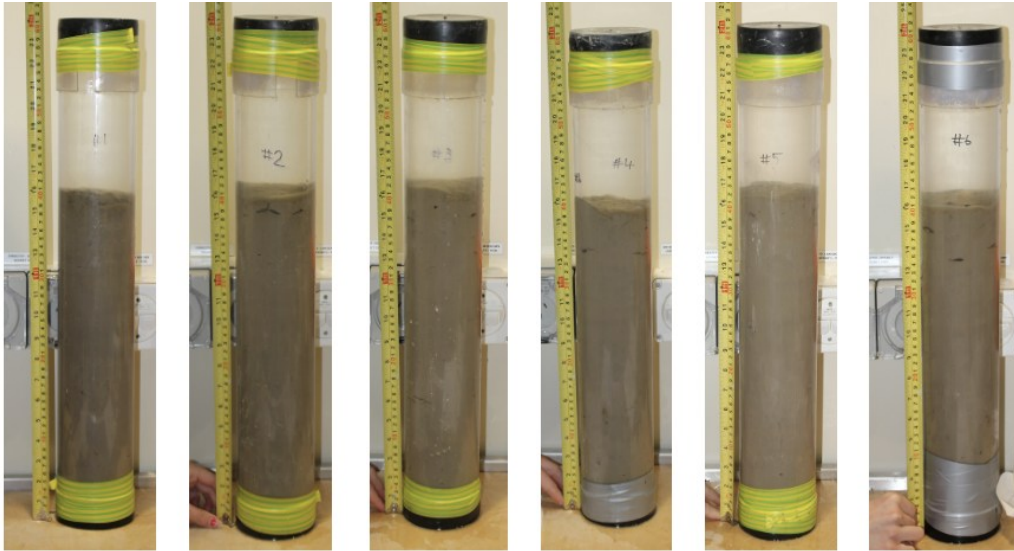


Figure 59: Example of core photographs taken immediately after MC04 retrieval (~40 cm of sediment collected).

12.5.3.1 Oxygen profiles

For multicores MC02 to MC08 (four cores), Core a was processed first, to obtain oxygen profiles with limited contamination from the air. Oxygen profiles were measured using UniSense O2 microsensors. A UniSense manual MicroProfiling System was set up above the extruder (Figure 60). The oxygen microsensors were calibrated according to the UniSense O2 Microsensor Manual, using the UniSense Calibration Chamber to obtain a high calibration point, and the zero-oxygen solution in the UniSense O2 sensor calibration kit as the low calibration point. Before beginning the profile, the remaining overlying water was syphoned off until 1 cm of water remained above the sediment. The core was extruded until the water was at the top of the core tube. The UniSense Logger program was used to take measurements every millimetre, starting in the overlying water. The system allowed a profile of up to 36 mm, and three replicates were taken for each profile. If oxygen levels had not reached zero in this profile, three centimetres were extruded using the technique described below, and a further profile was taken. For multicores MC09 to MC14 (five cores), the microsensors were too damaged to use, so the porewater cores (b, c, d, e) were processed before Core a.

12. Sediment (AAS 4630)

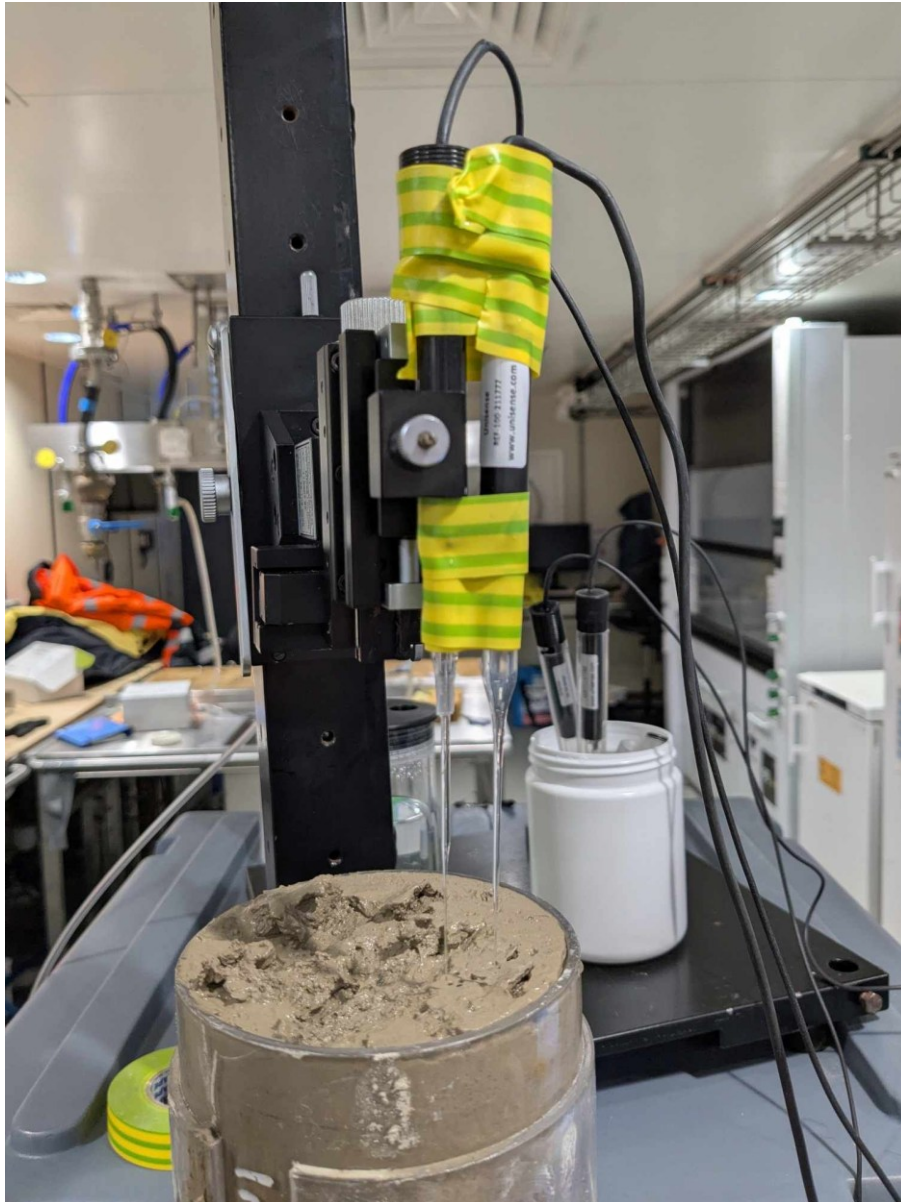


Figure 60: Set up for oxygen profiling of multicores.

12.5.3.2 Core slicing and porewater sampling methods

After oxygen profiling, Core a was extruded for diatom and excess samples. The core was extruded in 1 cm intervals. The core was sliced using a plastic spatula with a greater width than the core tube, and the slice was divided into quarters using a second plastic spatula. One quarter was sampled into a Whirl-Pak bag for diatom analysis, and the remainder was placed in a zip lock bag as an excess sample. The spatulas were cleaned with Milli-Q water after each slice. Once the core had been sampled, the samples were stored in a 3 °C fridge.

Cores b, c, d and e were sampled under a nitrogen atmosphere in an airtight glove box to minimise oxygen contamination which could change the redox chemistry of the sediments and porewaters. The remaining overlying water was syphoned off using a syringe while inside the glove box. The cores were extruded in 1 cm slices, except for the surface sediment where 0-2 cm was sliced into two centrifuge tubes. For Core b, one 2 cm x 2 cm dry bulk density (DBD)

12. Sediment (AAS 4630)

cube was filled with sediment for each slice. For one core in each multicore, a fifty-cent piece sized sample was taken from the upper two centimetres for particulate organic carbon (POC) analysis. The spatulas were cleaned with Milli-Q water and Kimwipes between slices. Once a rack of 12 centrifuge tubes was filled, the tubes were taken out of the glove box, the outside was washed with Milli-Q water, and they were taken to the temperature-controlled container to be centrifuged. For Core b, the DBD cubes were also removed, wiped down, wrapped in Parafilm, and stored at 3 °C. The POC samples were stored in the -20 °C freezer.

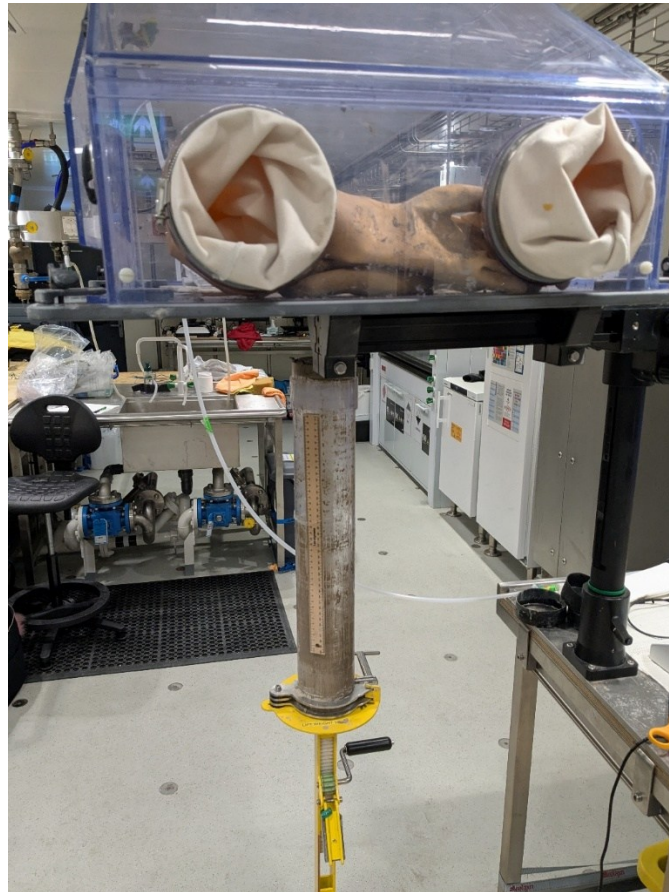


Figure 61: Multicore extruder and glove box set up.

In the temperature-controlled lab (named “BORIS” the Box Of Really Icy Scientists), the centrifuge tubes were centrifuged at 4200 rpm for 30 minutes. The tubes were transferred to a rack inside the second nitrogen filled glove box. The porewaters, which had been separated from the sediment, were poured into an acid washed 12 mL syringe with an acid washed 0.45 µm filter attached. The porewaters were filtered into acid washed 10 mL polypropylene tubes.

In the case of MC13, for one of the cores not used for DNA, a u-channel was inserted into one replicate core before extrusion, and extrusion was done around this u-channel. This u-channel was analysed for magnetic susceptibility using the same methods outlined in the kasten core section (see ‘Magnetic susceptibility’).

12. Sediment (AAS 4630)

12.5.3.3 Nutrients, Ferrozine and Sulphide methods

The porewaters from Core b were subsampled for onboard analysis: 1 mL was sampled for nutrients, 1 mL sampled for dissolved iron, and 1.5 mL was sampled into a tube which contained 0.6 mL of 50 mmol/L zinc acetate for dissolved sulphide analysis.

The nutrient sample was diluted to a dilution factor of 10 for measurements of silicate, nitrite, NO_x, phosphate and ammonia concentrations by the MNF hydrochemistry team. After initial analysis, further dilutions were required due to high concentrations of various nutrients in different multicores, ranging from dilution factors of 50 to 5000. Nutrient samples were also taken from the overlying seawater collected in the jerry cans.

The dissolved iron sample was analysed using the Ferrozine Method for natural waters, as described by Viollier et al. (2000). In this method, 100 µL of 10⁻² mol/L Ferrozine was added to a 1 mL porewater sample, and the absorbance at 562 nm was measured using a spectrophotometer (Absorbance "A1"). The solution was reduced by adding 150 µL of freshly made 1.4 mol/L hydroxylamine hydrochloride and reacting for 10 minutes. 50 µL of 10 mol/L ammonium acetate buffer was added, and the absorbance at 562 nm was remeasured (Absorbance "A2"). The concentrations of dissolved Fe (II) and Fe (III) were calculated using a calibration curve, and the formula found in Viollier et al. (2000).

The dissolved sulphide sample was analysed using the methylene blue method as described by Cline (1969): 30 µL of colour reagent and 60 µL of catalyst were added to 1 mL of the prepared porewater and zinc acetate solution. After 30 minutes of reaction time, the absorbance of the solution at 670 nm was measured using a spectrophotometer and the sulphide concentration was calculated using a calibration curve.

After on board analysis of Core b was complete, all remaining porewaters were acidified with 40 µL of 6M HCl per millilitre of porewater and stored at 3 °C. The overlying seawaters were acidified at the same ratio. After centrifuging, the sediment remaining in the centrifuge tubes was stored at 3 °C. The centrifuged sediment from Core #2 was stored in the -85 °C freezer.

12.5.3.4 Sedimentary Ancient DNA (sedaDNA) sampling from Multicore

Please refer to 'Sedimentary Ancient DNA (sedaDNA) sampling from Multicores' for details. Samples for *sedaDNA* were taken from Core f in multicores: 02, 11 and 13.

12.5.3.5 Smith-McIntyre grab

After repeated failed multicore deployments at Station 64, the Smith-McIntyre grab ("Smith-Mac") was successfully deployed. The Smith-Mac grab relies on the impact of the Smith-Mac's foot plates on the seafloor triggering the release of heavy-duty springs that rapidly force the bucket jaws to clamp shut into the sediment. It is a powerful and swift action that ensures penetration even in stiff sediment not suitable for multicoring. On retrieval, the lifting force of the wire closes the jaws and holds them shut, keeping the sediment within the device.

The mud sample from the Smith-McIntyre grab was sampled into 12 small mini cores using 2 cm x 2 cm channels. The internal layering of the sediment was not preserved by this deployment operation, a key objective for the science goals. The mud-rich sandy layers were sliced up samples bagged for IRD, diatoms and excess mud.

12. Sediment (AAS 4630)

12.5.3.6 Portable X-Ray Fluorescence (pXRF)

pXRF scanning was undertaken for every multicore using a handheld Olympus Delta X Premium pXRF set to “Geochem” mode. Usually just one core from each multicore was measured for pXRF, and measurements were done on the diatom / excess sample bags (refer to tables in ‘Sample description & preliminary results’). A powdered standard (“Tas Bas”) was measured through a ziplock thrice before and after each multicore. Data was not corrected for drift and preliminary results provided useful insight into the cyclicity of elemental ratios related to changes in lithology.

12.5.4 Sample description & preliminary results

12.5.4.1 Multicore deployment 1

MC01 deployment failed. The sea conditions were rough, and the multicorer was hit by a large wave when it was lowered to the sea surface. Rather than retrieve and reset the operators preferred to continue to provide experience for the crew, who were not involved with the trial voyages.

12.5.4.2 Multicore deployment 2

MC02 successfully recovered 6 sediment cores, however as this was the first successful recovery for the RSV *Nuyina*, it was discovered that the pucks used were too large for the coring tubes. Core 4 was the first to be extruded during which the puck got stuck and the core had to be abandoned. This problem was solved for subsequent cores. All cores exhibited a well-preserved sediment-water interface. The upper 5 cm displayed evidence of bioturbation within a brown, homogeneous clay layer, which extends unaltered until approximately 16 cm depth. Below this, a transition into mottled grey silt/clay imbedded with brown clay, progressively shifting to a predominantly grey silty sediment from ~30 cm downward.

Table 32: Samples and data collected from MC02

Core	Height (cm)	Samples / data taken
1	40	DBD, porewater
2	38	eDNA
3	43	Porewater, ferrozine, sulphide, nutrients, excess sediment
4	33	Discarded
5	33	O2, diatoms, grain size, TOC, pXRF
6	38	Porewater, excess sediment, pXRF

12.5.4.3 Multicore deployment 3

Multicore deployment 3 successfully recovered six sediment cores. The pin for core six did not fire, despite this, a full 37 cm core was still recovered, it is suspected that suction kept the sediment in the core during retrieval. The surface sediment of most cores contained dropstones and exhibited a high biological deposition, with a thin, fluffy layer blanketing the sediment-water interface. Bioturbation was observed in the upper ~8 cm, with multiple cores containing evidence of bioturbation, including worms and a brittle star. The sediment composition remained consistent throughout the cores, characterized by sticky, clay-rich material.

12. Sediment (AAS 4630)

Table 33: Samples and data collected from MC03

Core	Height (cm)	Samples / data taken
1	29	Porewater, excess sediment
2	25	Discarded
3	26	O2, Diatoms, pXRF
4	32	Grain size, porewater
5	37	DBD, porewater, ferrozine, sulphide, nutrients
6	37	Porewater, Si isotopes, TOC, excess sediment

12.5.4.4 Multicore deployment 4

Six sediment cores were recovered from deployment 4, all cores exhibited a fluffy/gelatinous layer 2-5 mm thick over the surface sediment, in some cores, this layer was more coagulated and thicker in areas. Bioturbation was present in all cores and ceased between 5 cm and 7 cm. The colour of sediment was consistent down the core (7.5 YR 4/2). Core 6 had four pieces of gravel sized rock clustered on the surface.

Table 34: Samples and data collected from MC04

Core	Height (cm)	Samples / data taken
1	41	Porewater, nutrients
2	42	Porewater, Si isotope
3	42.5	DBD, Porewater, ferrozine, sulphide, nutrients
4	42	O2, diatoms, grain size, pXRF
5	43.5	
6	42	Porewater

12.5.4.5 Multicore deployment 5,6,7

Multicore deployments 5, 6 and 7 were all unsuccessful and located at the first Process Station. This is likely due to faulty cords resulting in firing prior to reaching the seafloor. The Smith-McIntyre Grab was subsequently deployed (successfully) at this location.

12.5.4.6 Multicore deployment 8

MC deployment 8 was the first deployment involving a new pin firing mechanism designed by Jamie, and where 78 kg of weight were added to address some of the concerns for MC5,6,7. Six cores were successfully recovered, and the top 0-6 cm of core was less compacted and slightly lighter and greener in colour and with modest bioturbation. The sediment colour then transitioned downward into grey/black sediment. For some cores this was a sharp transition, while others exhibited a mottling of light brown and dark grey sediment before transitioning into exclusively darker more compacted sediment. Core 3 had a large boulder at the base of the core.

Table 35: Samples and data collected from MC08

Core	Height (cm)	Samples / data taken
------	-------------	----------------------

12. Sediment (AAS 4630)

1	16	Discarded
2	16	Porewater
3	16	Porewater, ferrozine, nutrients, sulphide
4	29	DBD, ferrozine, nutrients, sulphide
5	22	O ₂ , diatoms, excess sediment
6	26	Porewater, Si isotopes, nutrients, pXRF

12.5.4.7 Multicore deployment 9

Deployment 9 successfully recovered 6 cores, all of which had a good water-sediment interface. All cores had a fluffy/gelatinous layer ~2 mm thick blanketing the sediment and had bioturbation in the top ~5 cm. Some cores had worms and worm poo in the surface sediment. From 6 cm downward the cores had lenses of grey, clayey homogenous mud within a more green/brown biogenic sediment. These lenses continued to the bottom in some cores and in others the base of the core became this grey sediment uniformly.

Table 36: Samples and data collected from MC09

Core	Height (cm)	Samples / data taken
1	30	Porewaters
2	35	Porewaters
3	33	Diatom, grain size, TOC, excess sediment, pXRF
4	39	DBD, porewater, ferrozine, nutrients, sulphide
5	33	Si isotope, Porewater
6	24	Porewaters

12.5.4.8 Multicore deployment 10

Deployment 10 recovered 6 sediment cores all with a good sediment-water interface. In some cores there were krill swimming in the water column. Core 1 contained multiple cracks and air pockets, meaning that below these imperfections, we cannot be certain that the depth within the core is true to the depth below sea floor. Thus core 1 was sectioned for eDNA analysis of the surface sediment and not used for porewaters. Some of these cores had a fluffy, biological layer as thick as 5 mm, whereas some had none. All cores had bioturbation up to 9 cm deep in the core. The sediment was grey with darker clayey mottling from 6 cm, some cores also had a green-grey lenses deeper at 13 cm. Below this the sediment is more uniformly grey clay with little biogenic material, similar to that of the base of MC09 cores.

Table 37: Samples and data collected from MC10

Core	Height (cm)	Samples / data taken
1	29	Discarded
2	26.5	Porewater, Si isotopes
3	33	Diatom, grain size, TOC, excess sediment, pXRF
4	40	Porewater,
5	42	Porewater, Si isotopes
6	30	Porewater, DBD, ferrozine, nutrients, sulphide

12. Sediment (AAS 4630)

12.5.4.9 Multicore deployment 11

MC deployment 11 recovered 6 sediment cores. Core 1 was clearly disturbed with suspended sediment in the water column, while the other 5 had a well-preserved sediment-water interface. The cores had a fluffy yellow/green biological layer on top of the sediment, below this there was sandy brown/black mud that is bioturbated and contained live worms in some cores, this layer ranges from 1-10 cm thick. This layer had a gradual/mottled transition into grey clayey mud that extended to the bottom of the core.

Table 38: Samples and data collected from MC11

Core	Height (cm)	Samples / data taken
1	10	Excess sediment
2	20	Porewater, eDNA
3	15	Porewater
4	18	Diatom, excess sediment, grain size, TOC, nutrients, pXRF
5	17	Porewater, DBD
6	22	Porewater, ferrozine, sulphide, nutrients

12.5.4.10 Multicore deployment 12

Multicore deployment 12 was unsuccessful in retrieving any sediment cores. It is likely that the seafloor was not suitable for multicoring thus no further deployments were attempted.

12.5.4.11 Multicore deployment 13

Deployment 13 recovered six cores, one of which had no water above the sediment but still appeared to reflect the five other replicate cores. All cores had a fluffy yellow biological layer blanketing the sediment. The top ~6 cm of each core consisted of olive/light sandy mud with worms present in some cores. This transitioned below into more olive grey clayey mud which is massive and extends down to approximately 20 cm. Below this the sediment transitions into a yellow diatom ooze with cottage cheese like texture. Core 6 was successfully recovered however was extruded for geotech prior to being photographed or described, thus it was not considered in the above lithological description.

Table 39: Samples and data collected from MC13

Core	Height (cm)	Samples / data taken
1	33	Porewater, Si isotopes
2	27	Porewater, eDNA
3	33.5	DBD, porewater, ferrozine, nutrients, sulphide
4	5	Porewater
5	30	Diatom, excess sediment, grain size, TOC, magnetic susceptibility, pXRF
6	-	Geotech, excess sediment

12.5.4.12 Multicore deployment 14

Deployment 14 successfully recovered 6 sediment cores, but the sediment-water interface was not as well preserved as in other deployments. Five cores had muddy standing water, and one

12. Sediment (AAS 4630)

(core 6) had no standing water. Most cores had a thin (2-5 mm) layer of silty mud on the surface of the sediment however due to the disturbed water column in the cores it is likely that this layer is due to the settling of suspended sediment and does not reflect the sediment-water interface at the seafloor. Below this silty layer was a coarse, well sorted sandy mud with some IRD.

Table 40: Samples and data collected from MC14

Core	Height (cm)	Samples / data taken
1	11	Porewater
2	10	Porewater
3	12	Porewater
4	13	Porewater, DBD
5	10	Porewater
6	6	Diatom, geotech, excess sed, grain size, TOC, pXRF

12.5.5 Recommendations:

- Oxygen probes are not recommended for use in sandy/rocky sediments, or in cores containing large numbers of IRD. Oxygen strips could be used, which indicate the oxygen penetration depth.
- Jamie Derrick's modifications to the trigger system of the multicorer are recommended for use in subsequent voyages.
- Clear communications with other teams looking to sample the multicorer. Several replicate cores were put aside for aDNA sample but had to be discarded after being left for too long
- Spare tracks for the glove box are needed, as this wore down over the voyage and made it difficult to move the box up and down over the extruder when setting up/packing away

12.6 Kasten Cores

12.6.1 Introduction

Kasten cores were chosen to reconstruct changes in the ice sheet and ocean over timescales of thousands of years. Sediment records on the continental shelf were targeted to reconstruct recent changes in ice shelf circulation, meltwater and biological productivity during the Holocene (the last 10,000 years). Cores on the continental slope further from the ice sheet generally have lower sedimentation rates but provide more continuous records over hundreds of thousands of years. The objectives were to 1) obtain Holocene records of sea ice, glacial meltwater input, mCDW incursion, and impacts on biological productivity (shelf cores), and 2) obtain glacial to interglacial records that capture changes in ice sheet retreat, sea ice expansion, Antarctic slope current variability, particularly for warmer than pre-industrial interglacials (Marine Isotope Stage 5e and 11).

12.6.2 Site selection & deck operations

Target sites were chosen based on pre-voyage analysis of seismic lines, combined with multibeam and sub-bottom profiles acquired during the voyage. Cross lines were used to confirm the sub-bottom profile stratigraphy. There were six kasten core (barrel dimensions of: 4 m x 0.15 m x 0.15 m) deployments, all of which were successful. Once the corer had been recovered, it was transferred from the back deck into Wet Lab 1. The kasten cores were then opened by removing one side of the barrel. For a map showing kasten core deployments, refer to Figure 56.

Table 41: Kasten core deployments

Station	Kasten core deployment	Latitude (DD)	Longitude (DD)	Ocean Depth (m)	Length of core recovered (m)
6	KC01	-63.283	97.307	1647	2.31
37	KC02	-65.2408	99.2527	887	3.96
53	KC03	-65.2894	99.2398	867	3.09
82	KC04	-64.4204	93.5990	2677	3.4
103	KC05	-66.0224	95.1993	748.96	3.49
140	KC06	-63.9536	97.2159	2164.5	3.31

12.6.3 Sample Collection Methods

12.6.3.1 Core photography

Kasten core photography, sampling, and logging was conducted in the Wet Lab 1 onboard the RSV *Nuyina*. A tape measure was placed alongside the core at the level of the core surface for reference during logging, sampling, and photography. Several operations were necessary prior to logging due to the clean conditions required for DNA sampling.

12. Sediment (AAS 4630)

The surface was first scraped by the aDNA team to remove any foreign DNA from the sediments at the interface with the core barrel and provide a smooth surface for core photography. Photographs were then taken by personnel wearing appropriate DNA PPE (gloves, facemask, long sleeves and hairnet). To keep the photography consistent, we employed a wheeled camera frame with light diffuser that kept the camera elevated at a constant height as we took multiple overlapping photographs along the entire core length. All lights in the wet lab were turned off to ensure consistent lighting throughout the core length. The photographs were taken every 30 cm using a Nikon D5300 camera and 35 mm lens. To minimize parallax error, the images were taken with 30 % overlap with the previous image and were compiled by stitching together in Illustrator.

The core logging team (wearing appropriate PPE described above) took an initial sketch of the core surface and visible structures as a reference for detailed logging following the DNA sampling.

12.6.3.2 Sedimentary ancient DNA (sedaDNA) protocols

Refer to 'Sedimentary ancient DNA (sedaDNA) sampling from Kasten cores'.

12.6.3.3 Visual core logging & Biostratigraphy

Visual core logging was completed immediately after sedaDNA work using a template which includes the Munsell colour, bioturbation, sedimentary structures, fossil content, grain size, nature of contacts, and general impression.

12.6.3.4 Temperature probes

Three Antares Temperature Data Loggers (Type 1854) were attached to the top, middle, and bottom of the side of the lid of the Kasten corer, and measurements were recorded every second for the duration of the deployment, providing both water column and sediment temperature data.

12.6.3.5 Thermal conductivity probes

Thermal conductivity was measured using a TEMPOS thermal properties analyser. Measurements were taken by inserting the probe into the sediment ensuring the tip of the probe stay a minimum of an inch from the bottom of the core barrel. The probe calibrated itself to the temperature of the sediment then took one minute to complete each measurement. This was done at 20 cm intervals from the base of the core with two replicate measurements taken at each depth.

12.6.3.6 Rhizomes / Porewaters

Rhizosphere rhizomes (5 cm porous membrane, 0.15 µm pore size, reinforced with glass fibre wire) were used to collect porewaters immediately during and after core logging at 20 cm intervals.

12. Sediment (AAS 4630)

12.6.3.7 Other sampling

All samples were labelled as follows: “NUY2025_V03_x_KC0y_z” where x = station number, y = kasten core deployment, and z = parameter sampled (e.g. IRD). Tables detailing the different samples and sampling resolutions collected for each kasten core are included on the following pages.

12.6.3.8 Archive u-channels

Archives were taken from all kasten cores using electrical ducting (PVC) u-channels of varying size. Depending on the availability of sediment, u-channels with widths of 2 cm x 2 cm, 5 cm x 5 cm, and 6 cm x 4 cm were inserted into the sediment, ensuring that at least one full record of the core was captured. U-channels were carefully removed from the core barrel using plastic fishing wire to separate the archive sediment from the bulk, and plastic spatulas to keep all sediment within the channel. Archives were cleaned, wrapped in plastic and refrigerated to best preserve the sediment for future use. They will be stored at IMAS.

12.6.3.9 Magnetic susceptibility

Magnetic susceptibility was analysed for the 5 cm x 5 cm archive u-channels using a Bartsoft MSC2 80 cm hoop sensor at 1 cm intervals. U-channels were held in a custom-built wooden frame and guided through the hoop sensor.



Figure 62: Photo taken inside the plastic "track" that was used to hold the archive u-channels which were pushed through the white hoop sensor (pictured). Photo: Jamie Derrick

12.6.3.10 Portable X-Ray Fluorescence (pXRF)

pXRF scanning was undertaken on the 5 cm x 5 cm archive u-channels for every kasten core using a handheld Olympus Delta X Premium pXRF set to “Geochem” mode. The archive u-channels were covered in MYLAR film and measurements were taken every 2.5 cm, higher resolution than this was not possible due to the size of the aperture window on the pXRF. The

12. Sediment (AAS 4630)

standard used was the powdered 'Tas Bas', with calibration checks and triplicates of the standard being completed before and after each section of sediment core was measured.

12.6.4 Sample description & preliminary results

12.6.4.1 KC01

Sediment core NUY2025_V03_06_KC01 is located on the Western Bruce Rise, at -63.283 °S, 97.306 °E at a depth of 1645 mbsl. The site survey based on previous seismic and EASI-3 PS141 voyage in 2023-2024 and new TOPAS data acquired on NUY2025_V03 (202425030PS18_Run01_002). Large scale seismic data show long term development of the sediment cap on the northern side of the Western Bruce Rise. The coring site is situated on relatively flat seafloor bathymetry, shallowing slightly to the northeast. The dominant mode of sediment deposition is current controlled, influenced by the bifurcation of the Antarctic Slope Current between the Antarctic continental shelf to the south, and the ASC flow to the north. The coring site was chosen to penetrate into highly laminated section, which is represented in the sub bottom profiler data by closely spaced, continuous reflectors.

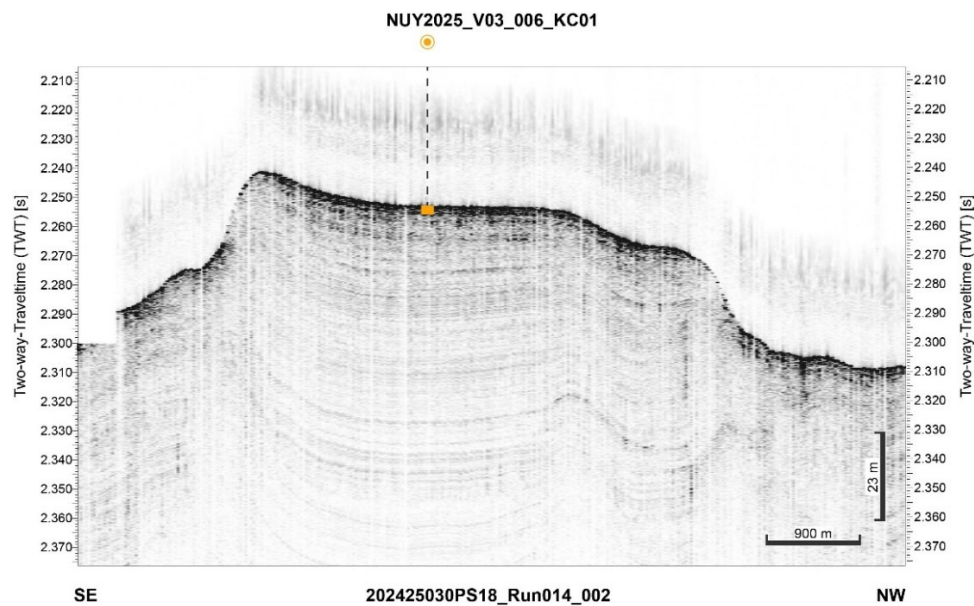


Figure 63: Sub bottom profile data for KC01 core site

The Kasten corer was deployed via the A-frame over the back deck, with temperature probes attached to the outside. On retrieval the top of the KC weight barrel had traces of mud, despite the core barrel being only 2/3 full. The base of the butter nose was indented so likely impact with large dropstones during coring.

Sampling

KC01 was sampled immediately after recovery (Figure 64). The order of operations was as follows: scraping, photography, *seda*DNA, thermal conductivity probes, core logging, rhizomes / porewater, removing dropstones, and finally implanting the XRF and archive U-channels. This was approximately a 17-hour long process. Smear slides were taken at 10 cm intervals and

12. Sediment (AAS 4630)

defined boundaries for onboard biostratigraphy. This was completed by Molly Husdell and Rachel Meyne by determining the last occurrence of an extinct diatom species, *Hemidiscus karstenii*, whose extinction occurred 190 thousand years ago (Barron 2003). In KC01, its last occurrence was at 175 cm which we interpreted as its extinction, thereby rendering KC01's base to be an estimated age of ~285 ka. Post sampling of magnetic susceptibility and pXRF datasets were acquired on the 5 cm x 5 cm archive u-channels following the methods outlined earlier in the report.

Table 42: Samples collected from KC01

Sample type	Intervals	Total samples
sedaDNA	At chosen depths	31
Ice rafted debris	Every 5 cm	46
Grainsize	Every 10 cm	24
Bulk Geochemistry/Total organic carbon	Every 10 cm	23
Porewater	Every 20 cm	13
$\delta^{15}\text{N}$	Every 10 cm	26
Be^{10}	Every 10 cm	24
Radiogenic isotopes	Every 10 cm	28
Diatoms	Every 5 cm	46
Ramped pyrolysis	At lithology boundaries	13
Dry bulk density	Every 10 cm	23
Dropstones	Wherever present	11
Cutter nose	Bottom of core	
Archive u-channels	5 cm x 5 cm set 2 cm x 2 cm set	2 sets

12. Sediment (AAS 4630)



Figure 64: Top left: KC02 post sampling. Top right: A. Wells, R. Meyne and J. Trihey core logging KC01. Bottom centre: sampling for sedaDNA.

12.6.4.2 KC02

NUY2025_V03_37_KC02 was collected from the east Antarctic continental shelf at (-65.2408 °S, 99.2527 °E) east of the Shackleton Ice Tongue in 887 m water depth. TOPAS sub bottom profiling revealed a thick (estimated 40 m) package of well-defined horizontally layered sediment and KC02 targeted the thickest area of this sediment package to retrieve a high-resolution record of the basin. The basin strikes northeast-southwest across the inner continental shelf of the eastern Denman region. The KC02 deployment over-penetrated the biosilicious mud, filling the barrel completely and with mud present between the weight plates. Around 250 kg of weight was removed from the subsequent deployment at the edge of the basin. The corresponding core KC03 is located 4.9 km away from KC02 near the edge of the basin where the sediment layers are truncated and aims to complement the high-resolution KC02 core with a lower resolution, stratigraphically older section, more condensed record. Some of the strata at this end of the basin is pinching out, which might result in a depositional hiatus. The relatively deep continental shelf (almost 900 m) and geometry of the basin likely shields this core location from strong currents, allowing for the primary method of sedimentation to be rain out from the overlying water column.

12. Sediment (AAS 4630)

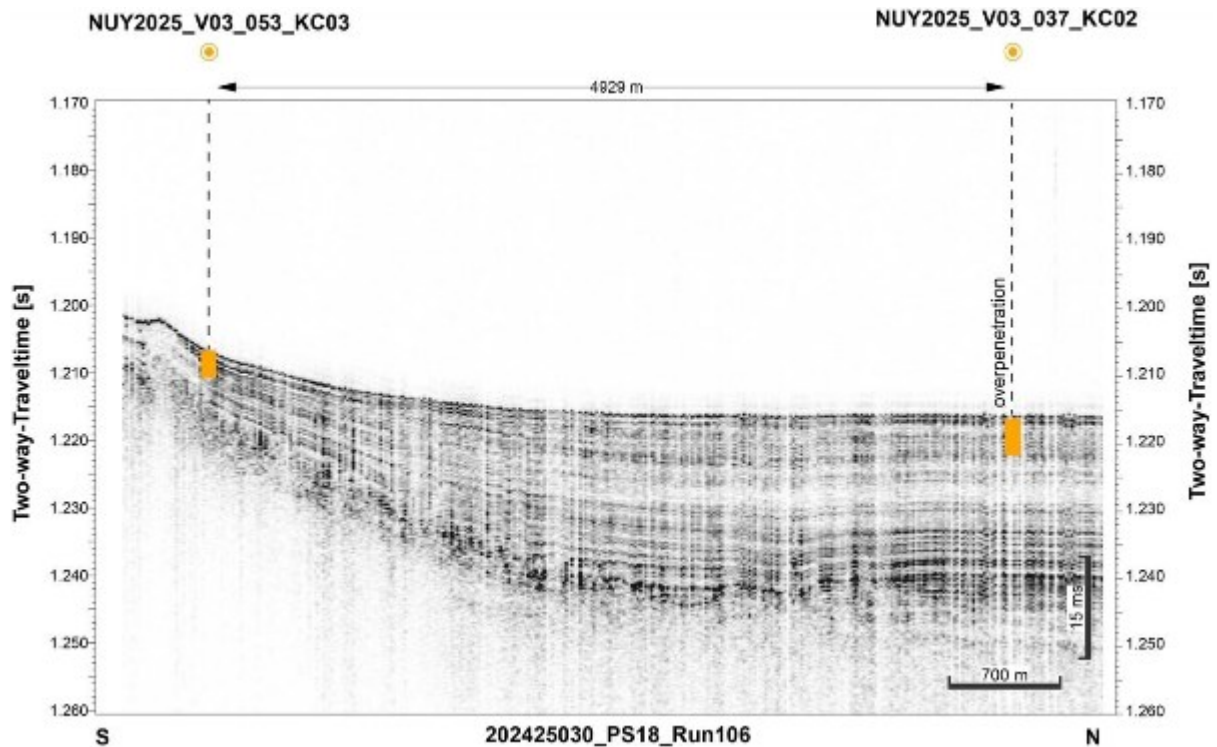


Figure 65: Sub bottom profile for KC02 and KC03

Sampling

KC02 was sampled immediately after recovery following the same order of operations as previous cores. Magnetic susceptibility and pXRF datasets were acquired on the 5 cm x 5 cm archive u-channels following the methods outlined earlier in the report.

Table 43: Samples collected from KC02

Sample type	Intervals	Total samples
sedaDNA	At chosen depths	40
Grainsize	Every 5 cm	80
Bulk Geochemistry/Total organic carbon	Every 5 cm	80
Porewater	Every 20 cm	20
d¹⁵N	Every 4 cm	102
Be¹⁰	Every 10 cm	44
Radiogenic isotopes	Every 5 cm	80
Diatoms	Every 2 cm	201
Ramped pyrolysis	Every 10 cm	41
Dry bulk density	Every 5 cm	80
Cutter nose	Bottom of core	1
Foraminifera	Every 50 cm	8
Archive u-channels	5 cm x 5 cm set 6 cm x 4 cm set 2 x cm x 2 cm set	3 sets

12. Sediment (AAS 4630)

12.6.4.3 KC03

NUY2025_V03_37_KC02 and NUY2025_53_KC03 were collected from the east Antarctic continental shelf, -65.2408 °S, 99.2527 °E and -65.2894 °S, 99.2398 °E respectively in 867 m water depth. TOPAS sub bottom profiling revealed a thick (estimated 40 m) package of acoustically well layered sediment in a basin that strikes northeast-southwest across the inner continental shelf of the eastern Denman region.

Sampling

KC03 was sampled immediately after recovery following the same order of operations as previous cores. Magnetic susceptibility and pXRF datasets were acquired on the 5 cm x 5 cm archive u-channels following the methods outlined earlier in the report.

Table 44: Samples collected from KC03

Sample type	Intervals	Total samples
sedaDNA	At chosen depths	36
Grainsize	Every 5 cm	80
Bulk Geochemistry/Total organic carbon	Every 5 cm	80
Porewater	Every 20 cm	22
d¹⁵N	Every 4 cm	102
Be¹⁰	Every 10 cm	44
Radiogenic isotopes	Every 5 cm	80
Diatoms	Every 2 cm	201
Ramped pyrolysis	Every 10 cm	41
Dry bulk density	Every 5 cm	80
Cutter nose	Bottom of core	1
Foraminifera	Every 50 cm	8
Archive u-channels	5 cm x 5 cm set 6 cm x 4 cm set 2 cm x 2 cm set	3 sets

12.6.4.4 KC04

Kasten core NUY2025_V03_082_KC04, was collected on the continental slope offshore of the Shackleton Ice Shelf (-64.4204 °S, 93.5990 °E). The weight on the head of the kasten core was increased to the original weight (~800 kg). The sediment echosounder data revealed a levee deposit at the western side of a channel system originating on the upper slope. The sediments deposited at this site therefore report on the interaction between the down-slope transport from the Shackleton Ice Shelf continental shelf and the Antarctic Slope Current. The site was selected based on sub-bottom profiler data collected by RV *Polarstern* in 2024 (Line 2024_0222_200301). The site was carefully chosen to avoid abundant slump-like features nearby, while recovering a continuous record.

12. Sediment (AAS 4630)

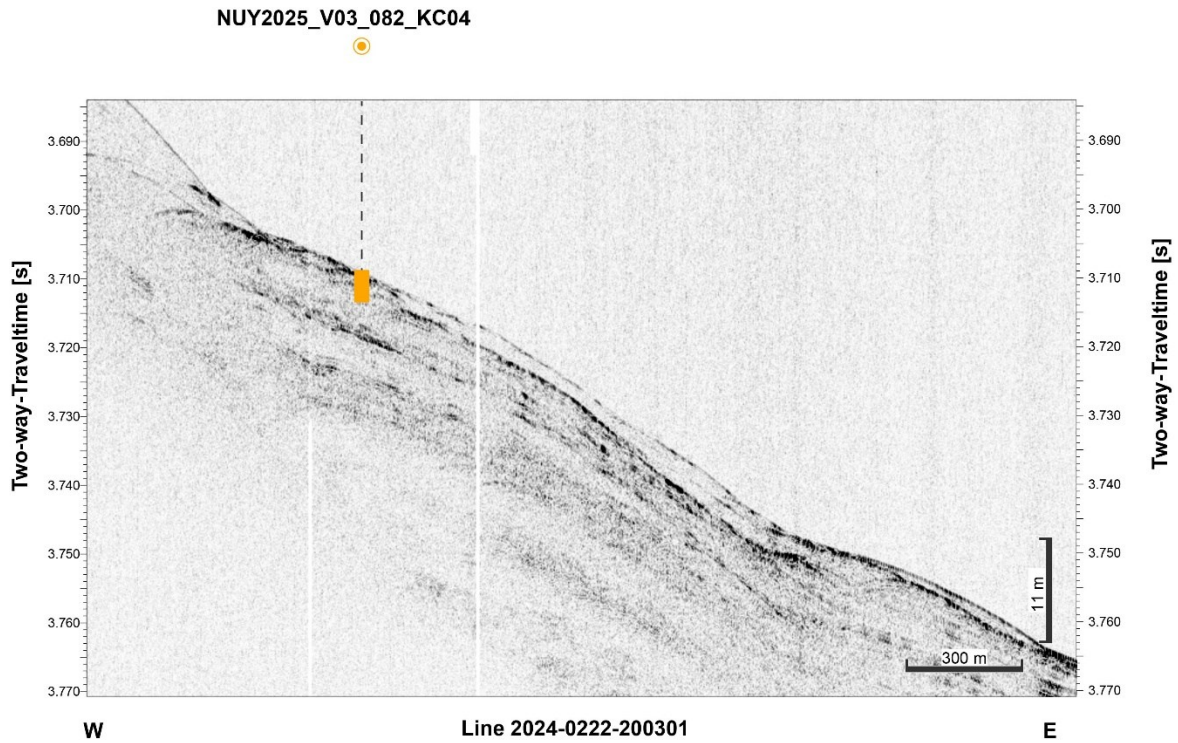


Figure 66: Sub bottom profile of KC04

Sampling

KC04 was sampled immediately after recovery following the same order of operations as previous cores over an approximate 17-hour period. Magnetic susceptibility and pXRF datasets were acquired on the 5 cm x 5 cm archive u-channels following the methods outlined earlier in the report and preliminary on-board biostratigraphy was completed. The methods for biostratigraphy are outlined in the KC01 sampling section. The last occurrence of *H. karstenii* in KC04 was at 218 cm, which we interpreted as its extinction. Therefore, KC04 is estimated to be ~290 ka at its base.

Table 45: Samples collected from KC04

Sample type	Intervals	Total samples
sedaDNA	At chosen depths	32
Thermal conductivity	20 cm	17
Porewater	20 cm plus boundaries of interest	20
Ice rafted debris	At boundaries only	17
Grainsize	5 cm	67
Bulk Geochemistry/Total organic carbon	5 cm	68
RPO	At boundaries only	10
TEX-86	5 cm	68
Foraminifera	5 cm for top 100 cm, then 10 cm	45

12. Sediment (AAS 4630)

Diatoms	2.5 cm	137
Dry bulk density	5 cm	68
Dropstones	Wherever present	32
Archive u-channels	5 cm x 5 cm set 6 cm x 4 cm set	Two sets

12.6.4.5 KC05

Kasten core NUY2025_V03_103_KC05 was collected on 9th April 2025 in a small basin on the continental shelf off the western Shackleton Ice Shelf (-66.0224 °S, 95.1993 °E). The sediment cored shows exemplary layering between diatomaceous oozes, diatom mats and clay-rich layers. It is expected that this core displays a high-resolution record of the recent environmental history of the inner Shackleton continental shelf. The E-W trending profile (shown below) shows an approximately 20 m thick sediment package, which is laminated in the centre of the basin and shows transparent features towards the basin's edges, which could be related to mass wasting deposits.

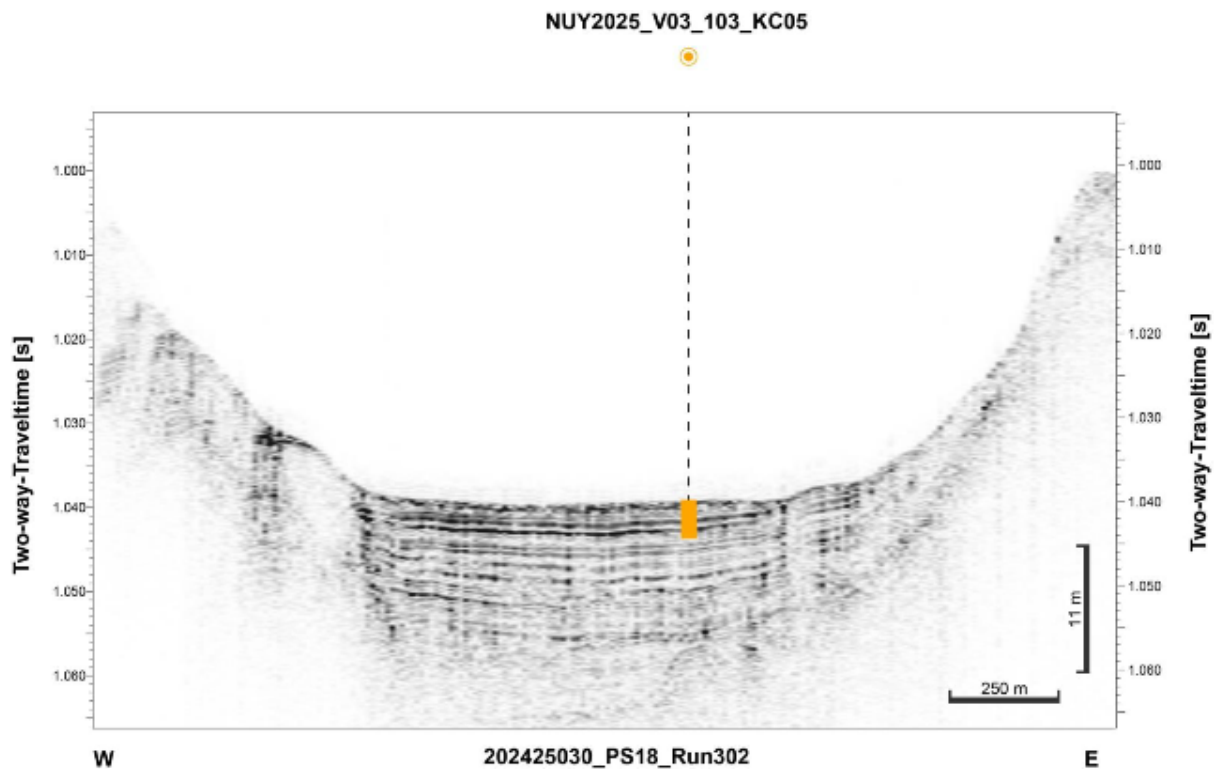


Figure 67: Sub bottom profile of KC05

Sampling

KC05 was sampled immediately after recovery following the same order of operations as previous cores. Magnetic susceptibility and pXRF datasets were acquired on the 5 cm x 5 cm archive u-channels following the methods outlined earlier in the report and preliminary on-board biostratigraphy was completed.

12. Sediment (AAS 4630)

Table 46: Samples collected from KC05

Sample type	Intervals	Total samples
sedaDNA	At chosen depths	54
Thermal conductivity	20 cm	18 measurements
Porewater	Boundaries	30
Grainsize	Every 5 cm	71
Bulk Geochemistry/Total organic carbon	Every 5 cm, with two layers sampled	137
TEX-86	Every 2 cm until 10 cm, then every 5 cm	70
Diatoms	Every 5 cm and Boundaries	86
Ramped pyrolysis	Lithological boundaries	15
Dry bulk density	5 cm	70
Dropstones	Sampled where present	7
Archive	2 cm x 2 cm set 5 cm x 5 cm set	Two sets

12.6.4.6 KC06

NUY2025_V03_140_KC06 was recovered on the continental slope north of the tip of the Shackleton Ice Shelf in a water depth of 2164.5 m (-63.9536 °S, 97.2159 °E). The coring target sits on a levee deposit, which records the interaction between down slope transport from the Denman region with the Antarctic Slope Current. The already available sub bottom profiler data (PS-141, 2024_0319-014932_freq_env) was carefully interrogated to show continuous sedimentation and be free of mass-wasting deposits.

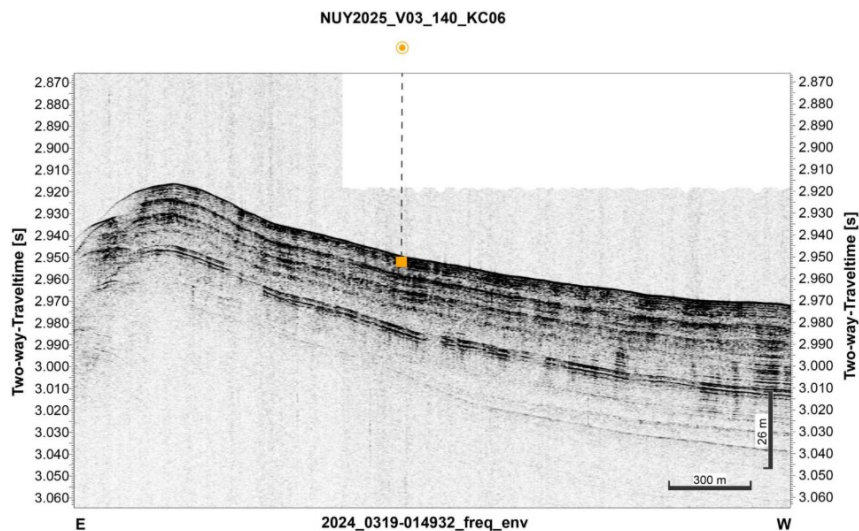


Figure 68: Sub bottom profile of KC06

KC06 was sampled immediately after recovery following the same order of operations as previous cores. Magnetic susceptibility and pXRF datasets were acquired on the 5 cm x 5 cm archive u-channels following the methods outlined earlier in the report and preliminary on-board biostratigraphy was completed. The methods for biostratigraphy are outlined in the KC01 sampling section. The last occurrence of *H. karstenii* in KC06 was at 175 cm, which we

12. Sediment (AAS 4630)

interpreted as its extinction. We sampled the core cutter carefully using a multicore tube which was sliced into 1 cm intervals because we believe we capture Marine Isotope Stage 11 at the base of the core. Therefore, KC06 is estimated to be ~450 ka at its base.

Table 47: Samples collected from KC06

Sample type	Intervals	Total samples
sedaDNA	At chosen depths	33
Thermal conductivity	20 cm	17 measurements
Porewater	Boundaries	24
Grainsize	Every 5 cm	69
Bulk Geochemistry/Total organic carbon	Every 5 cm	67
TEX-86	Every 5 cm and boundaries	68
Diatoms	Every 5 cm	67
Foraminifera	Every 5 cm	66
Ramped pyrolysis	Depths of interest	3
Dry bulk density	5 cm	66
Dropstones	Sampled where present	48
Archive u-channels	5 cm x 5 cm	One set

12.7 Data Management

All preliminary data will be published through the Australian Antarctic Data Centre (AADC) (<https://data.aad.gov.au/>) following standard AADC procedures, and subject to the moratorium of 2 years.

12.8 Acknowledgements

The sediments team would like to thank a number of people. The Serco crew, AAD gear officers and technicians were extremely helpful, and this work wouldn't have been possible without them. In particular a huge thank you to Dom Weller for fixing the centrifuge and allowing multicore processing to continue, and Jamie Derrick for fixing the multicore trigger system which enabled the multicore success rate to dramatically improve. Thank you to the hydrochemists on board, Julie Janssens and Merinda McMahon, for the macronutrient analysis of the porewater samples (sometimes 4 or 5 run throughs for the one sample). Special thank you to the sound witches for providing outstanding mapping of the ocean floor and below, and the whale watchers for keeping the sub-bottom profiler running! To those who volunteered to help with the Kasten core mud parties (Dr's Cath Deacon and Jess Johnson Ling, Frances Perry, Christian Pagel, Tim Scott, Tess Chapman, Dom Weller, Liam Byrne, and others), it was great fun having the extra company in the lab! Thank you.

12.9 References

- Barron, J.A. (2003). Planktonic marine diatom record of the past 18 M.Y.: Appearances and extinctions in the Pacific and Southern oceans. *Diatom Research*, 18(2), 103–224. <https://doi.org/10.1080/0269249X.2003.9705588>
- Cline, J. D. (1969). Spectrophotometric determination of hydrogen sulfide in natural waters. *Limnology and Oceanography*, 14(3), 454–458. <https://doi.org/10.4319/lo.1969.14.3.0454>
- Cutter, Gregory, Casciotti, Karen, Croot, Peter, Geibert, Walter, Heimbürger, Lars-Eric, Lohan, Maeve, Planquette, H  l  ne, van de Flierdt, Tina (2017) Sampling and Sample-handling Protocols for GEOTRACES Cruises. Version 3, August 2017. Toulouse, France, GEOTRACES International Project Office, 139pp. & Appendices. DOI: <http://dx.doi.org/10.25607/OBP-2>
- Cytiva. (2025). *Cytiva*. Cytiva. <https://www.cytivalifesciences.com/en/us/shop/lab-filtration/capsule-filters/pes-capsule-filters/acropak-200-capsules-with-supor-membrane-p-36449>
- Matsuoka, K., Skoglund, A., Roth, G., de Pomereu, J., Griffiths, H., Headland, R., Herried, B., Katsumata, K., Le Brocq, A., Licht, K., Morgan, F., Neff, P. D., Ritz, C., Scheinert, M., Tamura, T., Van de Putte, A., van den Broeke, M., von Deschwanen, A., Deschamps-Berger, C., . . . Melv  r, Y. (2021). Quantarctica, an integrated mapping environment for Antarctica, the Southern Ocean, and sub-Antarctic islands. *Environmental Modelling & Software*, 140, 105015. <https://doi.org/https://doi.org/10.1016/j.envsoft.2021.105015>
- Multi corer 6 x  110 mm, KC Denmark · Oceanography · Limnology · Hydrobiology. (2025). Kc-Denmark.dk. <https://www.kc-denmark.dk/products/sediment-samplers/multi-corer/multi-corer-6-x-oe110-mm.aspx>
- Viollier, E., Inglett, P. W., Hunter, K., Roychoudhury, A. N., & Van Cappellen, P. (2000). The ferrozine method revisited: Fe(II)/Fe(III) determination in natural waters. *Applied Geochemistry*, 15(6), 785–790. [https://doi.org/10.1016/s0883-2927\(99\)00097-9](https://doi.org/10.1016/s0883-2927(99)00097-9)

13. Towed camera / Seafloor imagery (AAS 4630)

By Craig Johnson

Personnel: Nicole Hill (Project Lead) (shore-based)
Jan Jansen (shore-based)
Craig Johnson (Shipboard Lead), IMAS
Noémie Friscourt, IMAS
Ilaria Stollberg, IMAS

13.1 Objectives

Our research questions centre around understanding the biodiversity, structure, distribution, and drivers of benthic communities and how this may change under future conditions. In particular, we aimed to validate circumpolar benthic models, develop a detailed understanding of regional patterns and examine the role of sea ice and productivity in shaping benthic communities. To support this, the objective of the work is to sample as broad a diversity of habitat types as possible using the AAD Towed Camera apparatus fitted with the VOYIS high-definition stereo camera system. Towed camera transects ~ 1 km in length were intended to sample benthic communities across a range of habitat types encompassing different depths, substratum type, slope angles, benthic rugosity, distances from the Denman Glacier and Shackleton Ice Shelf, productivity regimes and distances from the edge of the continental slope.

13.2 Methods

The towed body supporting the VOYIS stereo camera system (Figure 69) was lowered to the seafloor with the ship stationary, and on arrival within 1-2 m of the seafloor was towed in a consistent direction for ~1 km at 1-1.5 knots. The AAD system stores 5 stereo image pairs per second. Our field server (Greybits Box) contained customised software that captures images, allows real time scoring and formats images, metadata and annotations ready for upload into IMOS' Underwater Marine Imagery National Facility. The frequency of images forwarded to *Squidle* and the Greybits Box was reduced to 2 images per second for technical reasons, while *Squidle*'s capture software harvested an image every 5 seconds. For the duration of the voyage the IMAS Greybits hardware and *Squidle* software system was integrated with the AAD image acquisition / storage and NUTTS systems.

Using the *Squidle* software provided with the Greybits box, brief annotation notes are made on selected images in real time while the tow is underway. This includes identifying key taxa, substratum type, and any particular additional notes deemed worthy of highlighting. However, this annotation is at a high level, does not include a complete list of taxa, and in some cases is inaccurate (reflecting that a new image is available for annotation every 5 seconds on the *Squidle* software). This real-time underway annotation is useful to identify frames with organisms to quantify.

Once ashore, suitable images every ~50 m along each transect will be examined in detail and coverage of organisms carefully quantified. This is achieved by overlaying a grid of 108 points on each selected image and scoring ('annotating') whatever lies beneath each point using the well-recognised and widely used CATAMI Morphospecies classification (Althaus et al., 2015).

13. Towed camera / Seafloor imagery (AAS 4630)



Figure 69: The towed body on the aft deck of the RSV Nuyina. Photo: Ilaria Stollberg



Figure 70: Voyis image from Towed Camera 16 showing a scaleworm, soft corals, bryozoans, brittle stars and a seaspider on an outcropping rock.

13. Towed camera / Seafloor imagery (AAS 4630)



Figure 71: Voyis image form Towed Camera 20 showing a large glass sponge hosting feather stars surrounded by other sponges and brittle stars.



Figure 72: Voyis image form Towed Camera 13 showing benthic fish with attached isopod parasite.

13. Towed camera / Seafloor imagery (AAS 4630)



Figure 73: Voyis image from Towed Camera 20 showing a sea pig and its trail in soft sediment.

13.3 Activity on the Voyage

A total of 23 towed camera transects were completed on the voyage. While this is less than the 30 transects outlined in the Service Level Agreement, the target of 30 transects was a ‘stretch target’ determined assuming no losses of time due to bad weather. The reduced number of tows completed is the direct result of poor weather or ice conditions preventing lowering a wire from the stern of the vessel, or time constraints in juggling other research priorities. Also, tow directions were limited by wind and ice conditions; it was generally necessary to tow directly into the wind. Accordingly, shallow sites, and sites furthest south and close to the glacier / iceshelf (i.e. on both sides of the Shackleton Ice Shelf) were under-represented.

Details of the tows are provided below (Table 48, Table 49, Table 50).

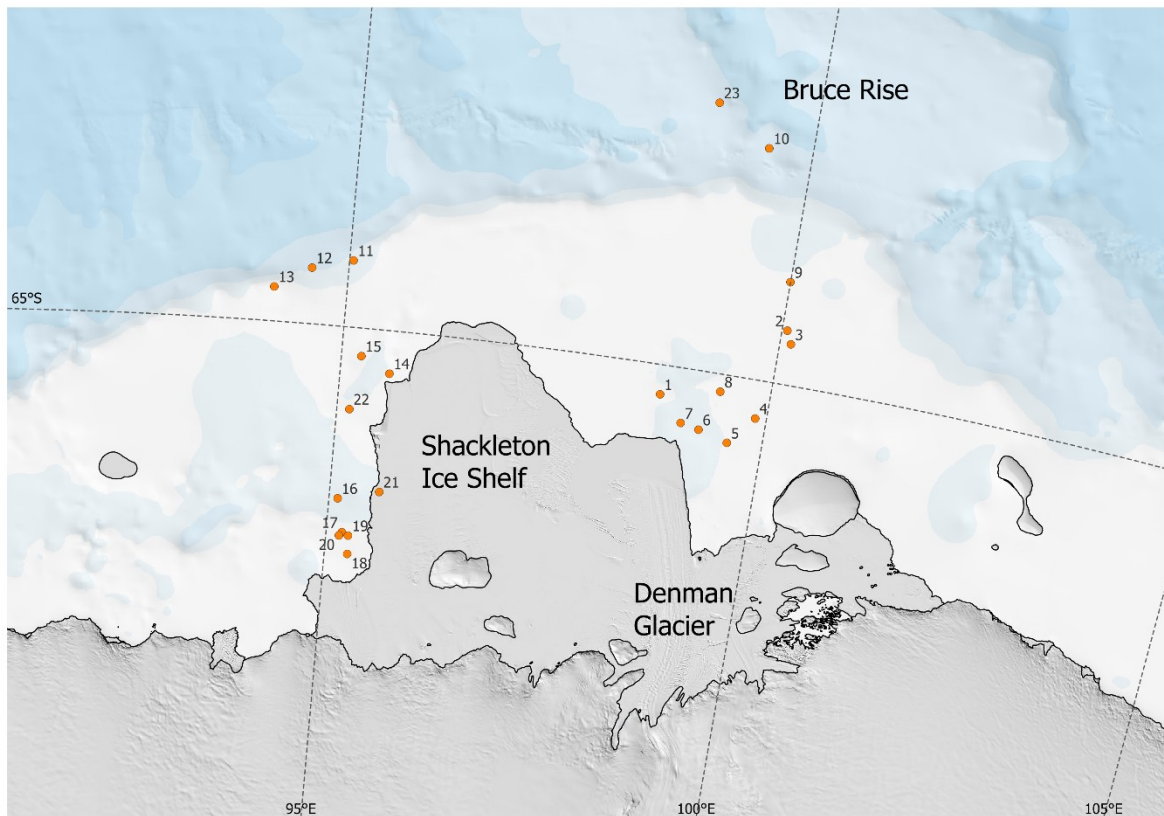


Figure 74: Deep Tow Camera locations. Basemap from Quantarctica (Matsuoka et al., 2021).

13. Towed camera / Seafloor imagery (AAS 4630)

Table 48: Towed Camera transect metadata.

Station	Transect Number	Images	Ship Sounder Depth (m)	Start Latitude (DD)	Start Longitude (DD)	End Latitude (DD)	End Longitude (DD)	Notes
30	1	500	625.83	-65.1458	98.8160	-65.1542	98.7483	
31	2	562	523.9	-64.7362	100.0589	-64.7363	100.0826	
33	3	296	505.02	-64.7993	100.1282	-64.8019	100.1753	
49	4	350	497.26	-65.1866	99.8728	-65.1882	99.9056	
50	5	348	612.01	-65.3304	99.5760	-65.3343	99.5440	
53	6	510	NA	NA	NA	NA	NA	No images
54	7	576	801.13	-65.2685	99.0211	-65.2757	99.0769	
60	8	741	819.97	-65.0862	99.4125	-65.0840	99.4475	
64	9	257	557.87	-64.5001	99.9996	-64.5126	100.0013	
66	10	417	1419.92	-63.8741	99.5123	-63.9010	99.4820	
80	11	436	352.3	-64.6715	95.1180	-64.6483	95.0595	
81	12	626	868.92	-64.7261	94.5797	-64.7150	94.6481	
83	13	573	277.55	-64.8320	94.1643	-64.8380	94.1422	
90	14	422	-455.82	-65.2101	95.5772	-65.2163	95.6031	
93	15	449	629.39	-65.1367	95.2322	-65.1360	95.2623	
99	16	561	459.91	-65.8422	95.1054	-65.8410	95.1357	
102	17	567	191.24	-66.0061	95.1914	-66.0081	95.2192	
107	18	398	325.1	-66.1097	95.2814	-66.1097	95.2811	
108	19	116	373.63	-66.0197	95.2758	-66.0197	95.2757	
109	20	400	699.37	-66.0229	95.1605	-66.0221	95.1883	
126	21	405	1279.67	-65.7918	95.4266	-65.7941	95.4571	
127	22	376	382.6	-65.4005	95.1497	-65.3975	95.1753	
142	23	397	1478.88	-63.6925	98.8940	-63.6940	98.9200	

13. Towed camera / Seafloor imagery (AAS 4630)

Table 49: High level notes on camera tows 1-13, DMV3, 2025 in the region of the Denman Glacier and Shackleton Ice Shelf. Technical information is provided in Table 50.

Tow	Notes
1	<p>... Transect starts on edge of paleoscour and moves away from scour scar @ ~25° angle to the scar.</p> <p>... High concentrations of marine snow and salps at the sea floor.</p> <p>... Soft sediment, well bioturbated, good diversity of fauna.</p>
2	<p>... Transect crosses pronounced paleoscour on seafloor.</p> <p>... High levels of marine snow at depth.</p> <p>... Technical issues with images freezing on Squidle as a result of attempted overwrite of images; resolution requires manually stopping and resetting the live frame feed, and filtering for 'VOYIS_USP'. In subsequent tows, we avoid need to filter for 'VOYIS_USP' by not turning on capture of images from forward facing camera, but overwrite issue persists.</p>
3	<p>... Transect commences in trough of paleoscour (~ 1 km in width) and runs obliquely upslope to a ridge. Difference in altitude trough-ridge ~ 10 m.</p> <p>... Bioturbation clearly evident.</p>
4	<p>... Transect length ~1500 m in silty mud.</p> <p>... Relatively high biodiversity in patches at scales 30-60 m.</p> <p>... Salps dense in water column, but not at seafloor.</p>
5	<p>... ~1500 m transect, crosses steep 'step down' of ~ 30 m drop.</p> <p>... Silty but with increasing patches of gravel as transect progressed.</p> <p>... Occasional drop stones.</p> <p>... Occasional high diversity patches.</p>
6	<p>... Deeper transect in a basin where Kasten core taken; v silty.</p> <p>... Sparse / depauperate community with little bioturbation.</p> <p>... Frame freezing problem continues. Buffer issue? Will try dropping AAD capture rate 5 to 2 per sec.</p>
7	<p>... ~ 1500 m; downslope and mostly fine silt, but crosses two ridges.</p> <p>... Sparse community, looks like possibly high current area (right to left).</p>
8	<p>... No particular comment.</p>
9	<p>... Camera porpoising with 4 m swell (and novice winch / wire driver), so suspect many frames not really usable.</p> <p>... Limited bioturbation.</p>
10	<p>... Podeba Canyon. Gravel and cobbles on sediment.</p> <p>... Step or ledge of what appears to be sedimentary rock overlain with sediment, but no major hard rock outcrops.</p> <p>... High abundances of crinoids, ophiuroids.</p>
11	<p>... Sediment coarser than sites further east (sandier), and possibly higher diversity than more eastern sites to date. High levels of bioturbation.</p> <p>... Tow crosses marked scour track; earlier beam trawl track? Illegal fishing?</p>
12	<p>... Through small scooped out valley off shelf break; steep in places.</p> <p>... Sediment with 20-80% overlay of gravel & cobbles; some consolidated sedimentary structures.</p>
13	<p>... High biodiversity and fish abundance; high abundance crustaceans at start (krill?).</p>

13. Towed camera / Seafloor imagery (AAS 4630)

14	<p>... No USBL due to ice conditions and risk to HIPAP pole.</p> <p>... Relatively low biodiversity. Muddy substratum with only moderate bioturbation, but with different type of bioturbation pattern than previously. Larger oblong shaped holes in benthos maybe subsurface molluscs?</p>
15	<p>... More sea pigs and stalked sea pens than usual; some notable sponges.</p>
16	<p>... Rich sponge community at beginning of transect.</p> <p>... Substratum looks like light sediment over hard base, giving way to pebbly gravel later in transect. Undulating in places.</p> <p>... Ophiuroids particularly abundant throughout.</p> <p>... Generally high biodiversity, high abundances.</p>
17	<p>... Hard bottom with high diversity / abundances. Lots of fish.</p>
18	<p>... No USBL due to ice conditions and risk to HIPAP pole.</p> <p>... Minimum depth = 260 m, generally towed up-slope.</p> <p>... mix of hard bottom and sediment; higher fish abundance earlier in transect.</p>
19	<p>... Very short transect to check suitability of substratum for beam trawl.</p> <p>... No USBL due to ice conditions and risk to HIPAP pole.</p> <p>... Blurred lens – dirty?</p>
20	<p>... No USBL due to ice conditions and risk to HIPAP pole.</p> <p>... Mostly sediment although lots of drop stones providing habitat for sponges.</p> <p>... High density sea pigs, especially towards end of transect.</p>
21	<p>... In deep trench . gutter running east-west approximately perpendicular to ice shelf.</p> <p>... Ship ran for ~1.5 km but camera covered only ~575 m due to high current and need to feed more wire to keep camera on the benthos; camera at least 800 m behind stern of vessel by the end of the transect.</p> <p>... High current also evident by orientation of benthic animals ‘streaming’ in the current and small scale scour striations on sea floor.</p>
22	<p>... No USBL due to ice conditions and risk to HIPAP pole.</p> <p>... This site identified by Mark Hindell as a ‘hotspot’ for benthic foraging by elephant seals.</p> <p>... High level of bioturbation, but surprisingly sparse diversity given level of bioturbation.</p> <p>... High abundance of fish, stalked sea pens. Remarkably few holothurians.</p>
23	<p>... Transect on NE facing slope on SW side of Pobeda Canyon on the Bruce Rise.</p> <p>... Pebbles on sediment, sparse community. Substratum appears semi-consolidated.</p> <p>... Camera porpoising along seafloor with swell.</p>
	END

13. Towed camera / Seafloor imagery (AAS 4630)

Table 50: Summary details of the 23 towed camera transects taken from RSV Nuyina on DMV3. Note that dates refer to ship time (operating on Bangkok time), while actual times of deployment and retrieval of the towed body are UTC. USBL 'y/no' indicates whether the USBL was able to be operated; when it was operational, lat/long coordinates refer to the position of the camera, otherwise the position of the stern of the vessel. Data from the AAD NUTTS stream provides information on depth, amount of wire out, and wire direction relative to the vessel, enabling dead reckoning estimates of camera location.

Tow No	Date*	Start	Finish	USBL	Way Point	Station No	Approx Heading	Start depth (m)	End depth (m)	UTC start (hr:min)	UTC end (hr:min)
1	19-Mar-25	65° 08.700'S, 98° 43.980'E	65° 09.240'S, 98° 45.420'E	y	NA	30	090	628	631	10:15	10:58
2	20-Mar-25	64° 44.160'S, 100° 03.660'E	64° 44.160'S, 100° 04.800'E	y	67	31	090	523	524	not recorded	05:40
3	20-Mar-25	64° 47.940'S, 100° 07.680'E	64° 48.000'S, 100° 09.360'E	y	68	33	095	504	498	14:22	15:05
4	25-Mar-25	65° 11.220'S, 99° 52.260'E	65° 11.280'S, 99° 53.880'E	y	106	49	120	496	486	12:07	13:00
5	25-Mar-25	65° 19.687'S, 99° 35.510'E	65° 19.971'S, 99° 33.680'E	y	107	50	255	592	627	16:44	17:26
6	26-Mar-25	65° 17.193'S, 99° 14.423'E	65° 17.625'S, 99° 15.248'E	y	110	53	125	889	880	08:41	09:31
7	26-Mar-25	65° 16.070'S, 99° 01.271'E	65° 16.129'S, 99° 03.202'E	y	111	54	125	801	849	12:52	13:46
8	27-Mar-25	65° 05.148'S, 99° 25.078'E	65° 05.101'S, 99° 25.628'E	y	116	60	090	814	799	12:15	12:49
9	29-Mar-25	64° 30.003'S, 99° 59.950'E	64° 30.339'S, 100° 00.052'E	y	128	64	175	555	551	15:15	15:44
10	31-Mar-25	63° 52.448'S, 99° 30.733'E	63° 52.448'S, 99° 30.733'E	y	130	66	213	1443	1605	09:20	09:56
11	3-Apr-25	64° 40.463'S, 95° 02.687'E	64° 39.496'S, 95° 03.204'E	y	148	80	005	421	560	12:40	13:31

13. Towed camera / Seafloor imagery (AAS 4630)

12	4-Apr-25	64° 43.555'S, 94° 34.797'E	64° 43.358'S, 94° 35.992'E	y	149	81	068	870	1207	00:26	00:47
13	5-Apr-25	64° 49.917'S, 94° 09.860'E	64° 50.235'S, 94° 08.788'E	y	151	83	230	278	295	17:50	18:22
14	6-Apr-25	65° 12.609'S, 95° 34.621'E	65° 12.898'S, 95° 35.706'E	no	161	90	120	557	523	13:10	13:41
15	7-Apr-25	65° 08.210'S, 95° 13.957'E	65° 08.165'S, 95° 15.208'E	y	163	93	085	634	608	01:59	02:34
16	8-Apr-25	65° 50.537'S, 95° 06.286'E	65° 50.487'S, 95° 07.880'E	y	169	99	086	460	431	15:08	15:52
17	9-Apr-25	66° 00.365'S, 95° 11.462'E	66° 00.161'S, 95° 12.554'E	y	173	102	100	190	240	10:08	10:53
18	11-Apr-25	66° 06.591'S, 95° 16.821'E	66° 06.494'S, 95° 18.141'E	no	176B	107	078	323	270	01:48	02:18
19	11-Apr-25	66° 01.211'S, 95° 16.190'E	66° 01.179'S, 95° 16.604'E	no	177	108	082	371	371	04:27	04:34
20	12-Apr-25	66° 01.383'S, 95° 09.619'E	66° 01.327'S, 95° 11.203'E	no	178	109	082	699	760	17:30	17:58
21	14-Apr-25	65° 47.494'S, 95° 35.555'E	65° 47.535'S, 95° 26.303'E	y	185	126	100	1279	1315	09:29	10:01
22	14-Apr-25	65° 24.036'S, 95° 08.960'E	65° 23.886'S, 95° 10.266'E	no	195	127	078	382	385	16:06	16:35
23	21-Apr-25	63° 41.555'S, 98° 53.628'E	63° 41.599'S, 98° 54.224'E	y	TC23	142	115	1480	1543	16:27	16:59

* The Date is NOT UTC but ship time, i.e. Bangkok time

13.4 Outcomes and data management

The detailed quantitative data will be provided to the Australian Antarctic Data Centre (AADC) (<https://data.aad.gov.au/>), and added to an existing global data base created by IMAS (Jansen et al., 2023) based on similar annotations of downward-facing camera images of the seafloor around Antarctica provided from voyages undertaken by Britain, France, Germany, USA, NZ, and previous campaigns by Australia and hosted at www.squidle.org (once embargoes are lifted). Collectively, these data inform complex statistical models to enable prediction of the distribution of biodiversity on the continental shelf right around Antarctica. The output from this work includes maps of the distribution of individual species and species complexes, bioregions, and vulnerable marine ecosystems. These maps are vital to informed policy development concerning marine spatial planning, marine conservation, and other aspects of marine management in Antarctica.

13.5 Acknowledgements

Given the aforementioned constraints, the achieved number of tows is an excellent outcome for the voyage and a credit to the efforts of the bridge crew, deck crew, wire operators, hydroacoustics team, and AAD electronics engineers whose combined teamwork underpins a successful tow.

13.6 References

- Althaus, F., Hill, N., Ferrari, R., Edwards, L., Przeslawski, R., Schönberg, C.H.L. *et al.* (2015). A Standardised Vocabulary for Identifying Benthic Biota and Substrata from Underwater Imagery: The CATAMI Classification Scheme. *PLOS ONE*, 10, e0141039.
- Jansen, J., Shelamoff, V., Gros, C., Windsor, T., Hill, N.A., Barnes, D.K. *et al.* (2023). The Antarctic Seafloor Annotated Imagery Database. *bioRxiv*, 2023.2002.2016.528770.
- Matsuoka, K., Skoglund, A., Roth, G., de Pomereu, J., Griffiths, H., Headland, R., Herried, B., Katsumata, K., Le Brocq, A., Licht, K., Morgan, F., Neff, P. D., Ritz, C., Scheinert, M., Tamura, T., Van de Putte, A., van den Broeke, M., von Deschwanden, A., Deschamps-Berger, C., . . . Melv er, Y. (2021). Quantarctica, an integrated mapping environment for Antarctica, the Southern Ocean, and sub-Antarctic islands. *Environmental Modelling & Software*, 140, 105015. <https://doi.org/https://doi.org/10.1016/j.envsoft.2021.105015>

14. Phytoplankton – Biogeochemistry (AAS 4630)

Team: The phytoplankton team had 2 researchers: Pauline Latour (ACEAS, UTAS) and Matthew Corkill (ACEAS, UTAS) and three researchers sharing their time between the trace metal and biology teams: Katie Nawrath (ACEAS, UTAS), Delphine Lannuzel (ACEAS, UTAS) and Talitha Nelson (ACEAS, UTAS). We also received help from Jakob Weis (ACEAS, UTAS), Abigail Smith (AAPP, AAD) and Noémie Friscourt (ACEAS, UTAS).

14.1 Overview and Acknowledgements

The team aimed to address two objectives:

1. What are the drivers of phytoplankton growth in coastal Antarctica in late summer-early Autumn?
2. What drives higher primary productivity in the Shackleton polynya compared to the Denman Glacier region?

The team collected > 4,800 samples (including over 2,200 samples analysed onboard) from the CTD, TMR, uncontaminated seawater (UCSW) underway system and deckboard incubations. We would like to acknowledge the Hydrochemistry team for analysing macronutrient samples collected in support of our deployments and experiments. We rely heavily on the macronutrient data to interpret our results and to monitor the state of our incubation experiments. Finally, we (Pauline and Matt) would like to thank all the people that stepped in to help us during times of intense work. We could not have collected such a rich dataset without you!

14.2 Aim and Hypotheses

During the Denman Marine Voyage, the aim of the phytoplankton team was to study the drivers of phytoplankton growth near the Denman Glacier and within the Shackleton Polynya. Phytoplankton are microscopic single-celled organisms playing key roles in the carbon cycle – through photosynthesis, and in supporting marine ecosystems at the base of most oceanic food webs. In the open Southern Ocean, phytoplankton is generally limited by iron, an essential micronutrient present in very low concentrations (Martin et al., 1990). Over the Antarctic continental shelf, particularly near ice shelves, primary productivity typically exceeds that of the open ocean due to enhanced iron availability from sedimentary, sea ice, and glacial sources (Lannuzel et al., 2010, Laufkotter et al., 2018, Raiswell et al., 2008, Smith et al., 2011). Primary productivity also shows significant regional variation across the Antarctic continental shelf. In the sea ice zone, much of this productivity is concentrated in coastal polynyas—ice-free areas that support highly productive food webs. This increased productivity is evidenced by ocean colour satellite observations, which show elevated surface chlorophyll concentrations in polynyas (Arrigo et al., 2003). Satellite observations suggest that phytoplankton growth is more elevated in the Shackleton polynya compared to waters near the Denman Glacier. However, satellite observations are limited to the first optical depth (~20 m below the surface) and therefore do not provide information on subsurface productivity. To gain a better understanding of phytoplankton productivity/processes both at the surface and at depth near the Denman Glacier and in the Shackleton Ice Shelf, we collected samples for multiple biological

14. Phytoplankton - Biogeochemistry (AAS 4630)

parameters (photophysiology, community composition, chlorophyll concentrations, particulate organic carbon, biogenic silica, carbon uptake and bacterial production), associated with trace metal measurements from nearby TMR deployments. We also performed bioassay incubations at two 'process stations', one near the Denman Glacier and one within the Shackleton Polynya, where we incubated natural phytoplankton communities under modified conditions (e.g., different light or metal levels). Additional underway and opportunistic samples were performed when encountering features of interest (e.g., subsurface iceberg meltwater, aerosols).

14.3 Sample Collection Methods

Photophysiological samples were directly analysed onboard using a Fast Repetition Rate Fluorometer (FRRF, Chelsea). Unfiltered seawater containing natural phytoplankton communities were left to low-light ($<2 \mu\text{mol photons m}^{-2} \text{s}^{-1}$) acclimate for 20 to 30 min before sample analyses. F_v/F_m (where $F_v = F_m - F_o$) was calculated from F_o and F_m , which refer to the minimum and maximum fluorescence, respectively, in the low light acclimated state. F_v/F_m and functional absorption cross section of photosystem II (σ_{PSII}) were determined after sample exposition to 120 flashes of light every $2 \mu\text{s}$ (saturation sequence) before the time interval between flashes was increased exponentially (relaxation sequence) for 40 flashes, measured at 450 nm. At least 15 acquisitions were measured for each sample and used to calculate the average value of F_v/F_m and σ_{PSII} .

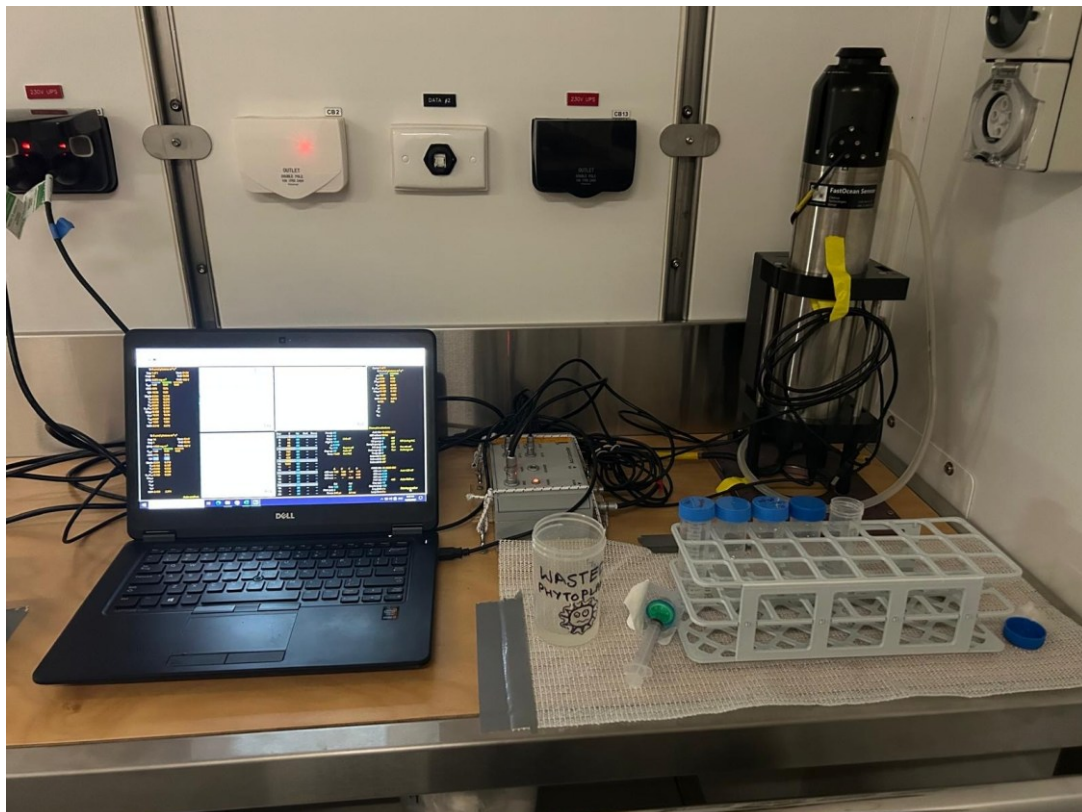


Figure 75: Station for photophysiological measurements through FRRF. These occurred in a refrigerated container, constantly maintained at +4 °C. Light levels were kept low when working on the FRRF.

14. Phytoplankton - Biogeochemistry (AAS 4630)

Chlorophyll-a (Chl-a) concentrations were measured directly onboard after filtration of about 1 L of seawater onto 25 mm diameter GF/F filters to retain phytoplankton pigments. The filters were stored in glass scintillation vials at -20 °C until analyses. The pigments were then extracted in 90 % acetone for 18 to 24 h at -20 °C. The Chl-a concentrations were measured using a Turner Trilogy fluorometer after blank correction using 90 % acetone and solid standard measurements (Holm-Hansen et al., 1965).

Biogenic silica (BSi) samples were collected by filtering ~1 L of seawater collected from the CTD onto 25 mm diameter 0.8 µm polycarbonate filters. The filters were stored in 60 mL polypropylene tubes at -20 °C until analyses. BSi concentrations will be determined after BSi conversion to silicic acid through leaching with 0.1 mol L⁻¹ sodium hydroxide at 85 °C for 2.15 h, before determination using spectrophotometry (Paasche, 1973).

Particulate organic carbon / nitrogen (POC / PON) samples were collected by filtering 2 L of seawater through pre-combusted 13 mm diameter QMA filters. The filters were stored in well plates, dried in the oven at 60 °C for several days, and then stored in a desiccator. Sample analyses are performed at the Central Science Laboratory (CSL), at the University of Tasmania following Martin (1993).

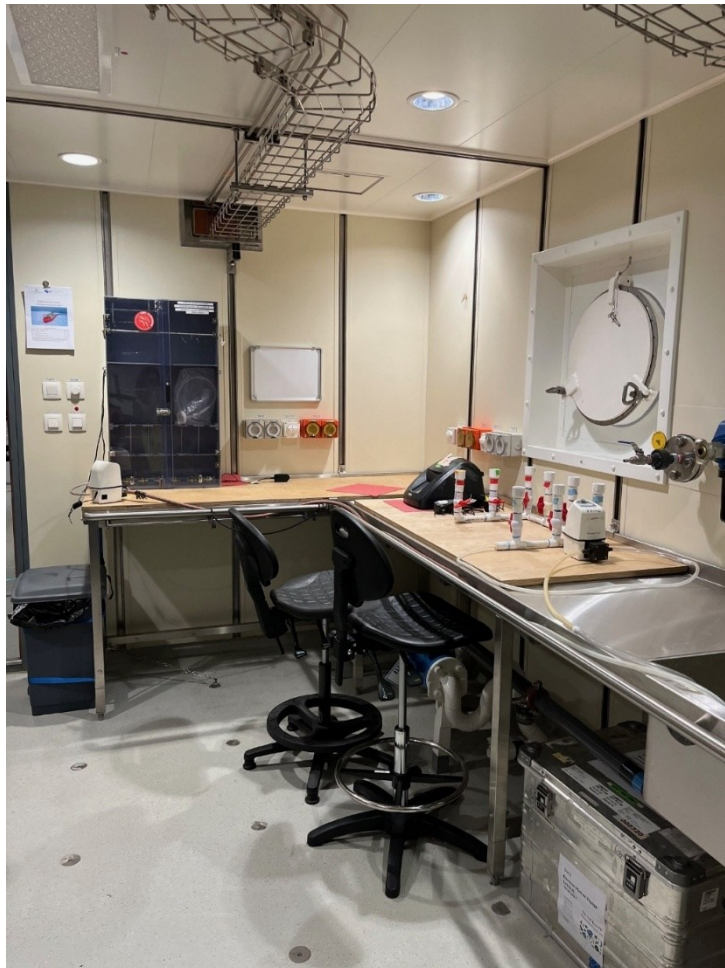


Figure 76: Filtration systems used for Chl-a/BSi sampling (on the right) and POC sampling (cabinet at the back). The POC filtration cabinet was borrowed from CSIRO (Australia).

Seawater for dissolved organic carbon/nitrogen (DOC / DON) were collected from the CTD into new sterile falcon tubes. This seawater was then filtered on pre-combusted 25 mm 0.7 µm GF/F

14. Phytoplankton - Biogeochemistry (AAS 4630)

filters in a 60 mL glass syringe. Pre-cleaned glass bottles were used to collect the filtrate for DOC analysis. The glass syringe was acid washed in a 30 % hydrochloric acid (HCl) bath for at least 8 hours, rinsed thrice in Milli-Q water, dried in an oven for 2 h at 80 °C and wrapped in aluminium foil prior the voyage. Glass materials, metal filter holders and GF/F filters were muffled and combusted in an oven at 450 °C for 8 hours. The filtrate was stored in the aluminium wrapped glass bottles to limit light exposure and stored at -20 °C. Samples will be analysed at the University of Tasmania using a Shimadzu total organic carbon (TOC) analyser.

We also collected a range of samples to help identify community composition: flow cytometry samples were collected through fixation of unfiltered seawater with glutaraldehyde (1 % for phytoplankton samples and 2 % for bacteria samples; Marie et al., 2005). Samples for pigment composition (HPLC) were also collected at specific stations by filtering ~1.5 L of seawater through a 13 mm GF/F filter and keeping it in liquid nitrogen until analyses at the AAD marine laboratory (Hayward et al., 2023; Wright et al., 2010). Additional HPLC samples were collected for combined pigment composition and phytoplankton absorption analysis at the CSIRO marine laboratory by filtering 4 L of seawater through 25 mm GF/F filter (stored at -80 °C). These samples were collected with the following objectives: (1) collection of NASA PACE satellite validation data and (2) intercomparison of the sampling techniques and subsequent analysis at the AAD and CSIRO marine laboratories. Finally, unfiltered seawater samples were collected from the CTD and from the incubation experiments (see incubation section below) for microscopy and scanning electron microscopy (SEM) analysis. 1 mL of acidic Lugol solution was pipetted into 100 mL glass amber bottles to preserve the samples. The unfiltered seawater was then filled to the neck of the bottles to 100 mL and stored at +4 °C in the dark. SEM samples will be filtered onshore within 6 months before analyses at the CSL (UTAS).

To gain more insights into biological rates, we used ¹⁴C to measure primary productivity (through phytoplankton carbon uptake) and ³H-leucine to measure bacterial production. Carbon uptake was measured after 24 h incubation of natural communities with 20 µCi of sodium ¹⁴C-bicarbonate followed by sequential filtration onto 20, 2 and 0.2 µm polycarbonate filters. Carbon uptake rates were determined onboard by measuring disintegrations per minute on a liquid scintillation counter (PerkinElmer Tri-Carb 2910 TR). Filters were incubated for over 24 h before analysis in 10 mL of Ultima Gold liquid scintillation cocktail (Hoppe et al., 2017). Bacterial production was measured after incubation of bacterial communities with a mix of hot and cold leucine (20 nM total concentration) for 4 h in the dark at in-situ temperatures (Smith et al., 1992; Fourquez et al., 2022). Five replicates were measured per samples, including two killed controls (at 5 % final trichloroacetic acid (TCA) concentrations). Samples were then centrifuged after addition of 50 µL of bovine serum albumin (3.4 g L⁻¹) at 12,000 g for 10 min (while keeping the centrifuge chamber at 4 °C). The supernatant was removed before washing the pellet with 5 % TCA and centrifuging a second time (using the same setting). Finally, the supernatant was removed and 1.5 mL of Ultima Gold scintillation cocktail LLT was added on the pellet. Bacterial production rates were determined by measuring disintegrations per minute on a liquid scintillation counter (PerkinElmer Tri-Carb 2910 TR), 24 h after cocktail addition.

14.4 Stations sampled during DMV

Table of locations sampled from can be found in the TMR section (Table 18).

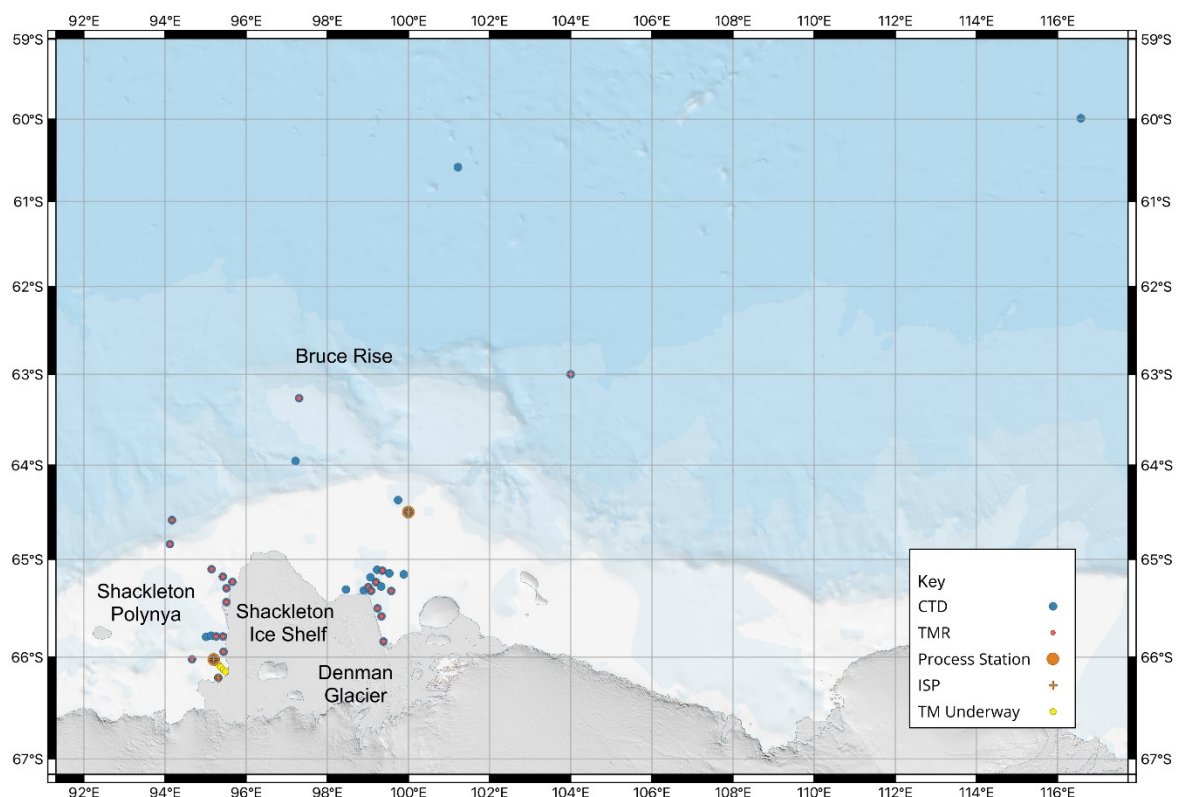


Figure 77: Map of the stations sampled for phytoplankton and biogeochemical parameters. CTD stations are shown in blue. TMR stations are shown in red. Process stations are shown in orange. ISP stations are shown by orange crosses. Underway locations shown in yellow. Phytoplankton and biogeochemical parameters were sampled from the Trace Metal Rosette (TMR) when the CTD was not deployed.

14. Phytoplankton - Biogeochemistry (AAS 4630)

Table 51: Summary of biological and biogeochemical variables collected by the phytoplankton team during DMV. RLC refers to rapid light curves measured on the FRRF.

Biological parameter	Description	# samples collected
Chl-a	Proxy for phytoplankton biomass	678
Flow cytometry	Sample for community composition	1,034
FRRF	Photophysiology measurements	445 + 62 RLC
POC / PON	Carbon content of particles	500
BSi	Silicate content of particles	456
DOC/DON	Recycled from POC/PON	56
Macronutrients	Macronutrient concentrations	57
SEM / Lugol	Phytoplankton taxonomy	136
Carbon uptake	Primary productivity	764
Bacterial production	Bacterial growth/biomass	573
HPLC (AAD)	Pigment measurements for community composition	60
HPLC (CSIRO)	Pigment measurements for community composition	55
Total	Total amount of samples collected	4,876

14.5 Preliminary Results

14.5.1 Chlorophyll-a concentrations

Chl-a concentrations measured during DMV averaged 0.6 mg m^{-3} near the Denman Glacier and 0.3 mg m^{-3} within the Shackleton Polynya. CTD002 was collected near the Bruce Rise (Figure 77) and was characteristic of late-summer open ocean profiles, with preliminary results suggesting a deep chlorophyll maximum (DCM) at 80 m. CTD021 illustrates the type of depth profiles encountered near the Denman Glacier. Surprisingly, elevated Chl-a concentrations were observed deep in the water column, where light levels would be expected to be limiting. CTD075 was collected in the Shackleton Polynya and illustrates the type of profile we encountered in this region (Figure 78). The features observed at the different sites (as well as their drivers) will be further investigated as the full suite of samples and variables are analysed (e.g. POC, BSi, HPLC).

14. Phytoplankton - Biogeochemistry (AAS 4630)

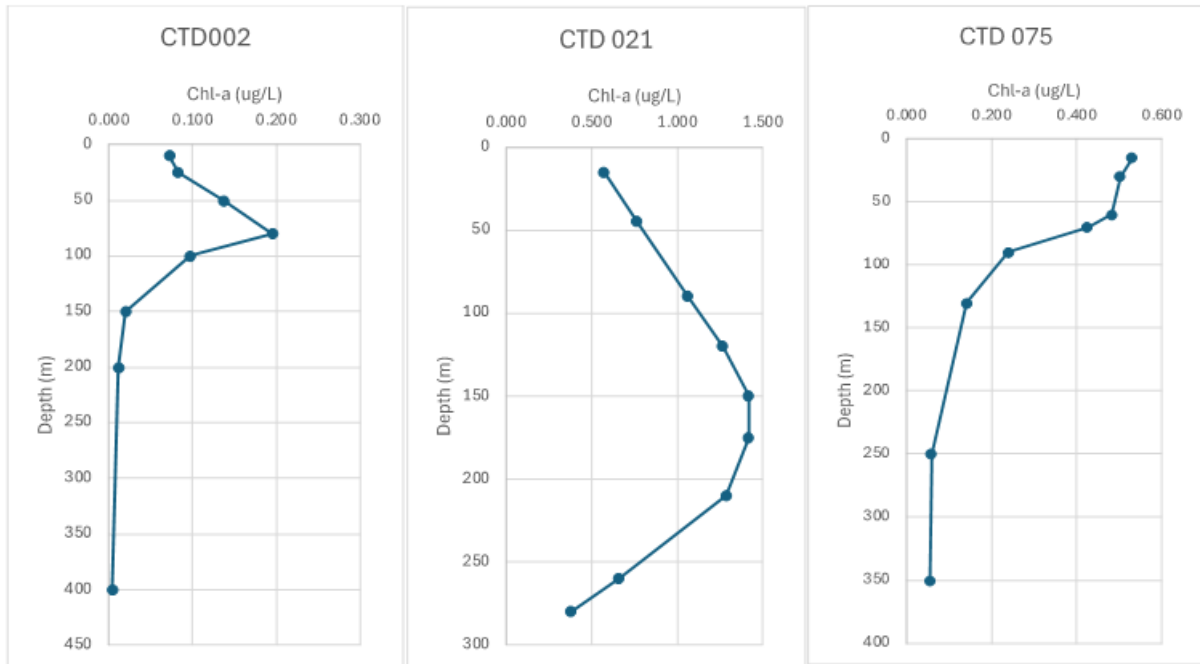


Figure 78: Examples of depth profiles of chlorophyll-a (Chl-a) concentrations measured during DMV (CTD002: offshore waters, CTD021: near the Denman Glacier and CTD075: within the Shackleton polynya). Samples for these profiles were collected from the CTD and extracted onboard.

14.5.2 Contribution of icebergs to localised ocean fluorescence

Enhanced fluorescence in the underway seawater system was observed near icebergs on several occasions as we transited towards the Denman region. These localised features matched lower temperatures and salinities (Figure 79), suggesting causality. Icebergs can release nutrients (such as iron), boosting local phytoplankton growth in their wake (Smith et al., 2011). Biological hotspots of primary productivity are visible from space near large icebergs, potentially contributing 20 % of the carbon export in the Southern Ocean (Duprat et al., 2016). The influence of iceberg meltwaters was also noted in vertical profiles from the CTD in the Denman region. Ongoing analysis of hydrography, CTD data, nutrients, Chl-a, BSi and POC samples collected over the course of the campaign will shed light on the contribution of icebergs to localised phytoplankton growth in the studied region.

14. Phytoplankton - Biogeochemistry (AAS 4630)

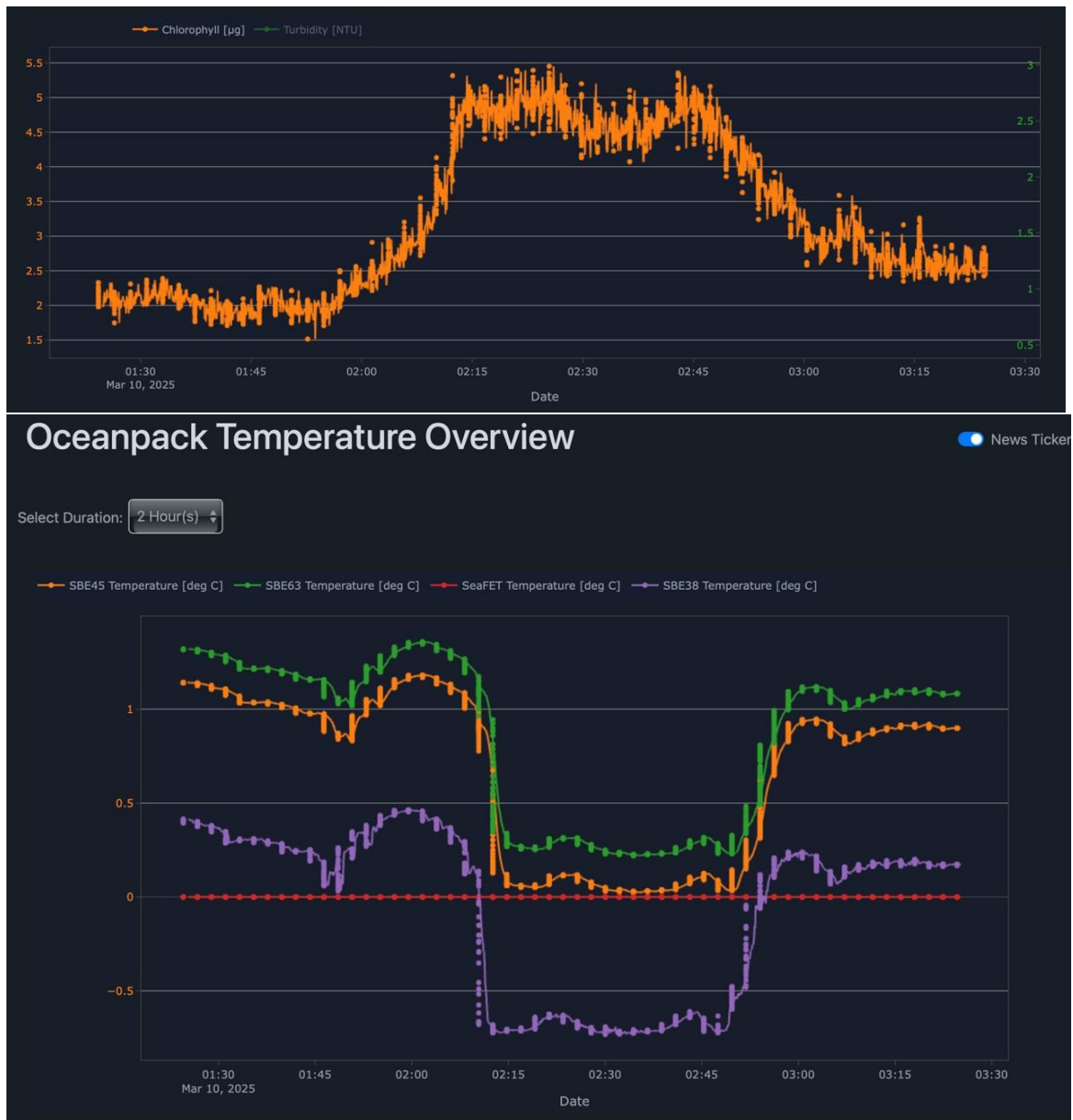


Figure 79: Estimated chlorophyll (derived from Fluorescence sensor, upper panel) and temperature (lower panel) measured from the underway seawater system (Oceanpack) on the 10th of March 2025 onboard RSV Nuyina near an iceberg.

14.5.3 Iron/manganese additions near the Denman Glacier and within the Shackleton Polynya

Manganese (Mn) has recently been observed to limit Southern Ocean phytoplankton growth (Browning et al., 2021). However, this limitation does not seem pervasive (Latour et al., 2024). Because this may directly influence the strength of the biological carbon pump, it is important to identify regions of Mn limitation. During the DMV voyage, we studied Mn control of phytoplankton growth by performing 2 incubation experiments at PS1 and PS2. Briefly, unfiltered trace metal clean seawater (collected with the TMR) was incubated in (trace metal clean) polycarbonate bottles with Mn, Fe or combined additions. Both Fe and Mn were added (using a 1:1 ratio of Fe or Mn:EDTA) to reach a final concentration of at least 2 nM within

14. Phytoplankton - Biogeochemistry (AAS 4630)

incubation bottles, using ultrapure salts of Fe and Mn chloride prepared in 0.01M HCl. We also incubated bottles at two light levels to study the combined effect of changing Fe, Mn and light conditions. Light levels were manipulated using neutral-density mesh screening as in Latour et al. (2024) and bottles were kept in deckboard incubators to allow regular diel light/dark cycles. These incubators maintained circulating seawater at in-situ temperatures. Bottles were sampled mid-experiment to measure nutrient consumption, their photophysiology and community composition through flow cytometry. These measurements were also made during the final sampling as well as additional parameters to better understand phytoplankton responses to Mn and Fe additions: Chl-a and BSi (both bulk and size-fractionated), POC, microscopy samples as well as carbon uptake and bacterial production.



Figure 80: Deckboard incubators used to perform all bioassays. These incubators recirculated seawater at constant temperature. We aimed for this temperature to be as close to in-situ conditions as possible, which oscillated between -1.5 °C and 1 °C.

14.5.4 Other secondary metals

Other trace metals have been known to influence phytoplankton growth in the Southern Ocean. Both cobalt (Co) and zinc (Zn) have been observed to limit phytoplankton growth while high concentrations of copper (Cu) may lead to toxicity and impact growth (Scharek et al., 1997; Yang et al., 2019). We tested the influence of increased Cu, Zn and Co concentrations on coastal Antarctic phytoplankton. Both Cu and Zn were added to have a final concentration of 4

14. Phytoplankton - Biogeochemistry (AAS 4630)

nM while Co was added to reach at least 1 nM within incubation bottles. Trace metal clean seawater was collected using the same protocol as described above, and final sampling was done for final Chl-a, BSi and POC concentrations, as well as FRRF and flow cytometry.

14.5.5 The influence of light and iron-binding ligands on Southern Ocean deep chlorophyll maximas in autumn

Iron (Fe) is present in low (nanomolar to sub-nanomolar) concentrations in most of the Southern Ocean, limiting phytoplankton growth (Martin et al., 1990). Over 99 % of Fe in the ocean is bound to molecules known as ligands (Thuroczy et al., 2011). Ligands play a key role in sustaining Fe in the surface ocean where it can be accessed by phytoplankton, with the ligand pool comprising a range of ligands with a range of binding strengths (Hassler et al., 2017). Weaker ligands (polysaccharides, exopolymeric substances and humic/fulvic substances) can be produced by phytoplankton, bacteria or the dissolution of terrestrial particles (Hansell, 2013; Norman et al., 2015). Stronger binding ligands, known as siderophores, can be actively produced by bacteria to capture Fe (Liu et al., 2022; Neilands, 1995; Wilhelm et al., 1994). Depending on the type of ligand, and the phytoplankton species, ligands can either increase or decrease the accessibility of Fe (Lis et al., 2015; Maldonado et al., 2005). Hence, understanding the response of natural phytoplankton communities to ligand bound Fe is important for understanding primary productivity now, and in the future.

The fluorescence depth profiles measured onboard showed deep fluorescence maximas at both process stations (60 m at PS1 and 160 m at PS2) and were sampled for incubation experiments. We aimed to test if Fe bound to different ligands, at increased light levels, affected the encountered deep productivity, and if this response differed between sites. Treatments included a control (no amendments), + 2.0 nM Fe bound to 2 nM of Ethylenediaminetetraacetic acid (EDTA), +2.0 nM Fe bound to 20 nM of the polysaccharide carrageenan (CAR), +2.0 nM Fe bound to 20 nM of Suwanee River fulvic acid (FA), and +2.0 nM Fe bound to 20 nM of the siderophore desferrioxamine b (DFB). Seawater was collected from the TMR and used to fill 1 L acid-cleaned polycarbonate (PC) bottles. PC bottles were cleaned onshore with a 2 % neutracon soak for one-week at room temperature, followed by another week in 10 % HCl at room temperature. Bottles were then rinsed at least four times with Milli-Q water and left to dry in a ducted laminar flow hood. They were then double bagged for transport. Six 1 L PC bottles were filled with filtered seawater from the TMR at the same depth where the unfiltered seawater was collected from. These were used as filtered controls to test the response of the natural ligand pool to different light levels. Samples were collected from the TMR for initial data on Chl-a, POC, SEM, flow cytometry, FRRF, macronutrients, trace metals, DOC and Fe-binding ligands. The incubation bottles (filtered and unfiltered) were then incubated in low light (only control and +Fe treatment) and high light conditions (all treatments) for 11 days. After 11 days, the incubation bottles were sub-sampled for carbon uptake and bacterial productivity. The remaining seawater was processed for FRRF, macronutrients, flow cytometry, Chl-a, SEM and POC. Filtered controls were processed for flow cytometry, DOC, trace metals and Fe-binding ligands.

14.5.6 Iron limitation DFB experiment

At each process station, an additional experiment was added to induce Fe limitation, since previous studies showed autumn phytoplankton were not Fe-limited (Singh et al., 2023; van Oijen et al., 2004). Seawater from the same depth as the ligand experiment was collected to fill 300 mL PC bottles. These PC bottles were cleaned as above. DFB was added in increasing additions, as +10 nM, +20 nM, +80 nM and +200 nM DFB. At PS1, bottles were incubated at low light conditions for 11 days. They were then processed for FRRF, flow cytometry, macronutrients and Chl-a concentrations. At PS2, the bottles were incubated at high light conditions for 11 days and then processed for FRRF, flow cytometry, macronutrients, chlorophyll and POC.

14.5.7 Krill-Assisted Resuspension of Material to Atmosphere (KARMA) Experiment

During the voyage, an opportunistic experiment investigated the role of Antarctic krill (*Euphausia superba*) in carbon cycling through diel vertical migration (DVM) and benthic feeding. Krill feeding in surface waters consume phytoplankton, contributing to the biological carbon pump by exporting organic matter to the seafloor. However, krill have also been observed feeding at depths exceeding 3000 m, potentially resuspending sediments and previously sequestered carbon, thereby altering carbon flux dynamics. This study aimed to quantify carbon egestion from krill feeding on both benthic and epipelagic sources. Krill were collected near the seafloor from beam trawls and from surface waters via the vessel's wet well, then preserved for SEM, POC and trace metal analysis of krill gut contents. We hypothesise that surface krill will show higher POC in their gut contents from phytoplankton, while benthic krill might contain sediment particles and lower POC but a higher ratio of Fe:Mn indicating sediment consumption.

The experimental component of the study involved incubating krill under three conditions: freshly fed on phytoplankton, starved, and fed sedimentary material. Across 12 h incubations, water samples were collected at multiple timepoints for DOC/POC, and macronutrient analysis, while bacterial production was measured at the start and end of each treatment. Sediment-fed krill were exposed to material from multicore samples, with DOC/POC measured before and after feeding. Preliminary results showed that bacterial production remained stable in starved krill, decreased in phytoplankton-fed krill, and increased in sediment-fed krill after 12 h, though variability was high and no statistically significant effects were observed based on treatment or krill length (Figure 81). All krill were adults with normally distributed lengths, and remaining analyses will be conducted post-voyage.

14. Phytoplankton - Biogeochemistry (AAS 4630)

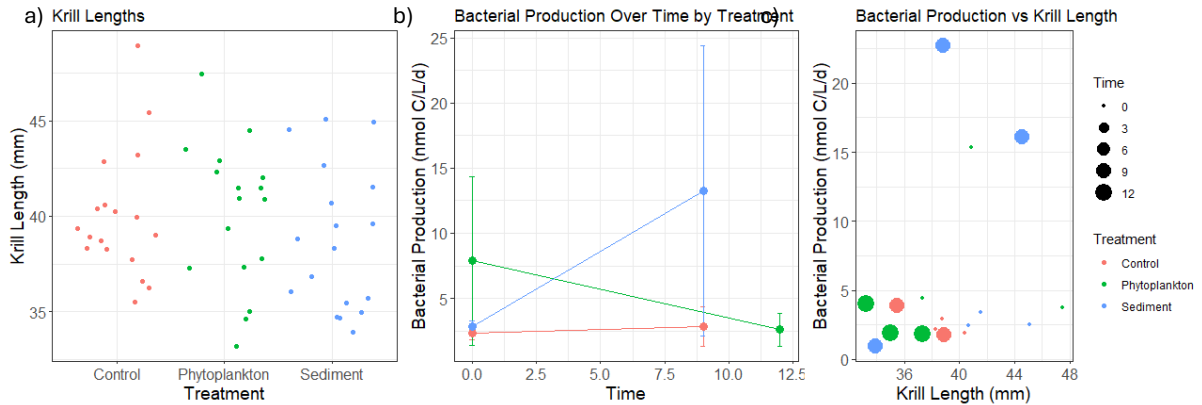


Figure 81: a) Distribution of krill lengths used in each treatment, b) bacterial production at the start and end of the incubations, and c) bacterial production as a product of krill length.

14.6 Data Management

All preliminary data will be published through the Australian Antarctic Data Centre (AADC) (<https://data.aad.gov.au/>) following standard AADC procedures, and subject to the moratorium of 2 years.

14.7 References

- Arrigo, K. R., & van Dijken, G. L. (2003). Phytoplankton dynamics within 37 Antarctic coastal polynya systems. *Journal of Geophysical Research: Oceans*, 108(C8).
- Browning, T. J., Achterberg, E.P., Engel, A. and Mawji, E. (2021). Manganese co-limitation of phytoplankton growth and major nutrient drawdown in the Southern Ocean. *Nature Communications* 12(1): 884. doi: <https://dx.doi.org/10.1038/s41467-021-21122-6>.
- Duprat, L. P., Bigg, G. R. & Wilton, D. J. (2016). Enhanced Southern Ocean marine productivity due to fertilization by giant icebergs. *Nature Geoscience*, 9(3), 219-221.
- Fourquez, M., Strzepek, R. F., Ellwood, M. J., Hassler, C., Cabanes, D., Eggins, S., Pearce I., Deppeler, S., Trull, T. W., Boyd, P. W. & Bressac, M. (2022). Phytoplankton responses to bacterially regenerated iron in a Southern Ocean eddy. *Microorganisms*, 10(8), 1655.
- Hansell, D. A. (2013). Recalcitrant dissolved organic carbon fractions. *Annual Review of Marine Science*, 5, 421–445
- Hassler, C.S., van den Berg, C.M.G. & Boyd, P.W. (2017). Toward a regional classification to provide a more inclusive examination of the ocean biogeochemistry of iron-binding ligands. *Frontiers in Marine Science*. 4, doi:10.3389/fmars.2017.00019
- Hayward, A., Pinkerton, M. H. & Gutierrez-Rodriguez, A. (2023). phytoclass: A pigment-based chemotaxonomic method to determine the biomass of phytoplankton classes. *Limnology and Oceanography: Methods* 21(4), 220-241.

14. Phytoplankton - Biogeochemistry (AAS 4630)

- Holm-Hansen, O., Lorenzen, C. J., Holmes, R. W., & Strickland, J. D. (1965). Fluorometric determination of chlorophyll. *ICES Journal of Marine Science*, 30(1), 3-15.
- Hoppe, C. J. M., Klaas, C., Ossebaar, S., Soppa, M. A., Cheah, W., Laglera, L. M., ... & Trimborn, S. (2017). Controls of primary production in two phytoplankton blooms in the Antarctic Circumpolar Current. *Deep Sea Research Part II: Topical Studies in Oceanography*, 138, 63-73.
- Lannuzel, D., Schoemann, V., De Jong, J., Pasquer, B., Van der Merwe, P., Masson, F., ... & Bowie, A. (2010). Distribution of dissolved iron in Antarctic sea ice: Spatial, seasonal, and inter-annual variability. *Journal of Geophysical Research: Biogeosciences*, 115(G3).
- Latour, P., Eggins, S., van der Merwe, P., Bach, L. T., Boyd, P. W., Ellwood, M. J., Bowie, A. R., Wuttig, K. & Strzepek, R. F. (2024). Characterization of a Southern Ocean deep chlorophyll maxima: Response of phytoplankton to light, iron and manganese enrichment. *Limnology and Oceanography Letters*, 9 (2), <https://doi.org/10.1002/lol2.10366>
- Laufkötter, C., Stern, A. A., John, J. G., Stock, C. A., & Dunne, J. P. (2018). Glacial iron sources stimulate the southern ocean carbon cycle. *Geophysical Research Letters*, 45(24), 13-377.
- Lis, H., Shaked, Y., Kranzler, C., Keren, N. & Morel, F. M. M. (2015). Iron bioavailability to phytoplankton: an empirical approach. *ISME J*, 9:1003–1013
- Liu L, Wang W, Wu S & Gao H. (2022). Recent Advances in the Siderophore Biology of *Shewanella*. *Front Microbiol.* 13:823758. [doi: 10.3389/fmicb.2022.823758](https://doi.org/10.3389/fmicb.2022.823758)
- Maldonado, M. T., Strzepek, R. F., Sander, S. & Boyd, P. W. (2005). Acquisition of iron bound to strong organic complexes, with different Fe binding groups and photochemical reactivities, by plankton communities in Fe-limited subantarctic waters. *Global Biogeochemical Cycles*. 19, [doi: 10.1029/2005GB002481](https://doi.org/10.1029/2005GB002481)
- Marie, D., Simon, N., & Vaulot, D. (2005). Phytoplankton cell counting by flow cytometry. *Algal culturing techniques*, 1, 253-267.
- Martin, J. H. (1990). Glacial-interglacial CO₂ change: the iron hypothesis. *Paleoceanography*. 5, 1-13, [doi: 10.1029/PA005i001p00001](https://doi.org/10.1029/PA005i001p00001)
- Martin, J. H. (1993). Determination of particulate organic carbon (POC) and nitrogen (PON) in seawater. In S. Kadar, M. Leinen, & J. W. Murray (Eds.), *Equatorial Pacific process study sampling and—Analytical protocol* (37–48). U. S. JGOFS.
- Neilands, J.B. (1995). Siderophores: structure and function of microbial iron transport compounds. *J Biol Chem*, 270(45):26723- 6. [doi: 10.1074/jbc.270.45.26723](https://doi.org/10.1074/jbc.270.45.26723)
- Norman, L., Worms, I. A. M., Angles, E., Bowie, A. R., Mancuso, N., Pham, A. N., Slaveykova, V. I., Townsend, A. T., Waite, D. & Hassler, C. S. (2015). The role of bacterial and algal exopolymeric substances in iron chemistry. *Mar. Chem*, 173, 148-161
- Paasche, E. (1973). Silicon and the ecology of marine plankton diatoms. I. *Thalassiosira*

14. Phytoplankton - Biogeochemistry (AAS 4630)

pseudonana (*Cyclotella nana*) grown in a chemostat with silicate as limiting nutrient. *Marine Biology*, 19(2), 117-126.

- Raiswell, R., Benning, L. G., Tranter, M., & Tulaczyk, S. (2008). Bioavailable iron in the Southern Ocean: the significance of the iceberg conveyor belt. *Geochemical transactions*, 9(1), 7.
- Scharek, R., Van Leeuwe, M. A., & De Baar, H. J. (1997). Responses of Southern Ocean phytoplankton to the addition of trace metals. *Deep Sea Research Part II: Topical Studies in Oceanography*, 44(1-2), 209-227.
- Singh, A., Fietz, S., Thomalla, S. J., Sanchez, N., Ardelan, M. V., Moreau, S., Kauko, H. M., Fransson, A., Chierici, M., Samanta, S., Mtshali, T. N., Roychoudhury, A. N., & Ryan-Keogh, T. J. (2023). Absence of photophysiological response to iron addition in autumn phytoplankton in the Antarctic sea-ice zone, *Biogeosciences*, 20, 3073–3091, <https://doi.org/10.5194/bg-20-3073>
- Smith, D.C., Azam, F. A Simple. (1992). Economical Method for Measuring Bacterial Protein Synthesis Rates in Seawater Using 3H-Leucine. *Mar. Microb. Food Webs*, 6, 107–114.
- Smith Jr, K. L., Sherman, A. D., Shaw, T. J., Murray, A. E., Vernet, M., & Cefarelli, A. O. (2011). Carbon export associated with free-drifting icebergs in the Southern Ocean. *Deep Sea Research Part II: Topical Studies in Oceanography*, 58(11-12), 1485-1496.
- Thuroczy, C.-E., Gerringa, L. J. A., Klunder, M. B., Laan, P. & H. J. W. de Baar. (2011). Observation of consistent trends in the organic complexation of dissolved iron in the Atlantic sector of the Southern Ocean. *Deep Sea Research Part II: Topical Studies in Oceanography*. 58, 2695-2706, doi: 10.1016/j.dsr2.2011.01.002
- van Oijen, T, van Leeuwe, MA, Granum, E, Weissing, FJ, Bellerby, RGJ, Gieskes, WWC & de Baar, HJW (2004). Light rather than iron controls photosynthate production and allocation in Southern Ocean phytoplankton populations during austral autumn, *Journal of Plankton Research*, vol. 26, no. 8, 885-900. <https://doi.org/10.1093/plankt/fbh088>
- Wilhelm, Steven W., Trick & Charles G. (1994). Iron-limited growth of cyanobacteria: Multiple siderophore production is a common response. *Limnology and Oceanography*, 39, doi: 10.4319/lo.1994.39.8.1979
- Wright, S., van den Enden, R., Pearce, I., Davidson, A.T., Scott, F.J. & Westwood, K.J., (2010). Phytoplankton community structure and stocks in the Southern Ocean (30°-80°E) determined by CHEMTAX analysis of HPLC pigment signatures. *Deep Sea Research II*, 57:758-778
- Yang, T., Chen, Y., Zhou, S., & Li, H. (2019). Impacts of Aerosol Copper on Marine Phytoplankton: A Review. *Atmosphere*, 10(7), 414. <https://doi.org/10.3390/atmos10070414>

15. Seal tagging (AAS 4630)

Team: David Green, Mark Hindell, Jakob Weis, Esther Tarszisz, Mick Stapleton

15.1 Introduction

The broad objective of the seal program was to use seals, as top predators, to better understand their role in the marine ecosystem of the region. In particular, by deploying various types of satellite tags the program aimed to provide data on seal movement and behaviour as well as krill distribution and physical and biological oceanography. The work feeds directly into ACEAS objective **7) understanding drivers of ecosystem processes and productivity in the Denman Glacier region.**

The tagging work had two components (i) deploying CTD and Fluro-CTD tags on elephant seals at Iles Kerguelen in January 2025 some of which, based on previous work, were likely to use the Denman Glacier region, and (ii) deploy CTD-tags on Weddell seals and prey-capture detection tags on crabeater seals from the RSV *Nuyina*. Another key objective was to calibrate an additional 20 CTD tags by deploying them on CTD casts during the voyage. This is crucial step in preparing the tags for deployment on elephant seals at Macquarie Island in May 2025. Other work to be performed on the voyage included using seal dive data to refine estimates of bathymetry in the region, to work with the towed camera team to identify sites of interest based on known seal distributions and to produce a seal sighting data base in eLog to record all seal sightings from the ship.

15.2 Methods, equipment and preliminary results

15.2.1 Elephant seal tagging at Iles Kerguelen and collection of biological and physical oceanography in the Denman Glacier region.

30 elephant seals were tagged with CTD satellite tags in December 2024 and January 2025. Eight of these seals used the Denman Glacier region between February and April 2025. These seals provided almost 1500 CTD profiles which will complement the oceanographic work conducted on RSV *Nuyina*.

15. Seal tagging (AAS 4630)

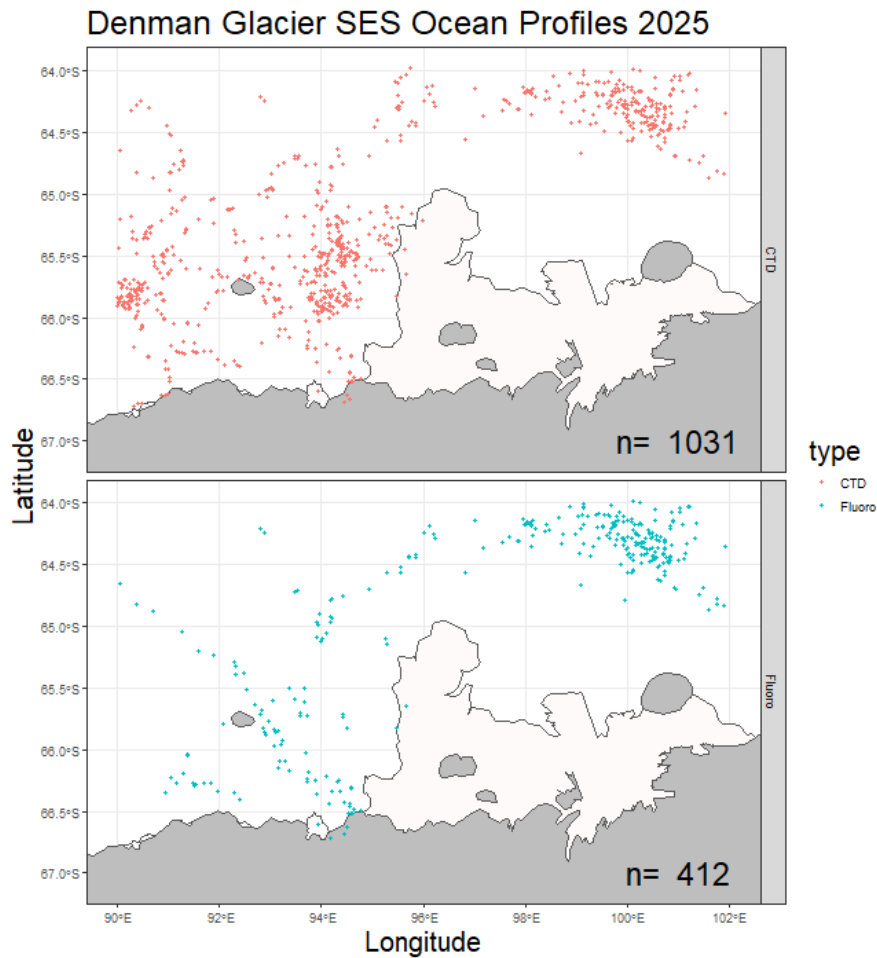


Figure 82: Maps of the oceanographic profiles collected by elephant seals in the Denman Glacier region between February and May 2025.

15.2.2 Constructing a new bathymetry for the Denman Glacier Study Area using seal dive data

A total of 78 instrumented seals visited the DG study area between March 2004 and April 2025. Of these, 69 used the Antarctic Continental Shelf (defined as < -1500 m on IBCSO2 bathymetry). This provided dive depths for a total of 114,672 dives, approximately 20 % of which were to the ocean floor. We divided the region into 2570 5 km x 5 km cells of which 2097 (81 %) had more than five dives. In these cells the deepest dive was assumed to be to the ocean floor. The remaining cells ($n = 473$, 18 %), had their bathymetry estimated by a spatial GAM based on the cells with at least five dives. This was deemed acceptable as these cells were invariably in close proximity to the more used cells and so were not requiring long-range (unreliable) extrapolation.

The dominant features in the study area are: 1) a deep depression at 66.5° S and 95° E, with a maximum depth of 1094 m, 2) a relatively shallow ridge extending northwest from the western edge of the ice shelf to the shelf break, and 3) two shallow banks (< 200 m), one to the north of the ice shelf and the other close the shelf break at 92° E. These features were either misrepresented in the IBCSO 2 dataset or were not as pronounced (Figure 83). Most notably IBCSO 2 underestimated the depths of the shallow banks associated with the shelf break and

15. Seal tagging (AAS 4630)

the depth of the ocean adjacent to the Antarctic continent, both regions frequently visited by elephant seals.

These data, while at significantly lower spatial resolution than the multi-beam surveys conducted during the DMV, nonetheless provided valuable additional data for regions that the ship did not visit.

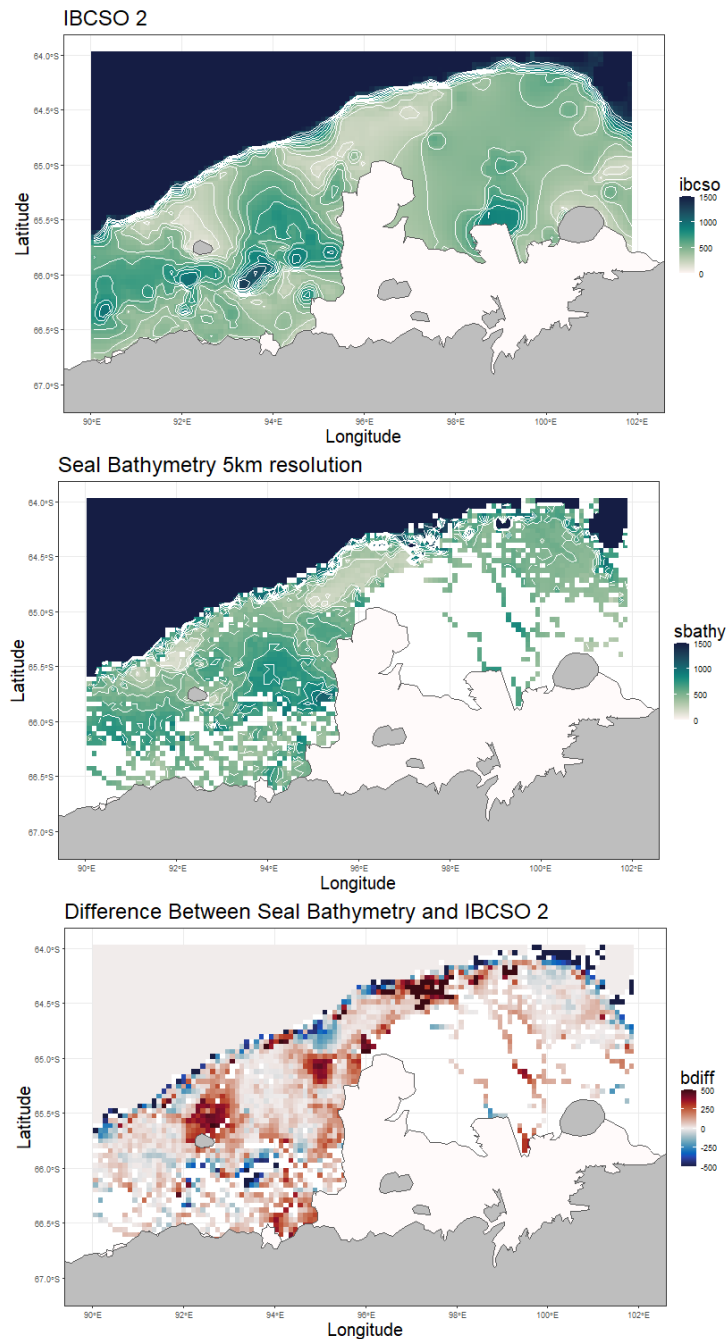


Figure 83: Bathymetry of the Denman Glacier Study Area derived from (a) the IBCSO 2 estimates of bathymetry, (b.) from seal dive depths and (c.) the difference between the two, where positive (red) values indicate the seal depth was deeper than IBCSO 2.

15. Seal tagging (AAS 4630)

15.2.3 Capturing seals on ice floes for the deployment of satellite telemetry tags

This component aimed to deploy satellite-relayed electronic tags on Weddell, crabeater and Ross seals hauled-out on ice floes, as well as to collect tissue samples for molecular work, generating a suite of *in situ* physical and biological data streams to support the Denman marine campaign.

15.2.3.1 Tag details and intended seal species

CTD-SRDLs – we aimed to deploy four Conductivity-Temperature-Depth Satellite Relay Devices (CTD-SRDL; Sea Mammal Research Unit) on Weddell seals, which forage benthically over the Antarctic shelf. These tags were provided by IMOS. They transmit up to four physical (salinity and temperature) profiles of the water column per day, contributing important observations of oceanographic processes, as well as measurements of seafloor depth.

DSA tags – we aimed to deploy nine dive segment activity (DSA; Wildlife Computers) tags on crabeater seals over the Antarctic shelf and shelf break. These tags record depth and triaxial acceleration, relaying summarised information on prey encounter rates in near real time via satellite. Crabeater seals forage almost exclusively on krill. Transmitted prey encounter rate summaries thus provide valuable inferred observations of krill distribution and densities.

Splash Tags – we aimed to deploy five Splash-10 tags (Wildlife Computers) on Ross seals. These tags transmit dive summaries of time, depth, and temperature along with position information. Ross seals are a specially protected species under the Antarctic Treaty, but their biology and foraging ecology remains poorly understood. This tracking work would provide foundational understanding of this species within the region.

15.2.3.2 Ice floe access and tag deployments

All seal capture, anaesthesia, tagging and sample collection procedures were conducted under approval from the University of Tasmania's animal ethics committee (A0028182). The capture and deployment of tags for seals on ice floes is an operation that has not been previously undertaken by the Australian Antarctic Program (AAP) from RSV *Nuyina*. A key objective of this work was therefore to develop a safe and sustainable working model for future efforts to conduct seal tagging as part of the AAP. Towards this, during the voyage protocols were successfully formalised for ship disembarkation and embarkation to and from ice floes via small watercraft, as well as standard operating procedures for working on ice floes. This was achieved through detailed consultation between the seal tagging team, the AAD FTO and Serco. Through this, we identified a set of safe operation conditions within which accessing ice floes and seals was achievable, including fair weather and ice condition guidelines.

The Standard Operating Procedures outlined in the seal tagging SMEAC developed by the FTO in conjunction with the seal team, AAD and Serco for attempting to catch a seal were:

- Non-fatigued staff with appropriate skill set and training for the task
- Wind less than 15 knots, sea state 1 or 2 and no sea swell
- Ice concentration 4/10 max
- Floe (with seals) greater than 15 m x 15 m

15. Seal tagging (AAS 4630)

- Floe visually assessed from the bridge to be at least 1 m thick
- Visibility greater than 2 nautical miles
- *Nuyina* able to effect immediate search and rescue response via personnel transfer tender (PTT) or other means if required.

Once on the ice, we trialled two separate approaches for capturing and sedating seals prior to tag deployment and sample collection. The first involved the team vet slowly approaching the seal alone and from a low angle to administer the anaesthetic intra-muscularly via a jabstick, before backing away to allow the sedative to take effect. In this approach, the team would wait for the seal to reach light sedation before approaching to perform deployment procedures. The second method was to first capture and restrain the seal using a hoop net, thereafter, administering the anaesthetic and waiting for a plane of light anaesthesia to be achieved. Once sedation has taken effect, the following procedures can be undertaken:

1. a satellite tag is glued to the hair on the seal's head
2. measurements of the seal's length and girth are recorded
3. blood samples, oral and rectal swabs, a whisker and faecal samples are collected for genetic and isotopic analyses
4. the seal is monitored until it regains full consciousness

15.2.3.3 Deployment attempts

On 6 April 2025, we had two separate attempts at tagging crabeater seals, to the north-west of the Shackleton Ice Shelf (-65.0988 °S, 95.0066 °E for the first attempt, and -65.0879 °S, 94.9947 °E for the second attempt). In our first encounter, we initially attempted to administer the anaesthetic without first capturing the seal. However, the seal was quickly alerted to our presence and would not allow our vet within range to deliver the intramuscular injection. We subsequently attempted to capture the seal but were unable to before it departed the ice floe. The seal did haul out on the same ice floe a second time but was again too alert to catch.

During our second tagging attempt on another seal, we again attempted to anaesthetise the seal without first catching it. On this occasion, our vet slowly crawled towards the seal, stopping each time it showed signs of increasing alertness. After approximately 20 min, she was able to approach within range of the jabstick and successfully delivered a needle jab. However, following this it was discovered that the anaesthetic solution had frozen and the anaesthetic had not been administered. We then successfully caught the seal in the hoop net and were able to deliver a partial dose intramuscularly using a syringe. Due to the seal's vigorous movements, delivery of a full dose was not possible. The seal nonetheless remained alert for 20 min following this, at which point the remainder of the dose was administered. However, after a further 20 min, the seal still showed little sign of sedation, and the decision was made not to administer further doses of anaesthetic. After establishing that the seal was fully conscious, we terminated the deployment attempt.

We had a further three days allocated for seal tagging activities on 15, 16 and 21 April. However, we found that ice conditions had changed significantly since the initial attempt on 6 April. There was considerably more newly formed ice, and storm events had created a dense pack of near 100 % cover, limiting access to suitably sized ice floes. Additionally, seals identified over these days tended to be hauled out on small floes, inaccessible by our team. This together with marginal weather conditions meant that further tagging attempts were not possible.

15. Seal tagging (AAS 4630)

We were therefore unsuccessful in deploying any tags during the voyage.

15.2.4 Seal Tag calibrations

15.2.4.1 Calibration data collection

On five CTD casts conducted over the Antarctic shelf, seal CTD tags were affixed to the CTD rosette frame to provide comparable data for tag calibration. To do this, seal tags were switched to calibration mode (using SMRU *TagConfig* software), and set to measure temperature, conductivity, depth and in some tags, fluorescence, once every five seconds when submerged in seawater. For each CTD cast, eight to 12 tags were cable-tied to the upper ring of the CTD frame approximately 50 cm apart. Tags with fluorescence/light sensors were calibrated on CTD casts sampled for biology, to be able to compare both CTD and tag fluorescence-derived chl to precise chl concentration measurements.

Each tag was deployed on 2–3 different CTD casts to obtain replicate calibration datasets. In the following, “replicate” refers to calibration data and results of a given tag collected during multiple CTD casts.

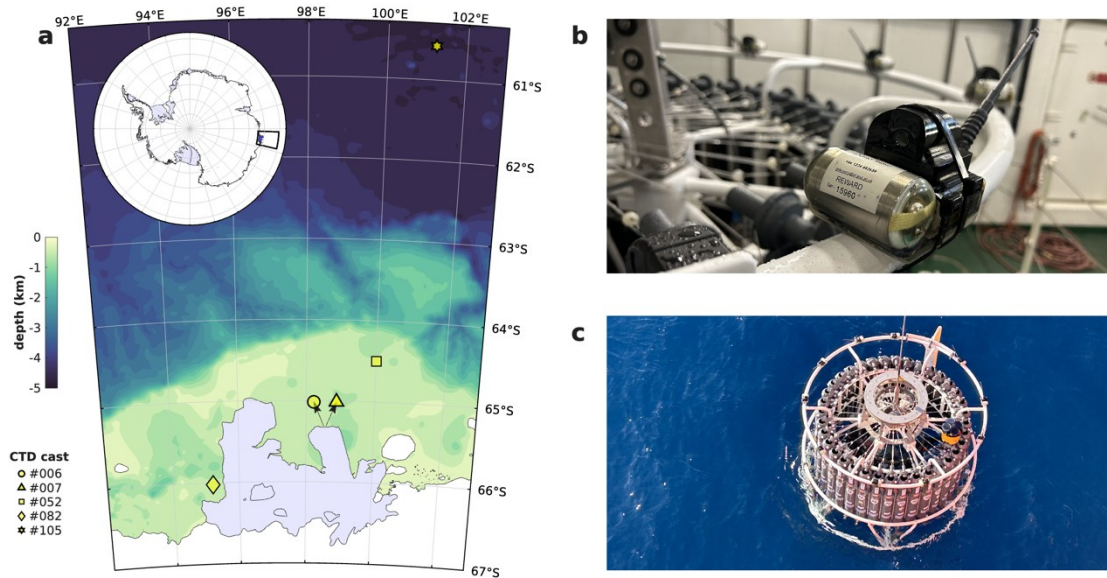


Figure 84: (a) Locations of calibration casts in the study region. (b, c) Experimental setup.

Table 52: Metadata of CTD casts where seal tag calibrations were undertaken.

CTD Cast No.	Station No.	Latitude (DD)	Longitude (DD)
6	9	-65.3136	98.5232
7	10	-65.3134	98.5899
52	64	-64.502	99.9987
82	109	-66.0218	95.1997
105	147	-60.5829	101.2168

15. Seal tagging (AAS 4630)

15.2.4.2 Calibration data analysis

Calibration coefficients (offset and slope) were calculated by regressing seal tag against CTD upcast measurements at corresponding depths using a reduced major axis linear regression (RMA; Figure 85). Because of the different sampling frequencies, measurements had to be interpolated onto the same depth grid first. The analysis focused on the up-cast tag data

15.2.4.3 Temperature, salinity and conductivity calibration results

Tag and CTD temperatures aligned very well in trend across all tags and replicates, with calibration slopes ranging around 1 (min = 0.96, max = 1.03, median = 0.99). 5 tags (12973, 14968, 15468, 15649, 15889) have notable negative temperature offsets (between -0.27 °C and -0.18 °C). The offsets of the remaining tags range around 0 (min = -0.06, max = 0.07 median = -0.01). Offsets and slopes are consistent across replicates of each tag (i.e. minor variations within tags).

Salinity offsets and slopes are broadly consistent with temperature. 3 of the 5 tags with notable temperature offsets (14968, 15468, 15649) also differed significantly in salinity, with offsets between -15.87 psu and -7.68 psu and slopes between 1.30 and 1.46 (drifting noticeably with depth). The remaining tags align well with CTD measurements, with offsets ranging around 0 (min = -3.02 psu, max = 3.70 psu, median = -0.96) and slopes ranging around 1 (min = 0.87, max = 1.07, median = 1.02). Offsets tend to be slightly negative and slopes slightly positive for most tags. All calibration coefficients are consistent across replicates.

Conductivity is generally in good agreement with CTD observations across all tags and replicates, including the three tags with offset and drifting salinity. Offsets ranged around 0 (min = -3.68, max = 1.77, median = -0.62) and slopes around 1 (min = 0.94, max = 1.12, median = 1.01). Consistent with salinity, offsets tend to be slightly negative and slopes slightly positive for most tags. All calibration coefficients are consistent across replicates.

The drift of salinity with depth noted for tags 14968, 15468, 15649 is the result of an erroneous conversion calculation performed by the tags. The tags use standard thermodynamic equations of sea water to calculate salinity from conductivity, temperature and depth. Using the respective equation provided by the TEOS-10 toolbox (<https://www.teos-10.org>), the salinity can be calculated from the CTD data. However, in the case of the three mentioned tags, plugging conductivity, temperature and pressure into the respective equation does not yield the salinity given in the tag's salinity.

15. Seal tagging (AAS 4630)

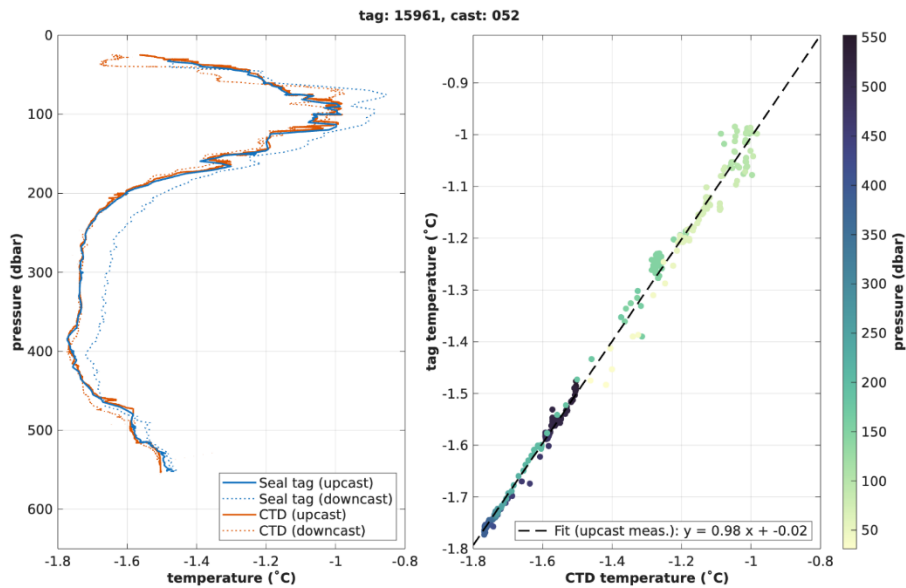


Figure 85: **Example calibration: Temperature (tag #15983 deployed on CTD #007).** (left) CTD (red) and seal tag (blue) temperature observations between 25 and 630 dbar (cast depth). Dotted and solid lines indicate down- and upcast measurements. (right) Tag temperature plotted against CTD temperature, colour-coded by pressure. A linear regression model was fitted to the data yielding the calibration line (dashed line, regression coefficients are displayed in the key). The slope and y-intercept are the calibration coefficients.

15.2.4.4 Key results

- Tag temperature and conductivity/salinity generally align very well with corresponding CTD measurements.
 - Temperature: None of the tags drifted (calibration slopes close to 1), most tags have minor offsets (calibration intercepts close to 0), four tags have a notable but consistent offset that can be corrected using calibration lines.
 - Conductivity: All tags are reasonably well aligned with CTD measurements both in trend and magnitude (minor regression slopes and intercepts), offsets tend to be negative for most tags, calibration lines are consistent for each tag
 - Salinity: **Apart from three tags**, all other tags are well aligned with CTD measurements both in trend and magnitude (offsets mostly negative consistent with conductivity), again, calibration lines are consistent for each tag. The salinity of tags 14968, 15468, and 15649 drift considerably with depth relative to the CTD. This was due to an error in the salinity calculation programmed in those tags which used a pressure of 0 throughout the profile, rather than the actual pressure at each depth.
 - Fluorescence aligned well with the CTD on all but one tag. Offsets are all near 0 which is to be expected, because both tag and CTD fluorescence were darked corrected prior to calibration, basically forcing the calibrations through (near) 0. Tag fluorescence is consistently lower than CTD fluorescence, by factors ranging between 0.3 and 0.9. These slopes are quite consistent for each tag.

15. Seal tagging (AAS 4630)

- Unfortunately, the light calibration is mostly unusable, because the CTD PAR sensors have been acting extremely strange for most of the casts that we deployed fluro/light tags on. The light curves of the tags look great though!
- Several of the tags had problematic sensors:
 - 12973: Failed to turn on at the surface on both casts
 - 14968, 15468, and 15649: Issue with on-tag salinity calculation
 - 15956: Fluro sensor clearly malfunctioned
 - 15982: Stopped logging after 150 m during first calibration cast but measured full during second cast.

Based on this work we have compiled a ranking of individual tag performance which will be used by the seal team at Macquarie Island to prioritise tags for deployments, as well as at least three tags which should not be deployed, but returned to the manufacturer. Most importantly the calibration data will be used to post-process the data returned from the seals to ensure the most reliable data are available for subsequent use by the multiple end-users of this data set.

15.2.5 Seal sightings database.

While in the pack-ice, a constant watch was kept to log all sighting of seals while the ship was underway during daylight hours. This was to provide information needed to plan seal capture events, by identifying where the seals were most concentrated, but it also provided valuable back data on the overall distribution of seals in the area (Figure 86). In total 142 seals were logged, the majority of which were crabeater seals ($n = 112$, 79 %), followed by Weddell seals ($n = 12$, 8 %) then elephant seals ($n = 2$, 1 %). 16 seals (11 %) could not be identified. The most notable feature of the sightings was the complete lack of seals seen in the polynya to the west of the Shackleton Ice Shelf, despite the considerable voyage time spent in the area. This undoubtedly was due to the lack of suitable ice floes in the polynya. The data will be incorporated into ongoing work in ACEAS developing species distribution models for pack-ice seals.

15. Seal tagging (AAS 4630)

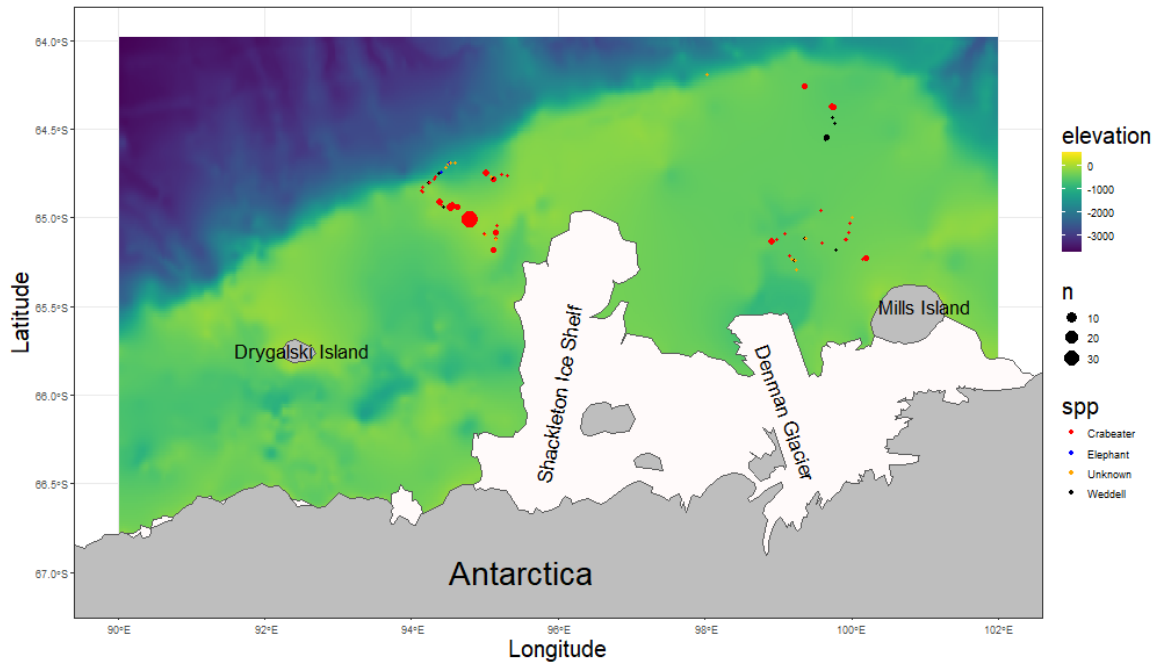


Figure 86: All sightings of seals entered in the "seal sighting" eLog during the Denman Marine Voyage in 2024. The background shows IBCSO 2 bathymetry.

15.3 Potential improvements

We identified a set of improvements that could lead to greater success of seal tag deployments over future voyages.

- **Finalising operational capacity early** – it took several weeks to identify and work through appropriate procedures for our team to disembark the ship and to access ice floes. This meant that we only had full operational capacity for deployments approximately halfway through the voyage and missed at least one attempt at deploying a tag. With these procedures now having been formalised, future work should have operational capacity from the start of the voyage, and greater potential to deploy tags as soon as conditions are suitable. Nonetheless future work would benefit from early engagement with Serco to identify/develop available options to support the project.
- **Taking early opportunities to tag** – given the dynamic nature of the sea ice zone, and the strict operational constraints on tagging, voyages attempting seal tagging work should look to capitalise on suitable opportunities as they present. This would require flexibility to increase the priority level of seal tagging activities opportunistically and may require several days if conditions are right.

This could be further assisted through extended dedicated seal tagging time rather than conducting other operations during the morning with seal tagging held off until the afternoon. Having a full day allocated would have provided greater opportunity to locate seals. Additionally, with other activities in the morning, ship's crew are not available to crew small boats until after the shift change at 12:30 pm. Having crew available for small boat and ice floe work throughout daylight hours (either through different shift

15. Seal tagging (AAS 4630)

times, or specific dedicated crew), would alleviate the operational time constraints imposed by crew shift changes.

- **Refinements to tagging techniques** – we identified a number of refinements to our procedures. Most notably, we prepared a system for preventing the anaesthetic from freezing in the jabstick cannister using chemical hand warmers and a strip of insulated rubber foam. We also identified that after capturing the seal, administration of anaesthesia would be best using the jabstick which administers the drug under pressure and allows greater potential quick delivery of a full dose.
- **Using drones or other aerial assets to locate seals** – we obtained an environmental clearance to use a drone onboard to scout for seals within 500 m of the vessel. However, the requirement of conducting drone operations within 12 nm of Australian Antarctic Territories meant that these operations were seldom possible. Future work could explore how drones could be used more effectively to locate seals. Alternatively, it may be worth considering the use of helicopters to find seals, as well as to carry the seal team to suitable deployment locations on ice floes.

15.4 Data Management

All preliminary data (including details of seal sightings) will be published through the Australian Antarctic Data Centre (AADC) (<https://data.aad.gov.au/>) following standard AADC procedures, and subject to the moratorium of 2 years.

16. Environmental DNA (eDNA) and sedimentary ancient DNA sampling (AAS 4556 and AAS 4636)

Team: Leonie Suter and Vishwadeep Rout

16.1 General Introduction

Environmental DNA (eDNA) is the genetic material shed by any living organism into the environment they live in. By taking a small environmental sample, e.g. a small seawater sample, this genetic information can be accessed through laboratory analyses, and through comparisons to DNA reference databases we can identify the species whose DNA is contained in a sample. This approach can be used to conduct non-invasive biodiversity surveys, capable of detecting species from microbes to blue whales, allowing us to describe community compositions of different ecosystems. Repeated monitoring and comparisons to physical and chemical ocean variables will allow us to identify drivers of community compositions and help us predict future impacts of climate change.

In the open ocean, eDNA generally degrades within hours to days below detectable levels. The signal detected in a sample therefore largely represents the current biodiversity present at the time of sampling. However, organic matter shed by living organisms can also sink to the seafloor, e.g. from faeces, moults or deceased organisms. Under the right conditions the DNA contained in this matter can remain relatively intact in seafloor sediments. Over thousands of years these sediments can build up to form a layered library of genetic information of past biodiversity, and this information can be accessed by taking sediment cores. Samples taken closer to the surface are generally younger, whereas samples taken from deeper in the sediments are generally older, with some cores going back in time for hundreds of thousands of years, spanning multiple glacial and interglacial periods. Studying this sedimentary ancient DNA (*sedaDNA*) can reveal biodiversity patterns of the past, how communities changed in relation to changing climates, and genomic adaptations of individual species over time.

Combining eDNA and *sedaDNA* data can put current biodiversity into historical perspective and help us predict how ecosystems may change or adapt to climate change.

16.2 Overall Aim and Hypothesis

Though eDNA and *sedaDNA* sampling we aim to describe the biodiversity of the present and past in the Denman Glacier region. In addition, we also aim to describe the animal biodiversity between Hobart and the survey area through transit sampling. As eDNA sampling can be quite labour intense, we investigate whether autonomous eDNA sampling can provide comparable data by testing two loaned eDNA samplers provided by the Monterey Bay Aquarium Research Institute (MBARI). Specifically, we ask

- iv) What is the animal biodiversity of the Denman Glacier region in surface waters and throughout the water column, and what physical and chemical ocean variables are shaping the observed diversity?

16. Environmental DNA (eDNA) and sedimentary ancient DNA sampling (AAS 4556 and AAS 4636)

- v) What is the animal biodiversity between Hobart and the survey area, how does it compare to eDNA data collected on past voyages, what are the drivers of biodiversity and can autonomous eDNA sampling provide comparable data?
- vi) How did the biodiversity change over the past glacial and interglacial periods, and how does it compare to current biodiversity?

16.3 Methods

16.3.1 Overview

eDNA samples were collected throughout the voyage to describe animal biodiversity in surface waters (underway sampling) and throughout the water column (CTD sampling). The following samples were collected:

- Underway sampling from the ship's uncontaminated seawater line (5 L) at 10 am, 2 pm and 10 pm ship time throughout the voyage, filtered by using a peristaltic pump.
- Underway sampling at matching times using two autonomous eDNA samplers loaned from MBARI.
- CTD sampling (5-10 L) generally collected from five depths between seafloor and surface from a total of 68 CTD casts.

In addition to eDNA sampling, we also collected sedaDNA samples from Kasten cores and multicores to describe the biodiversity of the past (see more detailed methods below).

16.3.2 Underway and CTD eDNA sampling

Underway eDNA sampling was undertaken in the RSV *Nuyina's* Wet Lab 1. At all times during setting up the sampling area and during sampling itself, appropriate PPE was worn that included a lab coat, safety glasses for bleach dilutions, and nitrile gloves.

Before collecting the first sample, the working surface, outside of tubing and filter holders were cleaned by wiping with 1 % sodium hypochlorite (bleach) using Kim Wipe (Kimtech), followed by Milli-Q water using Kim Wipe. Sampling bottles (5 L volume) were washed by rinsing with Milli-Q water, soaking the inside of each bottle with 50 mL of 1 % bleach for 10 minutes followed by further rinsing with Milli-Q water. The cleaned bottles were stored with closed lids until used for sampling. The insides of the tubing and filter holders were cleaned by flushing them with 50 mL of 1 % bleach followed by 1 L of Milli-Q water, using a peristaltic pump (Masterflex® L/S®). Two pairs of tweezers and one pair of scissors were soaked in 1 % bleach for 10 minutes, then rinsed with Milli-Q water and dried with a Kim Wipe (Kimtech). See Figure 87 for sampling set up.

16. Environmental DNA (eDNA) and sedimentary ancient DNA sampling (AAS 4556 and AAS 4636)

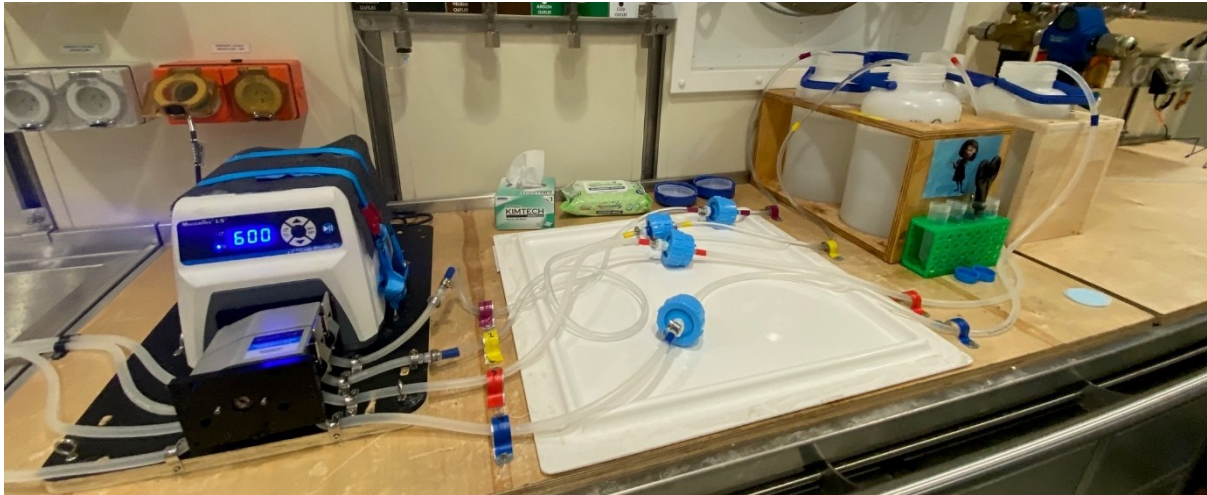


Figure 87: eDNA sampling set up in Wet Lab 1 of the RSV Nuyina to filter four eDNA samples in parallel.

Samples for eDNA analysis were collected during the transits, three times per day at 10 am, 2 pm, and 10 pm local ship time (UTC +7). Approximately 20 minutes prior to the sampling time, we opened the uncontaminated seawater line in Wet Lab 1. At the sampling times, we first rinsed one of the pre-cleaned sampling bottles with seawater and then collected 5 L of this seawater in the bottle. Water samples were logged in the RSV *Nuyina*'s eLog system to capture the sample's metadata (latitude, longitude, date, time, seawater temperature), as well as in a separate excel log sheet.

Next, a Durapore[®] Membrane Filter (5 µm SVPP, 47 mm; Millipore) was placed onto a filter holder and tightened. Using tubing and the peristaltic pump, the 5 L seawater sample was run through the filter at 600 rpm (usually taking 5-10 min). Then the filter was cut in half with sterilised scissors, and each half transferred into a separate 1.7 mL microcentrifuge tube (LoBind, Eppendorf). The tubes were labelled with a running number (DMV-001 etc) and 'A' or 'B' for the two halves. Replicates were stored in separate -80 °C freezer. For every 10th sample, we filtered 5 L of Milli-Q water using the same procedure as for the seawater samples described above as a control.

After the sampling, we repeated the cleaning procedure that was undertaken before the first sampling (described above) for the working surface, tubing, filter holders, pump, sampling bottles, scissors and tweezers.

eDNA sampling from CTD casts followed the same approach as the underway sampling for sterilizing surfaces and equipment and for filtering. Most CTD casts were between 500 m and 1000 m, and for these casts, samples were collected from five depths: 10 m above the seafloor, at around 500 m depth, below the deep chlorophyll maximum (DCM), at the DCM and at the surface (10-20 m depths). At the seafloor and 500 m depths, 10 L of seawater were collected due to low eDNA concentrations at these depths, whereas from the shallower depths, 5 L of seawater was collected. If the seafloor was deeper than 1000 m, additional samples were collected at 1000 m, and if the seafloor was shallower than 500 m, the 500 m sample was dropped. Up to four samples were filtered in parallel using a multi-channel pump head (Figure 87). As for the underway samples, tubes were labelled with a running number (DMV-001 etc) and 'A' or 'B' for the two halves – the metadata identified which sample was an underway, a CTD or a negative control sample. All metadata was entered into a log sheet as well as the *Nuyina*'s

16. Environmental DNA (eDNA) and sedimentary ancient DNA sampling (AAS 4556 and AAS 4636)

eLog system. In total, 166 samples were collected from the uncontaminated seawater line, 335 samples from 68 CTD casts as well as 56 negative controls.

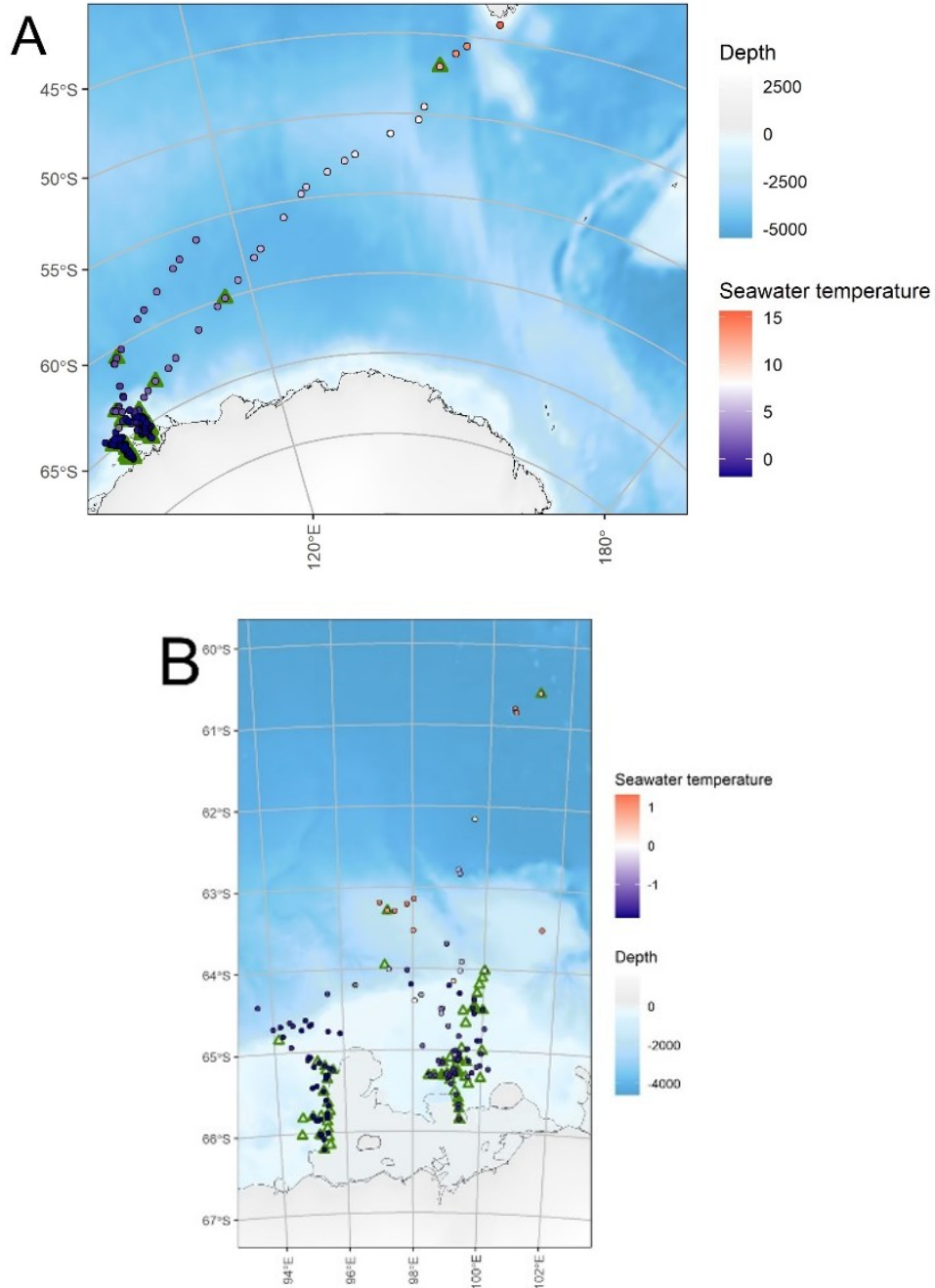


Figure 88: eDNA samples collected from the uncontaminated seawater line (circles coloured by seawater temperature) and from CTD casts (triangles), shown for the overall voyage (A) and the survey area (B).

16. Environmental DNA (eDNA) and sedimentary ancient DNA sampling (AAS 4556 and AAS 4636)

16.3.3 Autonomous eDNA sampling

Two autonomous eDNA samplers were loaned from MBARI for the voyage. The Environmental Sample Processor (ESP) contained 60 cartridges and could be programmed to filter 2 L of seawater onto 5 μ M SVPP, 25 mm filters at pre-determined times, followed by sample preservation in RNAlater buffer. The Filtering Instrument for DNA Observations (FIDO) sampler contained 144 sampling pucks and could be programmed to sample up to 5 L of seawater within 30 minutes onto 5 μ M SVPP, 47 mm filters, followed by soaking in RNAlater buffer and evacuation of all liquids from the puck using Nitrogen gas.

The ESP sampler was programmed to collect eDNA samples at 10 am and 10 pm during transit to and from the survey area, as well as at selective days in the survey area, both in the central area east of the Shackleton Ice Shelf, as well as in the western region, amounting to a total of 54 samples plus two negative controls. The FIDO sampler was programmed to collect samples throughout the voyage at 10 am and 10 pm, and towards the end of the voyage also at 2 pm, amounting to a total of 121 samples plus negative controls.

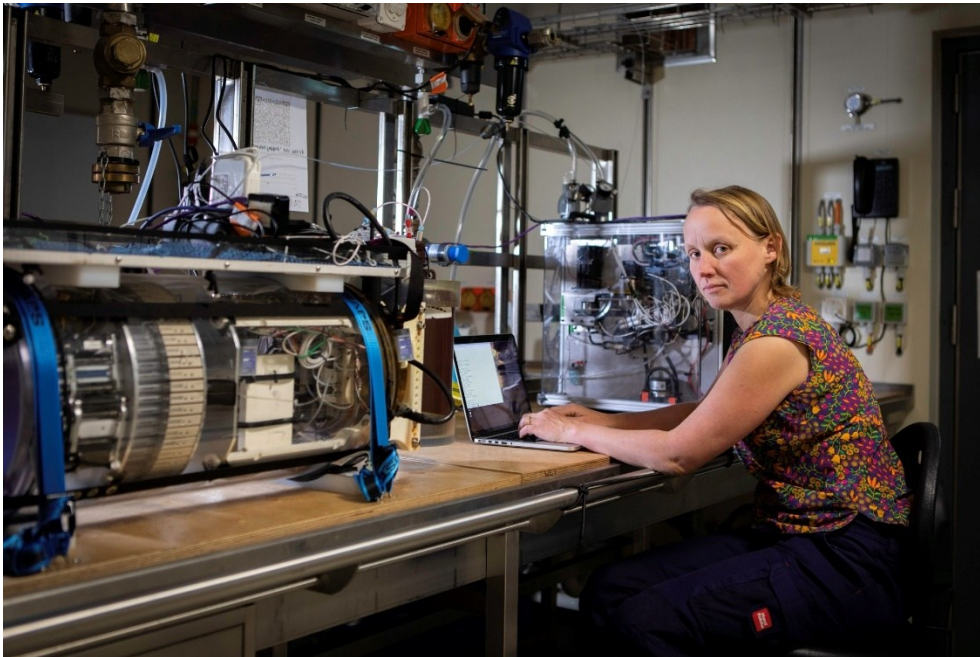


Figure 89: Dr Leonie Suter programming two autonomous eDNA samplers, the Environmental Sample Processor (ESP) on the left, and the Filtering Instrument for DNA Observations (FIDO) on the right, to collect, filter and preserve eDNA samples at pre-determined times. Photo: Pete Harmsen, AAD.

16.3.4 Sedimentary ancient DNA (sedaDNA) sampling from Kasten cores

Before collecting the sedaDNA samples from kasten cores, the floor of the Wet lab 2 and surfaces in the working area were cleaned with 3 % sodium hypochlorite (bleach). Metal surfaces were additionally wiped with 80 % ethanol. Plastic spatulas and scrapers to be used for sampling were also decontaminated with bleach. 5 mL centrifuge tubes were labelled and kept in a separate Ziplock bag before use. The sedaDNA sampling was performed in Wet Lab 2

16. Environmental DNA (eDNA) and sedimentary ancient DNA sampling (AAS 4556 and AAS 4636)

of the RSV *Nuyina*. It was commenced immediately after photographing the core as sampling for *sedaDNA* is time-sensitive (to avoid exposure to oxygen, high temperatures and contamination). The number of personnel and their movement around the lab was limited to further reduce the risk of contamination. While setting up the sampling area and during the sampling itself, appropriate PPE was worn that included a coverall, safety glasses, head cover, facemask and double nitrile gloves. After the Kasten core was placed on the roller rack, the top of the core barrel was removed sequentially from top to bottom. Upon removal, the upper 4 mm was scraped with a clean scraper in a perpendicular fashion, from the bottom to the top of the core, with a clean (3 % bleach and 70 % ethanol treated) scraper used for each scrape. A measuring tape was placed along the side of the core for reference. Starting from the bottom of the core, sediment samples were collected with a clean plastic spatula and were placed in 5 mL tubes. For each sample, a new clean spatula was used. The upper pair of gloves were changed between samples if contaminated with sediment. Samples (~2 cm³) were collected every 2 cm from 0-10 cm, every 10 cm from 10 cm to mid-core, and every 20 cm from mid core to the deepest part of the core. In addition, extra samples were collected at visible transitions (based on colour) in the sediments. Each sample tube was carefully wiped clean, sealed, labelled, and placed into an individually labelled Ziplock bag. All sample tubes were then grouped in a larger labelled bag containing the voyage ID, station number, core ID, and date, and immediately stored at -20 °C.

All six kasten cores were sampled for *sedaDNA* (see 'Table 41' and 'Figure 56' in sediments section for locations).



Figure 90: Collecting sedimentary ancient DNA from Kasten cores required carefully implemented controls to avoid contaminations of the ancient sediments with modern DNA, e.g. wearing appropriate PPE.

16. Environmental DNA (eDNA) and sedimentary ancient DNA sampling (AAS 4556 and AAS 4636)

16.3.5 Sedimentary Ancient DNA (sedaDNA) sampling from Multicores

Before collecting multi-core sediment samples, all equipment—including the core extruder, scrapers, and spatulas—was thoroughly decontaminated with a 3 % bleach solution, followed by 70 % ethanol wipes. Sampling took place in Dry Lab 2 of the RSV *Nuyina* under a quarantine-style, closed-door setup to reduce the risk of airborne contamination. The floor was mopped in advance using 1 % bleach and with tap water after 15 mins. Only authorized samplers were present, each adhering to stringent clean protocols, which included wearing face masks, hair covers, lab coats or disposable coveralls, safety glasses, and double gloves.

Excess seawater was first removed from the top of each multi-core cylinder using a sterilized syringe (treated with 3 % bleach and 70 % ethanol). The cores were then vertically extruded (i.e., gently pushed upwards from the bottom) to the desired depth, allowing sediment layers to be accessed cleanly from the top. Sterilized scrapers were used to take sediment slices (perpendicular the core). From each slice, approximately 2 cm³ of sediment was collected from the center using a clean plastic spatula and placed into 5 mL tubes. The first sample was collected from 0–1 cm, followed by core extrusion to access subsequent intervals at 2–3 cm, 4–5 cm, and so on. The core was progressively extruded at each sampling interval to expose fresh sediment layers. Sampling was conducted at every 2 cm intervals from 0–10 cm, and at 5 cm intervals from 10 cm to the bottom of the multi-core. A new clean scraper and spatula were used for each sample, and the upper pair of gloves was changed between samples if contaminated with sediment. Each sample tube was carefully wiped clean, sealed, labelled, and placed into an individually labelled Ziplock bag. All sample tubes were then grouped in a larger labelled bag containing the voyage ID, station number, core ID, and date, and immediately stored at –20 °C.

Samples were taken from multicores: 02, 11 and 13 (see ‘Table 30’ and ‘Figure 56’ in sediments section for location details).

16.4 Issues encountered

We encountered multiple issues with the autonomous eDNA samplers. The ESP and FIDO sampler were initially programmed to start sampling at the same time, but due to some interference of the instruments with each other, the ESP sampler had to be programmed to start sampling 15 minutes after the FIDO sampler. Mid-voyage, the FIDO sampler stopped sampling due to some broken parts and leaking tubing. We managed to take things apart, glue parts back together and re-wire some tubing and got the sampler to reliably sample for the remainder of the voyage, but we lost approximately one week of sampling mid-voyage.

Manual sampling in Wet Lab 1 generally worked well, however, at times there was a lot of traffic through the lab due to people using it as a thoroughfare between the CTD hangar and other work spaces, increasing the risk of contaminating samples with either human DNA or marine DNA carried around by people coming from the CTD hangar.

16.5 Recommendations

Careful consideration should be given as to who shares the lab space with the eDNA work, as using the lab as a thoroughfare can contaminate eDNA samples. Autonomous eDNA sampling

16. Environmental DNA (eDNA) and sedimentary ancient DNA sampling (AAS 4556 and AAS 4636)

may be a desirable alternative for underway sampling in the future, but we need to analyse the collected data first to ensure that the data quality is comparable to manual sampling.

16.6 Data Management

All preliminary data will be published through the Australian Antarctic Data Centre (AADC) (<https://data.aad.gov.au/>) following standard AADC procedures, and subject to the moratorium of 2 years.

16.7 Acknowledgements

We would like to thank the RSV *Nuyina*'s crew, voyage management, our science collaborators and all the AAD folks who contributed to this voyage. Special thanks are extended to Roland Painter and Adam Duraj for fixing the FIDO sampler.

The successful collection of sedimentary ancient DNA (*sedaDNA*) samples from both kasten and multi-core sediments aboard the RSV *Nuyina* would not have been possible without the invaluable assistance and support of several individuals. We sincerely thank **Molly, Jim, Rachel, Neve, Taryn, Katharina, Jo, Noah and Amy** for their hands-on help throughout the planning and execution of the sampling process. Their dedication to maintaining stringent contamination control and clean lab practices was critical in ensuring the integrity of the *sedaDNA* samples. We are deeply grateful for their time, help, and shared commitment to this work.

17. eDNA invasives (AAS 4628)

By Frances Perry

17.1 Introduction

Invasive species are one of the biggest threats to marine ecosystems, with vessel biofouling identified as the most common pathway for the spread of marine invasive species (Hewitt and Campbell, 2010). Antarctica is one of the few remaining regions without any known established populations of non-native marine species (McCarthy et al., 2022), but extensive biofouling communities have been identified on vessels operating in the Antarctic, including globally significant invasive species (Lewis et al., 2005).

This work is using environmental DNA (eDNA) analysis from seawater samples collected onboard to investigate the marine invasion risk posed by vessel biofouling in the Antarctic and Southern Ocean, using the RSV *Nuyina* as a case study. We aim to identify any biofouling species present within the internal niche areas of the vessel and use this information to inform ongoing biofouling management.

17.2 Sample Collection Methods

Samples were collected from three different points on the vessel: the uncontaminated seawater line (intake point at the bow), raw water (intake from the sea chests) and the moon pool (Figure 91). Five litres of seawater were collected from each location and filtered using a peristaltic pump (Sartorius, Microsart e.jet pump and 3-branch manifold) through a 1.2 µm pore size glass filter membrane (Sigma Aldrich). The filters were immediately preserved in ATL buffer (Qiagen) and stored at -20 °C until analysis. A field control was also collected after each day of sampling, by filtering 5 L of Milli-Q water following the same protocol. All sampling and filtration equipment was soaked in 10 % bleach solution for a minimum of 10 minutes and triple rinsed with MQW water before sampling. The temperature of each sample was also measured, to identify any effects of warming from the vessel between intake location and collection point onboard. There were 23 sampling events, with a total of 90 samples collected across the voyage (Table 53, Figure 92). Samples were named based on the location (uncontaminated sea water: US; raw water: RW; moon pool: MP; control: CON) and the sample number (1 - 23) e.g. US-1. On return, samples will be sequenced, and bioinformatics used to determine the taxonomic identity of the DNA sequences collected.

17. eDNA invasives (AAS 4628)



Figure 91: Sample collection from the moon pool (top doors closed) (left). The moon pool with the top doors open (centre). eDNA sampling process in Wet Lab 1 (right).

17.3 Locations

Seawater samples were collected daily during the transit between Hobart and Antarctica (02/03/25 – 08/03/25), weekly whilst at the Denman Glacier (15/03/25 – 19/04/25) and daily on the transit back to Hobart (23/04/25 – 01/05/25) at approximately 9 am ship time. Dates in Table 53 are in UTC.

Table 53: Timing and location of each sampling point for the eDNA invasives project.

Sampling event	Date & Time (UTC)	Latitude (DD)	Longitude (DD)
1	2025-03-02T01:30:00+00:00	-45.9551	143.7321
2	2025-03-02T21:45:00+00:00	-49.2866	140.9002
3	2025-03-04T01:15:00+00:00	-52.6656	133.4959
4	2025-03-05T01:30:00+00:00	-54.3465	128.3977
5	2025-03-06T01:35:00+00:00	-57.6783	122.1708
6	2025-03-07T01:50:00+00:00	-59.9930	116.5735
7	2025-03-08T01:30:00+00:00	-62.1907	108.4971
8	2025-03-15T00:05:00+00:00	-65.0143	98.6789
9	2025-03-16T02:15:00+00:00	-65.3211	98.9014
10	2025-03-22T01:00:00+00:00	-64.8731	99.0584
11	2025-03-29T02:30:00+00:00	-64.9484	99.6116
12	2025-04-05T02:30:30+00:00	-64.9218	94.3986
13	2025-04-12T02:40:30+00:00	-66.0218	95.1997
14	2025-04-14T00:45:00+00:00	-65.4095	95.2757
15	2025-04-23T01:15:00+00:00	-60.8490	100.6269
16	2025-04-24T01:30:00+00:00	-60.6235	101.1161
17	2025-04-25T01:33:51+00:00	-59.3202	105.2302
18	2025-04-25T23:15:54+00:00	-57.3873	111.4062
19	2025-04-26T22:15:43+00:00	-55.0486	118.3266
20	2025-04-27T22:20:00+00:00	-52.7539	125.1354
21	2025-04-28T22:30:09+00:00	-50.1705	131.5369
22	2025-04-29T22:40:00+00:00	-47.7502	137.5796
23	2025-04-30T22:30:15+00:00	-45.3526	143.3233

17. eDNA invasives (AAS 4628)

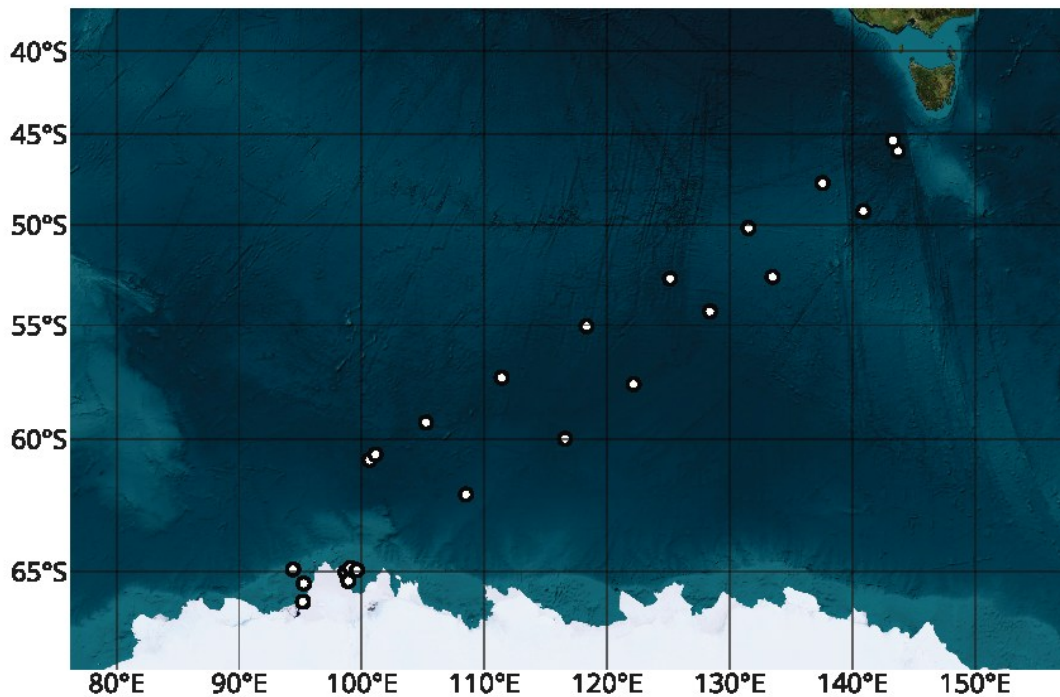


Figure 92: Map showing each sample location for the eDNA invasives project.

17.4 Data Management

All preliminary data will be published through the Australian Antarctic Data Centre (AADC) (<https://data.aad.gov.au/>) following standard AADC procedures, and subject to the moratorium of 2 years.

17.5 Acknowledgements

Thanks to the DVL's Nick Watt and Anthony Macfarlane as well as Tim Sharpe (Chief Mate) for helping to facilitate the sampling through the moon pool.

17.6 References

- Hewitt, C. & Campbell, M. 2010. The relative contribution of vectors to the introduction and translocation of marine invasive species. *In*: THE DEPARTMENT OF AGRICULTURE, F. A. F. D. (ed.). The National Centre for Marine Conservation and Resource Sustainability within the Australian Maritime College.
- Lewis, P. N., Riddle, M. J. & Smith, S. D. A. 2005. Assisted passage or passive drift: a comparison of alternative transport mechanisms for non-indigenous coastal species into the Southern Ocean. *Antarctic Science*, 17, 183-191.
- McCarthy, A. H., Peck, L. S. & Aldridge, D. C. 2022. Ship traffic connects Antarctica's fragile coasts to worldwide ecosystems. *Proceedings of the National Academy of Sciences*, 119, e2110303118

18. Zooplankton / Wet Well (AAS 4631)

Personnel: Haiting Zhang, Luke Brokensha, Inessa Corney, Pimnara Riengchan

18.1 General Introduction

Zooplankton play a key role in marine food webs and biogeochemical cycling, particularly in polar ecosystems where they contribute significantly to carbon export and energy transfer. Understanding their physiological responses to environmental change is essential for predicting the resilience of Southern Ocean ecosystems. During the Denman Marine Voyage, we conducted respiration rate experiments on live zooplankton collected from a range of sites including the Denman Glacier region and sites at lower latitude. These experiments tested the metabolic responses of multiple species to varying temperatures and pCO₂ conditions, simulating present-day and future climate scenarios. By examining interspecific and spatial variation in zooplankton respiration under these stressors, our study aims to inform projections of zooplankton functioning under ongoing ocean warming and acidification.

In addition to the experimental work, we conducted zooplankton net tows and collected phytoplankton samples across the transect to support broader ecological assessments, including spatial patterns in plankton abundance and community diversity. Notably, we collected live *Clio pyramidata*, a pteropod species, and successfully documented its egg development from initial laying through to hatching - the first time this process has ever been recorded. Together, these data provide new insights into the physiological plasticity, reproductive biology, and community structure of key plankton taxa in a changing Southern Ocean.

18.2 Overall Aim and Hypothesis

The zooplankton (Wet Well) team were seeking to:

- Collect live zooplankton from multiple locations and maintain them in the onboard aquarium for experimental work.
- Conduct physiological tolerance experiments using live zooplankton to examine their responses to environmental stressors, such as varying temperature and pCO₂ levels, by measuring respiration rates.
- Investigate heat shock protein responses by exposing zooplankton to extreme temperatures, assessing their capacity to respond and recover from ocean extremes.
- Collect live shelled pteropods from Antarctic waters and near the ice edge and run trial experiments to explore their calcification responses under ocean acidification scenarios.
- Monitor and document *Clio pyramidata* egg and larval development.
- Develop a simulated plankton tow method using the Wet Well system to collect underway samples, enabling analysis of spatial patterns in plankton abundance and community diversity.
- Collect phytoplankton samples associated with sea ice and analyse their distribution and taxonomy.

18. Zooplankton / Wet Well (AAS 4631)

- Collect fish samples from Wet Well for future DNA work and collect trace metal free zooplankton along with the TMR sites for further studies.

18.3 Methods

18.3.1 Simulated Plankton tow

The initiative of the development of a simulated plankton tow method was to quantify zooplankton collected via the Wet Well system over a defined time period, allowing for comparisons between Wet Well-derived abundance data and that from conventional trawl nets. This method was implemented using the newly installed Wet Well, which features a bottom drain that enables complete transfer of the catch tank contents into a plankton net. The top and side filter screen used were 200 µm, which is similar to the common plankton net mesh size.

18.3.1.1 Plankton tow operation

1. Check the pipe and valve to make sure the correct pipe (surface valve, middle valve, keel valve) is attached to the new wet well.
2. Before each tow, wet well should be running for at least ~10 minutes to make sure no remaining water in the pipe and in the view tank from the last running.
3. Stop valve, clean screens and catch tank using fresh sea water from view tank, or using freshwater hose but rinse with fresh sea water.
4. Close the drain and attach plankton net to the bottom joint? of the drain (attach net from the beginning in case of any leakage).
5. Turn hydraulic valve on (eLog activity: trawl start), ideally run wet well for 30 minutes. Assess running time based on the phytoplankton density, sea ice density, flow rate, and time limit for other operations, no less than 20 minutes if manageable.
6. Then turn hydraulic valve off (eLog activity: trawl end). Put the plankton net in a bucket to buffer the heavy water flow then open drain.
7. Use seawater from view tank to rinse top and side screens until clear, then rinse catch tank to make sure no visible plankton items left.
8. Take off plankton net. Filter and lightly rinse all samples into sample jar (ideally 500 mL to 1 L, this step is conducted in wet lab 2).
9. Preserve samples in 10 % Formalin as soon as possible.
10. Label jars. Store sample in hazardous chemical storage room on deck 4, ideally in UN certificated carton box.

18.3.1.2 Sampling frequency

The initial sampling plan aimed to collect one sample per degree of latitude along the transect from 47 °S to 65 °S, but this was adjusted to one sample every two degrees due to the absence of shift work in our team. Sampling was carried out primarily at night, with occasional daytime collections to enable day-night comparisons. When operators were available, plankton tows were conducted daily within research areas. Tows were skipped at repeat sites or when heavy sea ice obstructed the Wet Well. For future voyage planning, allocating dedicated ship time to sample open waters in ice-heavy regions would be valuable, as sea ice conditions during this voyage forced a temporary halt in plankton tow operations for several days.

18. Zooplankton / Wet Well (AAS 4631)

18.3.1.3 Laboratory analysis

Plankton tow samples will be used for zooplankton taxonomy identification, biomass determination, abundance calculation, and size analysis using microscopes and zooscan at IMAS zooplankton lab.

18.3.2 Zooplankton physiological tolerance experiments

18.3.2.1 Equipment and Materials

Bucket, handheld zooplankton net, sampling jars, petri dishes, holding dish, pipette, microscopes, camera for image recording, Presens SDR Plate system, 4 mL and 2 mL Presens sensor vials, Presens Oxygen Sensor Spot SP-PSt3-NAU, Presens Microx 4 system.

18.3.2.2 Thermal experiments procedure

Live zooplankton were collected from the Wet well, once hundreds of each species collected, specimen collection for experimental work began. Specimen collection – live copepods were collected from kreisels using a net, then washed into a holding dish. Copepod specimens were then individually picked out, to be photographed and identified before being placed into the 4 mL and 2 mL sensor vials for experimentation. This work targeted one known species of copepod *Calanus propinquus*. Once all sensor vials are filled, they were then placed into a temperature-controlled cabinet to begin thermal ramping experiments. Animals spent at least 24 hours at each temperature in the temperature-controlled environment before the experiment concluded. Amphipod specimens were picked out and placed into 150 mL glass bottles with 2 specimens in each bottle.

The target temperatures for thermal experiments were the ambient temperature the specimens were collected at: 1 °C, 5 °C, 10 °C, 15 °C. At the end of each 24-hour period, specimens were imaged and snap frozen for further analysis. New animals were used for each temperature. Post experiment processing includes taking wet weights, dry weights and size measurement of zooplankton, as well as further molecular work.

18.3.2.3 pCO₂ experiment procedure

Three pCO₂ sea water conditions were selected to reflect the ocean conditions under ambient (~400 ppm), low carbon emission scenario (~700 ppm) and high carbon emission scenario (~1000 ppm) climate factors.

The approach of three conditions were broken down into 6 blank vials (3 x 3 pCO₂ treatment), leaving 18 vials free, allowing for 6 vials per treatment of pCO₂, which were 6 replicates per species (focusing on two target species, one from temperature experiments and *Thysanoessa macrura* furcilia) per treatment.

pCO₂ experiments followed the same collection procedure as temperature experiments, all individuals were identified before being placed in vials for initial pCO₂ experimentation. Individuals in pCO₂ experiments were carefully monitored during experiments to determine when a significant decline in the individual's respiration has occurred and then animals followed the same post processing procedure as for the thermal experiments.

18. Zooplankton / Wet Well (AAS 4631)

18.3.2.4 Heat shock protein experiment procedure

Heat shock proteins (HSPs) are a family of proteins produced by cells in response to stressful conditions. To analyse the physiological response of zooplankton to thermal stress, the copepod *Calanus propinquus* and the amphipod *Themisto gaudichaudii*, collected from the Wet Well, were selected for HSP expression experiments. Thirty individuals of each species were maintained at ambient temperature for 24 hours, then 10 were exposed to a target temperature of 10 °C and ten were exposed to 5 °C for 36 hours. After exposure, specimens were preserved in RNAlater at 4 °C overnight before being transferred to –80 °C for return to Australia and further molecular analysis.

18.3.3 Pteropod egg development documentation

Pteropod *Clio paramidata* cultured in the kreisel in the aquarium unexpectedly laid egg masses, which enabled the documentation of the egg development for the first time on this species.

Egg masses were initially found in the kreisel and then carefully transferred into individual 5 L buckets and culture chambers to allow for better observation. During the first two weeks, the capsules were imaged under the same microscope at same magnifications four times every 4 hours. As development progressed, the observation frequency was gradually reduced, first to every 8 hours, then every 12 hours, and eventually once per day. Egg transferring was kept in cold using outer bucket filled with ice. All the process required extreme delicate handling and training was essential to make sure the minimum impact on the egg masses.

Base respiration rate of egg capsule was measured using the same sensor vial (2 mL) used for zooplankton thermal tolerance experiment.

18.3.3.1 Pteropod shell growth experiment

Pteropods (*Limacina helicina*) collected from the Wet Well were used for calcein incubation experiments to investigate their calcification responses under varying pCO₂ levels. Specimens were transferred to 15 L buckets and maintained in the aquarium at 1 °C. Respiration rates were measured under three treatments: (1) ambient pCO₂ (~400 ppm), (2) ambient pCO₂ with EIPA treatment, and (3) elevated pCO₂ (~1000 ppm). For each treatment, five individuals were pooled as one replicate, and respiration rate was measured using 2 mL sensor vials. Each treatment included six samples and two blanks. Sensor vials were first prepared in the aquarium, then placed in the culture cabinet at –1 °C for 24 hours of measurement.

18.4 Recommendations

The culture cabinet in Wet Lab 2, provided by AAD, was not functioning at the start of the voyage. It took 2–3 weeks to fix the issue, which delayed the start of the experiment. This highlights the importance of testing equipment prior to departure. While an alternative culture cabinet was available in the eDNA lab, the strict contamination-free requirements of that space made it unsuitable for our work. The cabinet was eventually relocated to Hold 1 Deck 4, but valuable time could have been saved if equipment setup had been planned in conjunction with lab space considerations.

18. Zooplankton / Wet Well (AAS 4631)

Experiment planning using the Wet Well should remain flexible and include alternative options due to the unpredictability of animal availability. Fragile organisms such as larval and gelatinous zooplankton were confirmed to be suitable for experimentation, allowing future experiments with these taxa to be planned with greater confidence. The use of microscopes equipped with cameras is highly recommended for photo identification. High-quality waterproof torches are essential when working in the Wet Well room.

During the sampling process, it was difficult to predict the types and numbers of animals that would be collected through Wet Well, which made pre-labelling of samples challenging. Zooplankton samples were mostly stored individually in cryovials (1.2 mL and 2 mL), and vials containing the same genus or same species from the same site were grouped in ziplock bags. For future work, it is recommended to include smaller vials (e.g., 0.5 mL) for preserving small copepods and zooplankton. Alternative storage methods, such as 96-well plates, can also be considered for preserving small individual animals.

Due to vertical migration, animals were more abundant at night, which was clearly reflected during Wet Well operations. When planning working hours or shift schedules, it is recommended to prioritise Wet Well use during the night and allocate daytime for experiments and other tasks. It's also important to allow some extra time for Wet Well operations, as collecting animals can easily take longer than expected, especially during a bloom. The peak time of animal appearance may vary and should be tested at the beginning of the voyage. On this voyage, our team's typical Wet Well working hours were from approximately 7 pm to 11 pm.

18.5 Preliminary Results (Voyage summary)

Overall,

- A total of 46 plankton tows were conducted. Site locations are shown in Figure 93, and the volume of filtered seawater for each tow is shown in Figure 94.
- Frozen phytoplankton samples (-80 °C) have been collected from 15 sites for future SEM analysis.
- Frozen zooplankton samples (-80 °C) have been collected from 23 sites.
- Preserved larval fish samples have been collected from four sites for further study.

18. Zooplankton / Wet Well (AAS 4631)

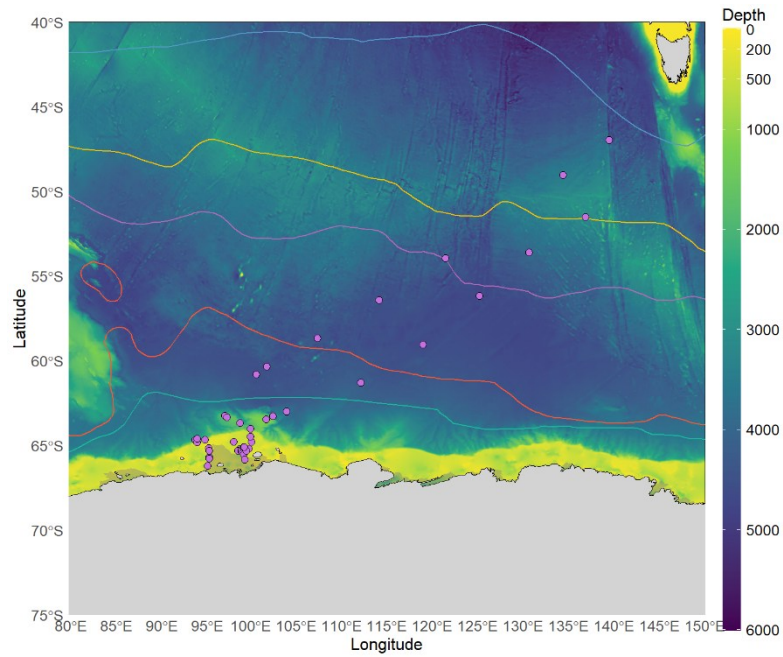


Figure 93: Plankton tow site location

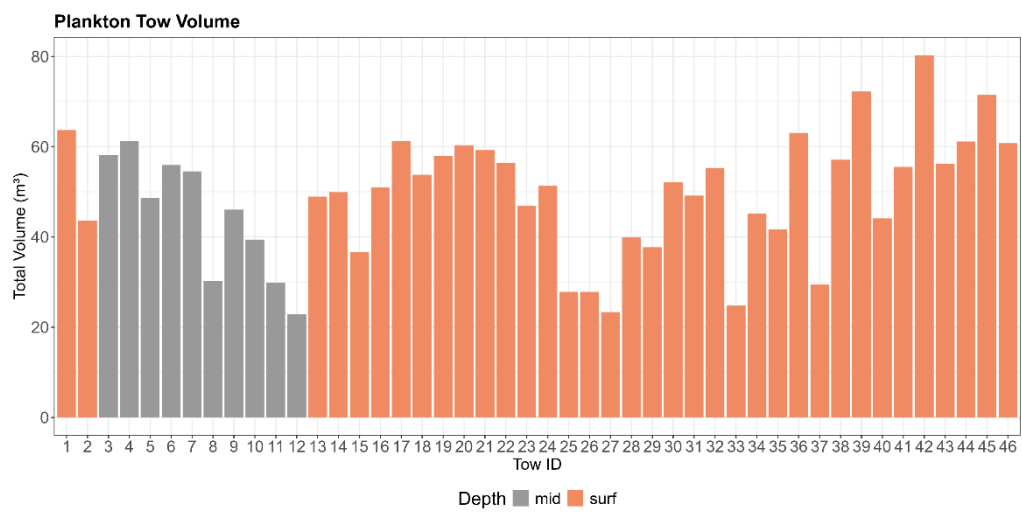


Figure 94: Volume of filtered seawater (m^3) for each plankton tow conducted using the Wet Well system.

18. Zooplankton / Wet Well (AAS 4631)

Table 54: Sampling log for plankton tows conducted using the Wet Well. Depth refers to the hose intake level: surf means the surface hose (~2 m below the waterline), and mid means the mid-depth hose (~5 m below the waterline).

Tow_id	Date (UTC)	Start time (UTC)	End time (UTC)	Start latitude (DD)	End latitude (DD)	Start longitude (DD)	End longitude (DD)	Depth
1	3/03/2025	13:55:25	14:24:32	-51.4994	-51.5495	136.9409	136.7901	surf
2	4/03/2025	13:04:48	13:24:00	-53.5951	-53.6201	130.679	130.6045	surf
3	5/03/2025	14:17:41	14:37:48	-56.1525	-56.1981	125.2246	125.1331	mid
4	6/03/2025	12:56:57	13:18:42	-59.0364	-59.0782	119.0468	118.9461	mid
5	7/03/2025	14:41:38	15:00:13	-61.2947	-61.318	112.1813	112.0874	mid
6	8/03/2025	14:25:00	14:48:02	-63	-63	104.0012	104.0012	mid
7	9/03/2025	8:00:59	8:23:00	-63.2897	-63.2897	102.4821	102.4821	mid
8	9/03/2025	14:21:48	14:34:07	-63.4552	-63.4681	101.7561	101.694	mid
9	11/03/2025	14:22:03	14:39:49	-63.2569	-63.2248	97.2464	97.1739	mid
10	13/03/2025	12:52:04	13:07:55	-63.3151	-63.346	97.3776	97.4491	mid
11	14/03/2025	13:28:50	13:42:28	-64.7922	-64.8197	98.1665	98.1478	mid
12	15/03/2025	1:30:36	1:42:19	-65.2187	-65.2414	98.7898	98.7904	mid
13	15/03/2025	14:11:20	14:31:23	-65.3139	-65.3139	98.6539	98.6539	surf
14	16/03/2025	7:31:34	7:52:27	-65.2869	-65.2869	99.0086	99.0086	surf
15	16/03/2025	14:00:29	14:15:48	-65.3383	-65.339	99.0238	99.0254	surf
16	17/03/2025	7:55:10	8:15:24	-65.4496	-65.4511	99.1679	99.1696	surf
17	17/03/2025	14:24:53	14:48:25	-65.5462	-65.5462	99.2754	99.2753	surf
18	18/03/2025	14:42:58	15:03:35	-65.8483	-65.8483	99.3858	99.3858	surf
19	19/03/2025	14:27:27	14:49:36	-65.1183	-65.1187	99.2095	99.2886	surf
20	20/03/2025	14:25:55	14:50:23	-64.7996	-64.8008	100.1327	100.1552	surf
21	21/03/2025	14:02:37	14:24:31	-65.2048	-65.2028	99.8127	99.9054	surf
22	22/03/2025	14:14:28	14:34:53	-65.3281	-65.3264	99.5505	99.6143	surf
23	24/03/2025	14:39:07	14:57:11	-65.1064	-65.1064	99.35073	99.35073	surf
24	29/03/2025	15:08:15	15:30:53	-64.501	-64.5049	99.99923	100	surf
25	30/03/2025	14:51:21	15:15:54	-64.5021	-64.5021	99.99828	99.99829	surf
26	31/03/2025	14:38:42	14:50:47	-64.0146	-64.0146	100.0204	100.0204	surf
27	31/03/2025	15:19:57	14:36:48	-64.0146	-64.0146	100.0204	100.0204	surf
28	3/04/2025	15:09:41	15:25:01	-64.6809	-64.6929	95.06042	95.03329	surf
29	4/04/2025	14:31:52	14:46:41	-64.6681	-64.6913	93.9317	93.95508	surf

18. Zooplankton / Wet Well (AAS 4631)

30	5/04/2025	14:17:50	14:39:37	-65.1798	-65.1799	95.42531	95.42548	surf
31	10/04/2025	14:17:05	14:36:48	-66.205	-66.205	95.31351	95.31351	surf
32	10/04/2025	15:53:59	16:16:10	-66.205	-66.205	95.3135	95.3135	surf
33	13/04/2025	13:38:31	13:48:36	-65.6773	-65.6774	95.49024	95.49669	surf
34	14/04/2025	7:18:12	7:36:07	-65.7911	-65.7911	95.45799	95.458	surf
35	16/04/2025	10:25:29	10:41:54	-64.8342	-64.8355	94.13591	94.13425	surf
36	18/04/2025	7:48:42	8:13:27	-65.3371	-65.3371	95.45039	95.45039	surf
37	19/04/2025	8:29:37	8:41:09	-64.6151	-64.619	94.16467	94.17695	surf
38	21/04/2025	15:57:26	16:21:27	-63.6929	-63.6928	98.89559	98.89558	surf
39_1	22/04/2025	12:23:16	12:35:54	-62.4746	-62.4584	99.53855	99.54613	surf
39_2	22/04/2025	12:43:19	13:03:16	-62.4505	-62.4097	99.54885	99.57381	surf
40	23/04/2025	11:59:56	12:23:32	-60.824	-60.8238	100.6379	100.6376	surf
41	24/04/2025	13:06:49	13:34:23	-60.375	-60.3384	101.7736	101.8844	surf
42	25/04/2025	8:18:52	8:51:06	-58.7183	-58.6617	107.294	107.4686	surf
43	26/04/2025	8:33:24	8:54:28	-56.4321	-56.3981	114.1021	114.2119	surf
44	27/04/2025	8:46:47	9:08:59	-53.9735	-53.9366	121.3991	121.5013	surf
45	29/04/2025	9:48:57	10:15:08	-49.0722	-49.0224	134.3415	134.4522	surf
46	30/04/2025	6:17:28	6:42:39	-46.9939	-46.9761	139.4418	139.4846	surf

18.5.1 Zooplankton Experiments

- Pteropod (*Clio pyramidata*): Successfully documented full egg development from initial egg release to hatching—the first time in recorded history.
- Pteropod (*Limacina helicina*): Two calcein incubation experiments completed to assess shell growth under changing pCO₂ conditions.
- Copepod and other zooplankton: Two experiments conducted using live animals from the Wet Well.
- Multi-stressor experiments: Completed 4 series of multi-stressor experiments involving: 2 copepod species, 1 amphipod species, 1 larval krill species. Each series included a minimum of 60 individual samples to examine stress response under combined environmental drivers.
- Heat shock protein assays: 2 experiments conducted on 1 copepod species and 1 amphipod species to assess molecular-level stress responses.

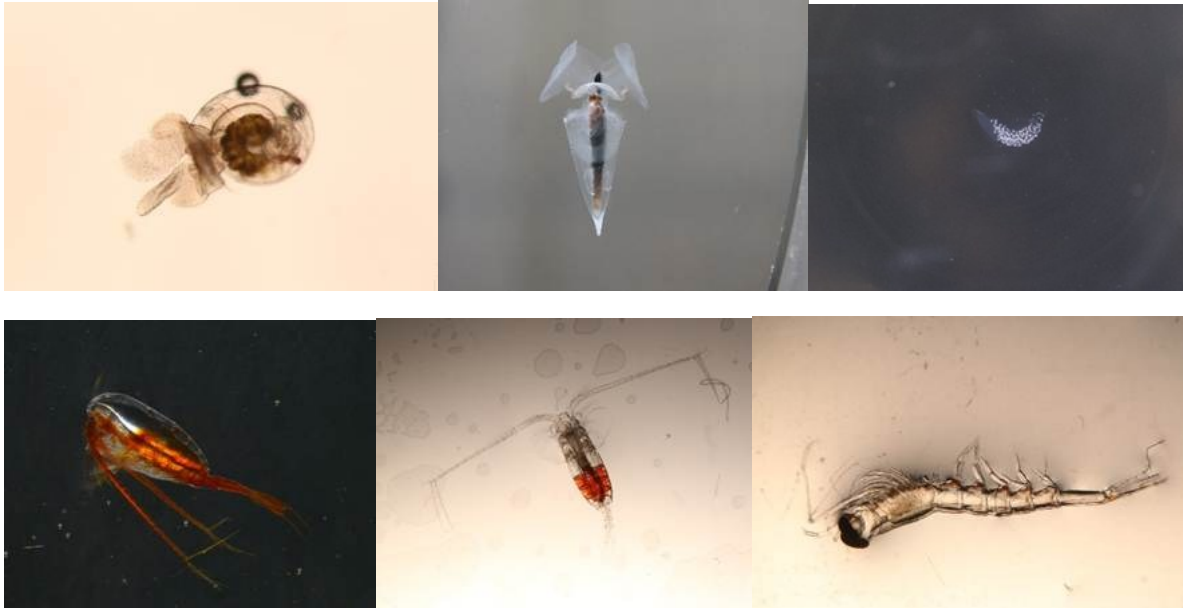


Figure 95: Photos of species used in the experiment. Top row (left to right): *Limacina helicina*, *Clio pyramidata*, *Clio pyramidata* egg mass. Bottom row (left to right): *Metridia* spp., *Calanus propinquus*, *Thysanoessa macrura*. Photo credits: Bottom left – Luke Brokensha; all others – Haiting Zhang

18.5.2 Continuous Plankton Recorder (CPR) Deployments

Ten CPR deployments were completed during the transits from Hobart to Denman and from Denman back to Hobart. Samples have been collected and stored at the Australian Antarctic Division and will be analysed in the future. The data will contribute to the Southern Ocean Continuous Zooplankton Records [AADC-00099] database.

18.6 Data Management

The preliminary datasets generated by the Wet Well team will be archived with the Australian Antarctic Data Centre (AADC) (<https://data.aad.gov.au/>) following standard AADC procedures, and subject to the moratorium of 2 years. In addition, working copies will be backed up on the UTAS/IMAS repository to support ongoing analyses and student projects.

18.7 Acknowledgements

Many thanks to Anton Rocconi for his dedicated support in operating the wet well and aquarium onboard, and for his valuable advice on working with live animals.

19. Media program

The Denman Marine Voyage media team, Lily West (Media Advisor) and Pete Harmsen (Videographer), worked collaboratively with all science, technical and leadership teams onboard RSV Nuyina.

They facilitated the filming, collection and distribution of content from the DMV.

The onboard media team attended daily briefings with voyage leadership and conducted weekly briefings with media representatives from the four scientific partner agencies.

Like the voyage itself, the media program was a coordinated effort between the four partner agencies.

Other key partners included the Department of Climate Change, Energy, the Environment and Water, University of Tasmania, CSIRO, SERCO and TasPorts.

The aim of the media program was to leverage different media formats and channels to reach audiences in ways that:

- Communicate the voyage's science and research activities and their importance for Australia and the world
- Showcase RSV Nuyina's cutting-edge scientific capabilities
- Enable all affiliated research groups to gain timely access to high quality content to support media engagement
- Generate material and story ideas for future use by all partner organisations
- Work together so all partner organisations are informed and can support others.

The onboard media team collated 107 vision packs, which were sent back to Australia for immediate distribution to the DMV's partner agencies.

Lily and Pete also captured hundreds of images and conducted 25 interviews with researchers on board.

There were six drone flights which captured some of the most iconic imagery from the voyage.

There were two periods of intense media coverage for the Denman Marine Voyage.

The first was the wharf side press conference prior to departure. This was attended by journalists from the ABC, 7 News, WIN News and AAPP, and the story gained national and international media coverage.

In the ensuing weeks, there was also a widespread distribution of a media package compiled by the onboard media team and the AAD media team back in Tasmania.

It contained stunning imagery and in-depth interviews with Australian researchers.

The package also detailed the scientific work happening during the voyage. The story was again picked up by a number of news stations and distributed across TV, print, social media and radio, nationally and internationally.

19. Media program

Early in the voyage, the Australian Government was placed into caretaker mode during the election period. As a division of the Australian Government, the AAD maintained caretaker conventions during this time and did not actively announce or pursue media opportunities.



Figure 96: The RSV Nuyina at the Denman Glacier. Photo: Pete Harmsen, AAD

20. ACEAS Outreach

By Neve Clippingdale

20.1 Overview

The Australian Centre for Excellence in Antarctic Science (ACEAS) conducted a series of outreach activities between 4th April and 1st May 2025. The initial planning phase began on 21st February 2025, when the first emails were sent to coordinate the logistics of the virtual calls.

These outreach sessions were collaboratively coordinated by members of the ACEAS team including Christina Schmidt, Jake Weis and Katharina Hochmuth, alongside the ACEAS Outreach Coordinator Neve Clippingdale. The calls were tailored to suit the age and educational level of participating students and were designed to highlight various aspects of life at sea and the practice of marine field science. Topics ranged from the daily operations of research vessels to conducting scientific work in remote Antarctic environments.

In total ACEAS facilitated nine virtual outreach calls involving three primary schools and four secondary schools located across three countries: Australia, the United States, and Germany (Table 55). Approximately 500 students aged between 4 and 18 years old participated in the program. This initiative not only expanded awareness of Antarctic science but also fostered international engagement with young learners in the field of marine and polar research. It is important to note however that each school participating in the program had an existing contact on board the Denman Marine Voyage. For future outreach initiatives, strategies to overcome this limitation and broaden school engagement should be considered.



Figure 97: Students from Our Lady of Mercy Catholic School ask ACEAS scientists Noah Menner, Katharina Hochmuth and Neve Clippingdale questions about the DMV and Antarctica (photos taken by Our Lady of Mercy staff).

20. ACEAS Outreach

Table 55: Schools that participated in ACEAS Outreach on the 2025 DMV

School	Age Range	Country	Number of Calls
Our Lady of Mercy Catholic School	4-10	Australia	1
Mount Nelson Primary School	9-12	Australia	1
Weston High School	15-17	USA	2
Colegio Alemán Guatemala	16-17	Germany	1
Kinderhouse	6-11	Germany	1
Jürgen-Fuhlendorf-Schule	16-18	Germany	2
Blue Mountains Grammar School	17-18	Australia	1

Schools were contacted in advance and during the initial stages of the Denman Marine Voyage, with regular communication required to coordinate and schedule the virtual calls. The number of calls per school varied depending on student participation levels and scheduling constraints; some schools hosted two sessions, while others participated in a single call. In certain instances schools divided sessions by age group however in one case the entire school attended a single call.

Each session typically lasted between 45 minutes and one hour. The content of the calls was adapted to suit the age range of the students, ensuring the material was both engaging and age appropriate. However, all calls consistently included a virtual tour component and concluded with a dedicated question-and-answer session, during which students had the opportunity to interact with the participating scientists, technicians, and crew members.

The structure of a typical call was as follows:

Primary School Sessions

- Welcome and introduction
- Presentation on essential clothing for working in Antarctica, including live modelling and demonstrations
- Tour of the RSV *Nuyina*, featuring exterior areas, recreational facilities, the bridge, mess hall, and scientific laboratories
- Interactive question-and-answer session with the team

High School Sessions

- Welcome and introduction
- Tour of the RSV *Nuyina*, highlighting key operational and scientific areas
- Presentations from up to six guest speakers, each discussing their specific roles on the Denman Marine Voyage and the scientific relevance of their work
- Group Q&A session, allowing students to engage directly with all guest speakers



Figure 98: Outreach in action! TOP: Neve Clippingdale, Jo Whittaker and Damien Stringer speak to students from Mount Nelson Primary School. BOTTOM LEFT: Maja Veit, Katharina Hochmuth and Christina Schmidt speak to students from Kinderhouse. BOTTOM RIGHT: Noah Menner and Neve Clippingdale speak to students from Our Lady of Mercy Catholic School.

The individual responsible for organising each call was generally also in charge of conducting the virtual tour and selecting the guest speakers. This approach enabled a diverse range of scientific disciplines to be presented to students, offering a broad and engaging overview of research conducted during the Denman Marine Voyage. Topics covered included physical oceanography, geology, paleoceanography, marine benthic ecology, marine biology, seal tagging, and hydro acoustics. Guest speakers represented a variety of organisations participating in the voyage, further enriching the students' exposure to real-world Antarctic science (Table 56).

20. ACEAS Outreach

Table 56: Table of ACEAS Outreach calls and involved scientists, technicians and crew on the DMV 2025.

ACEAS Outreach Call	Scientists Involved
Our Lady of Mercy Catholic School	Neve Clippingdale (ACEAS) Katharina Hochmuth (ACEAS) Noah Menner (ACEAS)
Mount Nelson Primary School	Neve Clippingdale (ACEAS) Katharina Hochmuth (ACEAS) Jo Whittaker (ACEAS) Damien Stringer (AAD)
Weston High School	Neve Clippingdale (ACEAS) Katharina Hochmuth (ACEAS) Joshua Lesicar (SAEF) Christina Schmidt (ACEAS) Floyd Howard (AAD) Luke Brokensha (AAD, AAPP) Rachel Meyne (ACEAS) Jim Trihey (ACEAS) Jess Brown (SAEF)
Colegio Alemán Guatemala	Jake Weis (ACEAS) Karin Orth (ACEAS) Katharina Hochmuth (ACEAS) David Green (ACEAS)
Kinderhouse	Katharina Hochmuth (ACEAS) Christina Schmidt (ACEAS) Jake Weis (ACEAS) Karin Orth (ACEAS) Maja Veit (Serco) Ole Rieke (AAPP) Neve Clippingdale (ACEAS)
Jürgen-Fuhlendorf-Schule	Christina Schmidt (ACEAS) Nicola Rodewald (SAEF) Ole Rieke (AAPP) Jake Weis (ACEAS) Katharina Hochmuth (ACEAS) Neve Clippingdale (ACEAS)
Blue Mountains Grammar School	Neve Clippingdale (ACEAS) Katharina Hochmuth (ACEAS) Jim Trihey (ACEAS) Chelsea Bekemeier (AAPP) Christina Schmidt (ACEAS) Jake Weis (ACEAS) Joshua Lesicar (SAEF) Rachel Meyne (ACEAS) Brett Cross (Serco)

Feedback received from participating schools was overwhelmingly positive with student engagement during the calls noted as particularly encouraging by the ACEAS team members involved. Many students came prepared with questions in advance, demonstrating a strong

20. ACEAS Outreach

interest in the topics presented. In addition to this, spontaneous questions frequently emerged during the sessions particularly when a topic sparked curiosity—an encouraging sign observed consistently across all age groups.

The high level of enthusiasm among participants on board the RSV *Nuyina* was noteworthy. Every scientist invited to contribute to the outreach calls accepted with enthusiasm, and there was never a shortage of willing volunteers. In some instances additional team members spontaneously joined the calls or took the opportunity to greet the students. This genuine eagerness created a warm and welcoming atmosphere, allowing students to witness firsthand the collaborative and supportive working environment aboard the RSV *Nuyina*.

This outreach initiative has not only succeeded in generating enthusiasm for Antarctic science but also holds promise for future opportunities. These may include ongoing mentoring relationships, as well as in-person school visits and guest talks. Overall, the program highlights the significant and meaningful impact of the ACEAS team's outreach efforts. All individuals involved in its delivery are to be commended for their dedication and contributions to its success.



Figure 99: Question time! TOP: Scientists pose for photo after a successful call with Weston High School. BOTTOM: Scientists answer questions from students from Kinderhouse and Jürgen-Fuhlendorf-Schule.

21. Appendix

21.1 Metadata

Metadata for all scientific voyage operations can be found in CSV form on the Australian Antarctic Data Centre. The following DOI is to the metadata for this voyage:

<http://dx.doi.org/doi:10.26179/k2n8-ph82>.

21.2 Station List

Table 58 contains a list of all 147 stations (a 'station' is defined as the location where a deployment entered the water, regardless of whether or not it was successful). Only events that were assigned station numbers have been included in this table. Dates and times are in UTC and refer to the start of the deployment.

The naming convention for stations was not agreed upon by the whole science team until Station 15. Stations before this were named retrospectively. Two TMR's early in the voyage failed and thus were not assigned TMR numbers. This changed later in the voyage when failed TMR's were given TMR numbers.

Table 57: Abbreviations used in Table 58 shown in order of appearance

Abbreviation	Phrase
CTD	Conductivity, Temperature, Depth
RD	Rock Dredge
TMR	Trace Metal Rosette
KC	Kasten Core
MC	Multicore
BT	Beam Trawl
TC	Towed Camera
PS	Process Station
SMG	Smith-McIntyre Grab
ISP	In Situ Pump

21. Appendix

Table 58: Station list for DMV deployments

Station	Latitude (DD)	Longitude (DD)	Activity	Date (UTC)	Time of deployment commencement (UTC)	Comments
1	-46.9992	142.0034	CTD1	2/03/2025	09:47:26	Trial
2	-59.993	116.5736	CTD2	6/03/2025	23:20:13	
3	-63	104.0012	CTD3	8/03/2025	13:00:00	
4	-63.286	102.4949	RD01	9/03/2025	00:18:41	
	-63.2897	102.4821	TMR1	9/03/2025	08:07:00	
5	-63.161	97.989	RD02	12/03/2025	09:52:33	
6	-63.2831	97.3054	CTD4	12/03/2025	16:15:52	
	-63.2930	97.3320	TMR2	12/03/2025	19:27:00	
	-63.2830	97.3069	KC01	13/03/2025	02:38:51	
	-63.2829	97.3068	MC01	13/03/2025	08:31:23	Fail
7	-64.500	98.795	BT01 (A)	14/03/2025	08:28:05	
8	-65.3036	98.4583	CTD5	15/03/2025	04:16:44	
	-65.3036	98.4583	TMR	15/03/2025	Not recorded	Fail
9	-65.3136	98.5232	CTD6	15/03/2025	07:37:22	
	-65.3136	98.5232	TMR	15/03/2025	Not recorded	Fail
10	-65.3134	98.5899	CTD7	15/03/2025	11:10:04	
11	-65.3139	98.6539	CTD8	15/03/2025	13:50:55	Aborted
	-65.3139	98.6539	CTD9	15/03/2025	17:26:52	
12	-65.3041	98.8436	CTD10	15/03/2025	20:59:59	
13	-65.3211	98.9014	CTD11	16/03/2025	00:56:06	
14	-65.2871	99.0096	CTD12	16/03/2025	06:14:01	
	-65.2869	99.0085	TMR3	16/03/2025	07:57:21	
	-65.2858	99.0044	MC02	16/03/2025	09:04:28	
15	-65.3231	99.0038	CTD13	16/03/2025	12:02:17	
16	-65.3434	99.0328	CTD14	16/03/2025	15:30:42	
17	-65.3254	99.0804	CTD15	16/03/2025	23:48:06	
	-65.3153	99.0828	TMR4	17/03/2025	02:19:22	
18	-65.3713	99.0989	CTD16	17/03/2025	03:54:30	
19	-65.4152	99.1336	CTD17	17/03/2025	06:13:56	

21. Appendix

20	-65.4511	99.1696	CTD18	17/03/2025	08:16:12	
21	-65.505	99.2378	CTD19	17/03/2025	10:46:44	
	-65.5047	99.2385	TMR5	17/03/2025	12:14:32	
22	-65.5462	99.2754	CTD20	17/03/2025	14:14:49	
23	-65.5867	99.3362	CTD21	17/03/2025	22:18:11	
	-65.5841	99.3382	TMR6	17/03/2025	11:55:42	
24	-65.6409	99.3404	CTD22	18/03/2025	01:41:58	
25	-65.6835	99.3329	CTD23	18/03/2025	03:50:27	
26	-65.72	99.3751	CTD24	18/03/2025	05:57:31	
27	-65.7566	99.3698	CTD25	18/03/2025	07:51:31	
28	-65.8065	99.4030	CTD26	18/03/2025	11:17:16	
29	-65.8483	99.3858	CTD27	18/03/2025	13:43:32	
	-65.8487	99.3858	TMR7	18/03/2025	15:10:00	
	-65.8483	99.3858	MC03	18/03/2025	16:48:12	
30	-65.145	98.787	BT02 (B)	19/03/2025	04:35:40	
	-65.1458	98.8160	TC01	19/03/2025	10:15:00	
31	-64.7362	100.0589	TC02	20/03/2025	04:48:48	
32	-64.7803	99.9043	CTD28	20/03/2025	09:26:55	
33	-64.7993	100.1282	TC03	20/03/2025	14:06:27	
34	-65.3264	99.5439	CTD29	22/03/2025	13:18:34	
	-65.3262	99.6169	TMR8	22/03/2025	15:26:24	
35	-65.2486	99.3112	CTD30	22/03/2025	19:08:10	
36	-65.291	99.4325	CTD31	22/03/2025	22:52:04	Fail
	-65.291	99.4325	CTD32	23/03/2025	00:06:13	
37	-65.2408	99.2527	KC02	23/03/2025	03:53:27	
38	-65.2355	99.1999	CTD33	23/03/2025	06:37:53	
	-65.2324	99.1814	TMR9	23/03/2025	08:04:11	
39	-65.1852	99.0618	CTD34	23/03/2025	10:44:20	
40	-65.1551	98.8839	CTD35	23/03/2025	14:03:47	
41	-65.0831	99.0035	CTD36	23/03/2025	16:32:21	
42	-65.092	99.1012	CTD37	23/03/2025	19:01:09	

21. Appendix

43	-65.1071	99.2269	CTD38	24/03/2025	06:20:10	
44	-65.1168	99.3618	CTD39	24/03/2025	09:00:00	
	-65.1114	99.3508	TMR10	24/03/2025	11:56:45	
	-65.1064	99.3507	MC04	24/03/2025	14:04:19	
45	-65.144	99.4629	CTD40	24/03/2025	19:52:52	
46	-65.1451	99.5634	CTD41	24/03/2025	22:16:28	
47	-65.232	100.167	BT03 (C)	25/03/2025	03:51:54	
48	-64.9988	100.0073	CTD42	25/03/2025	07:51:45	Polarstern Rep1
49	-65.1866	99.8728	TC04	25/03/2025	11:51:49	
50	-65.3304	99.5760	TC05	25/03/2025	16:42:19	
51	-65.3375	99.9811	CTD43	25/03/2025	20:30:18	
52	-65.4158	99.6358	CTD44	26/03/2025	00:02:52	
53	-65.2894	99.2398	KC03	26/03/2025	04:49:18	
	-65.2866	99.24038	CTD45	26/03/2025	06:41:48	
	-65.289	99.24067	TC06	26/03/2025	08:41:00	
54	-65.2685	99.0211	TC07	26/03/2025	12:30:45	
55	-65.3002	99.2018	CTD46	26/03/2025	16:34:39	
56	-65.2986	99.2732	CTD47	26/03/2025	19:15:17	
57	-65.281	99.3255	CTD48	26/03/2025	21:32:19	
58	-65.204	99.869	BT04 (D)	27/03/2025	02:58:35	Fail
59	-65.176	99.933	BT05 (E)	27/03/2025	04:55:03	
60	-65.0862	99.4125	TC08	27/03/2025	12:15:00	
61	-64.9761	99.3953	CTD49	27/03/2025	18:45:49	
62	-65.1179	99.3084	CTD50	27/03/2025	23:42:44	
63	-64.873	99.918	BT06 (F)	29/03/2025	06:05:32	
64	-64.5000	100.0000	PS1	29/03/2025	14:53:18	
	-64.5001	99.9996	TC09	29/03/2025	15:15:00	
	-64.5001	99.99971	CTD51	29/03/2025	19:11:35	
	-64.5000	99.9990	TMR11	29/03/2025	20:38:36	
	-64.5001	99.9998	MC5	29/03/2025	22:35:47	Fail
	-64.5001	99.9998	MC6	29/03/2025	23:51:00	Fail

21. Appendix

	-64.5001	99.9997	SMG1	30/03/2025	03:20:58	
	-64.5000	100.0000	ISP1	30/03/2025	08:00:00	
	-64.5012	99.99931	MC7	30/03/2025	12:36:31	Fail
	-64.502	99.99871	CTD52	30/03/2025	14:39:13	
	-64.5021	99.9983	CTD53	30/03/2025	15:00:09	
	-64.5020	99.9980	TMR12	30/03/2025	18:05:00	
	-64.5004	100.0001	TMR13	30/03/2025	21:15:07	
65	-64.218	99.060	BT07 (G)	31/03/2025	04:18:21	
66	-63.8741	99.5123	TC10	31/03/2025	08:48:15	
67	-64.0146	100.0204	CTD54	31/03/2025	14:57:00	
68	-64.1009	99.9641	CTD55	31/03/2025	18:17:05	
69	-64.1859	99.8776	CTD56	31/03/2025	21:16:22	
70	-64.2943	99.8283	CTD57	31/03/2025	23:49:34	
71	-64.3744	99.7449	CTD58	1/04/2025	02:59:58	
72	-64.4787	99.7154	CTD59	1/04/2025	06:22:43	
73	-64.5755	99.6369	CTD60	1/04/2025	09:00:22	
74	-64.6653	99.5142	CTD61	1/04/2025	12:13:34	
75	-64.4947	99.8066	CTD62	1/04/2025	16:31:32	
76	-64.5006	99.6418	CTD63	1/04/2025	19:06:18	
77	-64.5063	99.4321	CTD64	1/04/2025	21:51:52	
78	-64.5	99.2294	CTD65	2/04/2025	00:49:05	
79	-64.672	95.083	BT08 (H)	3/04/2025	09:04:21	
80	-64.6715	95.1180	TC11	3/04/2025	12:30:19	
81	-64.7261	94.5797	TC12	3/04/2025	23:39:31	
82	-64.4204	93.5990	KC04	4/04/2025	07:58:34	
83	-64.8320	94.1643	TC13	4/04/2025	17:50:00	
	-64.8396	94.1286	CTD66	4/04/2025	19:28:39	
	-64.8393	94.1283	TMR14	4/04/2025	21:06:00	
	-64.837	94.147	BT09 (I)	5/04/2025	00:02:23	
84	-65.2325	95.6596	CTD67	5/04/2025	07:15:05	
	-65.2325	95.6597	TMR15	5/04/2025	08:06:00	

21. Appendix

	-65.2325	95.6597	MC08	5/04/2025	09:20:46	
85	-65.1979	95.5323	CTD68	5/04/2025	11:46:08	
86	-65.1797	95.4251	CTD69	5/04/2025	13:27:36	
	-65.1798	95.4255	TMR16	5/04/2025	15:03:00	
87	-65.156	95.3211	CTD70	5/04/2025	16:15:40	
88	-65.1236	95.2167	CTD71	5/04/2025	19:13:18	
89	-65.0976	95.1007	CTD72	5/04/2025	22:01:50	
90	-65.2101	95.5772	TC14	6/04/2025	13:10:00	
91	-65.1802	95.4287	MC09	6/04/2025	16:20:07	
92	-65.1024	95.1461	MC10	6/04/2025	20:05:07	
	-65.1022	95.1472	TMR17	6/04/2025	22:06:00	
93	-65.1367	95.2322	TC15	7/04/2025	01:59:00	
	-65.135	95.267	BT10 (J)	7/04/2025	06:42:56	
94	-65.8129	94.7108	CTD73	7/04/2025	21:20:04	
95	-65.801	94.8687	CTD74	7/04/2025	23:54:37	
96	-65.7950	95.0116	MC11	8/04/2025	02:57:07	
	-65.795	95.0116	CTD75	8/04/2025	04:21:03	
	-65.795	95.0116	TMR18	8/04/2025	06:24:00	Fail
97	-65.783	95.1358	CTD76	8/04/2025	09:15:17	
98	-65.7908	95.2628	CTD77	8/04/2025	12:18:43	
99	-65.8422	95.1054	TC16	8/04/2025	15:08:00	
100	-66.021	94.6659	CTD78	8/04/2025	19:19:20	
	-66.021	94.6659	TMR19	8/04/2025	20:43:15	Fail
101	-65.842	95.147	BT11 (K)	9/04/2025	02:28:14	
102	-66.0061	95.1914	TC17	9/04/2025	10:08:00	
103	-66.0224	95.1993	KC05	9/04/2025	14:33:55	
104	-66.0281	95.2196	CTD79	9/04/2025	21:15:03	
105	-66.0110	95.2062	RD03	10/04/2025	07:38:19	Fail
106	-66.2050	95.3135	CTD80	10/04/2025	13:26:19	
	-66.2050	95.3135	TMR20	10/04/2025	14:29:56	
	-66.2050	95.3133	ISP2	10/04/2025	17:48:00	

21. Appendix

	-66.2058	95.3148	MC12	10/04/2025	21:39:07	
107	-66.1097	95.2814	TC18	11/04/2025	01:45:09	
108	-66.0197	95.2758	TC19	11/04/2025	04:23:15	
	-66.019	95.280	BT12 (L)	11/4/2025	07:22:28	
109	-66.022	95.1995	PS2	11/04/2025	12:14:48	
	-66.0220	95.1995	ISP3	11/04/2025	12:15:00	
	-66.0229	95.1605	TC20	11/04/2025	17:30:00	
	-66.0217	95.1995	CTD81	11/04/2025	19:49:31	
	-66.0217	95.1995	TMR21	11/04/2025	21:47:24	
	-66.0218	95.1995	MC13	12/04/2025	01:39:13	
	-66.0218	95.1997	TMR22	12/04/2025	04:21:00	
	-66.0218	95.1997	CTD82	12/04/2025	05:35:09	
110	-66.1465	95.5043	CTD83	12/04/2025	09:37:32	
111	-66.0969	95.4907	CTD84	12/04/2025	11:39:00	
112	-66.0511	95.4695	CTD85	12/04/2025	13:27:09	
113	-65.9989	95.4579	CTD86	12/04/2025	15:21:02	
114	-65.9454	95.4415	CTD87	12/04/2025	17:30:41	
115	-65.8957	95.4389	CTD88	12/04/2025	19:55:54	
116	-65.8592	95.4438	CTD89	12/04/2025	21:57:14	
117	-65.8235	95.4481	CTD90	13/04/2025	01:45:39	
118	-65.7911	95.4462	CTD91	13/04/2025	04:47:19	
119	-65.7602	95.4877	CTD92	13/04/2025	08:50:37	
120	-65.733	95.5251	CTD93	13/04/2025	11:42:48	
121	-65.6774	95.4967	CTD94	13/04/2025	13:59:53	
122	-65.6327	95.4767	CTD95	13/04/2025	16:08:23	
123	-65.5381	95.4077	CTD96	13/04/2025	19:00:01	
124	-65.4923	95.3555	CTD97	13/04/2025	21:12:19	
125	-65.7915	95.4274	TMR23	14/04/2025	08:30:53	Polarstern repeat
126	-65.7918	95.4266	TC21	14/04/2025	9:05:40	
127	-65.4005	95.1497	TC22	14/04/2025	16:41:47	
128	-65.0660	94.994	BT13 (M)	15/04/2025	02:29:00	

21. Appendix

129	-65.4408	95.5126	TMR24	15/04/2025	11:27:25	
130	-65.2991	95.5134	TMR25	15/04/2025	15:05:00	
131	-64.778	95.960	BT14 (N)	16/04/2025	01:42:55	
132	-64.8485	94.1449	MC14	16/04/2025	12:27:15	
133	-65.4917	95.3702	CTD98	17/04/2025	07:00:30	
134	-65.4404	95.3974	CTD99	17/04/2025	09:17:00	
135	-65.3421	95.4825	CTD100	17/04/2025	12:47:15	
136	-65.2998	95.4542	CTD101	17/04/2025	14:59:53	
137	-65.2363	95.4531	CTD102	17/04/2025	17:58:53	
138	-64.5883	94.1748	TMR26	19/04/2025	12:20:18	
139	-64.799	94.236	BT15 (O)	20/04/2025	02:10:10	
140	-63.9542	97.2165	CTD103	20/04/2025	19:11:24	
	-63.9536	97.2159	KC06	20/04/2025	22:49:25	
141	-64.192	98.037	BT16 (P)	21/04/2025	08:09:07	Fail
142	-63.6925	98.8940	TC23	21/04/2025	16:00:55	
143	-62.8316	99.2773	RD04	22/04/2025	04:19:01	
144	-60.7854	100.5907	RD05	23/04/2025	02:50:52	
145	-60.8240	100.6379	RD06	23/04/2025	11:42:49	
146	-60.6226	101.1314	RD07	23/04/2025	22:13:33	
147	-60.5869	101.2188	CTD104	24/04/2025	03:51:27	
	-60.5829	101.2168	CTD105	24/04/2025	10:03:24	

21. Appendix

21.3 Fish caught during DMV

Table 59: List of fish caught during beam trawls

Trawl	Fish ID #	ID	Euthanized (Y/N)	Sent Back (Alive)	Notes
A	NY010001	<i>Neopagetopsis ionah</i>	N	N	
A	NY010002	<i>Neopagetopsis ionah</i>	N	N	
A	NY010003	<i>Bathyraco marri</i>	N	N	
A	NY010004	<i>Neopagetopsis ionah</i>	N	N	
A	NY010005	<i>Chaenodraco wilsoni</i>	N	N	
A	NY010006	<i>Chaenodraco wilsoni</i>	N	N	
A	NY010007	<i>Racovitzia glacialis</i>	Y	N	
A	NY010008	<i>Racovitzia glacialis</i>	N	N	
A	NY010009	<i>Bathyraco marri</i>	N	N	
A	NY010010	<i>Bathyraco marri</i>	N	N	
A	NY010011	<i>Bathyraco marri</i>	N	N	
A	NY010012	<i>Macrourus carinatus</i>	N	N	
A	NY010013	<i>Macrourus carinatus</i>	N	N	
A	NY010014	<i>Macrourus carinatus</i>	N	N	
A	NY010015	<i>Harpagifer antarcticus</i>	N	N	
A	NY010016	<i>Harpagifer antarcticus</i>	N	N	
A	NY010017	<i>Trematomus hansonii</i>	N	N	
A	NY010018	<i>Trematomus hansonii</i>	N	N	
A	NY010019	<i>Trematomus hansonii</i>	N	N	
A	NY010020	<i>Trematomus hansonii</i>	N	N	
A	NY010021	<i>Trematomus hansonii</i>	N	N	
A	NY010022	<i>Trematomus hansonii</i>	N	N	
A	NY010023	<i>Pleuragramma antarctica</i>	N	N	
A	NY010024	<i>Pleuragramma antarctica</i>	N	N	
A	NY010025	<i>Pleuragramma antarctica</i>	N	N	
A	NY010026	<i>Pleuragramma antarctica</i>	N	N	
A	NY010027	<i>Pleuragramma antarctica</i>	N	N	
A	NY010028	<i>Pleuragramma antarctica</i>	N	N	
A	NY010029	<i>Pleuragramma antarctica</i>	N	N	
A	NY010030	<i>Pleuragramma antarctica</i>	N	N	
B	NY010031	<i>Pleuragramma antarctica</i>	Y	N	
B	NY010032	<i>Pleuragramma antarctica</i>	Y	N	
B	NY010033	<i>Pleuragramma antarctica</i>	N	N	
B	NY010034	<i>Macrourus carinatus</i>	Y	N	
B	NY010035	<i>Nototheniops larseni</i>	N	N	
B	NY010036	<i>Nototheniops larseni</i>	N	N	
B	NY010037	<i>Macrourus carinatus</i>	N	N	
B	NY010038	<i>Nototheniops larseni</i>	N	N	
B	NY010039	<i>Chaenodraco wilsoni</i>	N	N	
B	NY010040	<i>Lindbergichthys mizops</i>	Y	N	
B	NY010041	<i>Lindbergichthys mizops</i>	Y	N	
B	NY010042	<i>Lindbergichthys mizops</i>	Y	N	
B	NY010043	<i>Lindbergichthys mizops</i>	Y	N	
B	NY010044	<i>Racovitzia glacialis</i>	Y	N	
B	NY010045	<i>Bathyraco marri</i>	N	N	
B	NY010046	<i>Bathyraco marri</i>	N	N	
B	NY010047	<i>Racovitzia glacialis</i>	Y	N	
C	NY010048	<i>Trematomus hansonii</i>	N	N	
C	NY010049	<i>Pleuragramma antarctica</i>	N	N	
D	NY010050	<i>Racovitzia glacialis</i>	N	N	
D	NY010051	<i>Racovitzia glacialis</i>	N	N	
D	NY010052	<i>Racovitzia glacialis</i>	N	N	
D	NY010053	<i>Bathyraco marri</i>	Y	N	
D	NY010054	<i>Bathyraco marri</i>	Y	N	
D	NY010055	<i>Bathyraco marri</i>	Y	N	
D	NY010056	<i>Macrourus whitsoni</i>	N	N	
D	NY010057	<i>Macrourus whitsoni</i>	N	N	
D	NY010058	<i>Pleuragramma antarctica</i>	N	N	
D	NY010059	<i>Pleuragramma antarctica</i>	N	N	
E	NY010060	<i>Bathyraco marri</i>	Y	N	
E	NY010061	<i>Bathyraco marri</i>	Y	N	

21. Appendix

E	NY010062	<i>Bathyraco marri</i>	Y	N	
E	NY010063	<i>Bathyraco marri</i>	Y	N	
E	NY010064	<i>Pleuragramma antarctica</i>	Y	N	
E	NY010065	<i>Racovitzia glacialis</i>	Y	N	
E	NY010066	<i>Racovitzia glacialis</i>	Y	N	
E	NY010067	<i>Racovitzia glacialis</i>	Y	N	
E	NY010068	<i>Racovitzia glacialis</i>	Y	N	
E	NY010069	<i>Racovitzia glacialis</i>	Y	N	
E	NY010070	<i>Bathyraco marri</i>	Y	N	
E	NY010071	<i>Bathyraco marri</i>	Y	N	
E	NY010072	<i>Pleuragramma antarctica</i>	Y	N	
E	NY010073	<i>Pleuragramma antarctica</i>	Y	N	
E	NY010074	<i>Harpagifer antarcticus</i>	Y	N	
E	NY010075	<i>Pleuragramma antarctica</i>	N	N	
E	NY010076	<i>Pleuragramma antarctica</i>	N	N	
E	NY010077	<i>Pleuragramma antarctica</i>	N	N	
E	NY010078	<i>Pleuragramma antarctica</i>	N	N	
E	NY010079	<i>Pleuragramma antarctica</i>	N	N	
E	NY010394	<i>Bathyraco marri</i>		Y	
E	NY010395	<i>Bathyraco marri</i>		Y	
E	NY010396	<i>Bathyraco marri</i>		Y	
E	NY010397	<i>Bathyraco marri</i>		Y	
E	NY010398	<i>Bathyraco marri</i>		Y	
E	NY010399	<i>Bathyraco marri</i>		Y	
E	NY010400	<i>Bathyraco marri</i>		Y	
E	NY010401	<i>Bathyraco marri</i>		Y	
F	NY010080	<i>Pleuragramma antarctica</i>	N		
F	NY010081	<i>Pleuragramma antarctica</i>	N		
F	NY010082	<i>Pleuragramma antarctica</i>	N		
F	NY010083	<i>Pleuragramma antarctica</i>	N		
F	NY010084	<i>Bathyraco marri</i>	N		
F	NY010085	<i>Racovitzia glacialis</i>	N		
F	NY010086	<i>Pleuragramma antarctica</i>	N		
F	NY010087	<i>Pleuragramma antarctica</i>	N		
F	NY010088	<i>Racovitzia glacialis</i>	N		
F	NY010089	<i>Pleuragramma antarctica</i>	N		
F	NY010090	<i>Pleuragramma antarctica</i>	N		
F	NY010091	<i>Pleuragramma antarctica</i>	N		
F	NY010402	<i>Neopagetopsis ionah</i>		Y	
F	NY010403	<i>Harpagifer antarcticus</i>		Y	
F	NY010404	<i>Trematomus hansonii</i>		Y	
F	NY010405	<i>Trematomus hansonii</i>		Y	
F	NY010406	<i>Trematomus hansonii</i>		Y	
F	NY010407	<i>Bathyraco marri</i>		Y	
F	NY010408	<i>Bathyraco marri</i>		Y	
F	NY010409	<i>Bathyraco antarcticus</i>		Y	
F	NY010410	<i>Bathyraco antarcticus</i>		Y	
F	NY010411	<i>Bathyraco antarcticus</i>		Y	
F	NY010412	<i>Bathyraco antarcticus</i>		Y	
F	NY010413	<i>Bathyraco antarcticus</i>		Y	
G	NY010092	<i>Pleuragramma antarctica</i>	N		
G	NY010093	<i>Pleuragramma antarctica</i>	N		
G	NY010094	<i>Pleuragramma antarctica</i>	N		
G	NY010095	<i>Pleuragramma antarctica</i>	N		
G	NY010096	<i>Pleuragramma antarctica</i>	N		
G	NY010097	<i>Harpagifer antarcticus</i>	N		
G	NY010098	<i>Neopagetopsis ionah</i>	N		
G	NY010099	<i>Neopagetopsis ionah</i>	N		
G	NY010100	<i>Pachycara brachycephalum</i>	N		
G	NY010101	<i>Neopagetopsis ionah</i>	N		
G	NY010102	<i>Neopagetopsis ionah</i>	N		
G	NY010103	<i>Chaenodraco wilsoni</i>	N		
G	NY010414	<i>Trematomus hansonii</i>		Y	
G	NY010415	<i>Neopagetopsis ionah</i>		Y	
H	NY010103.B	<i>Neopagetopsis ionah</i>	N		
H	NY010104	<i>Neopagetopsis ionah</i>	N		
H	NY010105	<i>Chaenodraco wilsoni</i>	N		

21. Appendix

H	NY010106	<i>Chaenodraco wilsoni</i>	N		
H	NY010107	<i>Chaenodraco wilsoni</i>	N		
H	NY010108	<i>Chaenodraco wilsoni</i>	N		
H	NY010109	<i>Chaenodraco wilsoni</i>	N		
H	NY010110	<i>Pleuragramma antarctica</i>	N		
H	NY010111	<i>Trematomus hansonii</i>	N		
H	NY010112	<i>Trematomus hansonii</i>	N		
H	NY010113	<i>Trematomus hansonii</i>	N		
H	NY010114	<i>Trematomus hansonii</i>	N		
H	NY010115	<i>Trematomus hansonii</i>	N		
H	NY010116	<i>Trematomus hansonii</i>	N		
H	NY010117	<i>Trematomus hansonii</i>	N		
H	NY010118	<i>Trematomus hansonii</i>	N		
H	NY010416	<i>Neopagetopsis ionah</i>		Y	
H	NY010417	<i>Neopagetopsis ionah</i>		Y	
H	NY010418	<i>Neopagetopsis ionah</i>		Y	
H	NY010419	<i>Neopagetopsis ionah</i>		Y	
H	NY010420	<i>Neopagetopsis ionah</i>		Y	
H	NY010421	<i>Neopagetopsis ionah</i>		Y	
H	NY010422	<i>Neopagetopsis ionah</i>		Y	
H	NY010423	<i>Neopagetopsis ionah</i>		Y	
H	NY010424	<i>Trematomus hansonii</i>		Y	
H	NY010425	<i>Trematomus hansonii</i>		Y	
H	NY010426	<i>Trematomus hansonii</i>		Y	
H	NY010427	<i>Trematomus hansonii</i>		Y	
H	NY010428	<i>Trematomus hansonii</i>		Y	
H	NY010429	<i>Trematomus hansonii</i>		Y	
H	NY010430	<i>Trematomus hansonii</i>		Y	
H	NY010431	<i>Trematomus hansonii</i>		Y	
H	NY010432	<i>Trematomus hansonii</i>		Y	
H	NY010433	<i>Trematomus hansonii</i>		Y	
H	NY010434	<i>Trematomus hansonii</i>		Y	
H	NY010435	<i>Trematomus hansonii</i>		Y	
H	NY010436	skate		Y	
I	NY010119	<i>Channichthys rhinoceros</i>	N		
I	NY010120	<i>Chionodraco hamatus</i>	N		
I	NY010121	<i>Chionodraco hamatus</i>	N		
I	NY010122	<i>Chionodraco hamatus</i>	N		
I	NY010123	<i>Chionodraco hamatus</i>	N		
I	NY010124	<i>Chionodraco hamatus</i>	N		
I	NY010125	<i>Chionodraco hamatus</i>	N		
I	NY010126	<i>Chionodraco hamatus</i>	N		
I	NY010127	<i>Chionodraco hamatus</i>	N		
I	NY010128	<i>Trematomus hansonii</i>	N		
I	NY010129	<i>Trematomus hansonii</i>	N		
I	NY010130	<i>Bathyraco antarcticus</i>	N		
I	NY010131	<i>Bathyraco antarcticus</i>	N		
I	NY010132	<i>Bathyraco antarcticus</i>	N		
I	NY010133	<i>Bathyraco antarcticus</i>	N		
I	NY010134	<i>Bathyraco antarcticus</i>	N		
I	NY010135	<i>Bathyraco antarcticus</i>	N		
I	NY010136	<i>Bathyraco antarcticus</i>	N		
I	NY010137	<i>Bathyraco antarcticus</i>	N		
I	NY010138	<i>Bathyraco antarcticus</i>	N		
I	NY010139	<i>Bathyraco antarcticus</i>	N		
I	NY010140	<i>Bathyraco antarcticus</i>	N		
I	NY010141	<i>Bathyraco antarcticus</i>	N		
I	NY010142	<i>Bathyraco antarcticus</i>	N		
I	NY010143	<i>Bathyraco antarcticus</i>	N		
I	NY010144	<i>Bathyraco antarcticus</i>	N		
I	NY010145	<i>Bathyraco antarcticus</i>	N		
I	NY010146	<i>Bathyraco antarcticus</i>	N		
I	NY010147	<i>Bathyraco antarcticus</i>	N		
I	NY010148	<i>Bathyraco antarcticus</i>	N		
I	NY010149	<i>Bathyraco antarcticus</i>	N		
I	NY010150	<i>Bathyraco antarcticus</i>	N		
I	NY010151	<i>Bathyraco antarcticus</i>	N		

21. Appendix

I	NY010466	<i>Bathyraco antarcticus</i>		Y	
I	NY010467	<i>Bathyraco antarcticus</i>		Y	
I	NY010468	<i>Bathyraco antarcticus</i>		Y	
I	NY010469	<i>Bathyraco antarcticus</i>		Y	
I	NY010470	<i>Bathyraco antarcticus</i>		Y	
I	NY010471	<i>Bathyraco antarcticus</i>		Y	
I	NY010472	<i>Bathyraco antarcticus</i>		Y	
I	NY010473	<i>Bathyraco antarcticus</i>		Y	
I	NY010474	<i>Bathyraco antarcticus</i>		Y	
I	NY010475	<i>Bathyraco antarcticus</i>		Y	
I	NY010476	<i>Bathyraco antarcticus</i>		Y	
I	NY010477	<i>Bathyraco antarcticus</i>		Y	
I	NY010478	<i>Bathyraco antarcticus</i>		Y	
I	NY010479	<i>Bathyraco antarcticus</i>		Y	
I	NY010480	<i>Bathyraco antarcticus</i>		Y	
I	NY010481	<i>Bathyraco antarcticus</i>		Y	
I	NY010482	<i>Bathyraco antarcticus</i>		Y	
I	NY010483	<i>Bathyraco antarcticus</i>		Y	
I	NY010484	<i>Bathyraco antarcticus</i>		Y	
I	NY010485	<i>Bathyraco antarcticus</i>		Y	
I	NY010486	<i>Bathyraco antarcticus</i>		Y	
I	NY010487	<i>Bathyraco antarcticus</i>		Y	
I	NY010488	<i>Bathyraco antarcticus</i>		Y	
I	NY010489	<i>Bathyraco antarcticus</i>		Y	
I	NY010490	<i>Bathyraco antarcticus</i>		Y	
I	NY010491	<i>Bathyraco antarcticus</i>		Y	
I	NY010492	<i>Bathyraco antarcticus</i>		Y	
I	NY010493	<i>Bathyraco antarcticus</i>		Y	
I	NY010494	<i>Bathyraco antarcticus</i>		Y	
I	NY010495	<i>Bathyraco antarcticus</i>		Y	
I	NY010496	<i>Bathyraco antarcticus</i>		Y	
I	NY010497	<i>Bathyraco antarcticus</i>		Y	
I	NY010498	<i>Bathyraco antarcticus</i>		Y	
I	NY010499	<i>Bathyraco antarcticus</i>		Y	
I	NY010500	<i>Bathyraco antarcticus</i>		Y	
J	NY010190	<i>Chionodraco hamatus</i>	N		
J	NY010191	<i>Chionodraco hamatus</i>	N		
J	NY010192	<i>Chionodraco hamatus</i>	N		
J	NY010193	<i>Chionodraco hamatus</i>	N		
J	NY010194	<i>Chionodraco hamatus</i>	N		
J	NY010195	<i>Chionodraco hamatus</i>	N		
J	NY010196	<i>Bathyraco antarcticus</i>	N		
J	NY010197	<i>Bathyraco antarcticus</i>	N		
J	NY010198	<i>Bathyraco marri</i>	N		
J	NY010199	<i>Bathyraco marri</i>	N		
J	NY010200	<i>Bathyraco marri</i>	N		
J	NY010201	<i>Bathyraco marri</i>	N		
J	NY010202	<i>Racovitzia glacialis</i>	N		
J	NY010203	<i>Racovitzia glacialis</i>	N		
J	NY010204	<i>Racovitzia glacialis</i>	N		
J	NY010205	<i>Bathyraco marri</i>	N		
J	NY010206	<i>Neopagetopsis ionah</i>	N		
J	NY010207	<i>Neopagetopsis ionah</i>	N		
J	NY010208	<i>Neopagetopsis ionah</i>	N		
J	NY010209	<i>Neopagetopsis ionah</i>	N		
J	NY010210	<i>Neopagetopsis ionah</i>	N		
J	NY010211	<i>Neopagetopsis ionah</i>	N		
J	NY010212	<i>Neopagetopsis ionah</i>	N		
J	NY010213	<i>Neopagetopsis ionah</i>	N		
J	NY010214	<i>Neopagetopsis ionah</i>	N		
J	NY010215	<i>Neopagetopsis ionah</i>	N		
J	NY010216	<i>Neopagetopsis ionah</i>	N		
J	NY010217	<i>Neopagetopsis ionah</i>	N		
J	NY010218	<i>Neopagetopsis ionah</i>	N		
J	NY010219	<i>Neopagetopsis ionah</i>	N		
J	NY010220	<i>Pleuragramma antarctica</i>	N		
J	NY010221	<i>Pleuragramma antarctica</i>	N		

21. Appendix

J	NY010289	<i>Pleuragramma antarctica</i>	N		
J	NY010290	<i>Pleuragramma antarctica</i>	N		
J	NY010291	<i>Pleuragramma antarctica</i>	N		
J	NY010292	<i>Pleuragramma antarctica</i>	N		
J	NY010293	<i>Pleuragramma antarctica</i>	N		
J	NY010294	<i>Pleuragramma antarctica</i>	N		
J	NY010295	<i>Pleuragramma antarctica</i>	N		
J	NY010296	<i>Pleuragramma antarctica</i>	N		
J	NY010297	<i>Pleuragramma antarctica</i>	N		
J	NY010298	<i>Pleuragramma antarctica</i>	N		
J	NY010299	<i>Pleuragramma antarctica</i>	N		
J	NY010300	<i>Pleuragramma antarctica</i>	N		
J	NY010301	<i>Pleuragramma antarctica</i>	N		
J	NY010302	<i>Pleuragramma antarctica</i>	N		
J	NY010303	<i>Pleuragramma antarctica</i>	N		
J	NY010304	<i>Pleuragramma antarctica</i>	N		
J	NY010305	<i>Pleuragramma antarctica</i>	N		
J	NY010306	<i>Pleuragramma antarctica</i>	N		
J	NY010307	<i>Pleuragramma antarctica</i>	N		
J	NY010308	<i>Pleuragramma antarctica</i>	N		
J	NY010309	<i>Pleuragramma antarctica</i>	N		
J	NY010310	<i>Pleuragramma antarctica</i>	N		
J	NY010311	<i>Pleuragramma antarctica</i>	N		
J	NY010312	<i>Pleuragramma antarctica</i>	N		
J	NY010313	<i>Pleuragramma antarctica</i>	N		
J	NY010314	<i>Pleuragramma antarctica</i>	N		
J	NY010315	<i>Pleuragramma antarctica</i>	N		
J	NY010316	<i>Pleuragramma antarctica</i>	N		
J	NY010317	<i>Pleuragramma antarctica</i>	N		
J	NY010318	<i>Pleuragramma antarctica</i>	N		
J	NY010319	<i>Pleuragramma antarctica</i>	N		
J	NY010320	<i>Pleuragramma antarctica</i>	N		
J	NY010321	<i>Pleuragramma antarctica</i>	N		
J	NY010501	<i>Trematomus hansonii</i>		Y	
J	NY010502	<i>Macrourus carinatus</i>		Y	
K	NY010322	<i>Pleuragramma antarctica</i>	N		
K	NY010323	<i>Pleuragramma antarctica</i>	N		
K	NY010324	<i>Pleuragramma antarctica</i>	N		
K	NY010325	<i>Pleuragramma antarctica</i>	N		
K	NY010326	<i>Pleuragramma antarctica</i>	N		
K	NY010327	<i>Trematomus hansonii</i>	N		
K	NY010328	<i>Trematomus hansonii</i>	N		
K	NY010329	<i>Trematomus hansonii</i>	N		
K	NY010330	<i>Trematomus hansonii</i>	N		
K	NY010331	<i>Trematomus hansonii</i>	N		
K	NY010332	<i>Trematomus hansonii</i>	N		
K	NY010333	<i>Trematomus hansonii</i>	N		
K	NY010334	<i>Trematomus hansonii</i>	N		
K	NY010335	<i>Trematomus hansonii</i>	N		
K	NY010503	<i>Neopagetopsis ionah</i>	N		
K	NY010504	<i>Trematomus hansonii</i>		Y	
K	NY010505	<i>Trematomus hansonii</i>		Y	
K	NY010506	<i>Trematomus hansonii</i>		Y	
K	NY010507	<i>Trematomus hansonii</i>		Y	
L	NY010337	<i>Pleuragramma antarctica</i>	N		
L	NY010338	<i>Pleuragramma antarctica</i>	N		
L	NY010339	<i>Pleuragramma antarctica</i>	N		
L	NY010340	<i>Pleuragramma antarctica</i>	N		
L	NY010341	<i>Pleuragramma antarctica</i>	N		
L	NY010342	<i>Pleuragramma antarctica</i>	N		
L	NY010343	<i>Pleuragramma antarctica</i>	N		
L	NY010344	<i>Pleuragramma antarctica</i>	N		
L	NY010345	<i>Pleuragramma antarctica</i>	N		
L	NY010346	<i>Pleuragramma antarctica</i>	N		
L	NY010347	<i>Pleuragramma antarctica</i>	N		
L	NY010348	<i>Pleuragramma antarctica</i>	N		
L	NY010349	<i>Bathydraco antarcticus</i>	N		

21. Appendix

L	NY010350	<i>Bathyraco antarcticus</i>	N		
L	NY010351	<i>Racovitzia glacialis</i>	N		
L	NY010352	<i>Trematomus hansonii</i>	N		
L	NY010353	<i>Trematomus hansonii</i>	N		
L	NY010354	<i>Trematomus hansonii</i>	N		
L	NY010355	<i>Trematomus hansonii</i>	N		
L	NY010508	<i>Trematomus hansonii</i>		Y	
L	NY010509	<i>Trematomus hansonii</i>		Y	
L	NY010510	<i>Trematomus hansonii</i>		Y	
L	NY010511	<i>Trematomus hansonii</i>		Y	
L	NY010512	<i>Bathyraco marri</i>		Y	
L	NY010513	<i>Bathyraco marri</i>		Y	
L	NY010514	<i>Bathyraco marri</i>		Y	
L	NY010515	<i>Macrourus carinatus</i>		Y	
L	NY010516	<i>Macrourus carinatus</i>		Y	
M	NY010356	<i>Neopagetopsis ionah</i>	N		
M	NY010357	<i>Neopagetopsis ionah</i>	N		
M	NY010358	<i>Neopagetopsis ionah</i>	N		
M	NY010359	<i>Neopagetopsis ionah</i>	Y		
M	NY010360	<i>Neopagetopsis ionah</i>	N		
M	NY010361	<i>Trematomus hansonii</i>	Y		
M	NY010362	<i>Pleuragramma antarctica</i>	N		
M	NY010363	<i>Pachycara brachycephalum</i>	N		
M	NY010364	<i>Notolepis coatsi</i>	N		
M	NY010517	<i>Neopagetopsis ionah</i>		Y	
M	NY010518	<i>Leindebergichthys mizops</i>		Y	potential rockcod
N	NY010365	<i>Neopagetopsis ionah</i>	N		
N	NY010366	<i>Neopagetopsis ionah</i>	N		
N	NY010367	<i>Neopagetopsis ionah</i>	N		
N	NY010368	<i>Neopagetopsis ionah</i>	N		
N	NY010369	<i>Neopagetopsis ionah</i>	N		
N	NY010370	<i>Neopagetopsis ionah</i>	N		
N	NY010371	<i>Neopagetopsis ionah</i>	N		
N	NY010372	<i>Neopagetopsis ionah</i>	N		
N	NY010373	<i>Neopagetopsis ionah</i>	N		
N	NY010374	<i>Pleuragramma antarctica</i>	N		
N	NY010375	<i>Trematomus hansonii</i>	N		
N	NY010376	<i>Trematomus hansonii</i>	Y		
N	NY010377	<i>Trematomus hansonii</i>	N		
N	NY010378	<i>Trematomus hansonii</i>	N		
N	NY010379	<i>Trematomus hansonii</i>	N		
N	NY010380	<i>Trematomus hansonii</i>	N		
N	NY010381	<i>Trematomus hansonii</i>	N		
N	NY010382	<i>Trematomus hansonii</i>	N		
N	NY010519	<i>Neopagetopsis ionah</i>		Y	
N	NY010520	<i>Neopagetopsis ionah</i>		Y	
N	NY010521	<i>Neopagetopsis ionah</i>		Y	
N	NY010522	<i>Trematomus hansonii</i>		Y	
O	NY010383	<i>Trematomus hansonii</i>	N		
O	NY010384	<i>Trematomus hansonii</i>	N		
O	NY010385	<i>Trematomus hansonii</i>	N		
O	NY010386	<i>Trematomus hansonii</i>	N		
O	NY010387	<i>Trematomus hansonii</i>	N		
O	NY010388	<i>Trematomus hansonii</i>	N		
O	NY010389	<i>Trematomus hansonii</i>	N		
O	NY010390	<i>Macrourus carinatus</i>	N		
O	NY010391	<i>Racovitzia glacialis</i>	N		
O	NY010392	<i>Neopagetopsis ionah</i>	N		
O	NY010393	<i>Neopagetopsis ionah</i>	N		
O	NY010394	<i>Bathyraco marri</i>		Y	
O	NY010523	<i>Neopagetopsis ionah</i>		Y	
O	NY010524	<i>Neopagetopsis ionah</i>		Y	
O	NY010525	<i>Neopagetopsis ionah</i>		Y	
O	NY010526	<i>Neopagetopsis ionah</i>		Y	
O	NY010527	<i>Neopagetopsis ionah</i>		Y	
O	NY010528	<i>Neopagetopsis ionah</i>		Y	
O	NY010529	<i>Neopagetopsis ionah</i>		Y	

21. Appendix

O	NY010530	<i>Bathyraco marri</i>		Y	
O	NY010531	<i>Bathyraco marri</i>		Y	
O	NY010532	<i>Bathyraco marri</i>		Y	
O	NY010533	<i>Racovitzia glacialis</i>		Y	
O	NY010534	<i>Racovitzia glacialis</i>		Y	
O	NY010535	<i>Racovitzia glacialis</i>		Y	
O	NY010536	<i>Trematomus hansonii</i>		Y	
O	NY010537	<i>Trematomus hansonii</i>		Y	
O	NY010538	<i>Trematomus hansonii</i>		Y	
O	NY010539	<i>Trematomus hansonii</i>		Y	

22. Supplementary Material

Published separately on the IMAS database is the following:

- CTD log sheets
- TMR log sheets
- Rock dredge reports
- Detailed sediment core reports for kasten and multi cores, including visual core logs and core photos